Biochimica et Biophysica Acta 1102 (1992) 269–352

BBABIO 43718

Review

The manganese and calcium ions of photosynthetic oxygen evolution

Richard J. Debus

Department of Biochemistry, University of California Riverside, Riverside, CA 92521, USA

(Received 28 May 1992)

Key words: Photosystem II; Water oxidation; Electron transfer; Photosynthesis

Contents

Correspondence to: R.J. Debus, Department of Biochemistry, University of California Riverside, Riverside, CA 92521-0129, USA.

Abbreviations: Chl, chlorophyll; DBMIB, dibromothymoquinone; DCBQ, dichloro-*p*-benzoquinone; DCCD, dicyclohexylcarbodiimide; DCIP, 2,6-dichlorophenolindophenol; DCMU, 3-(3,4-dichlorophenyl)-1,1-dimethylurea; DPC, 1,5-diphenylcarbazide; EDC, 1-ethyl-3-[3-(dimethylamino)propyl]carbodiimide hydrochloride; EDTA, ethylenediaminetetraacetic acid; EGTA, ethylene glycol bis(β-aminoethyl ether)-*N*,*N*,*N*′,*N*′-tetraacetic acid; EPR, electron paramagnetic resonance; ENDOR, electron nuclear double resonance; ESEEM, electron spin echo envelope modulation; EXAFS, extended X-ray absorption fine structure; HEDTA, *N*-hydroxyethylethylenediaminetriacetic acid; LHC, light harvesting complex; LHCII, light harvesting complex specifically associated with PS II; LF-1, low fluorescence mutant of *Scenedesmus obliquus*; Mes, 2-(*N*-morpholino)ethanesulfonic acid; Pheo, pheophytin; PS, photosystem; Q, plastoquinone; SERS, surface-enhanced Raman scattering; Tris, tris(hydroxymethyl)aminomethane; XANES, X-ray absorption near edge structure.

I. Introduction

The most important function of manganese in biology is to catalyze the conversion of water to molecular oxygen. This process takes place in Photosystem II near the lumenal surface of the thylakoid membrane. The catalytic reaction is driven by light and requires four manganese, 2–3 calcium and several Cl^- ions. Our understanding of the catalytic process has advanced dramatically in the last decade. Three major sets of developments have been responsible for this progress. First, methods to separate PS II from other components of the thylakoid membrane were developed [1–4] and refined, both for higher plants [5–13] and cyanobacteria (see subsection III-F). The high concentrations of PS II and relative lack of contaminating pigments in these preparations have made the catalytic process increasingly accessible to sophisticated spectroscopic analysis. Second, the development of methods to isolate specific genes has resulted in the determination of the amino-acid sequence of every constituent polypeptide of PS II from a wide variety of organisms. These sequences have yielded insight into the structure of these polypeptides and into their possible evolutionary relationships and have made it possible to analyze structure/function relationships by directed mutagenesis. For recommended nomenclature for the corresponding genes, see Ref. 14; for compendia of published sequences, see Refs. 15,16. For reviews of mutagenesis studies, see Refs. 17–19. Finally, the determinations of the structures of reaction centers from the purple non-sulfur bacteria *Rhodopseudomonas viridis* [20] and *Rhodobacter sphaeroides* [21,22] at < 3 Å resolution (reviewed in Refs. 23–28)

have supplied a model for the structure of the core of PS II (for review, see Refs. 24,29). The aim of this review is to critically assess our current knowledge of the manganese and calcium ions in PS II and their roles in catalyzing the oxidation of water. Many excellent reviews that emphasize other aspects of PS II, or other points of view, have appeared recently [30–38]. For a comprehensive earlier review, see Ref. 39. For a recent review that emphasizes the molecular biology of PS II, see Ref. 16, also see Ref. 19.

I-A. Cofactors and electron transfer

Photosystem II (PS II) couples the oxidation of water with the reduction of plastoquinone. Molecular oxygen is released as a by-product of water oxidation. The entire process begins with the absorption of light by a light-harvesting pigment-protein antenna complex that is located peripherally to PS II. In higher plants and green algae the main antenna complex is known as LHCII [16,40–44]. The LHCII complex spans the thylakoid membrane and contains non-covalently bound chlorophyll *a*, chlorophyll *b* and carotenoid molecules. The three-dimensional structure of LHCII at 6 Å resolution has recently been reported [45]. In red algae and cyanobacteria the antenna complex is the phycobilisome [23,46]. Phycobilisomes are located on the stromal surface of the thylakoid membrane and contain many water soluble proteins that have covalently attached linear tetrapyrrole pigments called bilins. The structures of two phycobilisome proteins from different organisms at ≤ 2.7 Å resolution have been reported [47–49]. In all organisms, the energy absorbed by the antenna complex is transferred to PS II and ultimately to a specialized monomer or dimer of chlorophyll *a* molecules known as P680 (see Fig. 1, for review, see Ref. 50). The energy from a single photon promotes P680 to an excited singlet state. Within approx. 3 ps of its formation [51,52] (and see Ref. 53), the excited singlet state of P680 reduces a nearby pheophytin (Pheo), forming $P680^+$ and $Pheo^-$. Stabilization of these species against charge recombination is achieved by the rapid (250–550 ps [54–59]) oxidation of $Pheo^-$ by a nearby plastoquinone molecule known as Q_A and by the rapid (40–280 ns, see subsection II-D.2) reduction of $P680^+$ by a redox-active tyrosine residue known as Y_Z [60,61,986]. This component was proposed to be a tyrosine residue on the basis of specific deuteration experiments [62–64]. This assignment has been supported by time-resolved optical absorption measurements in the ultraviolet [61] and by directed mutagenesis studies [65–68]. The latter studies identified Y_Z as Tyr-161 of the D1 polypeptide [67,68] (see below and subsection I.B-1). Charge recombination between Q_A^- and Y_Z^+ is prevented by further electron transfer events: a second plastoquinone molecule, Q_B, oxidizes Q_A^-

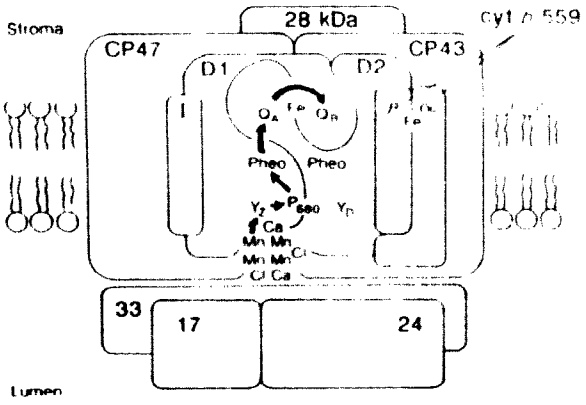

Fig. 1. Schematic illustration of the major polypeptide components of PS II. Numerous other polypeptides whose functions are unknown are not depicted (see Table I). Solid arrows show the direction of electron transfer.

within 100–200 μs [69–71] (forming Q_B^-) and the water-oxidizing complex, which contains the four Mn ions, reduces Y_Z^+ within 30–1300 μs (see subsection II-D.1). Plastoquinone binds only weakly to the Q_B site [70,72]. Many herbicides, such as DCMU, inhibit electron transfer from Q_A^- to Q_B by competing with plastoquinone for the Q_B site [73–75]. (For reviews of Q_A and Q_B function in PS II, see Refs. 71,76,77; for recent reviews of herbicide binding in PS II, see Refs. 78–80, also see Ref. 81). Before charge recombination between Q_B^- and the water-oxidizing complex takes place, a second charge-separation generates Y_Z^+ and Q_A^- a second time. The water-oxidizing complex then again reduces Y_Z^+, thereby accumulating a second oxidizing equivalent, while Q_A^- reduces Q_B^-. In reaction centers from purple non-sulfur bacteria, electron transfer from Q_A^- to Q_B is accompanied by protonation events, resulting in the formation of Q_BH_2 (for review, see Ref. 82). The resulting Q_BH_2 hydroquinone leaves the reaction center [83] (also see Ref. 84) and is replaced by an oxidized quinone from the membrane-associated quinone pool. In PS II, Q_BH_2 is believed to form and exchange analogously [33,71,76,77].

Water oxidation requires that the water-oxidizing complex accumulates a total of four oxidizing equivalents. Consequently, two plastohydroquinone molecules are formed for each O_2 molecule released by the oxidation of water. As it accumulates four oxidizing equivalents, the water-oxidizing complex cycles through a series of five oxidation states, termed S-states and designated S_n, where n denotes the number of oxidizing equivalents stored (see Fig. 2). In dark-adapted samples, the S_1 state predominates; even the S_0 state becomes oxidized to the S_1 state during prolonged (tens of minutes) dark adaptation [86–88]. The S_2 state is believed to be a transient intermediate that spontaneously reverts to the S_0 state with the concomitant

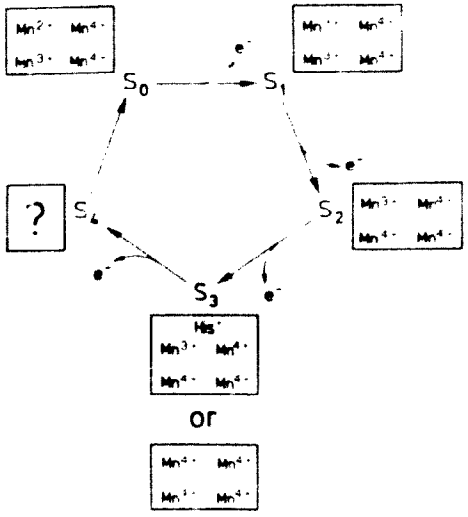

Fig. 2. The S-state cycle. Shown are the redox states of the four Mn ions in each S state consistent with most recent interpretations of X-ray absorption data (see subsection II-C.2). Whether a Mn ion or another redox active component (e.g., a histidine residue) is oxidized during the $S_1 \rightarrow S_2$ transition is currently a matter of controversy (see subsections II-C.2, II-D.1 and II-E.1). The Mn redox states in the transiently-lived S_4 state are unknown. Modified from Ref. 85.
Reprinted with permission (copyright 1991, Gauthier-Villars).

release of O_2. The oxidation of two molecules of water is generally believed to occur during the $S_3 \rightarrow (S_4) \rightarrow S_0$ transition, but this belief is not universally accepted and will be discussed in subsection II-H. The S-state model was originally formulated by Kok and co-workers [89,90] to explain why the yield of O_2 given off by chloroplasts in response to a series of light flashes oscillates with a period of four [89,91] (reviewed in Refs. 92,93). The Mn ions of the water-oxidizing complex are arranged as a multinuclear complex. The structure of the Mn complex and whether it accumulates all four oxidizing equivalents in response to the four successive charge-separations that are required for water oxidation, is currently a subject of vigorous debate and will be discussed in section II.

Both Q_A [94–97] and Q_B [98–100] interact magnetically with a nearby non-heme Fe^{2+} ion. The role of the Fe^{2+} ion is not clearly understood (for review, see Refs. 77,101). In reaction centers from purple non-sulfur bacteria, it can be replaced by Mn^{2+}, Co^{2+}, Ni^{2+}, Cu^{2+} or Zn^{2+} without changing the rate of electron transfer from Q_A to Q_B [102] (also see Refs. 103,104), even though the Fe^{2+} ion is located between the two quinones [20–22]. Even in the complete absence of a transition metal ion at the Fe^{2+} site, electron transfer from Q_A to Q_B is slowed by only a factor of 2–3 [102]. In these Fe^{2+}-depleted reaction centers, obtained from *Rhodobacter sphaeroides* R-26.1, electron transfer from $Pheo^-$ to Q_A was slowed by a factor of 20–50 [102,105] and the quantum yield of Q_A formation was diminished by 50% [105]. Conflicting data have been reported for metal-depleted reaction centers obtained from *Rhodobacter sphaeroides* strain Y, however [106] (also see Refs. 107). The non-heme Fe^{2+} ion has been extracted from PS II [108,109]. It has recently been reported that electron transfer from $Pheo^-$ to Q_A is not appreciably slowed in PS II in the absence of the Fe^{2+} ion [50]. Under special non-physiological conditions, the Fe^{2+} ion in PS II can be oxidized to Fe^{3+} [99,110,111] (for review, see Ref. 101). This oxidation has not been observed in purple non-sulfur bacteria. In reaction centers from these bacteria, the Fe^{2+} ion is coordinated by four histidine residues and one glutamate [20–22]. In PS II the non-heme Fe^{2+} ion is also believed to be coordinated by four histidine residues (e.g., see Fig. 3), but the fifth ligand may be supplied by bicarbonate [101,112,113] (for review, see Refs. 17,18,77).

In addition to Y_Z, there is a second redox-active tyrosine in PS II, known as Y_D. This component was shown to be a tyrosine residue on the basis of the specific deuteration experiments mentioned above [62–64]. Site-directed mutagenesis studies later identified Y_D as Tyr-161 of the D2 polypeptide [65,66] (in the sequence numbering system of spinach, see Fig. 3). The oxidized form of Y_D, Y_D^+, gives rise to the dark-stable EPR signal known as Signal II (reviewed in Refs. 35,62,986.). The Y_D tyrosine has no known function; cyanobacterial mutants that lack Y_D grow photoautotrophically and evolve oxygen, although at somewhat diminished rates (see discussions in Refs. 65,66). While Y_D can reduce the S_2 and S_3 states in darkness [86–88,117–122] and Y_D^+ can oxidize the S_0 state to S_1 [87,88,122], these processes take place slowly and their physiological relevance is unknown. Nevertheless, the oxidation of S_0 to S_1 by Y_D^+ has been proposed to stabilize the Mn complex during prolonged periods of darkness by oxidizing a Mn^{2+} ion that is postulated to be present in the S_0 state [87]. Recent data indicate that Y_D can be oxidized by $P680^+$ as well as by the Mn complex [122,123]. At cryogenic temperatures, Y_D^+ can be reduced by Q_A^- [119–121] and possibly by cytochrome *b*-559 [124]. It should be noted that Y_Z^+ and Y_D^+ are believed to be neutral radicals [32,62,63, 65,125,126] that form hydrogen bonds with nearby basic residues [32,65,125,126]. These basic residues have been proposed to be His-190 of the D1 and D2 polypeptides [35,65,114,116,122] (in the sequence numbering system of spinach) (see Figs. 3 and 5).

I-B. Polypeptides

I-B.1. The D1 and D2 polypeptides

The minimal oxygen-evolving PS-II complex consists of seven major polypeptides, plus one or more small

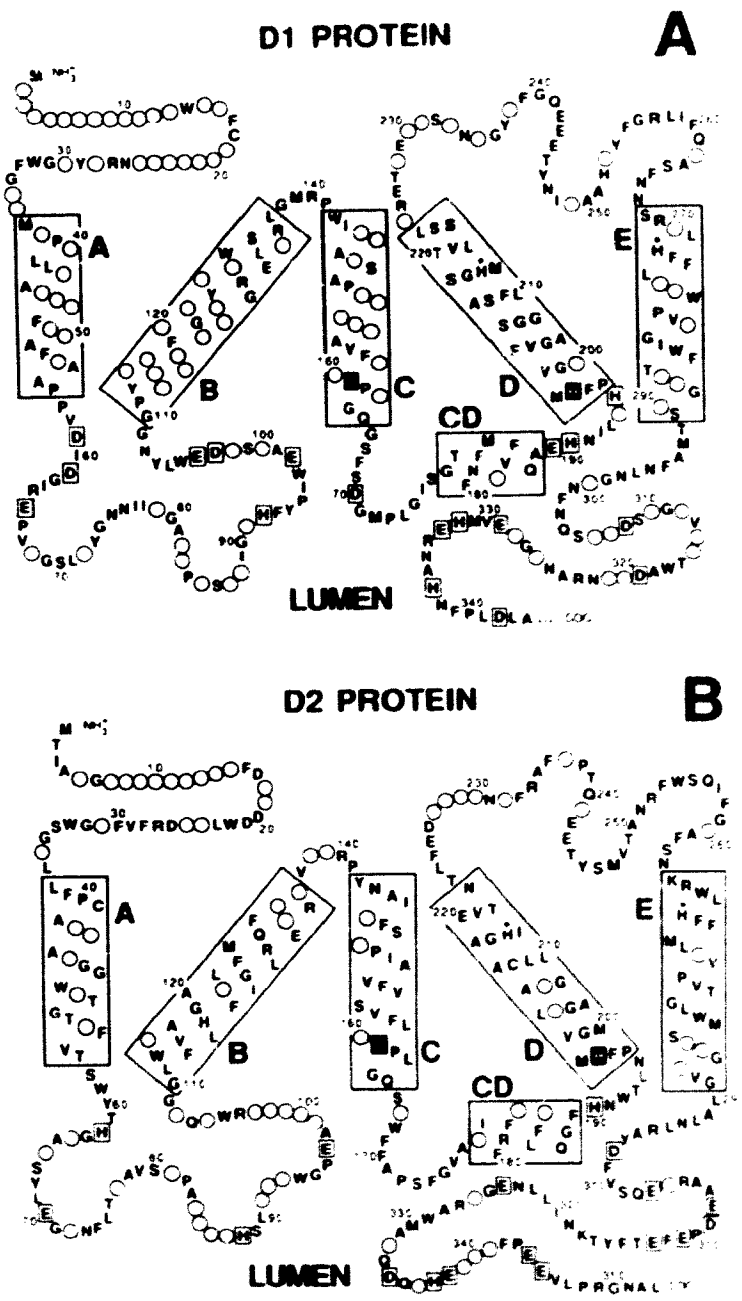

Fig. 3. The predicted folding patterns for the D1 polypeptide (A) and the D2 polypeptide (B). In both polypeptides the five predicted membrane-spanning α-helices are denoted 'A' through 'E,' while a helical domain predicted to be on the lumenal side of the membrane is denoted 'CD.' Residues conserved in 38 sequences of the D1 polypeptide and 15 sequences of the D2 polypeptide [114] are shown by their one letter symbols. The circles represent non-conserved residues. The sequence numberings correspond to those in spinach. The Y_z and Y_D tyrosine residues (Tyr-161 of D1 and D2, respectively) and the proposed histidine ligands for P680 (His 198 of both D1 and D2) are denoted by white letters on a black background. The proposed histidine ligands for the non-heme iron atom (His-215 and His-272 from D1 and His-215 and His-269 from D2) are marked with asterisks. Conserved carboxylate and histidine residues that are located on the lumenal side of the membrane are enclosed in boxes. Note that the published sequence from *Vicia faba* [115] has been determined to contain four errors: residues 13, 164, 198 and 215 are actually Glu, Glu, Asn and His, respectively (J. Hirschberg, B. Svensson and K. Ko, personal communication, 1989). The figures were kindly modified from Ref. 116 by B. Svensson and S. Styring. Reprinted with permission (copyright 1990, Oxford University Press).

polypeptides of ≤ 10 kDa (Fig. 1). However, PS-II complexes in vivo may contain at least 20 polypeptides (see Table I; for review, see Refs. 32–36,128–130). Charge separation takes place in a heterodimer of two 38–39 kDa polypeptides known as D1 and D2, which are encoded by the chloroplast *psb*A and *psb*D genes, respectively. (For a comparison of the amino-acid sequences of 38 D1 and 15 D2 polypeptides, see Ref. 131, also see Fig. 3 and Ref. 16). The sequences of these two polypeptides are highly homologous to one another and exhibit striking similarities to the sequences of the L-and M-subunits of reaction centers from purple non-sulfur bacteria. These similarities led many authors to propose that the D1 and D2 polypeptides form a core structure similar to that in the reaction centers from *Rhodopseudomonas viridis* and *Rhodobacter sphaeroides* (reviewed in Refs. 24,29). The chlorophyll, pheophytin and carotenoid contents of isolated D1/D2 complexes (isolated as a complex that included the polypeptides of cytochrome *b*-559 and the product of the *psb*I gene, see subsections I-B.3 and I-B.5) were originally reported be similar to those of bacterial reaction centers [132–134]. However, recent analyses indicate that the D1/D2 heterodimer, isolated either with [13,135–139] or without [140] the cytochrome *b*-559 polypeptides and the *psb*I gene product, contains significantly more chlorophyll and carotenoids than bacterial reaction centers. Estimates of approx. 6 chlorophyll *a* molecules per D1/D2 heterodimer (assuming that PS II contains 2 pheophytin molecules per P680 and that no chlorophyll is converted to pheophytin during isolation of the complex) [13,136–140], or 10–12 chlorophyll *a* molecules per D1/D2 heterodimer (assuming that PS II contains 2 cytochrome *b*-559 hemes per P680, see subsection I-B.3) [135] and 2 β-carotene molecules [136,137] have been reported, compared to 4 bacteriochlorophyll molecules and 1 carotenoid in bacterial reaction centers. The difference in pigment content between the D1/D2 heterodimer and bacterial reaction centers suggests that, while the latter may serve as a reasonable model for the structure of the D1/D2 complex in the vicinity of the pheophytin and quinone electron acceptors, it may not accurately reflect the structure of the D1/D2 complex near P680. Furthermore, the regions of the D1 and D2 polypeptides that are believed to protrude from the lumenal side of the thylakoid membrane contain many more residues than the corresponding

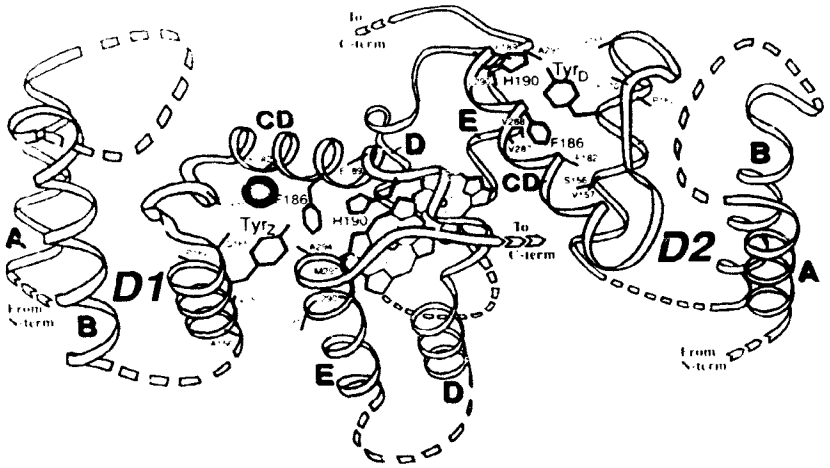

Fig. 4. A model of the donor side of the D1 and D2 polypeptides of PS II as viewed obliquely from above the lumenal surface of the thylakoid membrane. The D1 polypeptide is in the lower-left half of the figure. The sequence numberings correspond to those in spinach. The peptide backbones of the D1 and D2 polypeptides correspond to those of the L and M subunits, respectively, of the reaction center from *Rhodopseudomonas viridis* [20]. The loops connecting the A and B helices are dashed and the carboxy-terminal sequences are omitted to signify that these regions of the D1 and D2 polypeptides contain more residues than L and M polypeptides of *Rp. viridis* and that their positions are not predicted in this model. The bacteriochlorophyll dimer from *Rp. viridis* is included without modification as indicating a possible location for P680 (assuming that P680 is a dimer and is oriented the same as in *Rp. viridis*, see Ref. 127 for discussion). The side chains of Tyr-161 and His-190 have been substituted for the corresponding L and M residues and are included to show the possible locations of Y_Z (Tyr_Z) and Y_D (Tyr_D) and their proposed [35,65,114,116,122] hydrogen bond partners (for details concerning the orientation of these residues in this model, see Refs. 35,114,116). In this model, developed by B. Svensson and S. Styring, Phe-186 of the D1 polypeptide is proposed to mediate electron transfer from Y_Z to $P680^+$ [35,116] and a Mn or Ca^{2+} ion (stippled sphere) is proposed to bind to Asp-170, Gln-165 and Glu-189 of the D1 polypeptide [114]. In addition, residues 170 and 189 (phenylalanines in D2 and aspartate and glutamate, respectively, in D1) are proposed to make the lumenal end of the Y_Z cavity more hydrophilic than the lumenal end of the Y_D cavity [35,114,116]. The figure was kindly modified from Ref. 114 by B. Svensson and S. Styring. Reprinted with permission (copyright 1991 by Zeitschrift der Naturforschung).

regions of bacterial reaction centers. Nevertheless, the bacterial model for the PS-II core led to the site-directed mutagenesis studies that identified Y_Z and Y_D as specific tyrosine residues on the D1 and D2 polypeptides [65–68]. The D1 polypeptide is post-translationally cleaved between Ala-344 and residue 345 [141,142] by a 33–35 kDa processing enzyme [143–146] and is transiently palmitoylated [147]. Both D1 and D2 are phosphorylated [148–151] and *N*-acetylated [150] at their amino-terminal threonine residues following post-translational cleavage of their initiating *N*-formyl-methionine residues. It has recently been reported that the D1/D2/1/cytochrome *b*-559 complex possesses a low intrinsic serine proteinase activity [152–155] that may be involved with the light-induced turnover of the D1 polypeptide (reviewed in Refs. 35,156,157,987).

I-B.2. The CP47 and CP43 polypeptides

In addition to the D1 and D2 polypeptides, oxygen-evolving PS II complexes contain two other chlorophyll-containing polypeptides known as CP47 and CP43. These polypeptides have molecular masses of approx. 51 and 46 kDa and are encoded by the chloroplast *psb*B and *psb*C genes, respectively. (For a comparison of amino-acid sequences of CP47 and CP43 from a number of organisms, see Ref. 130, also see Refs. 15,16). The CP47, CP43, D1 and D2 polypeptides are present in a 1 : 1 : 1 : 1 stoichiometry based on the incorporation of [^{14}C]acetate [158] or [^{14}C]bicarbonate [159] into unicellular green algae. The first two [160,161] amino-acid residues of CP43 are post-translationally cleaved and the resulting amino-terminal threonine residue is *O*-phosphorylated and *N*-acetylated [150]. Both CP47 and CP43 appear to contain six transmem-

TABLE I

Photosystem II polypeptides

(a), In smallest complex shown by EPR measurements at cryogenic temperatures to carry out charge-separation; (b), in smallest complexes that evolve oxygen at high rates in vitro; (c), not in PS II; (A component of a NADH or NADPH plastoquinone oxidoreductase); (d), stabilizes the Mn complex and is required for optimal rates of oxygen evolution; (e), maintains high-affinity binding of Ca^{2+}; (f), maintains high-affinity binding of Cl^-; (g), required for normal functioning of Q_B.

Gene	Nuclear or chloroplast	Polypeptide	Location or function	Amino acids in mature polypeptide	References
*psb*A	C	D1	a,b	343	[141,142,150]
*psb*C	C	CP47	b	507	[130]
*psb*C	C	CP43	b	459	[150]
*psb*D	C	D2	a,b	352	[142,150]
*psb*E	C	cytochrome *b*-559 α	a,b	82	[195]
*psb*F	C	cytochrome *b*-559 β	a,b	43	[193]
*psb*G	C	-	c	248	[335,337]
*psb*H	C	8 kDa "phosphoprotein"	?	72 [2]	[310–312]
*psb*I	C	I	?	36	[297,299,300]
*psb*J	C	(not yet identified)	?	40	[306,307]
*psb*K	C	K	?	37	[289,295,298]
*psb*L	C	L	?	37	[296,298,300]
*psb*M	C	M [3]	?	33	[301]
*psb*N	C	N [3]	?	42	[301]
*psb*O	C	33 kDa extrinsic	b,d	248	[220,221]
*psb*P	N	24 kDa extrinsic [4]	e	180	[254,255]
*psb*Q	N	17 kDa extrinsic [4]	f	149	[255]
*psb*R	N	10 kDa extrinsic [4]	?	69	[315]
–	N	22 kDa intrinsic [4]	?	?	
–	N	28 kDa intrinsic [5]	g		
–	N	6.1 kDa [4]	?		[294,298]
–	N	5 kDa [6]	?	?	[291,298,301]
–	N	4.1 kDa	?		[298,301]

[1] Determined entirely from the nucleotide sequence of the corresponding gene.

[2] Polypeptide consists of 60–63 amino-acid residues in cyanobacteria; the N-terminal region is shorter by approx. 12 residues [289,324,325].

[3] Not yet detected in plants.

[4] Not detected in cyanobacteria.

[5] This polypeptide has been proposed to be CP29. However, the sequences attributed to CP29 in tomato [331] (284 amino-acid residues including transitpeptide) and barley [332] (286 amino-acid residues including transit polypeptide) appear to correspond to different proteins.

[6] The approx. 5 kDa polypeptide in cyanobacteria is apparently unrelated to that found in plants [301,302].

brane regions and a very large hydrophilic loop that is located on the lumenal side of the thylakoid membrane [130,162]. This loop contains approx. 190 residues in CP47 and approx. 130 residues in CP43 [130] (see loops 'E' in Fig. 5). Both CP47 and CP43 are believed to serve as tightly-bound light-harvesting antennae, but may have other functions that remain undetermined (for review, see Ref. 130). It has recently been proposed that CP43 may possess an intrinsic serine proteinase activity that cleaves the D1 polypeptide following photoinhibitory treatments [163]. PS II complexes that are depleted of CP43 (and which consequently contain CP47, D1, D2, cytochrome *b*-559 and the product of the *psb*I gene) have been estimated to contain 30–34 chlorophyll *a* molecules per P680 based on their contents of cytochrome *b*-559 [135,164] or photoreducible Q_A [165] (see also Ref. 166). However, similar complexes have been reported to contain only 17–18 chlorophylls based on the assumption that PS II contains only two molecules of pheophytin [134,137,167]. Also, some oxygen-evolving PS II complexes (whose constituent polypeptides include CP47, CP43, D1 and D2) have been reported to contain as few as 31–35 chlorophylls per P680 based on the amount of photoreducible Q_A present [13,168]. Consequently, CP47 has been estimated to contain 19–26 [135,165] or 10–13 [137,167] chlorophyll *a* molecules. The CP43 polypeptide has been estimated to contain 10–12 [167] or approx. 15 chlorophyll *a* molecules [165].

The CP47 polypeptide appears to be required for the stable assembly of PS II complexes: neither D1 nor D2 accumulates in thylakoid membranes of the cyanobacterium *Synechocystis* sp. PCC 6803 when the *psb*B gene is inactivated [169]. The CP47 polypeptide also appears to be required for Q_A and Y_Z to function normally. Indirect evidence indicates that PS II preparations that have been stripped of CP47 can photoreduce added quinones [170–172], possibly with high quantum efficiency [173–175]. However, there is little direct evidence that photoreduction of quinones takes place at the Q_A site in D1/D2/I/cytochrome *b*-559 complexes. Such evidence, as outlined in Ref. 176, should include flash-induced optical absorption changes in the ultraviolet that can be unambiguously attributed to Q_A [177–179], the flash-induced formation of C550 (an electrochromic blue-shift of a pheophytin *a* absorption band near 545 nm that is caused by the formation of Q_A^- [177,180]) and light-saturation of Q_A^- formation as the intensity of the flashes is increased. When quinones bind to non-Q_A sites, light saturation is not achieved [176]. Flash-induced absorption changes in the ultraviolet have recently been reported for D1/D2/I/cytochrome *b*-559 complexes incubated with dibromothymoquinone (DBMIB) [181], but they differ from those previously attributed to Q_A^- [177–179], no C550 was detected and no light-saturation studies were reported. It seems likely that the Q_A site is altered or absent in the absence of CP47. In PS II complexes that contain CP47 and CP43, the specificity of the Q_A site for quinones [108,176,182] appears to be more stringent than in reaction centers from purple non-sulfur bacteria [183]. There is no direct evidence for the formation of Y_Z^+ in the D1/D2/I/cytochrome *b*-559 complexes [184] (also see Ref. 185), although a 5 μs

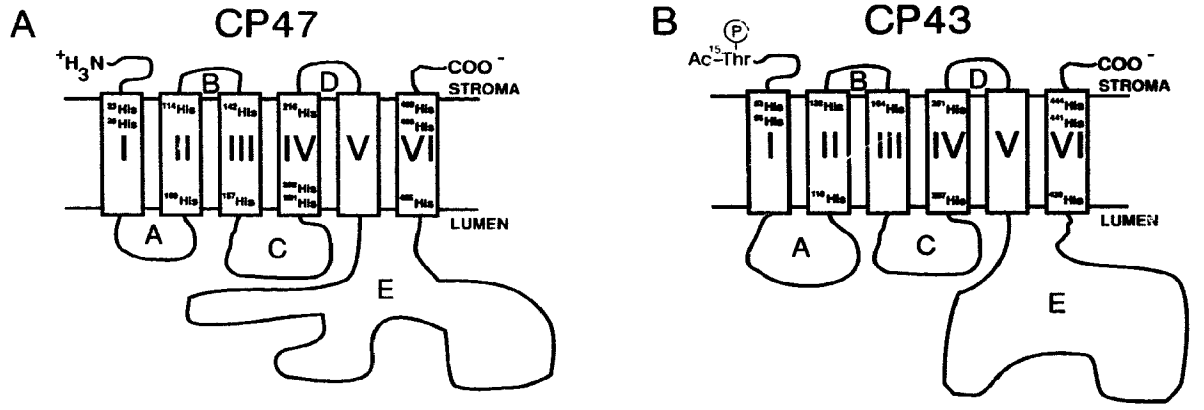

Fig. 5. The predicted folding patterns for the CP47 polypeptide (A) and the CP43 polypeptide (B). In both polypeptides, the six predicted membrane-spanning α-helices are denoted 'I' through 'VI.' Extrinsic hydrophilic loops are denoted 'A' through 'E.' The approximate locations of conserved histidine residues are shown (note that His-430 of CP43 is not conserved in *Synechococcus* sp. PCC 7942 (also known as *Anacystis nidulans* R2) [130,160], where it is a proline). In the sequence numbering shown for CP43, the start codon occurs at position 13 [160,161]. The large approx. 190 residue loop 'E' of CP47 has been proposed to extend approximately from residue 257 to residue 450 [130]. The large approx. 130 residue loop 'E' of CP43 has been proposed to extend approximately from residues 292 to 426 [130] or from residues 280 to 412 [884]. Figures kindly provided by T.M. Bricker.

phase in the kinetics of reduction of $P680^+$ observed in one such complex has been attributed to electron donation by Y_Z [173].

The CP43 polypeptide can be readily removed from PS II preparations that lack the extrinsic 33, 24 and 17 kDa polypeptides (see subsection I-B.4) by treatment with chaotropic agents [135,166,186] or with detergents [134,187,188]. EPR signals that resemble tyrosine radicals have been generated in some of the resulting preparations [184,189]. These have been attributed to Y_Z^+ and/or Y_D^+ [184,189]. However, whether these preparations contain [166,187,188] or lack [134,184] photoreducible Q_A has been disputed. Recently, however, both the photoreduction of Q_A and the photooxidation of Y_Z have been demonstrated to proceed with normal quantum efficiencies in PS II complexes that were isolated from mutants of the cyanobacterium *Synechocystis* sp. PCC 6803 that lack *psb*C and hence that lack CP43 [165]. The earlier dispute over Q_A function may have resulted from the concurrent extraction of Q_A or from partial denaturation of the complex during removal of CP43 (see discussions in Ref. 165,190), or from the concurrent removal of one or more small polypeptides [138] (see subsection I-B.5). Electron transfer from Q_A^- to Q_B is slowed [165] and specific binding of the herbicide DCMU is absent [191] in the CP43-less PS II complexes isolated from the *Synechocystis* mutants. The CP43 polypeptide may facilitate the assembly of PS II: cells and thylakoid membranes of *Synechocystis* 6803 accumulate partially functional PS II complexes at only approx. 10% of wild-type levels when the *psb*C gene (which encodes CP43) is inactivated or deleted [165,169]. Similar complexes have been detected in mutants of *Chlamydomonas reinhardtii* that are unable to synthesize CP43 [192].

I-B.3. Cytochrome b-559

Oxygen-evolving PS II complexes also contain polypeptides of approx. 9 kDa and approx. 4 kDa which coordinate the heme of cytochrome *b*-559. These polypeptides are present in a 1 : 1 stoichiometry [193]. They are known as the α- and β-polypeptides and are encoded by the chloroplast *psb*E and *psb*F genes, respectively. (For a comparison of amino-acid sequences of the α-and β-polypeptides from a number of organisms, see Ref. 194, also see Refs. 15,16). Both polypeptides have a single membrane-spanning region [193,195]. The α-polypeptide is oriented with its carboxy-terminus on the lumenal side of the thylakoid membrane [196–198]. Based on preliminary data, the β-polypeptide has been proposed to be oriented similarly [199]. The cytochrome has been proposed to be a heterodimer of the α- and β-polypeptides [193,200]. The α- and β-polypeptides each contain a single histidine residue [193,195], whereas the cytochrome *b*-559 heme is coordinated by two histidine residues [201]. Consequently, if cytochrome *b*-559 consists of an $(\alpha\beta)$ heterodimer, a parallel orientation of the α- and β-polypeptides would require that the heme be located near the stromal edge of the thylakoid membrane [196–199]. However, in a recent preliminary report, the carboxy-terminus of the a subunit was linked to the amino-terminus of the β subunit by fusing the *psb*E and *psb*F genes of the cyanobacterium *Synechocystis* sp. PCC 6803 [18]. In the resulting mutant, PS II activity was not severely impaired [18]. Because the α- and β-polypeptides in the mutant are expected to be oriented antiparallel to one another, the histidine residues implicated in coordinating the heme in the $(\alpha\beta)$ heterodimer model would be located on opposite edges of the thylakoid membrane. However, the cytochrome *b*-559 content of the mutant was reported to be similar to that of wild-type cells [18]. On the basis of this result, it was suggested that cytochrome *b*-559 may consist of $(\alpha)_2$ and $(\beta)_2$ homodimers, with each homodimer coordinating one heme [18]. In this model, one heme would be located near the stromal edge of the thylakoid membrane and one heme would be located near the lumenal edge [18].

It is currently controversial whether PS II complexes contain one [13,137,167,202,203] or two [12,204–209] cytochrome *b*-559 per P680 in vivo. (For a recent review of this controversy, see Ref. 203, for earlier discussions, see Refs. 135,200,202.) The analyses of the *psb*E–*psb*F fusion mutant described in the preceding paragraph, if confirmed, could severely impact this controversy.

The redox potential of cytochrome *b*-559 is heterogeneous (reviewed in Ref. 210 and see Ref. 211). In intact, oxygen-evolving PS II centers, the cytochrome is predominantly in a high potential form and is reduced in dark-adapted samples [210,211]. Removal of the extrinsic 24 and 17 kDa extrinsic polypeptides, despite the apparent proximity of the cytochrome heme to the opposite side of the thylakoid membrane in the $(\alpha\beta)$ heterodimer model, causes a substantial decrease in the cytochrome's redox potential, resulting in the oxidation of the cytochrome in dark-adapted samples [207,211–214]. In intact PS-II centers, the heme is oxidized at low quantum yield [215] by $P680^+$ via a chlorophyll monomer [216] (also see Ref. 123). It is rereduced by the plastoquinone pool [217], reportedly via the Q_B site [215]. The function of cytochrome *b*-559 is unknown; several proposals for its function have appeared [200,210,215,216,218,219] (for review, see Refs. 199,200).

I-B.4. The 33, 24 and 17 kDa extrinsic polypeptides

The seventh major polypeptide in oxygen-evolving PS-II complexes is an extrinsic polypeptide of 33 kDa. It has recently been determined to be present in a 1 : 1

stoichiometry with CP47 based on cross-linking studies that measured the degree of cross-linking as the amount of the cross-linking reagent was increased [222] (earlier estimates had yielded 1 [205,223], 2 [224,225] or 1–3 [226] 33 kDa polypeptides per P680). The 33 kDa polypeptide protects the Mn complex and maintains it in a configuration that optimizes the catalytic efficiency of water oxidation. It is encoded by the recently renamed [14] nuclear *psb*O gene, previously known as *psb*1, *eee*1 or *wox*A. (For comparisons of amino-acid sequences from a number of organisms, see Refs. 227,228, also see Ref. 16). The 33 kDa polypeptide contains one intrachain disulfide bond that is located in the interior of the protein and is essential for maintaining the protein's conformation and ability to rebind to PS II preparations [229,230]. The 33 kDa polypeptide binds directly to the intrinsic polypeptides and its binding is stabilized by the Mn complex [231–234]. Carboxylate residues from the 33 kDa polypeptide have been suggested to be involved in binding [235]. These residues appear to be in the polypeptide's amino-terminal domain: removal of 16 to 18 residues from the amino-terminus prevents the 33 kDa polypeptide from binding without disrupting its overall conformation [236]. A 15 kDa fragment of the 33 kDa polypeptide remains attached to PS II membranes that have been treated with trypsin at pH < 7.25 and sustains the functional activity of the Mn complex [237]. It was not ascertained whether this fragment was from the amino-terminal domain. The 33 kDa polypeptide can be readily released from PS II by treatment of samples with 0.8 M Tris at pH 8.0–8.2 [238–241], 0.7 M NaSCN [223], 1 M $CaCl_2$ or $MgCl_2$ [232,242,243], or high concentrations of urea [223,244–246]. (Most of these treatments fail to remove the 33 kDa polypeptide from PS II particles of the cyanobacterium *Phormidium laminosum*, however [247]). Most of these treatments concurrently extract manganese (also see subsection II-A.2), but treatment with 2.6 M urea in the presence of 0.2 M Cl^- [246,248] or with 1 M $CaCl_2$ or $MgCl_2$ [232,242,243,248] leaves the Mn cluster intact (see subsection II-J.1). However, if samples that have been depleted of the 33 kDa polypeptide are not maintained in high concentrations of Cl^- (> 100 mM), two Mn ions become paramagnetically uncoupled [249,250] and are slowly released [232,245,246,251–253]. For further discussion of the effects of removing the 33 kDa polypeptide, see subsection II-J.1.

Two other extrinsic polypeptides of 24 and 17 kDa are also associated with oxygen-evolving PS II preparations. They are the products of the recently renamed [14] nuclear *psb*P and *psb*Q genes, respectively. (For a comparison of amino-acid sequences of the 24 kDa polypeptide from a number of organisms, see Ref. 256, also see Ref. 16). The 24 and 17 kDa polypeptides are present in a 1:1:1 stoichiometry with the 33 kDa polypeptide [205,223,226]. They can be readily released from PS II by washing samples with 1–2 M NaCl [223,240,241,257,258]. The 17 kDa polypeptide can be completely released (along with approx. 35% of the 24 kDa polypeptide) by 60 mM $MgCl_2$ or $CaCl_2$ [259]. In the absence of the 24 and 17 kDa polypeptides, high rates of oxygen evolution can only be obtained in the presence of high concentrations of Ca^{2+} [260–262] and Cl^- [262–265] (for review, see Refs. 33,34,37,38,128, 266–270). The 24 kDa polypeptide enhances the binding of at least one Ca^{2+} ion to its functional site in PS II (see section III-A), while the 17 kDa polypeptide has been reported to enhance the binding of Cl^- to PS II [264,265]. Such a role for the 17 kDa polypeptide has been disputed, however [259,263]. The manganese complex becomes susceptible to attack by exogenous reductants when the 24 and 17 kDa polypeptides are removed [231,259,271–277]. This protection appears to be provided specifically by the 24 kDa polypeptide [259].

The binding of the 24 and 17 kDa polypeptides is stabilized by the manganese complex [234,278,279] and appears to involve their amino-terminal domains [280,281]. The 24 kDa polypeptide appears to bind to a site created by conformational changes that are caused by the binding of the 33 kDa polypeptide [233]. Cross-linking of the 24 kDa polypeptide with the 33 kDa polypeptide has been reported [282]. Similarly, the 17 kDa polypeptide appears to bind to a site created by conformational changes that are caused by the binding of the 24 kDa polypeptide [233]. Crosslinking of the 17 kDa polypeptide with the 24 kDa polypeptide has been reported [283]. It is not known whether the 24 and 17 kDa polypeptides bind directly to the intrinsic polypeptides or to sites on the 33 and/or 24 kDa polypeptides. However, a specific interaction between the 24 kDa polypeptide and CP43 has been suggested based on the accumulation of the 24 kDa polypeptide in stacked regions of the thylakoid membrane in the presence, but not in the absence, of the CP43 polypeptide in mutants of the alga *Chlamydomonas reinhardtii* [192]. Neither the 24 kDa nor the 17 kDa polypeptide appears to be present in cyanobacteria [168,247,284–290].

I-B.5. Small polypeptides

In addition to the major polypeptides described above, several small polypeptides (3–7 kDa) are also associated with oxygen-evolving PS II preparations [289,291–303] (Table I). Their functions are unknown (for review, see Ref. 16,18,302,304). One of these polypeptides, the approx. 4.8 kDa product of the chloroplast *psb*I gene, copurifies with the D1/D2/cytochrome *b*-559 complex [293,297,299,300]. It appears to have one membrane-spanning hydrophobic domain and a hydrophilic carboxy-terminal region that contains

several acidic and basic residues [297,299]. Its stoichiometry in relation to the α and β kDa polypeptides of cytochrome *b*-559 has been estimated to be 1:1:1 based on SDS-PAGE profiles that were stained with Coomassie blue [293,297]. A recent dissociation/reconstitution study suggests that one or two additional small polypeptides may be required for the photoreduction of Q_A to proceed with normal quantum efficiency [138]. The authors of this study propose that the approx. 5 kDa product of the chloroplast *psb*L gene [296,298,300] and/or a nuclearly-encoded 4.1 kDa polypeptide [293,298] (also see Ref. 301) are the required polypeptides. However, the band assigned to the 4.1 kDa polypeptide in the published SDS-PAGE profiles appears to be present in substantial amounts in all of the authors' preparations that contain quinone [138], including those that are incapable of photoreducing Q_A with high quantum efficiency. Furthermore, several polypeptides appear to comigrate with the band assigned to the *psb*L polypeptide [138]. Consequently, further work will be required to substantiate the proposed involvement of either the 4.1 kDa polypeptide or the *psb*L product in Q_A function. The *psb*L gene is cotranscribed with the *psb*E and *psb*F genes that encode the α and β polypeptides of cytochrome *b*-559 [194,296,305,306] and its product has been reported to be more tightly associated with the D1/D2 heterodimer in cyanobacteria than in higher plants [300]. The product of the *psb*L gene may be essential for the assembly of PS II: the deletion of the *psb*L gene from the cyanobacterium *Synechocystis* sp. PCC 6803 is reported to abolish PS II function [18]. The *psb*J gene is cotranscribed with *psb*E, *psb*F and *psb*L [194,296,305,306], but no polypeptide that corresponds to this gene has yet been reported. However, a mutant of *Synechocystis* 6803 that should be unable to synthesize the *psb*J product grows photoautotrophically and evolves oxygen, although at somewhat diminished rates [308]. This result suggests that the *psb*J product may influence PS II function [308]. Two approx. 4.7 kDa polypeptides that correspond to the chloroplast *psb*M and *psb*N genes have been found in PS II complexes isolated from the cyanobacterium *Synechococcus vulcanus* [301,302], but no corresponding polypeptides have yet been detected in higher plants. Additional nuclear encoded polypeptides of 6.1 kDa [294,298] and approx. 5 kDa [291,298] have been detected in PS II membranes from spinach and wheat. The 6.1 kDa polypeptide is not essential for oxygen evolution [293] and does not appear to be present in cyanobacteria [289,300–302]. Although a approx. 5 kDa polypeptide has been detected in oxygen-evolving PS II complexes from the cyanobacterium *Synechococcus vulcanus*, it appears to be unrelated to the approx. 5 kDa polypeptide detected in plants [301,302].

An approx. 3.9 kDa polypeptide that is associated with oxygen-evolving PS-II complexes is encoded by the chloroplast *psb*K gene [289,295,298,309]. The polypeptide's amino-terminus is post-translationally cleaved [295,298,309] to yield a product that is believed to be have its amino-terminus exposed on the lumenal side of the thylakoid membrane [289,309]. This polypeptide is not essential for oxygen evolution because it can be removed during isolation of oxygen-evolving PS-II complexes [295] and because mutants of *Synechocystis* sp. PCC 6803 that lack the *psb*K gene grow photoautotrophically and evolve oxygen, although at somewhat diminished rates [309]. Interestingly, the addition of glucose to these *Synechocystis* mutants does not restore their growth rates to wild-type levels [309]. Consequently, the *psb*K product has been suggested to influence some process unrelated to PS II in addition to being required for maximal rates of oxygen evolution [309].

I-B.6. Other polypeptides

Polypeptides of approx. 8 kDa (the product of the chloroplast *psb*H gene) [16,44,298,310–312], approx. 10 kDa (the product of the nuclear *psb*R gene) [16,298,313–316] and approx. 22 kDa (a nuclear gene product) [313,314] are also associated with isolated PS II complexes. The functions of these polypeptides are unknown. They have been removed biochemically [8,9,12,128,129,314] or, in the case of the *psb*R product, by inhibiting translation with anti-sense RNA [317], without severely disrupting oxygen evolution. Deletion of the *psb*H gene from *Synechocystis* sp. PCC 6803 does not abolish photoautotrophic growth at low light intensities (5 μE $m^{-2}s^{-1}$), but prevents photoautotrophic growth at high light intensities (S.R. Mayes, Z.H. Zhang and J. Barber, cited in Ref. 18). The approx. 10 kDa *psb*R product is not required for the 24 kDa extrinsic polypeptide to bind to the PS-II core complex [318], in contrast to an earlier report [314]. In contrast to a preliminary report [128] the approx. 22 polypeptide is not required for Q_B to function normally [129,319,320]. However, Q_A appears to become more exposed to exogenous oxidants in the absence of both the approx. 22 kDa and the approx. 10 kDa *psb*R polypeptides [129,319,320]. The approx. 10 kDa *psb*R product does not appear to be present in cyanobacteria [168,284,286–289,301,302,314,321]. The approx. 22 kDa polypeptide has been reported to be present in the cyanobacterium *Synechocystis* sp. PCC 6803 [321]. In higher plants [322] and in the alga *Chlamydomonas reinhardtii* [323] the *psb*H product is phosphorylated near its amino-terminus at a threonine residue. The *psb*H product does not appear to be phosphorylated in cyanobacteria [289,324]. In both *Synechococcus vulcanus* [289] and *Synechocystis* sp. PCC 6803 [324,325] the *psb*H product lacks the first 12 amino-acid residues found in plants and *Chlamydomonas*, including the

threonine residue that is phosphorylated in eukaryotic organisms.

An additional chlorophyll-containing polypeptide of approx. 28 kDa is required for Q_B to function normally [129,319,320]. In the absence of this polypeptide, herbicide-sensitive electron transfer from Q_A to Q_B is disrupted. Q_A becomes more easily oxidized by exogenous agents and the magnetic coupling between Q_A and the non-heme Fe^{2+} becomes disrupted [129,319,320]. Some of these alterations are reminiscent of those caused by the removal of the H-subunit from bacterial reaction centers [326], although whether the similarities have any evolutionary significance is not known. The stability of Y_D^+ appears to be diminished in the absence of the 28 kDa polypeptide [319,320], suggesting that this polypeptide may influence the donor side of PS II as well as the acceptor side. It has been reported that the 28 kDa polypeptide can be crosslinked to CP47 in samples that lack the extrinsic 33 kDa polypeptide [980]. The 28 kDa polypeptide has been proposed to be the light-harvesting chlorophyll *a*/*b*-containing polypeptide known as CP29 [327–330]. However, there appears to be some confusion over the identity of CP29. The sequences that have been attributed to CP29 in tomato [331] and barley [332] appear to correspond to different proteins; one of these has been suggested to be CP26, another LHCII polypeptide [332]. It has also been reported that CP29 consists of two non-identical polypeptides of approx. 26 and 28 kDa [988].

An extrinsic approx. 9 kDa polypeptide has been proposed to be essential for water oxidation in the cyanobacterium *Phormidium laminosum*: its loss from PS II particles correlated with the loss of oxygen evolution [333,334] and its subsequent reconstitution restored oxygen evolution [334]. This polypeptide also appears to be present in PS II particles from the cyanobacterium *Synechococcus vulcanus*, although it has a molecular mass of approx. 12 kDa in this organism [290]. The two polypeptides share extensive sequence homologies in their amino-terminal regions [290]. The approx. 9 kDa polypeptide can be extracted from *Phormidium laminosum* PS II particles by treatment with 0.8 M Tris (pH 8.5), 1 M NaCl, $CaCl_2$ or $MgCl_2$, or by incubation in the presence of low concentrations of glycerol [247,333,334]. The approx. 12 kDa polypeptide can be extracted from *Synechococcus vulcanus* PS II particles by treatment with 1 M Tris (pH 8.5) or 1 M $CaCl_2$ [290]. The same treatments remove an additional approx. 17 kDa polypeptide from *Synechococcus vulcanus* PS II particles. It is attributed to cytochrome c-550 [290], a cytochrome that has been found in other cyanobacteria and in a red alga (see discussion in Ref. 290).

A 24–28 kDa polypeptide that was originally found in PS II-enriched membranes and whose chloroplast-encoded gene was labeled *psbG* [335] has since been shown to be unrelated to PS II and has been proposed to be a component of a NADH or NADPH plastoquinone oxidoreductase [336,337].

II. Manganese

II-A. General considerations

II-A.1. Stoichiometry

A requirement for Mn in photosynthetic water oxidation has long been known (for early reviews, see Refs. 93,338,339). On the basis of atomic absorption measurements or EPR quantifications of Mn^{2+} ions released by HCl, numerous workers have concluded that active (oxygen-evolving) PS II complexes contain four Mn ions per P680 [8,10,11,209,241,271,284,286, 340–344]. Determining the Mn content of active PS-II centers requires accurate quantification of active PS-II centers. In early studies, active PS II centers were quantified on the basis of O_2-flash-yield measurements [340,345]. These flash-yield measurements gave estimates of the chlorophyll/P680 stoichiometry in chloroplasts. These or similar estimates were used in subsequent determinations of the Mn content of active PS-II centers [284,341,346]. In some studies, chlorophyll/P680 stoichiometries relative to those in chloroplasts were estimated from the rise kinetics of O_2 evolution [346] or variable fluorescence [284] produced by a weak or modulated light beam. In preparations of isolated PS II particles, quantifications of PS-II centers generally have been based on quantifications of $P680^+$ [342, 346], Q_A^- [8,10,11,286,342,344] or Y_D^+ [209,241,271,343]. However, these determinations can be challenged on grounds that quantification of $P680^+$, Q_A^- or Y_D^+ does not necessarily quantify oxygen-evolving PS-II centers [347]. The measured Mn/PS II stoichiometries would have underestimated the Mn content of active centers if the analyzed samples contained inactive centers that could form $P680^+$, Q_A^- or Y_D^+, but lacked Mn. Based on quantifications of active PS-II centers in purified PS II particles by O_2 flash yield measurements, Pauly and Witt recently proposed that active PS-II centers contain six Mn ions per P680, rather than four [347]. These authors argue that PS II preparations previously analyzed for Mn content contained significant fractions of Mn-deficient inactive centers. If this was true, it should be possible to photoaccumulate significant quantities of Y_Z^+ in such preparations; however, this does not appear to be the case (e.g., Refs. 2,209,342). Photoaccumulation of Y_Z^+ in such preparations requires the removal of Mn (e.g., Refs. 2,209,342,348) or the inhibition of S-state turnover (e.g., see subsection III-C). An alternate explanation for the data of Pauly and Witt is that their samples contained significant fractions of inactive PS-II centers that contained residual Mn ions.

Even the most active samples analyzed by Pauly and Witt contained no more than approx. 50% active PS-II centers [347]. If any of the inactive centers contained Mn ions, the measured stoichiometry would have overestimated the Mn content of active centers. In appreciation of this fact, Pauly and Witt also examined samples that had been partially depleted of Mn. They concluded that their inactive PS-II centers contained no Mn ions [347]. Their argument was based on plotting the Mn content of active centers as a function of the fraction of active centers present in samples depleted of varying amounts of Mn [347]. The data were fit with a horizontal line signifying 6 Mn ions per active PS II complex in all Mn-depleted samples. However, because no samples containing more than approx. 50% active centers were examined, the data can easily be fit by a line that extrapolates to four Mn ions per center in samples that contain no inactive centers (see Fig. 4 of Ref. 347). No independent corroborating data (e.g., charge recombination assays) were presented. Consequently, the conclusion that the inactive centers contained no Mn ions may not be valid. The reinvestigation of the Mn content of active PS-II centers by Pauly and Witt should be repeated with samples that contain larger fractions of active centers. Such samples should be characterized by EPR and charge recombination assays in addition to O_2 flash yield measurements.

II-A.2. Extraction

All but 0.4–0.8 Mn can be released from PS II concomitant with the loss of the 33, 24 and 17 kDa polypeptides by treatment of samples with 0.8 M Tris at pH 8.0–8.5 [223,240,349,350] (also see subsection I-B.4), with 0.7 M NaSCN [223], or with 2 mM La^{3+} in the presence of reducing agents [39]. Similar amounts of Mn can be released if reducing agents are added to samples depleted of the 24 and 17 kDa polypeptides [231,273]. More complete release of Mn has been reported in samples that were treated with 1.0 M Tris in the presence of 0.5 M $MgCl_2$ [351,352], or in samples that were treated with 1 mM NH_2OH following removal of the 24 and 17 kDa polypeptides [353]. Not all treatments to extract Mn release the 33, 24 and 17 kDa polypeptides. Treatment of intact PS II membranes with 5 mM NH_2OH releases all but 0.1–0.4 Mn concomitant with the loss of only approx. 5% of the 33 kDa polypeptide and 25–40% of the 24 and 17 kDa polypeptides [272,349,350,354]. One pair of Mn ions appears to be more weakly bound than the other: as mentioned in subsection I-B.4, if samples that have been depleted of the 33 kDa polypeptide are not maintained in high concentrations of Cl^- (> 100 mM), two Mn ions are slowly released [232,245,246,251–253].

II-A.3. Binding and photoactivation

Assembly of the functional Mn complex requires light. This process is known as 'photoactivation' and has a very low quantum yield (estimated to be approx. 0.01 [355]). During assembly of the Mn tetramer, a stable intermediate is formed by two light-dependent steps that are separated by a light-independent step [93,357–360]. This sequence of light-dark-light events is believed to correspond to (i) photooxidation of a ligated Mn^{2+} ion to form a ligated mononuclear Mn^{3+} intermediate, (ii) ligation of a second Mn^{2+} ion to form a binuclear Mn^{3+}-Mn^{2+} intermediate and (iii) photooxidation of the second Mn^{2+} ion to form a stable Mn^{3+}-Mn^{3+} complex [349,350,354,359,361,362]. The mononuclear Mn^{3+} and binuclear Mn^{3+}–Mn^{2+} intermediates are very unstable [349,354,359,361–363], with the former being less stable than the latter. Charge recombination between Q_A^- or Q_B^- and the ligated Mn^{3+} ion has recently been shown to account for much of the instability [363], confirming earlier indications [349,353,362]. Reduction of the Mn^{3+} ion by exogenous reductants also contributes to the instability of the intermediates [353,359,361,363,364]. The instability of the two intermediates largely explains the low quantum yield of the overall photoactivation process. In addition, the photooxidation of the second Mn^{2+} ion may occur with a low quantum efficiency [350,365], which would also contribute to the low overall yield of photoactivation. The photooxidation of the first Mn^{2+} ion occurs with high quantum efficiency [366–368,981]). The conversion of the mononuclear Mn^{3+} intermediate to the binuclear Mn^{3+}–Mn^{2+} intermediate is believed to be the rate-limiting step in the photoactivation process [349,354] and is believed to be accompanied by conformational rearrangements of the PS-II core polypeptides [3–9,359,362]. These conformational rearrangements change the susceptibility of the ligated Mn^{3+} to exogenous reductants [359,361,362] and may facilitate the binding of the second Mn^{2+} ion [349,359,362]. Once the stable binuclear Mn^{3+}–Mn^{3+} complex is formed, the spontaneous light-independent coordination of two further Mn^{2+} ions is believed to complete the assembly of the Mn tetramer [349,350, 354,361,362]. This second pair of Mn^{2+} ions may correspond to the more weakly bound pair that was noted in the preceding paragraph. Activation of the Mn tetramer requires calcium [349,369–375] and 1–2 Ca^{2+} ions are believed to bind near the Mn complex after it is assembled [349,354,362,375]. At least one Ca^{2+} site appears to be created during the assembly of the Mn complex [362]. Chloride ions are also required for functional assembly of the Mn complex [364,376]. For recent discussions of the optimal conditions for photoactivation of PS II membranes or particles, see [353,363,364,377].

Two binding sites for Mn^{2+} in Mn-depleted PS II preparations have been reported. One of these has a K_m of 0.4–2 μM, as estimated from steady-state assays of Mn^{2+}-supported electron transfer in the presence of

H_2O_2 [378–380] and estimated from single-turnover assays of the reduction of Y_Z^+ by Mn^{2+} [367,368,981] (also see Ref. 366). Smaller apparent K_m (or K_d) values (< 0.2 μM), estimated by some workers on the basis of steady-state assays [352,381], probably reflect the slow dissociation of a Mn^{2+} ion from the same site (see discussions in Refs. 354,365,981). This Mn^{2+} site is presumably the first Mn site occupied during the photoactivation process [354,365,368,382]. A second Mn^{2+} site, having a K_d estimated to be 40–50 μM, has been inferred from studies of the kinetics of photoactivation [354,371]. This site has been proposed to be the second Mn site occupied during the photoactivation process [354] (also see discussions in Refs. 365,382). Essentially the same K_d value was estimated from a study demonstrating that Mn^{2+} slows the rate of electron transfer from Y_Z to $P680^+$ in Mn-depleted preparations [382]. It was proposed that the binding of Mn^{2+} to the tightly-binding Mn site has no net electrostatic influence on the rate of electron transfer from Y_Z to $P680^+$, while the binding of Mn^{2+} to the weaker site electrostatically retards this rate [382]. As pointed out by the authors [382], this proposal seems remarkable. Because the reduction of Y_Z^+ by Mn^{2+} in the tightly-binding site is quite rapid [366–368], this site is expected to be located closer to Y_Z than the weaker binding Mn site. It might be expected, therefore, that Mn^{2+} in the tightly-binding site would have a greater electrostatic influence on electron transfer from Y_Z to $P680^+$ than Mn^{2+} in the weaker site, but just the opposite is proposed [382]. The proposal may have implications for the location of the two Mn sites relative to the positions of P680 and Y_Z. Electrostatic interactions are believed to account for the slower rate of electron transfer from Y_Z to $P680^+$ in intact PS II preparations when the water oxidizing complex is in the S_2 or S_3 states (see subsection II-D.2). Such interactions are also believed to account for the pH-dependence of this rate in Mn-depleted PS II preparations [383,384].

The Mn complex has long been assumed to accumulate the oxidizing equivalents that correspond to the S-state transitions and to serve as the catalytic site of water oxidation (e.g., see Refs. 93,338,339). Evaluation of these assumptions has been achieved over the past decade on the basis of EPR, X-ray aosorption and optical absorption measurements.

II-B. EPR studies

II-B.1. The multiline and g = 4.1 EPR signals

Two EPR signals have been attributed to the Mn complex in the S_2 state. These signals, observable only at temperatures < 35 K, are known as the 'multiline' and 'g = 4.1' signals (for recent reviews, see Refs. 38,85,385–389). The multiline signal was first observed in samples that had been rapidly frozen following a flash given at room temperature [390–392]. This signal is centered at $g = 1.982 \pm 0.002$ [393,394] and has a linewidth of 1500–1800 Gauss. At X-band (9.1–9.4 GHz), the signal exhibits 18–20 partially resolved hyperfine lines that are spaced by 85–90 Gauss and are often superimposed on a broad Gaussian-shaped signal near $g = 2$ (see Fig. 6A). At high resolution, these hyperfine lines have numerous small peaks and shoulders superimposed (e.g., see Refs. 395–398). At S band (3.9 GHz), the multiline signal exhibits 40–50 hyperfine lines, with most being separated by 20–25 Gauss [399,400] (see Fig. 7). The signal has also been examined at Q-band (34 GHz) [393,394]. The orientation-

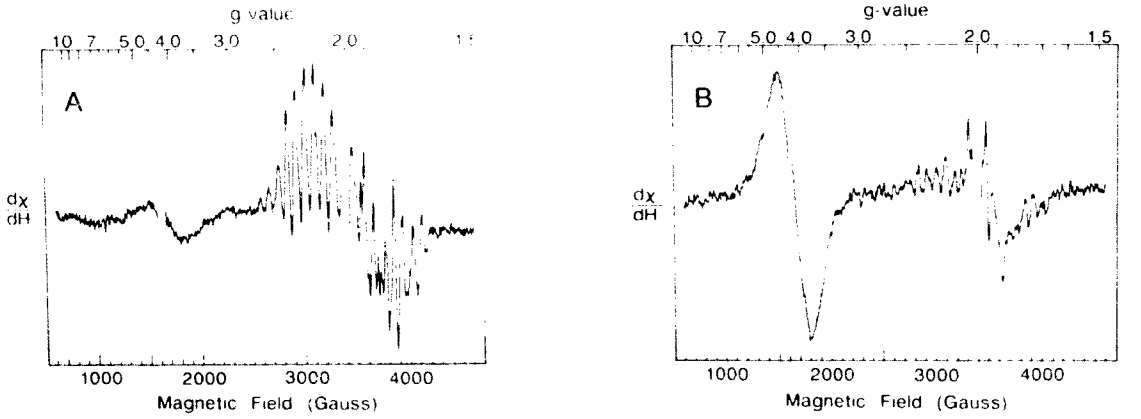

Fig. 6. The multiline (A) and g = 4.1 (B) EPR signals observed in PS II membranes illuminated at 195 K in the presence of 0.4 M sucrose. (A) Sample contained 5% ethanol to suppress formation of the g = 4.1 signal. (B) Sample contained 50 mM F^- to enhance the g = 4.1 signal at the expense of the multiline signal. Spectra represent the difference between spectra recorded after and before illumination and were recorded at 8 K. The microwave frequency was 9.50 GHz. The narrow signal of Y_D^+ near g = 2 and a subtraction artifact near g = 4.3 caused by the presence of adventitious rhombic Fe^{3+} in the preparations have been omitted for clarity. Figures kindly provided by R.D. Britt.

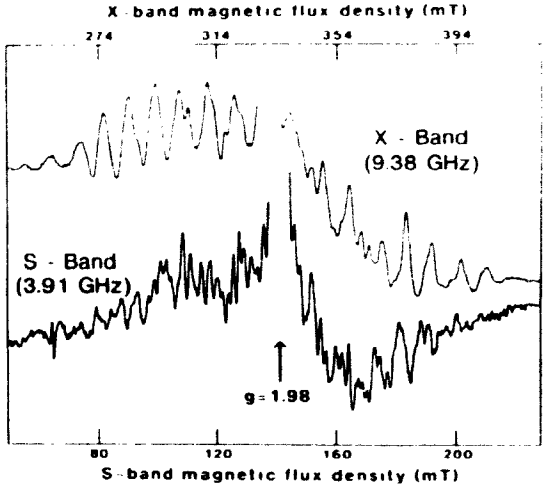

Fig. 7. Comparison of multiline EPR signals recorded at X-band (top spectrum) and at S-band (bottom spectrum). Isolated PS II particles in 0.4 M sucrose were illuminated at 200 K in the presence of 2% ethanol and 100 μM DCMU. The spectra represent the difference between spectra recorded after and before illumination and were recorded at 12 K (top) or 15 K (bottom). The central portion of each spectrum, containing the narrow signal of Y_D^{ox}, has been omitted for clarity. Modified from Ref. 399. Reprinted with permission (copyright 1989 by the American Chemical Society)

dependence of the multiline signal has been examined at both X-band [401,402] and S-band [399,400]. Significant anisotropy was observed, particularly at S-band and was attributed primarily to hyperfine anisotropy. This anisotropy explains the many small peaks and shoulders that are superimposed on the main hyperfine lines in unoriented samples.

The amplitude of the multiline signal oscillates with a period of four in response to a series of flashes given before freezing [390,391,403,404]. Because its amplitude is maximal following the first and fifth flashes, the signal was attributed to the S_2 state [391,403,404]. This assignment was confirmed by studies of the signal's rate of decay and temperature-dependence of formation [392,395,403]. The signal can also be generated by continuous illumination under conditions that limit PS II to a single charge separation (illumination at 160–200 K [392,395], or while simultaneously freezing to 77 K in the presence of DCMU [405]). Because the multiline signal, with its many hyperfine lines, resembled the EPR spectrum of a synthetic mixed-valent dinuclear Mn compound [406] (also see Ref. 407) and because the signal was abolished by treatments that extract Mn [391,405], the signal was originally proposed to arise from an $S = 1/2$ magnetic ground state of either an exchange-coupled Mn(III)$_2$-Mn(IV) tetramer [391,408] or a Mn(II)-Mn(III) or Mn(III)-Mn(IV) dimer [405,409,410]. More recent models will be discussed below. The flash-induced periodicity of the amplitude of the multiline signal has been interpreted as demonstrating that Mn is oxidized during the S-state transitions. This interpretation is supported by X-ray absorption measurements that correlate the formation of the multiline signal with the oxidation of Mn during the $S_1 \rightarrow S_2$ transition [343,411,412] (see subsection II-C.2). The multiline signal has been observed in PS II preparations from several species of cyanobacteria [209,342,343,413–415] and displays a similar temperature-dependence [414], response to NH_3 [414,415] and response to Sr^{2+} after Ca^{2+}-depletion [415], compared to its properties in preparations from higher plants (see below and subsection II-G.1).

The $g = 4.1$ signal has a width of 320–360 Gauss and lacks resolved hyperfine structure (see Fig. 6B). It has essentially the same appearance at S-band as at X-band [400,416]. The signal was first observed in samples that were continuously illuminated at 140 K, a temperature lower than that required for generation of the multiline signal [417]. It was also observed in samples illuminated at 200 K in the presence of sucrose [403]. In samples not containing sucrose, the $g = 4.1$ signal was shown to convert into the multiline signal when samples that had been illuminated at 140 K were subsequently warmed in darkness [208,417,418]. Like the multiline signal, the $g = 4.1$ signal was shown to be abolished by treatments that remove Mn [403,417] and a correlation between its formation and the oxidation of Mn was demonstrated by X-ray absorption measurements [412,419]. Although the $g = 4.1$ signal lacks resolved hyperfine structure, it has been suggested to have underlying hyperfine structure [416] because the signal is not appreciably narrower at S-band than at X-band [400,416]. Indeed, at least 16 partially resolved hyperfine lines, spaced by approx. 36 Gauss, have been observed on the $g = 4.1$ signal in oriented PS II membranes that had been treated with NH_3 [402,420] (see Fig. 8). The $g = 4.1$ signal has not been observed in samples depleted of the extrinsic 24 and 17 kDa polypeptides [214,421] unless these samples have been supplemented with Sr^{2+} [421]. The $g = 4.1$ signal has also not been observed in Ca^{2+}-depleted samples that retain the 24 and 17 kDa polypeptides [422–424] unless these samples have been supplemented with Sr^{2+} [422]. Reconstitution of these samples with Ca^{2+} does not restore the $g = 4.1$ signal [422–424].

The $g = 4.1$ signal has not yet been reported in any PS II preparation from a cyanobacterium (e.g., Refs. 343,415). Its absence probably does not reflect the apparent lack of the 24 and 17 kDa polypeptides in cyanobacteria, however. Without these polypeptides, PS II membranes from spinach oxidize a chlorophyll molecule when illuminated at 130–200 K [214]. In contrast, a PS II preparation from the cyanobacterium

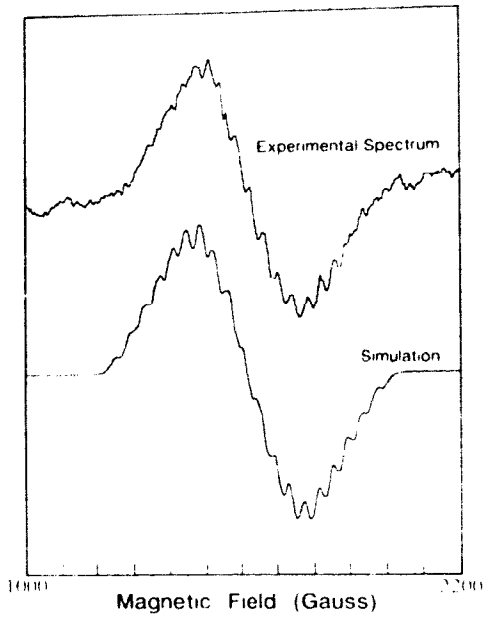

Fig. 8. Ammonia modified $g = 4.1$ EPR signal observed in oriented PS II membranes (top spectrum). The membrane normal was oriented parallel to the applied magnetic field. The PS II membranes were treated with 100 mM NH_4Cl at pH 7.5 in the presence of 0.4 M sucrose and were oriented by drying them onto mylar films. The signal was generated by illumination at 195 K. The spectrum represents the difference between the spectrum recorded after and before illumination and was recorded at 8 K. The bottom spectrum shows a simulation of the experimental spectrum calculated assuming that the experimental spectrum arises from a tetranuclear Mn cluster that has a ground state of $S = 3/2$. Modified from Ref. 402. Reprinted with permission (copyright 1992 by the American Chemical Society).

Synechococcus elongatus (formerly known as *Synechococcus* sp. [425]) was shown by X-ray absorption measurements to have oxidized the Mn complex when illuminated at 140 K, although no $g = 4.1$ signal was observed [343]. Consequently, a reason other than the apparent lack of the 24 and 17 kDa polypeptides must be responsible for the absence of the $g = 4.1$ signal in this cyanobacterial preparation. It should be noted, however, that only one systematic search for the $g = 4.1$ signal in a cyanobacterial preparation has been reported [343] and that the glycerol that was employed in this study as a cryoprotectant (and reported to be necessary for the observation of the multiline signal) may have prevented the $g = 4.1$ signal from being observed [426] (see below).

The $g = 4.1$ signal was originally attributed to an electron transfer intermediate between Mn and $P680^+$ [403,417]. However, because it was found to be a precursor of only the multiline signal and not of the S_3 state [208] and because its amplitude was found to oscillate with a period of four in response to a series of flashes given before illumination and to be maximal following the first and fifth flashes [426], it was subsequently assigned to an alternate form of the S_2 state [208,418,426,492]. The form of the S_2 state that exhibits the $g = 4.1$ signal has been reported to recombine with Q_A^- more rapidly than the form that exhibits the multiline signal [426].

The two forms of the S_2 state that give rise to the multiline and $g = 4.1$ signals have been proposed to be linked by an equilibrium [394,426–428] that is influenced by many factors [428]. Indeed, the relative amplitudes of the two signals are sensitive to a variety of treatments. For example, the choice of cryoprotectant is critical. Both signals are observed in samples illuminated at approx. 200 K in the presence of 0.4 M sucrose [418,426], but a smaller $g = 4.1$ signal is observed in the absence of cryoprotectant [429] and little or none is observed in the presence of 30% ethylene glycol [418,426] or 50% glycerol [426], or when 4–6% ethanol [393,394,416,426,430] (see Fig. 6A) or 3% methanol [431] is added to samples that contain 0.4 M sucrose. The amplitude of the $g = 4.1$ signal has been reported to be increased relative to that of the multiline signal when Ca^{2+} is replaced by Sr^{2+} [421,422,432], when samples are depleted of Cl^- in the presence of SO_4^{2-} [428,433,434], when Cl^- is replaced by F^- [417,428,434] (see Fig. 6B), NO_3^- [434] or I^- [434], or when samples are treated with NH_3 [427–429,435,436] (even in the presence of 4% ethanol [402]) or methylamine [428]. In contrast, the amplitude of the $g = 4.1$ signal has been reported to be diminished when Cl^- is replaced by Br^- [428,434]. Because NH_3 [437–439], methylamine [439] and F^- [439] compete for a Cl^- site on Mn (see subsection II-G.1), it has been suggested that the conversion of the $g = 4.1$ to the multiline form of the S_2 state involves the binding of Cl^- [38,85,428], even at temperatures as low as 160 K [38]. Because the amplitude of the $g = 4.1$ signal is increased both by the presence of sucrose and by the depletion of Cl^-, sucrose has been proposed to interfere with the binding of Cl^- to PS II [428].

Many of the treatments just described alter the linewidths of the multiline and $g = 4.1$ signals. For example, subtle changes in the hyperfine structure of the multiline signal have been observed depending on whether sucrose, ethylene glycol, ethanol or methanol is present [393,394,400,418,426,431]. The widths of the component lines of ENDOR spectra of the multiline signal are also influenced by whether sucrose, glycerol, or ethylene glycol is present [440,441]. The addition of 4–5% ethanol to samples that contain 0.4 M sucrose has been reported to shift the positions of the hyperfine lines of the multiline signal at S-band [400], to narrow the hyperfine lines of the signal at X-band, allowing additional structure to be resolved [393,394,426] and to make the signal easier to saturate

[394,426]. The addition of 3% methanol to samples containing 0.4 M sucrose has recently been reported to eliminate the broad Gaussian-shaped signal that appears to underlie the multiline signal [431]. Treatment with NH_3 in the presence of sucrose [436,442], or in the absence of cryoprotectant [429], has been reported to shift the $g = 4.1$ signal to g approx. 4.2 and to narrow the signal to approx. 300 Gauss (also see Ref. 402). This treatment also induces the resolution of at least 16 hyperfine lines on the $g = 4.1$ signal in oriented samples [402,420] (Fig. 8), as mentioned earlier. Substitution of F^- for Cl^- has been reported to narrow the $g = 4.1$ signal by approx. 10% [417] (see Fig. 6B). Treatment with NH_3 also alters the multiline signal. The NH_3-altered signal has more lines (21–22 vs. 18–20) and smaller hyperfine splittings (67.5 vs. 87.5 Gauss) than the unmodified signal [414,415,427–429,436,442–446] (see Fig. 9). This NH_3-induced alteration of the multiline signal was originally reported to require illumination at 0°C [443] or incubation at temperatures near 0°C following illumination at 195 K [427,444,446], but has more recently been reported to occur with a halftime of approx. 15 min when samples

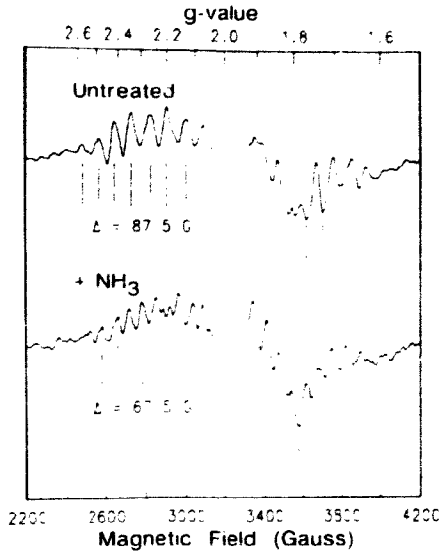

Fig. 9. Comparison of normal (top spectrum) and NH_4Cl-modified (bottom spectrum) multiline EPR signals observed in PS II membranes. Samples in 30% (v/v) ethylene glycol were illuminated at 0°C in the presence of 250 μM 2,5-dichloro-*p*-benzoquinone and 50 μM DCMU in the absence (top spectrum) or presence (bottom spectrum) of 100 mM NH_4Cl before being frozen to 77 K. Spectra represent the difference between spectra recorded after and before illumination and were recorded at 8 K. The vertical lines show the positions of the hyperfine lines. The average spacing between lines in each spectrum is indicated by Δ. The central portion of each spectrum, containing the narrow signal of $Y_D^{\cdot}$, has been omitted for clarity. Modified from Ref. 443. Reprinted with permission (copyright 1986 by the American Chemical Society).

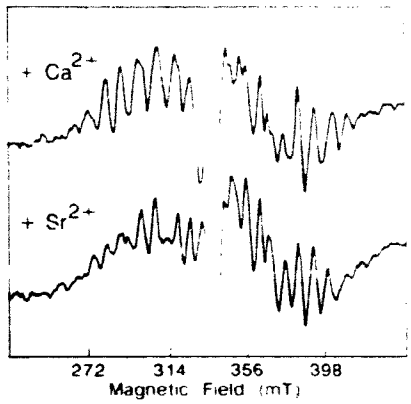

Fig. 10. Comparison of normal (top spectrum) and Sr^{2+}-modified (bottom spectrum) multiline EPR signals observed in PS II membranes. Samples were depleted of Ca^{2+} with 1.2 M NaCl and 50 μM EGTA at pH 6.5 during illumination, then were reconstituted with either 20 mM $CaCl_2$ (top spectrum) or 20 mM $SrCl_2$ (bottom spectrum). The samples were illuminated at 200 K. The samples were not reconstituted with the 24 and 17 kDa polypeptides and no cryoprotectant was added. The spectra represent the difference between spectra recorded after and before illumination and were recorded at 10 K. The right half of each trace has been shifted upward. The central portion of each spectrum, containing the narrow signal of $Y_D^{\cdot}$, has been omitted for clarity. Modified from Ref. 421. Reprinted with permission (copyright 1988 by the American Chemical Society).

are incubated at 198 K following illumination at 188 K [429]. Substituting Sr^{2+} for Ca^{2+} also alters the multiline signal [415,421,422,432] (see Fig. 10). The Sr^{2+}-modified signal superficially resembles the NH_3-modified signal (compare Figs. 9 and 10). Depletion of Ca^{2+} under some conditions results in another altered multiline signal that exhibits approx. 26 hyperfine lines spaced by 55–65 Gauss and that is stable in darkness [423,447–456] (see below). The interaction of NH_3 and other amines with PS II will be discussed in greater detail in subsection II-G.1. The hyperfine lines of the multiline signal have been reported to be broadened by $H_2^{17}O$ [436,457] and to be narrowed by ^2H_2O [458], although two other groups have been unable to reproduce the narrowing reportedly caused by ^2H_2O [396,399]. The lineshape of the multiline signal is also influenced by the length of time that the sample is dark-adapted before the S_2 state is formed [459,460].

The multiline and $g = 4.1$ signals have been proposed to represent the only forms of the S_2 state [428]. This may be incorrect. While the amplitude of the $g = 4.1$ signal has been reported to be enhanced at the expense of the multiline signal in samples that were depleted of Cl^- in the presence of ethylene glycol [428], the amplitude of the $g = 4.1$ signal has been reported to be diminished by 5–20% concurrent with loss of the multiline signal in samples depleted of Cl^- in the presence of sucrose [433,434]. Moreover, substi-

tution of Br^- for Cl^- in the presence of sucrose has been reported to diminish the amplitude of the $g = 4.1$ signal by approx. 30% without significantly increasing the amplitude of the multiline signal [434], while substitution of Br^- for Cl^- in the presence of sucrose plus 4% ethanol (added to inhibit the formation of the $g = 4.1$ signal), has been reported to diminish the amplitude of the multiline signal by approx. 30% [461]. Finally, the substitution of NO_3^- for Cl^- has been reported to only slightly enhance the $g = 4.1$ signal [434] while nearly abolishing the multiline signal [434,461]. The decrease in the amplitudes of the multiline signal observed in some Br^-- and NO_3^--substituted samples has been at least partially attributed to g-strain broadening [461]. Nevertheless, the frequently reported absence of a complementary relationship between the amplitudes of the multiline and $g = 4.1$ signals suggests that there may be other forms of the S_2 state that exhibit EPR spectra with features that are too broad to be recognizable. Broadened, unrecognizable EPR signals have previously been attributed to the S_2 state in Ca^{2+}-depleted [404,421,432] and Cl^--depleted [433] samples (see subsections III-C and III-D). Such signals have also been invoked to explain why no $g = 4.1$ or other Mn EPR signal is observed when PS-II preparations from *Synechococcus elongatus* are illuminated at 140 K, or are warmed to 215 K after being illuminated at 140 K, despite the appearance of the $Q_A Fe^{2+}$ signal and despite the X-ray absorption data showing that the Mn complex was oxidized in these samples [343]. It should be noted, however, that determining the absolute amounts of the multiline and $g = 4.1$ signals present in samples poised in the S_2 state may be complicated by difficulties associated with quantifying the amount of the S_2 state present. The amount of the S_2 state produced during illumination is generally determined from the amplitude of the EPR spectrum of the $Q_A Fe^{2+}$ complex at $g = 1.8$–1.9 [208]. However, this signal is very broad, extending over several thousand Gauss [462] and its intensity at $g = 1.8$–1.9 can be greatly influenced by sample conditions [97,462–464] (for review, see Refs. 386,465). For example, the amplitude of the $Q_A Fe^{2+}$ signal at $g = 1.9$ has been reported to increase 2-fold in the presence of some herbicides [463] and by more than 12-fold in the presence of formate [464].

The $g = 4.1$ signal has been proposed to arise from an inactive form of the Mn complex that is unable to advance to the S_3 state [428]. This proposal was based on reports that the depletion of Cl^- blocks the $S_2 \rightarrow S_3$ transition [433,466–470] (however, see below and see subsection III-D) and on observations that the depletion of Cl^- (in the presence of SO_4^{2-}) enhances the $g = 4.1$ signal relative to the multiline signal [428,433,434]. Because F^- [417,428], NH_3 [427–429,435,436] and methylamine [428] inhibit steady-state oxygen evolution and enhance the $g = 4.1$ signal relative to the multiline signal, inhibitory anions and small primary amines were proposed to inhibit steady-state oxygen evolution by favoring an 'inactive' conformation of the Mn complex [428]. However, recent data contradict this proposal. Neither steady-state oxygen evolution nor O_2 flash yields were affected when the relative proportions of the multiline and $g = 4.1$ signals were varied by the addition of ethanol [430]. Furthermore, while substitution of NO_3^- for Cl^- enhances the $g = 4.1$ EPR signal and almost completely abolishes the multiline signal [434] (and see Ref. 461), only the $S_3 \rightarrow (S_4) \rightarrow S_0$ transition appears to be slowed [471] and the rate of steady-state oxygen evolution compared to untreated samples remains as high as 40–75% [434,461, 472,473]. Finally, new evidence suggests that the depletion of Cl^- in the presence of SO_4^{2-} may not block the $S_2 \rightarrow S_3$ transition (see below and see subsection III-D).

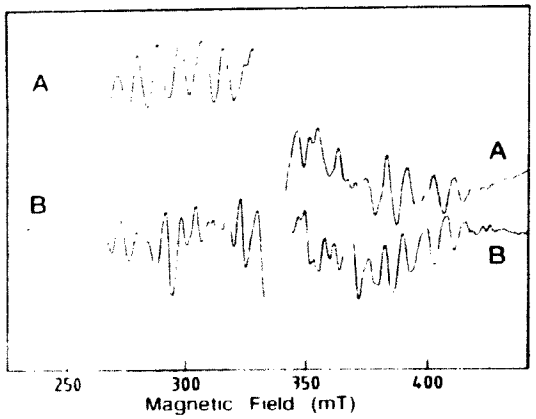

Fig. 11. Normal (A) and dark-stable (B) multiline EPR signals observed in Ca^{2+}-depleted PS II membranes. Samples were depleted of Ca^{2+} with 1.2 M NaCl and 50 μM EGTA at pH 6.5 during illumination. The samples were not reconstituted with the 24 and 17 kDa polypeptides. (A) Sample was illuminated at 198 K in the presence of 10 mM EGTA. (B) Sample was illuminated at 0°C for 2 min in the presence of 10 mM EGTA and then incubated in darkness at 0°C for 60 min before the spectrum was recorded. Spectra represent the difference between spectra recorded after and before illumination and were recorded at 10 K. The central portion of each spectrum, containing the narrow signal of $Y_D^{\bullet}$, has been omitted for clarity. Modified from Ref. 454.

Recently, an altered form of the multiline signal, having at least 26 hyperfine lines spaced by 55–65 Gauss, has been reported in spinach PS II membranes depleted of Ca^{2+} either by washing with 1–2 M NaCl and 1–20 mM EDTA or EGTA at pH 6.5 in the presence of light [447,449,453,454,456], or by incubation with 10–20 mM sodium citrate at pH 3 in darkness [423,424,448,450,455,456,982] (M.J. Latimer, V.J. DeRose, V.K. Yachandra, I. Mukerji, K. Sauer and M.P. Klein, personal communication) (See Fig. 11). The new signal has been attributed to a modified form

of the S_2 state and is stable in darkness for many hours. The extrinsic 24 and 17 kDa polypeptides are retained during some of these Ca^{2+} extraction procedures [423,447,448,450], but not during others [449,453,454]. Consequently, the presence of neither polypeptide is required for generation of the signal (also see the discussion in Ref. 454 and see Ref. 456), but their presence has been reported to influence the observed hyperfine pattern to a small extent [454]. When the 24 and 17 kDa polypeptides are absent, the addition of Ca^{2+} rapidly converts the altered multiline signal into the normal signal [449,453]. When these polypeptides are present, the addition of Ca^{2+} appears to restore the normal S_2 state much more slowly than it decays [447]. This may reflect the 24 and 17 kDa polypeptides acting as apparent diffusion barriers to Ca^{2+} rebinding in darkness, as has been demonstrated previously [274,474–476] (see subsection III-C). However, the presence of these polypeptides does not prevent added Ca^{2+} from rapidly deactivating the modified S_3 state [447]. This observation agrees with reports that binding and dissociation of Ca^{2+} occurs most readily in the S_3 state [447,477] and may support suggestions that structural changes accompany the $S_2 \rightarrow S_3$ transition [427,429,443,477–479] (for review, see Refs. 38,387 and subsections II-G.1 and II-H).

Generation of the altered multiline signal requires illumination at temperatures near 0°C [423,424,450, 454]. These temperatures are approx. 70°C higher than the temperatures that are sufficient for generation of the normal multiline signal in untreated samples [208,417,418]. In samples incubated with sodium citrate at pH 3 in darkness, the half-inhibition temperature of the altered signal was determined to be 240–250 K [423,424,450], close to that for the $S_2 \rightarrow S_3$ transition in untreated samples [480–482]. In samples washed with NaCl and high concentrations of chelating agents during illumination [447,449,452–454,456], the altered signal is generated during the Ca^{2+}-depletion process. However, when the altered signal in these samples was allowed to decay by an approx. 48 hour incubation in darkness at 0°C, regeneration of the signal required illumination at temperatures near 0°C [454].

Generation of the altered signal also requires the presence of high concentrations of chelating agents (at least 0.2 mM EDTA [453]). If samples are depleted of Ca^{2+} by treatment with only 50 μM EGTA, only the normal multiline signal, with normal stability characteristics, can be generated [421,454]. The altered signal can be produced following the subsequent addition of 10 mM EGTA or 40 mM citrate, but only after the samples are illuminated at 0°C; illumination at 198 K generates only the normal signal [454]. On the basis of these observations, the properties of the altered multiline signal have been proposed to result from the direct ligation of Mn by EGTA, EDTA, or citrate [454], in agreement with earlier suggestions [37,447,449]. Flexible poly-carboxylic acids appear to be required because the altered signal could not be produced in the presence of either acetate or rigid poly-carboxylic acids such as phthalic acid or terephthalic acid [454].

The amplitude of the altered signal has been reported to be maximal when samples are illuminated under conditions that permit the achievement and subsequent deactivation of an apparent S_3 state (e.g., illumination in the absence of DCMU) [454] (also see Ref. 982). This may explain the relatively small amplitudes of the altered multiline signals reported in some studies [423,448,450]. Consequently, the susceptibility of the Mn complex to ligation by flexible poly-carboxylic acids has been proposed to be greatest in the S_3 state, much less in the S_2 state and minimal in the S_1 state [454]. Assuming that chelators gain access to the Mn via the vacant Ca^{2+} site, this proposal also agrees with the previous indications [447,477] that the Ca site is most accessible in the S_3 state [454,982] (see subsection III-A). Because the presence of 200 mM sodium acetate did not lead to generation of the altered signal [454], it is unlikely that the properties of this signal are significantly influenced by occupancy of a Ca^{2+} site by Na^+, as was previously suggested [37,447]. The properties of the altered multiline signal will be further discussed in subsection III-C.

No dark-stable altered multiline signal was detected in an earlier study of Ca^{2+}-depleted PS II membranes that were prepared by methods similar to those described above [483]. Interestingly, 20% glycerol was employed as a cryoprotectant in this study [483], whereas 0.3–0.4 M sucrose has been employed as a cryoprotectant in all studies that have reported the altered multiline signal. Because the choice of cryoprotectant influences the properties of the normal multiline and $g = 4.1$ signals (see above), it might be worthwhile to investigate whether effects of cryoprotectants influence the properties of the altered multiline signal in Ca^{2+}-depleted samples.

II-B.2. The 130–160 Gauss wide EPR signal

Three groups have reported that the altered multiline signal disappears upon either flash or continuous illumination at temperatures near 0°C [447,448,451, 452,454–456,484]. It is replaced by a signal centered at $g = 2.004$ that has a linewidth of approx. 164 Gauss in the presence of the 24 and 17 kDa polypeptides [447, 448,451,452,455,456,484] (see Fig. 12) and 130–140 Gauss in their absence [454,485]. Unlike the modified multiline signal, generation of the 130–164 Gauss-wide signal does not require high concentrations of chelating agents because it can be observed in samples washed with NaCl in the presence of only 50 μM EGTA [454]. However, one group has recently reported that only a small amount of this signal is produced when only 50

μM EGTA is present [456]. Although the signal was originally reported to have a near-Gaussian lineshape [447,448,451], it was later reported to be a doublet [452] (Fig. 12) and more recently has been reported to have a more complex structure [485]. The earlier near-Gaussian spectra have been attributed to a superpositioning of the approx. 130 Gauss and approx. 164 Gauss forms of the signal [454]. This signal has been proposed to arise from an oxidized organic component that is magnetically coupled to the S_2-state Mn complex [447,448,452,454,484–487]. The signal has been attributed to a modified form of the S_3 state [447,448,452,454,485–487]. Alternatively, it has been suggested to arise from an interaction between Y_Z^+ and the modified S_2-state Mn complex, possibly as a result of a perturbation of the Mn complex caused by Y_Z^+ [456]. This 'S_3' or 'S_2-plus-radical' state has been reported to have a considerably longer lifetime in the presence of the 24 and 17 kDa polypeptides than in their absence [454]. From a determination of the optical absorption changes in the ultraviolet that accompany the formation of the approx. 164 Gauss-wide signal, the oxidized species has been proposed to be a histidine radical [452] (see Fig. 13), although this assignment has been disputed [456] (see subsection II-F.1). Models of the magnetic coupling between the putative histidine radical and the Mn complex suggest that the radical does not directly ligate Mn [452,454,484,486]. To account for the absence of an EPR signal from the S_3 state in untreated samples, it has been proposed that the radical is located closer to the Mn in the untreated system, so that its spectrum is broadened beyond recognition [452,484,486]. Whether the 130–164 Gauss-wide signal represents an altered form of the S_3 state [447,448,452,454,486], a precursor of the S_3 state [453], an organic radical formed (reversibly) because the normal oxidation of Mn is blocked [453], or an interaction between Y_Z^+ and the modified S_2-state Mn complex [456], remains unknown and will be discussed further in subsection II-F.1. The addition of NH_3 to Ca^{2+}-depleted samples that lack the 24 and 17 kDa polypeptides narrows the signal to approx. 100 Gauss [485]. In Ca^{2+}-depleted PS II particles isolated from the cyanobacterium *Synechocystis* sp. PCC 6803, the signal of the 'S_2-plus-radical' state has been reported to have a linewidth of < 90 Gauss [415].

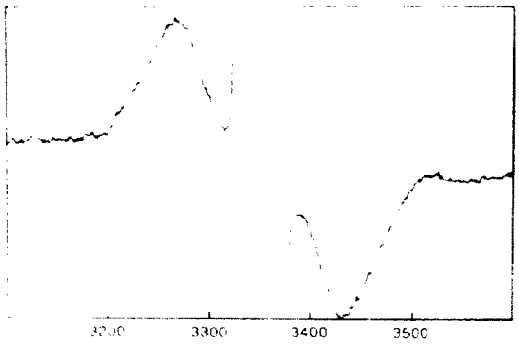

Fig. 12. The approx. 164 Gauss-wide EPR signal observed in Ca^{2+}-depleted PS II membranes that had been reconstituted with the 24 and 17 kDa polypeptides. Sample was depleted of Ca^{2+} with 1.2 M NaCl and 20 mM EGTA at pH 6.5 during illumination. The signal was generated by flash illumination at 20°C, followed by rapid freezing in darkness. The spectrum represents the difference between spectra recorded after and before illumination and was recorded at 15 K. The central portion of the spectrum, containing the narrow signal of Y_D^+, has been omitted for clarity. Modified from Ref. 85. Reprinted with permission (copyright 1991, Gauthier-Villars).

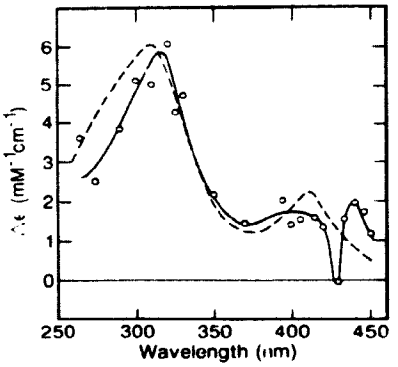

Fig. 13. Optical absorption spectrum induced by flash illumination of Ca^{2+}-depleted PS II membranes that had been poised in the dark-stable S_2 state before illumination (circles and solid line) in comparison to the in vitro spectrum of a [histidine-OH] radical (dashed line). PS II membranes were depleted of Ca^{2+} with 1.2 M NaCl and 20 mM EGTA at pH 6.5 during illumination and were subsequently reconstituted with the 24 and 17 kDa polypeptides. Modified from Ref. 452. Reprinted with permission (copyright 1990 by Macmillan Magazines Ltd.).

A fourth group has reported that a broad EPR signal at $g = 2$ is induced by illumination of NaCl/EDTA-washed spinach PS II membranes, but without the loss of the altered multiline signal [453]. This $g = 2$ signal was also postulated to arise from an oxidized histidine residue, but the signal was not well characterized, its linewidth was not reported and the possibility of magnetic coupling with the Mn complex was not considered [453]. The observation of both the altered multiline signal and the 130–164 Gauss-wide signals in the same samples [453] conflicts with the work described in the preceding paragraph. The reasons for the discrepancy are unknown. However, the 24 and 17 kDa polypeptides were absent from the samples examined by in this group [453]. Because the state that gives rise to the approx. 164 Gauss signal has been reported to be much less stable in the absence of these polypeptides than in their presence [454], the spectra reported in Ref. 453 may reflect a combination of

spectra from PS-II centers in the S_2 and 'S_2-plus-radical' states.

The loss of the altered multiline signal in parallel with the formation of the 130–164 Gauss-wide signal has been attributed to the same magnetic coupling that gives rise to the latter signal [447,452,484]. Spectral simulations have been advanced to support this view [452]. However, in a recent study, when samples exhibiting the approx. 164 Gauss-wide signal were stored at 77 K for one week, about 50% of this signal decayed whereas no parallel formation of the altered multiline signal was detected [456]. When these samples were subsequently illuminated at 8–77 K, the approx. 164 Gauss-wide signal was immediately restored. Ordinarily, no formation of this signal is detected when samples are illuminated at 200 K [447]. Furthermore, the ability to regenerate this signal was lost when samples that had been stored at 77 K for one week were incubated at 200 K for 15 min before being illuminated at 77 K [456]. These results suggest that a structural change involving the manganese cluster accompanies the oxidation of the organic component that gives rise to the 130–160 Gauss-wide signal and that the concurrent loss of the altered multiline signal may be caused by this structural change rather than by magnetic coupling to the oxidized radical [456]. Conformational rearrangements of the manganese complex are believed to accompany the S-state transitions [427,443, 477–479], even at temperatures as low as 198 K [429] (for review, see Refs. 38,387 and subsections II-G.1 and II-H).

A new EPR signal centered at g approx. 2 and having a linewidth of 160 ± 20 Gauss [486] or < 90 Gauss [487] was recently reported in spinach PS II membranes depleted of Cl^- in the presence of SO_4^{2-} [486,487] and in samples inhibited with F^- [486]. These signals resemble the 130–164 Gauss-wide signal observed in Ca^{2+}-depleted samples. They have also been attributed to a magnetic interaction between an organic radical and the S_2-state Mn complex and have also been referred to as a modified form of the S_3 state [486,487]. Similar signals with linewidths ≤ 100 Gauss have recently been reported in samples treated with NH_3 [456,485]. A similar signal was previously reported in NH_2OH-treated samples illuminated at 200 K, even after treatment with Tris to extract the Mn complex (see subsection II-A) [488]. This signal was attributed to an unidentified component associated with the acceptor side of PS II [488]. A similar signal, reported near $g \approx 2.1$ in NH_2OH-treated samples, was attributed to a modified form of the signal from $Q_A^- Fe^{2+}$ [489,490], although this assignment has been questioned [386,456]. It has been suggested that the signals observed in Ca^{2+}-depleted, Cl^--depleted, F^--inhibited, NH_3-treated and NH_2OH-treated samples all arise from the same interaction between an organic radical and the S_2-state Mn complex [456]. The relationship between Ca^{2+}-depletion, Cl^--depletion, F^--treatment, NH_3-treatment and the 90–164 Gauss-wide EPR signals will be further discussed in subsection III-D.

II-B.3. Structural implications for the manganese cluster

The multiline and $g = 4.1$ signals were originally attributed to two slightly different conformations of a tetranuclear Mn cluster with different spin states [208,418,426,492]. This model was supported by reports that the amplitude of the multiline signal diminished below 7 K [418,459,491–493]; this non-Curie temperature-dependence could only be explained if the four manganese ions were arranged as an exchange-coupled tetramer [418,492]. Because the $g = 4.1$ signal was observed to exhibit Curie temperature-dependence [388, 393,394,492] (but see Ref. 431, discussed below), the multiline and $g = 4.1$ signals were attributed to an $S = 1/2$ excited state and an $S = 3/2$ ground state, respectively, of a single tetranuclear cluster [418,426, 492] (see also Ref. 459). However, the observations of non-Curie temperature-dependence for the multiline signal have not been reproduced subsequently [85,388, 389,393,394,410,414,431]. In spite of the precautions taken to avoid saturation [418,459,492], the earlier observations of non-Curie behavior are now believed to have been caused by saturation of the multiline signal at temperatures below 7 K [388]. The multiline signal is now generally believed to arise from an $S = 1/2$ ground state [31,33,38,85,385,388,389,431]. Consequently, the non-Curie argument in favor of an exchange-coupled tetranuclear cluster no longer exists. Nevertheless, having the multiline and $g = 4.1$ EPR signals originate from two different conformations of a single tetranuclear cluster still remains an attractive model (see below). Several models for the mechanism of water oxidation based on tetranuclear clusters have been advanced [478,479,494,495] (see also the model of Moravsky and Khramov cited in Refs. 30,496, and see subsection II-H) and numerous tetranuclear clusters having spectroscopic properties that resemble those of the manganese in PS II have been synthesized (reviewed in Refs. 387,495–504 and see Refs. 505–508).

Trimeric Mn compounds can give rise to EPR signals that resemble the multiline and $g = 4.1$ signals [509–511]. Consequently, it has been suggested that the multiline and $g = 4.1$ signals may arise from two different conformations of a trinuclear Mn cluster and that the fourth Mn ion in PS II may serve as an electron transfer intermediate between the trimer and Y_Z [509,512]. The possible relevance to PS II of the trinuclear/mononuclear copper centers in ascorbate oxidase [513,514], which catalyze the four-electron oxidation of O_2 to H_2O, has been suggested [23,511] (also see the discussion in Ref. 388).

An alternate model for the origin of the multiline

and $g = 4.1$ signals involves a redox equilibrium between a monomeric Mn(IV) ion and a mixed-valent Mn dimer [393,394,414] or trimer [498,509,512]. Numerous dimeric and trimeric Mn clusters with properties similar to those of the manganese in PS II have been synthesized (reviewed in Refs. 495–502,504,511,515) and studies of inorganic Mn(IV) compounds indicate that a mononuclear Mn(IV) ion could exhibit a $g = 4.1$ signal similar to that observed in PS II [510,511,516]. However, the recent observation of hyperfine structure on the $g = 4.1$ signal in oriented NH_3-treated samples [402,420] (Fig. 8) undermines the redox-equilibrium model. The number of hyperfine lines and their spacing demonstrate that the $g = 4.1$ signal cannot arise from a Mn monomer [402,420]. Furthermore, the signal has been asserted to arise from a cluster that contains at least three Mn ions [420]. An isolated Mn(II)-Mn(III) or Mn(III)-Mn(IV) dimer with a Mn-Mn distance that is compatible with EXAFS measurements on PS II (see subsection II-C.1) would be strongly antiferromagnetically coupled and consequently would have an $S = 1/2$ ground state and exhibit an EPR signal near $g = 2$ [385,499,517]. Furthermore, even if the $g = 4.1$ signal were to arise from an excited state of such a dimer, it would exhibit an additional EPR signal near $g = 2$ [385,420,499,517]. Nevertheless, it should be noted that one group has recently reported that, under some conditions, there is an EPR signal centered near g approx. 2 that is associated with the Mn that give rise to the $g = 4.1$ signal [431]. This signal is the broad Gaussian-shaped signal that, under some conditions, underlies the multiline signal [431]. On the basis of an orientation study and spectral simulations, the NH_3-modified $g = 4.1$ signal has been proposed to arise from an $S \geq 3/2$ ground state of a manganese tetramer and most likely from an $S = 5/2$ ground state [402] (also see the discussion in Ref. 389).

An $S = 5/2$ ground state origin for the $g = 4.1$ signal was originally proposed based on a recent multifrequency EPR study that involved comparing the $g = 4.1$ signal at S-band (3.9 GHz), X-band (9.2 GHz) and P-band (15.5 GHz) [416]. On the basis of spectral simulations, these data were interpreted as indicating that the $g = 4.1$ signal arises from the middle Kramer's doublet of a near rhombic $S = 5/2$ system. This origin for the $g = 4.1$ signal predicts that it would exhibit apparent Curie-law behavior above 2 K [416], in agreement with the earlier studies that reported [492] or suggested [393,394] that this signal exhibits Curie temperature-dependence. The signal was proposed to arise from an exchange-coupled trinuclear or tetranuclear Mn cluster [416], in agreement with the studies of the NH_3-modified signal [402,420]. However, another recent study disagrees with the assignment of the $g = 4.1$ signal to an $S = 5/2$ ground state [431]. From an investigation of the saturation properties and temperature-dependencies of both the multiline and $g = 4.1$ signals, the $g = 4.1$ signal is reported to exhibit non-Curie behavior when generated by illumination at 180–240 K in the presence of 0.4 M sucrose [431]. This conflicts with the earlier studies that reported [492] or suggested [393,394] Curie temperature-dependence for this signal. The conflict with one of the earlier studies [492] is attributed to a postulated difference in the exchange couplings of a manganese tetramer when the $g = 4.1$ signal is generated at different temperatures: the signal is suggested to arise from an $S = 3/2$ ground state when generated at approx. 130 K (as in Ref. 492) and from an $S = 3/2$ excited state when generated at 180–240 K [431]. The conflict with the other studies [393,394] is attributed to the broad Gaussian-shaped signal that is suggested [431] to be present beneath the multiline signals reported in Refs. 393,394. This broad signal, centered near $g = 2$, is reported to be associated with the $g = 4.1$ signal generated at 180–240 K and to exhibit the same non-Curie temperature-dependence [431]. The broad Gaussian-shaped signal is reported to contribute significantly to the apparent integrated intensity of the multiline signal [431]. Consequently, the relative integrated intensities of the $g = 4.1$ and multiline signals appear to change little with temperature, giving the impression [393,394] that the $g = 4.1$ signal exhibits Curie behavior [431]. The authors attribute the $g = 4.1$ signal generated at 180–240 K to the first excited $S = 3/2$ state of an $S = 7/2$ multiplet [431]. The reasons for the conflicts between this study [431] and the multifrequency EPR study discussed above [416] are not understood; in both studies the $g = 4.1$ signal was generated by illumination at approx. 200 K in the presence of 0.4 M sucrose. Nevertheless, both studies [416,431] attribute the $g = 4.1$ EPR signal to an exchange-coupled trimer or tetramer of Mn, in agreement with the studies of the NH_3-modified $g = 4.1$ signal [402,420].

Recent data indicate that the multiline signal may also arise from a exchange-couple Mn trimer or tetramer. Preliminary orientation studies of the altered, approx. 26-line multiline signal in Ca^{2+}-depleted samples (see Fig. 11) have been interpreted as indicating that the multiline signal arises from a Mn cluster that is larger than a dimer [447,451]: the number of lines does not depend on orientation, suggesting that their number cannot be explained solely on the basis of anisotropic hyperfine couplings [447,451] (also see the arguments in Refs. 38,85). The large number of hyperfine lines exhibited by the multiline signal at S-band [399,400] (Fig. 7) also suggests that the multiline signal may arise from a complex of more than two Mn ions. However, this number of hyperfine lines could arise from a dimer if the hyperfine interactions are anisotropic and include second order contributions [399,400]. Recent magnetic susceptibility measure-

ments have been interpreted as indicating that both the multiline and $g = 4.1$ signals arise from the same Mn cluster [486] and that this cluster is larger than a dimer [518]. The change in susceptibility induced by a flash given at room temperature is reported to be identical in Cl^--reconstituted and F^--inhibited samples that exhibit predominantly the multiline and $g = 4.1$ signals, respectively [486], suggesting that the same cluster is oxidized when either signal is formed. However, it is not clear that the two samples contained significantly different proportions of 'multiline' and '$g = 4.1$' centers: the amplitude of the $g = 4.1$ signal was not significantly enhanced in the F^--inhibited sample compared to its amplitude in the sample that had been reconstituted with Cl^- (compare Fig. 1 of Ref. 486 with Figs. 6A and 6B of subsection II-B.1), suggesting that both samples may have contained the same fraction of centers that gave rise to the $g = 4.1$ signal. The lack of the multiline signal in the F^--inhibited sample (Fig. 1 of Ref. 486) might have resulted from the prior depletion of Cl^- from this sample: the multiline signal is not observed in Cl^--depleted preparations in the presence of SO_4^{2-} [214,433,434,487,519] (see subsection III-D). Further magnetic susceptibility measurements seem warranted.

If both the multiline and $g = 4.1$ signals arise from Mn clusters that contain more than two Mn ions, then the four manganese ions in PS II must be arranged either as a tetramer (possibly arranged as a pair of interacting dimers as in the inorganic model compound reported in Ref. 505 (see Fig. 14C) or as depicted in Fig. 15 in subsection II-C.1), or as a trimer that gives rise to both EPR signals, with an EPR silent monomer located some distance away. While the trimer model cannot be excluded at present, a tetranuclear origin for the multiline signal is favored on theoretical grounds [520]: if only Mn(III) and Mn(IV) ions are present in the S_2 state (see subsection II-C.2), and if the multiline signal exhibits little or no g anisotropy [393,394], it is argued that the width of the multiline signal cannot be accounted for by a Mn dimer or trimer [520] (also see the arguments in Ref. 385). Depending on the magnetic couplings, an exchange-coupled tetranuclear cluster could have an $S = 1/2$ ground state in one conformation and an $S = 3/2$ [385,418,420,517] or $S = 5/2$ [402] ground state in another. These two conformations could give rise to the multiline and $g = 4.1$ signals, respectively [385,402,418,420,517], as was proposed originally [208,418,426,492]. Different exchange couplings within a manganese tetramer have also been invoked to explain the recent report that the $g = 4.1$ signal arises from an excited $S = 3/2$ state and exhibits Curie temperature-dependence when generated under some conditions [431]. Perturbation of the exchange couplings by inhibitory amines and anions, different cryoprotectants and by the substitution of Sr^{2+} for

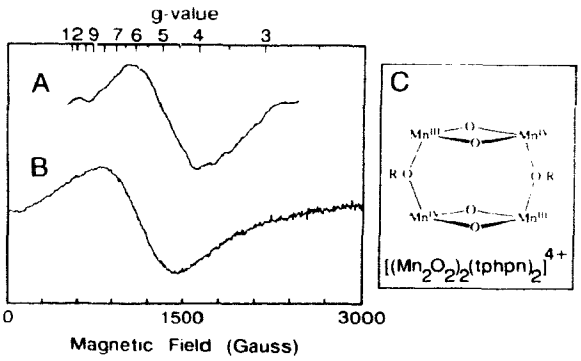

Fig. 14. Comparison of EPR spectra from PS II membranes poised in the S_1 state (A) and from a model compound that contains a bridged pair of di-μ-oxo bridged Mn(III)-Mn(IV) dimers (B). A schematic illustration of this compound, $[(Mn_2O_2)_2(tphpn)_2]^{4+}$ (tphpn = *N,N,N',N'*-tetrakis(2-pyridylmethyl)-2-hydroxypropane-1,3-diamine) is presented in (C). Spectra were recorded with parallel polarization spectrometer geometry at 4.2 K (A) or 4 K (B). The S_1 state PS II spectrum represents the difference between spectra recorded before and after illumination at 200 K [521,522]. Left panel was modified from Ref. 505. Reprinted with permission (copyright 1991 by the American Chemical Society).

Ca^{2+}, presumably causes the alterations in the multiline and $g = 4.1$ signals that are described in subsection II-B.1 [38,85,389,428].

The S_1-state EPR signal. Not all available data necessarily agree with a tetranuclear (or trinuclear) origin for both the multiline and $g = 4.1$ signals. In one recent study, the relationship between these signals and an EPR signal that was recently observed in dark-adapted PS II membranes and assigned to the S_1-state Mn complex was examined [521,522]. This signal (see Fig. 14), detected by parallel polarization EPR, is centered at g approx. 4.8 and has a peak-to-peak width of approx. 600 Gauss [521,522]. It appears to be a precursor of the multiline signal, but not of the $g = 4.1$ signal; when the $g = 4.1$ signal is produced, the S_1-state signal is unaffected, whereas when the multiline signal is produced, the S_1-state signal disappears. On the basis of these results, the S_1-state signal and the multiline signal have been proposed to arise from a different Mn center than the $g = 4.1$ signal [521,522]. This proposal favors the monomer-dimer/trimer redox equilibrium model. To rationalize the behavior of the S_1-state signal with a tetranuclear origin for the multiline signal, it has been suggested that the S_1-state signal might arise from an isolated Mn(III) ion, that the S_2-state $g = 4.1$ signal might arise from an exchange-coupled Mn trimer and that the multiline signal might result from a conformation- or ligand-induced coupling of the monomer and trimer to yield an exchange-coupled tetramer [85]. This model is similar to one presented to rationalize the non-Curie temperature-dependence of

the $g = 4.1$ signal under some conditions [431]. In a related development, a parallel-polarized EPR signal, centered near $g = 6$ and having a peak-to-peak width of approx. 700 Gauss, has been detected in a tetranuclear Mn complex that contains a symmetrical, bridged dimer of di-μ_2-oxo bridged Mn(III)-Mn(IV) dimers [504,505] (see Fig. 14). This compound has been proposed to be a model of the Mn complex in the S_1 state in terms of its electronic properties and Mn oxidation states (see subsection II-C.2) [504,505]. However, if the S_1-state signal arises from magnetic coupling between two Mn(III)-Mn(IV) dimers in PS II, as is proposed for this compound [504,505], it is unclear why the S_1-state signal would seem to be related to the multiline signal in the S_2 state, but not to the $g = 4.1$ signal.

NMR proton relaxation enhancement studies. Comparison of the NMR relaxation rates of bulk solvent water protons interacting with PS II in the S_1, S_2 and S_3 states [523–527] were originally interpreted as favoring the redox equilibrium model [526]. The relaxation rates are increased in the S_2 and S_3 states and are most consistent with a rapid chemical exchange of water protons between the bulk solvent and the coordination sphere of a monomeric Mn(IV) ion [523–527]. The observed relaxation rate enhancements are more difficult to reconcile with a polynuclear cluster that contains a Mn(III) ion [526,527]. Nevertheless, a model that reconciles these data with a tetranuclear origin for the multiline and $g = 4.1$ signals has recently been proposed [527]. In this model, PS II contains a tightly coupled Mn trimer that is magnetically coupled with a Mn monomer. The coupling between the monomer and the trimer is proposed to be weak at room temperature, but to be strong at cryogenic temperatures. The chemically-exchanging water molecules are proposed to interact only with the monomer. Consequently, the strongly-coupled trimer would influence the measured proton relaxation enhancements only through its weak coupling with the monomer. In the S_1 state, the Mn oxidation states would be Mn(III) for the monomer and either $Mn(III)_3$ or $Mn(IV)_2$-Mn(III) for the trimer. The Mn monomer is proposed to be oxidized to Mn(IV) in the S_2 state and to persist as Mn(IV) in the S_3 state, whereas the oxidation states of the Mn ions in the trimer are proposed to remain the same in the S_1, S_2 and S_3 states. The weak coupling between the Mn trimer ($S = 1$) and monomer ($S = 3/2$) in the S_2 state at room temperature would give rise to the NMR proton relaxation enhancements that appear to originate from a monomeric Mn(IV) ion, while strong antiferromagnetic or ferromagnetic coupling between the monomer and trimer at cryogenic temperatures would give rise to the multiline (from an $S = 1/2$ state) and $g = 4.1$ signals (from an $S = 5/2$ state), respectively [527]. This model does not appear to account for the behavior of the S_1-state EPR signal, however.

Future work must reconcile the relationship between the S_1-state EPR signal and the S_2-state multiline and $g = 4.1$ signals, the NMR proton relaxation enhancement data and the disparate conclusions of the recent temperature dependence and multifrequency EPR studies that propose different magnetic origins for the S_2-state $g = 4.1$ signal.

II-C. X-ray absorption studies

II-C.1. The structure of the manganese complex – EXAFS studies

The original EXAFS measurements on PS II [412,528–530] were performed by Klein, Sauer and co-workers on broken chloroplasts or PS II membranes. These authors concluded that the Mn ions are coordinated by oxygen or nitrogen atoms with Mn–O or Mn–N distances of 1.75 Å and 2.0 Å. Between one and two Mn-Mn interactions, having Mn–Mn distances of approx. 2.7 Å, were also detected [412,529] and a possible approx. 3.3 Å M-Mn interaction was reported [412,530]. These distances were interpreted in terms of a di-μ_2-oxo bridged Mn dimer, with either two Mn monomers or a second dimer located approx. 3.3 Å distant. In work published in 1988–1990 [343,531–533], the Klein/Sauer group examined PS II membranes from both spinach and the cyanobacterium *Synechococcus elongatus* with an improved detection system. From these data they concluded that each Mn is ligated by 1–2 and 2–4 oxygen or nitrogen atoms at 1.75–1.8 Å and 1.9–2.2 Å, respectively and that there are 2–3 Mn–Mn interactions with distances of 2.73 ± 0.05 Å. No 3.3 Å Mn–Mn interaction was detected, however. The results were interpreted in terms of two inequivalent di-μ_2-oxo bridged Mn dimers that are located > 3.0 Å apart, although a linear or bent trimeric di-μ_2-oxo bridged Mn structure, with a monomeric Mn located > 3.0 Å distant, would also be consistent with these data [343,531–533] (reviewed in Ref. 534).

Two other EXAFS studies on PS II also appeared in 1989–1990: Penner-Hahn and co-workers [535,536] analyzed a highly-purified oxygen-evolving PS II complex from spinach that lacks the 24 and 17 kDa polypeptides, while Cramer, George and Prince [537,538] analyzed oriented chloroplast membranes. Both groups reported Mn–O or Mn–N distances of 1.9–2.1 Å and either 2–3 [535,536] or 3–5 [537,538] Mn–Mn interactions with a distance of approx. 2.7 Å. Both groups also reported 1–2 Mn–Mn interactions with a distance of approx. 3.3 Å. The measurements on the oriented chloroplast membranes demonstrated that the 3.3 Å interaction is strongly dichroic and is oriented perpendicularly to the plane of the membrane [537,538]. Weak dichroism was also reported for the 2.7 Å interactions. These interactions were reported to be oriented at an

average angle of 62° to the membrane normal [537,538]. Penner-Hahn and co-workers proposed that the 3.3 Å interaction represents a combination of Mn–Mn and Mn-carbon interactions, with the latter arising from coordination of Mn by carboxylate, alkoxide, or phenoxide ligands [535,536]. These workers suggested that the approx. 3.3 Å interaction could also represent either an Mn–Mn or an Mn–Ca interaction [535], but favored the former because 3.3 Å is short for an Mn–Ca distance. However, based on investigations of trinuclear compounds containing both Mn and Na [510,516,539], Pecoraro and co-workers have proposed that such a short Mn–Ca distance is possible [510,511,516]. In contrast to the work of the Klein/Sauer group, no 1.75 Å interaction was detected by either the Penner-Hahn or the Cramer/George/Prince groups. Penner-Hahn and co-workers concluded that their data do not exclude the existence of a small number of 1.75–1.8 Å interactions [535,536], but argued that such short Mn–O distances are found only in model compounds that have strongly donating nitrogen ligands (such as phenanthroline or pyridines) *trans* to the μ_2-oxo bridges, a situation not likely to exist with amino acid ligands, which are weaker donors. Two other groups have recently begun XANES or EXAFS measurements on PS II membranes [540–542] and one of these reports that each Mn is ligated by 2.0 ± 0.4 oxygen or nitrogen atoms at 1.79 Å [540], in agreement with the Klein/Sauer group.

More recently, the Klein/Sauer group has collected data at 10 K with the same type of detector as employed by the Cramer/George/Prince and Penner-Hahn groups [389,543]. An interaction of approx. 3.3 Å is clearly visible at the lower temperature and is attributed to approximately one Mn–Mn or Mn–Ca interaction [389,543]. With the higher signal-to-noise ratio achieved in the most recent measurements, the Klein/Sauer group now reports approx. 2 oxygen or nitrogen atoms (per Mn) at 1.80 ± 0.05 Å, and 2–4 at 1.9–2.2 Å, with the number of 2.7 Å Mn–Mn interactions remaining at 2–3 [389]. The orientations of the 2.7 Å and 3.3 Å interactions were also studied in the most recent studies [389]. The 3.3 Å interaction was found to be strongly dichroic and to be oriented perpendicular to the plane of the thylakoid membrane [389,543], as was previously reported by the Cramer/George/Prince group [537,538]. In addition, the 2.7 Å interactions were also found to be weakly dichroic and to be oriented approx. parallel to the thylakoid membrane [389]. Nevertheless, the amplitudes of the Fourier peaks in EXAFS spectra taken at different orientations by the Klein/Sauer group were reported to differ significantly [389] from those reported earlier by the Cramer/George/Prince group.

In all of the reported EXAFS studies, the environments of the Mn ions have been concluded to be very heterogeneous, being characterized by a distribution of Mn–O and Mn–N distances. The anisotropy and observed quantities of 2.7 Å Mn–Mn interactions are inconsistent with the published symmetric tetranuclear models for the Mn complex [478,479,494,495], but a highly distorted tetramer, a dimer of dimers, or a trimer plus monomer would be consistent with the data. If the S_2-state $g = 4.1$ EPR signal were to arise from a monomeric Mn(IV) ion, then Penner-Hahn and co-workers argued that the remaining Mn must be arranged as a trimer [535,536]. However, as discussed in subsection II-B.2, a monomeric origin for the $g = 4.1$ signal has recently been excluded by the hyperfine structure observed on this signal in oriented NH_3-treated PS II membranes [402,420].

All groups agree that the 2.7 Å Mn–Mn interaction suggests that the Mn ions involved are linked by more than one short bridging ligand. All groups have proposed di-μ_2-oxo bridged structures; at issue is the length of the Mn–O bonds. Because neither the Penner-Hahn group nor the Cramer/George/Prince group required a 1.75 Å interaction to fit their data, both groups suggested that μ_3-oxo or μ_2-hydroxo bridges may also be involved. However, the Penner-Hahn group has since discovered that the mylar tape employed to mount some of their samples was contaminated with Mn(II) ions amounting to approx. 25% of the observed Mn signal intensity [544]. Also, the Cramer/George/Prince group has since discovered that the prolonged dehydration times employed to orient their samples onto mylar sheets led to the formation of Mn(II) ions; as much as approx. 25% of the Mn in the analyzed samples may have been Mn(II) (S.P. Cramer, personal communication). In spectral simulations, the Klein/Sauer group has reported that they can reproduce the X-ray absorption edge (XANES) data of the Penner-Hahn and Cramer/George/Prince groups by assuming that the mounted samples of these groups contained 25% and 40% adventitious Mn(II), respectively [389]. Contamination by Mn(II) would have led to overestimation of the Mn–O or Mn–N distances [389] (S.P. Cramer, personal communication). Contamination by Mn(II) may also partially explain why the amplitudes of the Fourier peaks in the oriented EXAFS spectra of the Cramer/Prince/George group differ from those of the Klein/Sauer group [389]. An additional contributing factor could be that the more rapid dehydration procedure employed by the Klein/Sauer group, which produces less adventitious Mn(II), produces samples that are less oriented (S.P. Cramer, personal communication).

Based on a correlation between Mn–Mn distances and Mn–O–Mn bond angles in 22 dimeric Mn model compounds, Pecoraro and co-workers have suggested that the 2.7 Å interaction arises from a di-μ_2-oxo or di-μ_2-oxo/carboxylato bridged structure with Mn–O–

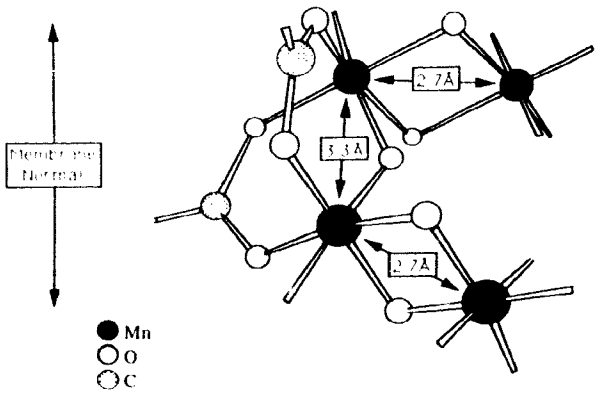

Fig. 15. Model for the Mn complex in PS II proposed by Klein, Sauer and co-workers on the basis of their EXAFS data [389]. The model consists of two di-μ-oxo bridged Mn dimers that are bridged by one mono-μ_3-oxo and two carboxylato bridges. The Mn–Mn distance in each di-μ-oxo bridged dimer is approx. 2.7 Å, while the closest Mn–Mn distance between the dimers is approx. 3.3 Å. The 3.3 Mn–Mn interaction is proposed to be oriented perpendicular to the plane of the thylakoid membrane. Note that the model predicts two 2.7 Å and one 3.3 Å Mn–Mn interactions. The experimental data have been interpreted as indicating the presence of 2–3 [389,535,536] or 3–5 [537,538] 2.7 Å Mn–Mn interactions and 1 [389] or 1–2 3.3 Å Mn-metal interactions [535–538]. Reprinted from Ref. 389 with permission (copyright 1992 by VCH, Inc.).

Mn bond angles of 95–100° [510,511,545]. The Penner-Hahn [535], Cramer/George/Prince [537,538] and Klein/Sauer groups [389] (also Pecoraro and co-workers [510,511]) have suggested that the approx. 3.3 Å interaction, if it corresponds to an Mn–Mn distance, may arise from bridging of Mn by some combination of oxo, hydroxo, alkoxo, phenoxo and carboxylato ligands, such as by one μ_3-oxo, μ_3-oxo, or μ_3-hydroxo bridge plus one or two carboxylato bridges (see Fig. 15).

Some of the discrepancies between the published work of the various groups may have resulted from differences in sample preparations, degrees of contamination by Mn(II), detection systems (the Penner-Hahn and Cramer/George/Prince groups used the same detection system), data analysis procedures, or sample temperatures (4 K by the Cramer/George/Prince group, 10 K or 80 K by the Penner-Hahn group, 10 K or 170–190 K by the Klein/Sauer group). For example, the approx. 3.3 Å distance attributed to a Mn–Mn or a Mn–Ca interaction is only observable at temperatures well below 80 K [389,536,543]. With all three groups now free of adventitious Mn(II) and employing the same sample temperatures and improved detection systems, a consensus concerning the numbers and distances of atoms coordinated to Mn is expected in the near future.

Calcium. Whether Ca^{2+} is located near Mn has been addressed by both the Penner-Hahn and Klein/Sauer groups. As mentioned earlier, Penner-Hahn and co-workers suggested that the approx. 3.3 Å distance could represent either a Mn–Mn or a Mn–Ca interaction, but favored the former assignment. These authors also observed a Mn-metal interaction of approx. 4.35 Å [535] and suggested that it, too, could represent either a Mn–Mn or a Mn–Ca interaction. As a precedent for such a 4.35 Å Mn–Ca interaction in PS II, these authors point out that concanavalin A contains a Mn^{2+}-Ca^{2+} heterodinuclear site, with the Mn^{2+} and Ca^{2+} ions separated by 4.25 Å [546] (or 4.6 Å [547]) and bridged by two carboxylate groups. The potential relevance of concanavalin A to PS II had been noted previously [539,548,549]. Klein, Sauer and co-workers have recently compared samples reconstituted with Ca^{2+} or Sr^{2+} following the depletion of Ca^{2+} by treatment with sodium citrate at pH 3 [543] (M.J. Latimer, V.J. DeRose, V.K. Yachandra, I. Mukerji, K. Sauer and M.P. Klein, personal communication). A second-derivative analysis of the absorption edge found little difference between untreated samples and samples reconstituted with Ca^{2+} or Sr^{2+}, but found significant changes in unreconstituted Ca^{2+}-depleted samples, suggesting that the structure of the Mn complex is altered in the absence of Ca^{2+} or Sr^{2+} (at least when Ca^{2+} is extracted at pH 3). A second group has also reported that depleting PS II membranes of Ca^{2+} with sodium citrate at pH 3 significantly perturbs the structure of the Mn complex [424]. The Klein/Sauer group has reported that the EXAFS scattering amplitude of the approx. 3.3 Å interaction is significantly larger in samples reconstituted with Sr^{2+} than in samples reconstituted with Ca^{2+} [543]. Because Sr has a greater scattering ability than Ca, these authors propose that there is a Ca^{2+} binding site located approx. 3.3 Å from Mn. From quantitative analyses, the approx. 3.3 Å interaction is proposed to arise either solely from a Mn–Ca interaction, or from a combination of Mn–Mn and Mn–Ca interactions [389,543] (M.J. Latimer, V.J. DeRose, V.K. Yachandra, I. Mukerji, K. Sauer and M.P. Klein, personal communication). Samples having Sr^{2+} substituted for Ca^{2+} have also been analyzed by the Penner-Hahn group. In contrast to the results of the Klein/Sauer group, the scattering amplitude of the approx. 3.3 Å interaction was not larger in the Penner-Hahn group's Sr^{2+}-supplemented samples compared to its amplitude in Ca^{2+}-supplemented samples. However, the multiline EPR signal was not examined in the Penner-Hahn group's EXAFS samples to show definitively that Sr^{2+} had replaced Ca^{2+}, although equivalently prepared samples exhibited the Sr^{2+}-modified multiline signal (see Fig. 10) (J.E. Penner-Hahn, personal communication). Further experiments are in progress. If the difference

between the Sr^{2+}-substituted samples of the Klein/Sauer and Penner-Hahn groups persists, it is unlikely to be caused by the lack of the extrinsic 24 and 17 kDa polypeptides in the Penner-Hahn group's samples, despite the lower apparent affinity for Ca^{2+} in such samples (see subsection III-A); both groups report similar data for their respective Ca^{2+}-supplemented samples (J.E. Penner-Hahn and C.F. Yocum, personal communication; V.K Yachandra and M.P. Klein, personal communication).

Chloride. Whether one or two Cl^- ions are present in the Mn coordination sphere, as postulated from inhibition studies with amines [437–439] (see subsection II-G.1), cannot be determined in untreated samples with the currently achievable EXAFS signal-to-noise ratios [412,535]. However, the substitution of F^- for Cl^- perturbs the structure of at least one of the di-μ_2-oxo bridged Mn dimers postulated to be present in PS II [543]. These data, in addition to a recent examination of samples having Br^- substituted for Cl^- (obtained by growing *Synechococcus elongatus* on Br salts in place of Cl^-), has led the Klein/Sauer group to suggest that one Cl^- ion may ligate the Mn complex as a terminal ligand with a Mn–Cl distance of approx. 2.3 Å [543] (M.P. Klein and V.K. Yachandra, personal communication). Klein, Sauer and co-workers argue that their data exclude the possibility that the Mn complex is ligated by more than one Cl^- ion, or that Cl^- is present as a bridging ligand, at least in the S_1 state [543].

Models. A model proposed by the Klein/Sauer group to account for their EXAFS data is presented in Fig. 15. A detailed structural model has also been proposed by Kusunoki and co-workers based on the pre-edge features of X-ray absorption edge (XANES) data and on considerations of ligand field theory [541,542]. This model includes a single di-μ_2-oxo bridged Mn dimer that is bridged on one side by a deprotonated water dimer $(HOHOH)^-$, ligated on the opposite side by an imidazole nitrogen and a carboxylate oxygen and bridged to two Mn monomers by additional carboxylate ligands. However, it is difficult to understand how these authors could have arrived at such a detailed model without the benefit of Mn–Mn or Mn-ligand distances derived by EXAFS spectroscopy and without additional experimental data.

II-C.2. The oxidation states of manganese – XANES studies

The S_1 state. In most XANES spectra of dark-adapted samples, the position of the absorption edge has been taken to indicate that the average oxidation state of the Mn in the S_1 state is Mn(III) [343,411,412, 419,529,530,534,535,541,542,550]. This assignment agrees with proton NMR relaxation enhancement measurements [523–527], and with both microwave power saturation [551] and spin-lattice relaxation time [552] measurements of $Y_D^{\bullet}$. Penner-Hahn and co-workers reported that the XANES absorption edge is unusually broad for model compounds containing Mn(III) and, from an analysis of the entire edge region, proposed that the S_1 state consists of one Mn(II), two Mn(III) and one Mn(IV) ions [535,536]. However, the mylar tape that was employed to mount some of the samples was subsequently found to be contaminated with Mn(II) ions [544] (see subsection II-C.1). Klein, Sauer and co-workers have argued against the presence of Mn(II) in the S_1 state, maintaining that the similarity of their S_1-, S_2- and S_3-state EXAFS data (see below), rules out the significant structural changes in the Mn coordination sphere that would be expected from oxidation of Mn(II) to Mn(III) during either the $S_1 \rightarrow S_2$ or $S_2 \rightarrow S_3$ transitions [389]. From second derivative analyses of the XANES edge and pre-edge features of samples poised in the S_1 and S_2 states, the Klein/Sauer group now favors an assignment of two Mn(III) plus two Mn(IV) ions to the S_1 state and one Mn(III) and three Mn(IV) ions to the S_2 state [389,533,543] (see Fig. 2). Penner-Hahn and co-workers now also favor the assignment of two Mn(III) and two Mn(IV) ions to the S_1 state based on their most recent data acquired with samples that were mounted with Mn-free polypropylene windows [544]. Such an oxidation state assignment would be consistent with the model compound that contains a symmetrical, bridged pair of Mn(III)-Mn(IV) dimers [504,505] and that gives rise to a parallel-polarized EPR signal that resembles the EPR signal observed in S_1-state samples [521,522] (see subsection II-B.3 and Fig. 14).

In a recent development, bond valence sums have been calculated for metal ions in a variety of model compounds and metalloenzymes, based on bond lengths determined crystallographically and/or by EXAFS measurements [553]. In all cases, the calculated bond valence sums correctly predict the oxidation state of the metal ion in question. When applied to PS II, assuming that (i) the average Mn–O distance is 1.91 Å, (ii) there are only 1–2 nitrogens to the Mn complex [389,398,554] (see subsection II-I), (iii) the S_2 state consists of either a $(III)_3(IV)$, $(III)(IV)_3$, or $(IV)_3(V)$ Mn tetramer (see subsection II-B.1) and (iv) the average Mn–O distance does not change significantly when the Mn cluster is oxidized to the S_2 state (as determined by EXAFS measurements, see below), the S_1 state is predicted to contain two Mn(III) and two Mn(IV) ions [553]. The bond valence sum analysis would be inconsistent with an assignment of four Mn(III) ions to the S_1 state [553]. It should be noted, however, that Kusunoki and co-workers favor an assignment of four Mn(III) ions to the S_1 state based on their XANES data [541,542].

The S_3 state. The edge energies of S_3-state samples are approx. 1 eV higher than those of S_1-state samples and the pre-edge features are different [343,411,412, 419,541,542]. By comparison with model compounds, these differences have been interpreted as demonstrating that one Mn(III) ion is oxidized to Mn(IV) during the $S_1 \rightarrow S_2$ transition [343,411,412,419,541,542] (reviewed in Ref. 389,534). Consistent with this interpretation, the S_1- and S_2-state EXAFS spectra appear nearly identical [343,389,412,533,534]. The similarity of these spectra demonstrates that no large structural rearrangements take place during the $S_1 \rightarrow S_2$ transition. Nevertheless, subtle differences between the S_1- and S_2-state samples were observed in spectra recorded at 10 K by the Klein/Sauer group. These differences are consistent with the oxidation of Mn(III) ion to Mn(IV) during the $S_1 \rightarrow S_2$ transition [389,543] (also see [542]). The NMR proton relaxation enhancement [523–527], microwave power saturation [551] and spin-lattice relaxation [552] measurements cited above have also been interpreted as indicating that one Mn(III) ion is oxidized to Mn (IV) during the $S_1 \rightarrow S_2$ transition, as have most measurements of flash-induced optical absorption changes in the ultraviolet (see subsection II-D.1).

The S_3 state. Samples trapped predominantly in the S_3 state (65% S_3, 35% S_2) have been reported by the Klein/Sauer group [389,531,533,534]. These samples were prepared under conditions that permit 2-electron oxidation of the Mn complex during illumination at cryogenic temperatures: prior to illumination at 240 K, the acceptor-side non-heme Fe^{2+} was oxidized to Fe^{3+} either by oxidation of dark-adapted samples with ferricyanide [555], followed by exchange of ferricyanide for DCMU, or by illumination at 77 K of samples containing the high-potential quinone phenyl-*p*-benzoquinone, followed by brief warming to 293 K [99,110]. Earlier attempts to poise samples in the S_3 state had achieved at most 47% S_3 [411,530]. The absorption edge of the S_3-state samples (following subtraction of spectra corresponding to residual S_2-state centers) was not significantly changed in shape or energy from that of samples poised in the S_2 state [411,530,531,533,534]. These results have been interpreted as demonstrating that Mn is not oxidized during the $S_2 \rightarrow S_3$ transition. The oxidizing equivalent is proposed to reside on a redox-active histidine or tyrosine residue either ligated to Mn, or located close enough to the Mn complex to be magnetically coupled with it. Such magnetic coupling has been proposed to account for the lack of an observable EPR signal from the S_3 state in native preparations [389,530,531,533]. However, the apparent lack of Mn oxidation during the $S_2 \rightarrow S_3$ transition has been challenged on two grounds. First, because no direct spectroscopic assay for the S_3 state yet exists, the authors are forced to assume that, following illumination, samples not displaying the S_2-state multiline EPR signal are in the S_3 state. Consequently, it is not yet possible to assess directly whether the authors' S_3-state samples are contaminated with PS II complexes that are in the S_0 or S_1 states, whose presence might offset an increase in edge energy associated with the $S_2 \rightarrow S_3$ transition [30,482,556,557]. Second, because the absorption edge data reflect only the electron density around the metal ion, changes in the Mn coordination sphere could mask a change in the Mn oxidation state [30,387,496,498,502,556]. While the EXAFS data do show small structural changes in the environment of the Mn ions during the $S_2 \rightarrow S_3$ transition, the Klein/Sauer group maintains that the Mn site symmetry remains virtually unchanged. Furthermore, they argue that it would be highly unlikely and unprecedented from studies of model compounds, for an increase in edge energy caused by the oxidation of the Mn complex to be coincidentally offset by a decrease in energy caused by ligand rearrangements [389,531]. Other workers dispute this point, however, arguing that electron-poor Mn(II) centers resemble Mn(III) centers in X-ray photoelectron spectra of model compounds [387,558].

Independent of the XANES and EXAFS data, the NMR proton relaxation enhancement measurements [524–527], the microwave power saturation [551] and spin-lattice relaxation [552] measurements of Y_D^+ and recent measurements of proton release and of electrochromic shifts near 440 nm [559] (see subsection II-E), have also been interpreted as indicating that the oxidation state of the Mn cluster remains unchanged during the $S_2 \rightarrow S_3$ transition. The 130–164 Gauss-wide EPR signal, recently observed in Ca^{2+}-depleted [423,447–456] and Cl^--depleted [486,487] samples (see subsection II-B.2), has also been interpreted as indicating that no Mn ions are oxidized during the $S_2 \rightarrow S_3$ transition; this signal has been proposed to arise from a histidine residue (or another organic component) that is oxidized during this transition, even in untreated samples [447,448,452,453,486]. However, whether oxidation of this putative histidine residue occurs in untreated samples (or occurs at all) remains in dispute (see subsection II-F). In contrast to the interpretations based on X-ray absorption, NMR and EPR spectroscopies, most interpretations of flash-induced optical absorption changes in the ultraviolet favor the oxidation of one Mn(III) ion to Mn(IV) during the $S_2 \rightarrow S_3$ transition (see subsection II-D.1).

The small structural changes in the environment of the Mn complex that result from the $S_2 \rightarrow S_3$ transition [389,531,533,534] have been attributed to a slight change in the 2.7 Å Mn–Mn distances: the distance between the Mn ions in one dimer was suggested to be approx. 0.15 Å larger than the distance between the Mn ions in the other dimer [389,531,533]. No evidence

for more extensive structural rearrangements was obtained, arguing against several recently proposed mechanisms based on rearrangements of tetranuclear Mn clusters [478,479,494,495] (see subsections II-B.3 and II-H). However, the S_3-state spectra were all recorded at 170–190 K, temperatures too high to permit observation of the approx. 3.3 Å interaction [389,536,543]. Consequently, if the Mn complex consists of two Mn centers (e.g., two dimers or a trimer plus a monomer) that are located approx. 3.3 Å apart, the currently available data cannot exclude the possibility that the distance between the two Mn centers changes significantly during the $S_2 \rightarrow S_3$ transition.

The S_0 state. Samples possibly trapped in the S_0 state have been prepared by the Klein/Sauer group by illumination at 195 K of samples incubated in darkness with low concentrations of hydroxylamine (40–60 μM) [389,530,532–534]. Prior to illumination, the XANES and EXAFS spectra of the NH_2OH-treated samples were identical to those of samples in the S_1 state. After illumination, the absorption edge shifted approx. 1 eV to lower energies and the EXAFS data showed evidence of structural rearrangements in the Mn environment. The authors proposed that NH_2OH has no effect on Mn in the S_1 state, but reduces Mn in the illumination-induced S_2 state by two electrons, forming the S_0 state. This mechanism for the action of hydroxylamine had been proposed previously on the basis of proton release measurements [560–564] and is consistent with a recent proposal that NH_2OH reduces a redox-active group near Mn [565,566] (see subsection II-G.2). However, in contrast to the findings of the Klein/Sauer group, Penner-Hahn and co-workers find that a similar concentration of NH_2OH reversibly shifts the absorption edge of the S_1 state to lower energies in darkness, without loss of activity [544]. This shift is consistent with reduction of the Mn complex to an 'S_{-1}' state, as proposed based on EPR [488,567] and flash-induced optical absorption measurements [568–571]. However, hydroquinone reversibly shifts the edge to a somewhat greater extent, also without loss of activity, indicating that NH_2OH and hydroquinone either reduce different Mn ions, or that different reduced 'states' of the Mn complex are produced by these two reductants [544]. The discrepancy between the findings of the Klein/Sauer and Penner-Hahn groups may arise from the absence of the extrinsic 24 and 17 kDa polypeptides in the samples of the latter: removal of these polypeptides increases the accessibility of NH_2OH and other reductants to the Mn complex [231,259,271–277].

It remains unclear whether illumination generates the true, physiological, S_0 state in NH_2OH-treated samples. For example, it has been reported that the reduction of Mn by NH_2OH alters the environment of the Mn complex, making it less susceptible to reduction during succeeding S-state cycles [572–574]. It also remains unclear whether oxidation products of NH_2OH contribute to the EXAFS spectrum of the illumination-induced state. Because of these uncertainties, Klein, Sauer and co-workers refer to the NH_2OH-induced state as the 'S_0^*' state [389,530,532–534]. Despite the uncertainties, the differences in the XANES and EXAFS spectra between samples in the S_1 and 'S_0^*' states have led these workers to suggest that one Mn(II) ion is oxidized to Mn(III) during the $S_0 \rightarrow S_1$ transition [389,530,532–534]. The structural rearrangements observed upon formation of the S_0^* state are consistent with this assignment. This interpretation agrees with the previously cited NMR proton relaxation enhancement [524–527], microwave power saturation [551] and spin-lattice relaxation measurements [552] and also with several interpretations of flash-induced optical absorption changes in the ultraviolet, but conflicts with others (see subsection II-D.1). The nature of the state induced by illumination of NH_2OH-treated samples should be further characterized.

II-D. Flash-induced optical absorption changes

II-D.1. Absorption changes in the ultraviolet

Spectra. The S-state transitions are accompanied by optical absorption changes in the ultraviolet that oscillate with a period of four in response to a series of flashes [575–577]. Numerous authors have attempted to quantify these changes and assign them to the individual S-state transitions [178,568,570,578–589]. The procedures are complicated and have been plagued with controversy [570,587,588,590] (for recent reviews, see the discussions in Refs. 557,589). Factors that must be considered are the initial distribution of PS-II centers in the S_1 and S_0 states in dark-adapted samples, an anomalous absorption change on the first flash given to dark-adapted samples that is associated with centers unable to reduce Q_B, the fraction of centers that undergo zero or two transitions in response to single flashes of light and the absorption changes that accompany the formation and reduction of semiquinone anion at the Q_B-site. Interpretations of some earlier investigations [581,582] are now believed to have been misled by the latter [570,584,587,591].

The absorption changes that accompany the $S_0 \rightarrow S_1$, $S_1 \rightarrow S_2$ and $S_2 \rightarrow S_3$ transitions were initially reported to be similar and to consist of broad absorption increases that are maximal near 305 nm and have shoulders near 350 nm [178,579,585]. This work was performed by Dekker, van Gorkom and co-workers, who employed PS II membranes isolated from spinach. Subsequently, Lavergne, working with an algal mutant that lacks PS I and part of the LHC complex, reported that the changes accompanying the $S_2 \rightarrow S_3$ transition are slightly different and somewhat smaller than those

accompanying the $S_1 \rightarrow S_2$ transition [583,584]. He also reported that the absorption changes that accompany the $S_0 \rightarrow S_1$ transition are negligible [583,584]. At the same time, Witt and co-workers, working with PS II preparations isolated from the cyanobacterium *Synechococcus elongatus*, reported spectra for the $S_1 \rightarrow S_2$ and $S_2 \rightarrow S_3$ transitions that were considerably different from those reported by Dekker et al. and by Lavergne [569,570,592]. The spectra of Witt and co-workers had maxima near 340 nm. Witt and co-workers also reported a different spectrum for the $S_0 \rightarrow S_1$ transition. This spectrum had a maximum near 310 nm and its amplitude at 355 nm was at least 3-fold smaller than the spectra of the other two transitions [569,570,586,592]. The spectra obtained by Witt and co-workers were obtained in the presence of 24 μM NH_2OH, which was added to synchronize all centers in the 'S_1' state (see subsection II-G.2). However, the desired synchronization of all centers in the 'S_1' state may not have been achieved; consequently, the examined samples may have contained a mixture of S-states (see discussions in Refs. 557,588,593). Also, because oxidation products of NH_2OH have been reported to alter the reactivity and environment of the Mn complex [572–574] (see subsection II-G.2), the spectra may be partly artifactual. Nevertheless, spectra obtained by Witt and co-workers in the absence of NH_2OH [570] also differed from those obtained with the algal and spinach preparations, suggesting that the absorption changes that accompany the S-state transitions may differ between cyanobacteria and eukaryotes. This suggestion has recently been disputed by Dekker, however [557].

Lavergne recently reported spectra obtained with PS II membranes isolated from spinach [589] (see Fig. 16). These spectra have higher resolution than Lavergne's previous spectra obtained with algal cells [589]. As originally reported by Lavergne [584], the latest spectrum of the $S_2 \rightarrow S_3$ transition is somewhat different than that of the $S_1 \rightarrow S_2$ transition and the absorption changes that accompany the $S_0 \rightarrow S_1$ transition are negligible [589]. The shoulders near 350 nm are clearly resolved in these latest spectra. The controversies surrounding the amplitudes and shapes of the spectra remain unresolved, however. On the basis of recent analyses, Dekker has concluded that the absorption changes that accompany the $S_0 \rightarrow S_1$ transition are at least 50% as large as those that accompany the $S_1 \rightarrow S_2$ and $S_2 \rightarrow S_3$ transitions and that all three spectra are similar, with those of the $S_1 \rightarrow S_2$ and $S_2 \rightarrow S_3$ transitions being essentially indistinguishable in shape or amplitude [557]. Renger and co-workers have recently reported [591] that absorption changes measured for the $S_0 \rightarrow S_1$ transition at 355 nm are smaller than reported by Dekker [557] but larger than reported by Lavergne [588,589]. Finally, Van Gorkom

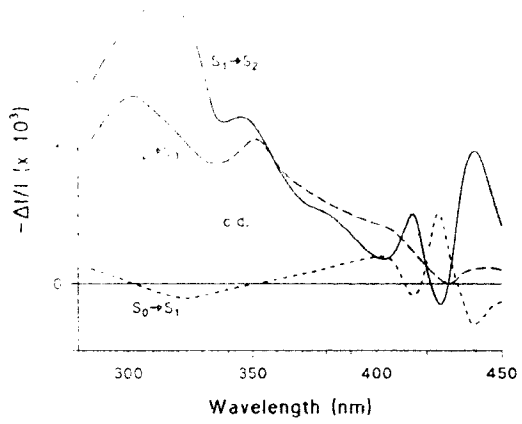

Fig. 16. Optical absorption spectra of the individual S-state transitions obtained with spinach PS II membranes. The dotted curve denoted 'c.d.' is the spectrum of flash-illuminated Ca^{2+}-depleted PS II membranes that had been poised in the dark-stable S_2 state before illumination (reproduced from Fig. 13). Reprinted from Ref. 589.

and co-workers maintain that the absorption changes for all three transitions are similar and have similar amplitudes [594]. (Note, however, that Lavergne's recent work [589] was performed in reply to Dekker [557] and Van Gorkom [594].)

The absorption increases that accompany the $S_0 \rightarrow S_1$, $S_1 \rightarrow S_2$ and $S_2 \rightarrow S_3$ transitions are reversed during the $S_3 \rightarrow (S_4) \rightarrow S_0$ transition [568,570,579,580,583–586,589,590]. Consequently, the optical absorption data have been interpreted in support of mechanisms of water oxidation that involve a concerted oxidation of water during the $S_4 \rightarrow S_0$ transition [557,568,570,579, 580,585,586,590] (see subsection II-H).

Interpretations. Based on comparisons with spectral changes in a binuclear Mn-gluconate complex, Dekker, van Gorkom and co-workers proposed that $S_0 \rightarrow S_1$, $S_1 \rightarrow S_2$ and $S_2 \rightarrow S_3$ transitions each represent the oxidation of one Mn(III) ion to Mn(IV) [178,557,579]. In contrast, Witt and co-workers [569,570,586] and Lavergne [584] proposed that the $S_0 \rightarrow S_1$ transition represents a Mn(II) to Mn(III) oxidation because of the smaller absorption increases which they attributed to this transition. However, some workers (including Lavergne) have cautioned that Mn oxidation states cannot be unambiguously assigned on the basis of optical absorption data alone [584,587,588,591,595–597]. For example, the spectral properties of Mn(II) to Mn(III) oxidations in tri- and tetranuclear μ_3-oxo bridged Mn-carboxylate complexes [595] resemble those of the $S_1 \rightarrow S_2$ and $S_2 \rightarrow S_3$ transitions reported by Dekker et al. and Lavergne. Oxidations of a Mn(II) ion to Mn(III) during the $S_0 \rightarrow S_1$ transition and of a Mn(III) ion to Mn(IV) during the $S_1 \rightarrow S_2$ transition would agree with the interpretations of the X-ray ab-

sorption and magnetic resonance data described in subsection II-C.2. However, the interpretation that a Mn ion is oxidized during the $S_2 \rightarrow S_3$ transition is clearly in conflict. Because the formation of the 130–164 Gauss-wide EPR signal observed in Ca^{2+}-depleted samples was attributed to the oxidation of a histidine residue (see Fig. 13 and subsection II-B.1) it has been proposed that the $S_2 \rightarrow S_3$ transition in native PS-II complexes also corresponds to the oxidation of a histidine residue [452]. This suggestion remains controversial, however (see subsection II-F). Indeed, Lavergne has recently suggested that this transition might correspond to the oxidation of a tryptophan residue [589]. Based on his spectra for the $S_0 \rightarrow S_1$ transition, Dekker has recently suggested that the $S_0 \rightarrow S_1$ transition may correspond to the oxidation of a histidine residue [557].

The rate of electron transfer from Mn to Y_Z^+. The mechanism driving the S-state transitions is the oxidation of Mn by Y_Z^+. The rates of the individual transitions have been determined by time-resolved measurements of optical absorption changes measured in the ultraviolet. Dekker, Van Gorkom and co-workers obtained halftimes of 30, 110, 350 and 1300 μs for the $S_0 \rightarrow S_1$, $S_1 \rightarrow S_2$, $S_2 \rightarrow S_3$ and $S_3 \rightarrow (S_4) \rightarrow S_0$ transitions, respectively [580] and subsequent authors have obtained similar values [480,570,582]. These values are consistent with those measured for the decay of Y_Z^+ in time-resolved EPR experiments [60,598–601] and in experiments involving measurements of electroluminescence [602] (also see Ref. 603). As might be expected from electrostatic considerations, the rate of electron transfer from Mn to Y_Z^+ decreases as the number of oxidizing equivalents that are stored in the water-oxidizing complex increases. The temperature-dependence of the S-state transitions has been determined by EPR [392,482], thermoluminescence [481,989] and optical absorption [480,591] measurements. Activation energies [480,591] and entropies [480] have been reported. The $S_1 \rightarrow S_2$ transition takes place at much lower temperatures (135–140 K) than the other transitions (220–235 K) [392,481,482]. The higher temperatures required for the other S-state transitions have been suggested to correlate with proton release or structural rearrangements that accompany all S-state transitions except the $S_1 \rightarrow S_2$ transition [38,481,482] (see subsections II-E and II-H).

II-D.2. Absorption changes in the visible and near-infrared

Flash-induced optical absorption changes in the visible [178,568,571,579,584,585,589,590,604–608] and possibly the near infrared [609] (see below), are also associated with the S-state transitions. Like those in the ultraviolet, these changes oscillate with a period of four in response to a series of flashes. The absorption changes in the visible have been attributed to electrochromic shifts of absorption bands of carotenoids or chlorophyll *a*: an apparent shift of a carotenoid band was observed at 514 nm [605], an apparent red-shift of the chlorophyll *a* Soret band was observed near 435 nm [178,579,584,589,604,608] (see Fig. 16) and an apparent blue-shift of other chlorophyll *a* transitions was observed near 680 nm [568,571,607,608]. The magnitudes of these shifts were observed to be maximal, but opposite in direction, during the $S_1 \rightarrow S_2$ and $S_3 \rightarrow (S_4) \rightarrow S_0$ transitions. A smaller shift, opposite in direction to that associated with the $S_1 \rightarrow S_2$ transition, was reported for the $S_0 \rightarrow S_1$ transition and a negligible shift was reported for the $S_2 \rightarrow S_3$ transition (see Refs. 585,589,590 in particular). The magnitudes of these shifts (at least those near 435 nm) have recently been shown to depend strongly on pH [559]. The shift associated with the $S_0 \rightarrow S_1$ transition appears to be maximal below pH 5.5, while that associated with the $S_1 \rightarrow S_2$ transition appears to be maximal near pH 7.75 [559]. These electrochromic shifts have been attributed to the creation an uncompensated positive charge (or pH-dependent fraction of charge, see subsection II-E) in the water-oxidizing complex during the $S_1 \rightarrow S_2$ transition [568–571,584,605,607,608] (see also the discussions in [585,589,590]). Because the uncompensated charge appears to be present primarily in the S_2 and S_3 states, it has been proposed that deprotonation events compensate for positive charge formed during the $S_0 \rightarrow S_1$ and $S_2 \rightarrow S_3$ oxidations, but not for a charge or fraction of charge formed during the $S_1 \rightarrow S_2$ oxidation [568–571,584,592,605,607] (for further discussion, see subsection II-E). The absence of a deprotonation event during the $S_1 \rightarrow S_2$ transition has been proposed to account for why this transition occurs at temperatures considerably lower than those required for the other transitions [480–482]. A strong electrochromic shift near 435 nm during the $S_2 \rightarrow S_3$ transition has recently been reported in Ca^{2+}-depleted samples [452] (see Fig. 16). On the basis of this observation, it has been proposed that the deprotonation event normally associated with the $S_2 \rightarrow S_3$ transition is prevented in the absence of Ca^{2+} [452]. The presence of uncompensated positive charge on or near the Mn complex in the S_2 and S_3 states has been proposed to account for why Cl^- ions appear to bind more strongly in the S_2 and S_3 states than in the S_0 or S_1 states [610] (see subsection III-D).

Optical absorption changes in the near infrared that are associated with the S-state transitions have been attributed to intervalence electronic transitions within a mixed-valent Mn cluster [609,611]. The optical spectrum corresponding to the S_2 state has been reported to extend out to 1050 nm and to have a maximum at 780 nm [609]. However, this assignment has been challenged and the spectral changes have been attributed instead to changes in sample scattering [608].

The rate of electron transfer from Y_Z to P680$^+$. In oxygen evolving samples, this electron transfer rate has been determined from chlorophyll *a* fluorescence measurements [612–614] and from optical absorption changes in the near infrared at 820–837 nm [615–618] and in the visible at 680–688 nm [617,619]. Under multiple flash conditions (conditions where the four S-states are equally populated), the rate was found to be multiphasic [615–617,619]. In approx. 70% of PS-II centers, halftimes of approx. 25 ns, approx. 50 ns, and approx. 300 ns were observed, while in approx. 30% of centers, halftimes of approx. 5 μs, approx. 35 μs, and approx. 200 μs were observed [617]. Subsequent measurements utilizing single flashes found that the rate has a halftime of approx. 20 ns when the water-oxidizing complex is in the S_0 and S_1 states and to have components of approximately equal magnitude with halftimes of approx. 40 and approx. 280 ns when the water-oxidizing complex is in the S_2 and S_3 states [618,620]. The approx. 5 μs and approx. 200 μs components were attributed to inactive centers (the latter to charge recombination between Q_A^- and P680$^+$), but the magnitude of the approx. 35 μs component was found to be S-state-dependent and to be maximal in the S_2 and S_3 states [621]. An involvement of the approx. 35 μs component in oxygen-evolving centers was suggested [621]. However, in more recent studies this component has been attributed to inactive PS-II centers [382,622]. It has been suggested to arise from the reduction of a monomeric Chl$^+$ molecule rather than of P680$^+$ [623] and its apparent S-state dependence has been suggested to be artifactual [382]. The presence of an uncompensated positive charge (or fraction of charge) on or near the Mn complex in the S_2 and S_3 states has been postulated to account for why the rate of electron transfer from Y_Z to P680$^+$ is slower in the S_2 and S_3 states than in the S_0 or S_1 states [569,618,620].

Treatments that perturb or extract the Mn complex eliminate the nanosecond components of the electron transfer reaction. These treatments include incubation with Tris or NH_2OH [383,384,615,616,624–627], extraction of Ca^{2+} [487] (see also Ref.628), or partial digestion with trypsin [629,630]. Treatment with 600–660 mM acetate, which reversibly inhibits oxygen evolution [631] and competes with Cl^- for a site possibly on the Mn complex [439] (see subsections II-G.1 and III-D), slows the reaction to 160–170 μs [631–633]. (It should be noted that retardation of electron transfer from Y_Z to P680$^+$ is apparently not a characteristic of all treatments that inhibit oxygen evolution [634].)

The temperature-dependence [635] and pH-dependence [620,622] of electron transfer from Y_Z to P680$^+$ have been examined in oxygen evolving samples, as well as in Mn-depleted samples [383,384,625,627,629, 636,637]. The reaction's activation energy is substantially greater in Mn-depleted [636] than in oxygen-evolving [635] samples (approx. 46 kJ/mol vs. approx. 10 kJ/mol). Based on the activation energy measured in oxygen-evolving samples, a reorganization parameter of 450–600 mV was estimated for the reaction from classical Marcus electron transfer theory [638]. In oxygen evolving samples, as the pH was lowered from pH 6.5 to pH 4, the rate of the reaction in the S_1 state slowed from approx. 20 ns to 40–50 ns [620]. Concurrently, the ratio of the approx. 40 ns phase to the approx. 280 ns phase in the S_2 state decreased to near zero [620] and the fraction of centers with rates in the μs time range increased from approx. 31% to approx. 77% [622]. To account for these data, the presence of an acidic group with a pK_a of 5.3 near the Mn complex was postulated [620]. The presence of an acidic group with a pK_a of 5.8–6.0 has also been proposed on the basis of the pH-dependence of the rates of Y_D oxidation and Y_D^+ reduction by the Mn complex [122]. Also, the presence of an acidic group with a pK_a of 6.05 has been postulated based on recent measurements of the pH-dependence of proton release [559] (see subsection II-E).

II-E. Proton release accompanying the S-state transitions

On the basis of the S-state-dependences of electrochromic shifts of optical absorption bands and the rate of P680$^+$ reduction (see subsection II-D.2), the stoichiometry of protons released from the water-oxidizing complex per P680 during the S-state oxidations was proposed to be 1:0:1:2 for the $S_0 \rightarrow S_1$, $S_1 \rightarrow S_2$, $S_2 \rightarrow S_3$ and $S_3 \rightarrow (S_4) \rightarrow S_0$ transitions, respectively [568–570,584,605,607,618]. This proposed pattern of 'intrinsic' proton release was found to coincide with direct measurements of the stoichiometry of protons released into solution during the S-state transitions; a stoichiometry of 1:0:1:2 for 'extrinsic' proton release was determined by several groups on the basis of measurements with sensitive glass electrodes [639], pH-sensitive dyes [564,574,640–645], or an EPR spin probe [646]. Measurements of delayed fluorescence as a function of S-state were interpreted as being qualitatively consistent with this stoichiometry [647,648].

However, on the basis of a new interpretation of proton release measurements and newer data, the measured proton release stoichiometry in intact preparations has recently been determined to be non-integer [559,649–651] and to depend on pH [559,651]. At pH 6.5, the stoichiometry was determined to be 1.2:0.2:0.95:1.65 for the $S_0 \rightarrow S_1$, $S_1 \rightarrow S_2$, $S_2 \rightarrow S_3$ and $S_3 \rightarrow (S_4) \rightarrow S_0$ transitions, respectively [559]. As the pH was increased from pH 5.5 to pH 8, the number of protons released during the $S_0 \rightarrow S_1$ transition decreased from 1.75 to 1, the number of protons released during $S_1 \rightarrow S_2$ transition increased from 0 to 0.5, and

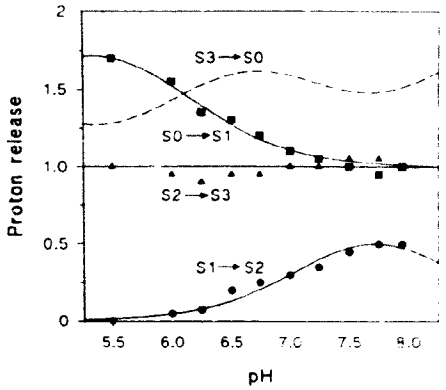

Fig. 17. The pH-dependence of the number of protons released into solution per P680 during the individual S-state transitions. The solid lines represent a fit of the data points to a model involving pK_a shifts or deprotonations of four separate groups located on or near the Mn complex. The dashed curve, representing the stoichiometry of proton release during the $S_3 \rightarrow (S_4) \rightarrow S_0$ transition, was calculated by assuming that four protons are released during each S state cycle. Reprinted from Ref. 559 with permission (copyright 1991 by the American Chemical Society).

the number of protons released during the $S_2 \rightarrow S_3$ transition remained close to 1 [559,651] (see Fig. 17). Earlier interpretations of proton release data are believed to have been misled by an expectation of an integer stoichiometry [559,649,650]. Some earlier work is also believed to have been misled by a transient alkalinization of the narrow external partitions that exist between appressed thylakoid membranes [559, 649,650]. This transient alkalinization was caused by proton uptake in response to the reduction of Q_B. The superposition of this alkalinization on the acidification caused by proton release created a slow phase of acidification that was ignored in earlier measurements. Correcting some earlier data [643] for this alkalinization yields the non-integer stoichiometry observed in recent studies [651]. The non-integer and pH-dependent stoichiometry of proton release has been interpreted in terms of a combination of specific deprotonations and electrostatically-induced pK_a shifts of protonatable amino-acid residues [559,649–651]. As a precedent for this interpretation, it has been pointed out [559,649–651] that non-integer and pH-dependent proton binding is associated with the single electron reductions of Q_A and Q_B in reaction centers from purple non-sulfur bacteria, and that these data have also been explained in terms of pK_a shifts of several near-by amino-acid residues [652–654] (also see Ref. 82).

The pH-dependences of the electrochromic shifts that accompany the $S_0 \rightarrow S_1$ and $S_1 \rightarrow S_2$ transitions correlate with the pH-dependences of the fractional numbers of protons released on these transitions [559]. Consequently, the agreement between the apparent intrinsic proton release pattern estimated from electrochromic shifts and the measured extrinsic proton release pattern still appears to hold. However, whether either pattern represents deprotonation events at the water oxidizing complex, or even in its vicinity, is under debate (see below). Furthermore, it has been argued that the proton release stoichiometry cannot be deduced solely from electrochromic shifts [559].

According to one view, the extrinsic proton release stoichiometry measured in intact samples reflects deprotonation events in the immediate vicinity of the water oxidizing complex and includes individual deprotonations and pK_a shifts of amino acid residues that are closely associated with the Mn complex [559]. At least four distinct protonatable groups are postulated to be involved [559]. Two of these groups are proposed to have pK_a values of 6.05 and 8.2 in the S_0 state [559]. As mentioned in subsection II-D.2, an acidic group with a pK_a of 5.8–6.0 has previously been proposed to influence electron transfer between Y_D and the Mn complex [122]. The numbers of protons released per P680 during the $S_0 \rightarrow S_1$ and $S_1 \rightarrow S_2$ transitions are proposed to result from changes in the pK_a values of at least three groups caused by electrostatic interactions with the Mn complex [559]. However, one proton released during the $S_0 \rightarrow S_1$ transition may correspond to a deprotonation of the Mn complex itself (J. Lavergne, personal communication). The proton released during the $S_2 \rightarrow S_3$ transition is proposed to result solely from the deprotonation of a specific residue; because no significant electrochromic shift accompanies the release of approximately one proton per P680 during this transition, it is proposed that an amino-acid residue rather than the Mn complex is oxidized during this transition [559]. This residue is suggested to have a pK_a of ≤ 9.5 in its reduced form and ≥ 3.5 in its oxidized form [559].

An alternate view is that the extrinsic proton release stoichiometry measures protons contributed by several sources and does not necessarily reflect deprotonation events at the water oxidizing site [508,569,571,574,596, 597,645,651,655–659]. It has been suggested that the protons released by water oxidation may equilibrate slowly with the external aqueous phase during the time scale of the proton release measurements [569,655, 656,659]. Consequently, the measured protons could arise from amino acid pK_a shifts that are indirectly caused by events at the water oxidizing site [571,574, 596,597,645,659]. Such residues could be located far from the Mn complex [597,645]. The pK_a values of such residues could change in response to the conformational rearrangements of the Mn complex that are believed to accompany the S-state transitions (see subsection II-G.1). Such pK_a changes of amino-acid

residues located far from the Mn complex may also contribute to the uncompensated positive charge in the S_2 and S_3 states that gives rise to the S-state-dependent electrochromic shifts and P680$^+$ reduction kinetics that were attributed to 'intrinsic' deprotonation events [597,645]. Consequently, the intrinsic and extrinsic proton release patterns could be different manifestations of a single phenomenon that does not directly reflect deprotonation events at the water oxidizing site.

If the measured proton release pattern is only indirectly related to deprotonation events at the water oxidizing site, the pattern should be sensitive to changes in the structure of PS II. Indeed, the pattern changes significantly when PS II membranes are purified to remove the extrinsic 24 and 17 kDa polypeptides and the LHC polypeptides [657,658] or are treated with trypsin [657,659]. A proton release stoichiometry of 1:1:1:1 was recently observed in thylakoid membranes from pea plants that were grown under intermittent light and that consequently lacked the LHC polypeptides [651,660]. On the basis of these data, it was suggested that (i) one proton is released from a specific group near the Mn complex during each of the $S_0 \rightarrow S_1$, $S_1 \rightarrow S_2$ and $S_2 \rightarrow S_3$ transitions, (ii) four protons and four electrons are abstracted from H_2O during the $S_3 \rightarrow (S_4) \rightarrow S_0$ transition, (iii) three of the protons that are released from H_2O during the $S_3 \rightarrow (S_4) \rightarrow S_0$ transition reprotonate the groups that had been deprotonated during the other transitions and (iv) the LHC polypeptides modulate proton release from the water oxidizing complex, imposing the pH-dependent, non-integer stoichiometry that is actually measured [651]. The involvement of LHC polypeptides in directing protons from the water oxidizing complex to the lumen will be discussed later in this subsection.

However, those workers who argue that the extrinsic proton release stoichiometry reflects deprotonation events at the water oxidizing site offer a different interpretation for the 1:1:1:1 stoichiometry observed in samples that lack the LHC polypeptides. According to this alternate interpretation, the absence of the LHC polypeptides exposes additional protonatable amino-acid residues near the Mn complex to the aqueous phase [559]. Deprotonation of these additional residues neutralizes charge accumulation in the vicinity of the water oxidizing complex caused by the S-state oxidations, giving rise to the altered proton release stoichiometries observed in these [559] and in trypsin-treated preparations. The debate over whether the extrinsic proton release stoichiometry measured in native samples directly reflects deprotonation events at the water oxidation site remains unresolved.

The rates at which protons are released during the individual S-state transitions have been reported [564,643,645]. Except for the $S_3 \rightarrow (S_4) \rightarrow S_0$ transition, these rates do not correspond to the rates at which the Mn complex is oxidized by Y_Z^+ (see subsection II-D.1) [564,643]. Proton release halftimes of 250 μs, 200 μs and 1.2 ms were estimated for the $S_0 \rightarrow S_1$, $S_2 \rightarrow S_3$ and $S_3 \rightarrow (S_4) \rightarrow S_0$ transitions in thylakoid membranes [564,643] and similar values were reported in PS II membrane fragments [645]. For the $S_0 \rightarrow S_1$ transition, the reported rates of proton release are slower than the rate of reduction of Y_Z^+ by the Mn complex. For the $S_2 \rightarrow S_3$ transition, however, the reported rates of proton release are faster than the rate of reduction of Y_Z^+ (200–250 μs for proton release [564,643,645] compared to 350–450 μs for the reduction of Y_Z^+ [480,570,580,582]). This result was explained in terms of a deprotonation of an acidic group near Y_Z [564,643]. However, the proton release halftimes measured in thylakoid membranes need to be reevaluated. It is now believed that the extent of proton release during each S-state transition was underestimated in these studies because of the transient alkalinization of the narrow external partitions between appressed thylakoid membranes [559,649,650]. These underestimates of the extent of proton release would have led to erroneous estimations of the proton release halftimes. These halftimes are now being remeasured in completely unstacked thylakoid membranes (P. Jahns and W. Junge, personal communication). In such preparations, the halftime of proton release during the $S_2 \rightarrow S_3$ transition remains faster than the rate of Y_Z^+ reduction (P. Jahns and W. Junge, personal communication). The kinetics of proton release are also being examined by time-resolved studies of the electrochromic shifts that accompany the S-state transitions (J. Lavergne, personal communication).

Covalent modification of stacked thylakoid membranes with *N,N'*-dicyclohexylcarbodiimide (DCCD) appears to interfere with normal proton release: instead of being released to the lumen, protons released by the water-oxidizing complex appear to be taken up at the Q_B site, diminishing the proton uptake from the external phase that is associated with reduction of Q_B [661–663]. Modification with [^{14}C]-DCCD results in the derivatization of polypeptides of 20–28 kDa [661,663]. These polypeptides have been identified as LHC polypeptides, although some of them are believed to be associated with PS I [663]. Consequently, it has been proposed that some LHCII polypeptides play a role in channeling protons from the water-oxidizing complex to the lumen [660,663]. As noted above, the measured proton release stoichiometry changes dramatically in the absence of these polypeptides [651,657,658]. Interestingly, the binding of Ca^{2+} ions to some LHC polypeptides interferes with proton release in the same fashion as DCCD (P. Jahns and W. Junge, personal communication).

II-F. The possible oxidation of histidine

II-F.1. Samples depleted of Ca^{2+}, Cl^- or manganese

As mentioned earlier (see subsection II-B.1), the 130–164 Gauss-wide EPR signal observed in Ca^{2+}-depleted and Cl^--depleted samples has been proposed to arise from an oxidized organic component that is magnetically coupled with the modified S_2-state Mn complex [447,448,452,454,484,486,487]. Based on the ultraviolet absorption spectrum that accompanies the oxidation of the modified S_2 state in Ca^{2+}-depleted samples (see Fig. 13), this organic component was proposed to be a histidine radical [452]. Specifically, the spectrum in Ca^{2+}-depleted samples was found to be similar [452] to that generated by the covalent addition of a hydroxyl radical to histidine in water at pH 9.2 [664]. It was suggested that the resulting histidine-$OH^{\cdot}$ radical might represent an intermediate of water-oxidation [452] (see subsection II-H). Similarities between optical absorption spectra generated in biological samples and with model compounds should be interpreted with caution, however. For example, earlier comparisons of such spectra [178,637,665] were interpreted in support of earlier proposals that Y_Z^+ and Y_D^+ are quinone cation radicals. Specific deuteration experiments subsequently demonstrated that Y_D^+ is a tyrosine radical [62–64] and directed mutagenesis studies subsequently identified Y_D and Y_Z as specific tyrosine residues of the D1 and D2 polypeptides [65–68]. Also, it should be emphasized that the spectrum that was compared to the spectrum generated in the Ca^{2+}-depleted samples was that of a covalent $OH^{\cdot}$ adduct of histidine, not that of an unmodified histidine radical. In fact, the spectrum represents a mixture of different histidine-$OH^{\cdot}$ radicals [664,666]. In one study it was concluded that the spectrum corresponds to at least three different radical species [666]. These correspond to the addition of the hydroxyl radical to different positions on the imidazole ring [664,666].

It has recently been suggested that the optical absorption changes that accompany the oxidation of the modified S_2 state in Ca^{2+}-depleted and Cl^--depleted samples may arise from Y_Z^+ [456] (although the possibility of tyrosine oxidation was earlier dismissed by Rutherford and co-workers [452]). It was proposed that the 130–164 Gauss-wide EPR signal observed in these samples arises from an interaction between Y_Z^+ and the modified S_2-state Mn complex [456]. This assignment is based on two observations: first, the 130–160 Gauss-wide and Y_Z^+ signals both decay with the same kinetics in the same samples at room temperature and second, both signals can reportedly be generated by illumination at 10 K after having been allowed to decay at 77 K for one week [456]. (Illumination at 10 K allows only a single charge separation to occur). However, if the 130–164 Gauss-wide signal arises from an organic radical that is magnetically coupled to the Mn complex, as was previously proposed [447,448,452,454,484,486,487], it seems unlikely that both the 130–164 Gauss-wide and Y_Z^+ signals would be present at 10 K, as reported [456]. Instead, the signal of Y_Z^+ should vanish, as does the signal of $Pheo^-$ when it interacts with the $Q_A^- Fe^{2+}$ complex to yield a doublet with a 40–60 Gauss-wide splitting that is visible at temperatures below 15 K [97,98,108,415,667,668]. In one version of the recent proposal, the modified S_2-state Mn complex gives rise to the 130–164 Gauss-wide signal as a result of a perturbation caused by the oxidation of Y_Z [456]. This proposal should be carefully evaluated. Indeed, if the 130–164 Gauss-wide and Y_Z^+ signals are not closely related, it is difficult to understand why they would decay at the same rate at room temperature [456]. (It should be noted that Boussac and Rutherford have recently argued that the signal attributed to Y_Z^+ in the presence of the 130–164 Gauss-wide signal [456] arises from an S_3- state relaxation enhancement of Y_D^+ [999].)

Photooxidation of a histidine residue has recently been proposed to occur Mn-depleted PS II membranes [669–672]. This proposal is based on the observation that the thermoluminescence 'A_T'-band previously observed in Mn-depleted samples [673,674] is reversibly quenched by treatment of Mn-depleted samples with diethylpyrocarbonate (DEPC) under conditions that favor the specific modification of histidine residues [669,671]. (For reviews of thermoluminescence measurements of PS II, see Refs. 675–677). Because the loss of the A_T-band during DEPC treatment [669,671], during photoinhibition [670], or after digestion with trypsin at pH 8 [672] does not correlate with the reported amplitudes of the EPR signals of Y_Z^+ or Y_D^+, it has been concluded that the A_T-band corresponds to charge recombination between Q_A^- and a photooxidized histidine residue [669–672]. This residue is proposed to be oxidized by Y_Z^+ with high quantum efficiency (the amplitude of the A_T-band that can be generated by a single flash is approx. 60% of that generated by multiple flashes and approx. 30% of that generated by continuous illumination [669]). This residue is also proposed to mediate the oxidation of Mn^{2+} during photoactivation [670,672]. Consequently, illumination is proposed to generate both Y_Z^+ and the oxidized histidine residue in the same Mn-depleted PS-II centers [669,672].

There appear to be several problems with assignment of the A_T-band to charge recombination involving an oxidized histidine residue, however. First, no EPR signal appears to be associated with the putative histidine radical [670–672,674]. Second, from the rate that $P680^+$ is reduced following each of two closely-spaced saturating flashes, both Mn-depleted PS-II membranes [383,624,625] and PS II complexes that lack functional Mn [678,679] have been shown to contain

only a single electron donor (Y_Z) to $P680^+$ and not two donors (Y_Z plus histidine), as is now proposed [669–672]. Both EPR [348,627,680,681] and optical absorption [68,178,179,637,665] studies have identified the single electron donor as Y_Z (also see Ref. 123). Finally, in the absence of exogenous electron donors or acceptors, 75% of the Q_A^- and Y_Z^+ generated by a single flash in Mn-depleted PS II particles decay with identical half-times, presumably by charge recombination [68]. Consequently, any donor to Y_Z^+ in Mn-depleted PS II preparations must be oxidized with a relatively low quantum yield.

The A_T-band had previously been assigned to charge recombination between Q_A^- and Y_Z^+ [673]. The involvement of Y_Z^+ in the charge recombination reaction that gives rise to the A_T-band had been suggested even earlier [682]. If these earlier assignments are correct, the quenching of the A_T-band by treatment with DEPC [669,671] could have resulted from an alteration of the redox potential of Y_Z (or of the quinone electron acceptors) in response to the chemical modification of nearby histidine residues. For example, if His-190 of the D1 polypeptide forms a hydrogen bond with Y_Z as recently proposed [35,65,114,116,122], then derivatization of His-190 with DEPC would be expected to significantly alter the redox properties of Y_Z. Changing His-190 to Gln or Asp by site-directed mutagenesis slows the oxidation of Y_Z by $P680^+$ by a factor of approx. 200 [17,19]. The conclusion that Y_Z^+ is not affected by treatment with DEPC [669,671] or by photoinhibition with intense yellow light [670] needs to be further substantiated. The observation of a low-field shoulder on an EPR signal that is centered at $g = 2$ [670] is not unambiguous proof for the presence of Y_Z^+. Light-induced radicals other than Y_D^+ have been observed in samples that lack Y_Z (e.g., samples that had been photoinhibited with weak white light [683] or samples in which the Y_Z tyrosine residue had been changed to phenylalanine [684]). These signals were attributed to a carotenoid radical [683] and to an unidentified oxidized amino-acid residue [684], respectively. In Mn-depleted samples that have been digested with trypsin at pH $\geq$ 7.4, the reduction of Y_Z^+ is greatly accelerated compared to its reduction rate in undigested Mn-depleted samples [629,630,665]. The instability of Y_Z^+ in such samples does not interfere with the ability of Y_Z to function in steady-state electron transfer assays [237,672] nor prevent the EPR signal of Y_Z^+ from being photoaccumulated in the presence of electron acceptors [672]. Nevertheless, the instability of Y_Z^+ in samples digested with trypsin at pH 8 [672] might explain the lack of an A_T band in such samples if the A_T-band arises from charge recombination involving Y_Z^+. Finally, the possibility that DEPC modifies the stability of Y_D^+, rendering it easily confused with Y_Z^+, must be considered. Unfortunately, only light-induced EPR signals were reported in the one study that presented EPR spectra of DEPC-modified samples [671]. An unambiguous assignment of the A_T-band in Mn-depleted samples will require that this band be correlated with changes in EPR and optical absorption spectra.

It should be noted that the EPR and optical studies which demonstrated that Y_Z is the only donor to $P680^+$ in Mn-depleted samples were performed at room temperature. The A_T-band is formed maximally by illumination at approx. 250 K [674]. The reduction of $P680^+$ by Y_Z is more drastically affected by temperature in Mn-depleted [636] than in oxygen-evolving [635] preparations. Because of the slower donation by Y_Z, the reduction of $P680^+$ in Mn-depleted samples at temperatures below 270 K has been described in terms of a competition between electron donation by Y_Z and Q_A^-; no other electron donors were invoked [636]. Nevertheless, it would be worthwhile to ascertain by EPR or optical absorption measurements whether a component other than Y_Z (e.g., an amino-acid residue) becomes oxidized in a fraction of Mn-depleted PS-II centers at temperatures near 250 K. Such a component might give rise to the A_T-band even if it were oxidized in only a small fraction of PS-II centers, provided that the A_T-band does not arise from charge recombination involving Y_Z^+.

II-F.2. Native samples

The optical absorption spectrum that accompanies the oxidation of the modified S_2 state in Ca^{2+}-treated samples [452] (Fig. 13) resembles the spectra reported by Dekker (e.g., Ref. 557) and Lavergne (e.g., Ref. 589) for the $S_2 \rightarrow S_3$ transition in untreated samples. A major difference, however, is that the shoulder near 350 nm is missing in the spectrum of Ca^{2+}-depleted samples [452] (see Fig. 16). Because of the similarities between the two spectra, Rutherford and co-workers proposed that histidine is oxidized during the $S_2 \rightarrow S_3$ transition in native samples [452]. This proposal would explain the apparent lack of Mn oxidation during the $S_2 \rightarrow S_3$ transition found in the X-ray absorption [389,411,530,531,533,534], NMR [524–527] and EPR [551,552] experiments (see subsection II-C.2). The differences between the two spectra, most notably the absence of the shoulder near 350 nm in the spectrum of Ca^{2+}-depleted samples, were attributed either to artifacts introduced by the deconvolution procedures that were employed to determine the $S_2 \rightarrow S_3$ spectrum in the untreated samples, or to structural changes that resulted from the removal of Ca^{2+} [452]. Problems with the deconvolution procedures appear to have been ruled out by recent optical absorption measurements reported by one of these authors [589] (see Fig. 16). However, as mentioned in subsection II-C.1, based on X-ray absorption edge measurements, extraction of

Ca^{2+} appears to alter the structure of the Mn environment, at least when Ca^{2+} is extracted with sodium citrate at pH 3 [424] (M.J. Latimer, V.J. DeRose, V.K. Yachandra, I. Mukerji, K. Sauer and M.P. Klein, personal communication).

In contrast to the arguments of Rutherford and co-workers, Dekker has argued that the presence of the shoulder at 350 nm in the spectrum of untreated samples indicates that Mn, not histidine, is normally oxidized during the $S_2 \rightarrow S_3$ transition [557]. Furthermore, Lavergne has recently suggested that the absorption changes that accompany this transition in untreated samples might correspond to the oxidation of a tryptophan residue [589]. Consequently, the controversy over whether the same component is oxidized in both native and Ca^{2+}-depleted samples during the $S_2 \rightarrow S_3$ transition remains unresolved. It has recently been suggested that the putative histidine residue and the Mn complex may normally be in redox equilibrium, with oxidation of the histidine residue being favored at the cryogenic temperatures that were employed for the EPR and X-ray absorption measurements and oxidation of the Mn complex being favored at the ambient temperatures that were employed for the optical absorption measurements [557,571] (G.T. Babcock, personal communication). This suggestion does not account for the NMR data, however, which were recorded at room temperature and have been interpreted as favoring no oxidation of manganese during the $S_2 \rightarrow S_3$ transition [524–527] (see subsection II-B.2).

To summarize, the evidence that a histidine residue is oxidized during the $S_2 \rightarrow S_3$ transition in native PS II complexes, or even in samples depleted of Ca^{2+}, Cl^-, or manganese, is far from conclusive. The recent proposals: that a tryptophan residue may be oxidized during this transition in native samples [589], that the manganese complex may be in redox equilibrium with an aromatic amino-acid residue [557,589] and that the 130–164 Gauss-wide EPR signal arises from an interaction between Y_Z^+ and a modified S_2-state of the Mn complex [456], all warrant further study.

II-G. Substrate analogues and the site of water oxidation

II-G.1. Amines

Many primary amines (ammonia, methyl amine, *tert*-butylamine, Tris, 2-amino-2-ethyl-1,3-propanediol), at low concentrations, are reversible inhibitors of water oxidation [437–439,685–689]. Their effectiveness as inhibitors is proportional to their nucleophilicity [439,689], suggesting that they act as Lewis bases to displace H_2O or other ligands from Mn [689]. Ammonia had previously been proposed to compete with substrate H_2O for a site on Mn [687]. The binding of amines is purely competitive with Cl^- in steady-state inhibition studies [437–439]. Because Cl^- is required for oxygen evolution [472,685] (for review see Refs. 38,270,690,691), these results have been interpreted as indicating that amines displace Cl^- from a site located on the Mn complex [437–439]. From experiments that were performed with electron acceptors having different efficiencies, it was proposed that amines bind to this site in the S_2 or S_3 states [439]. Ammonia is unique among amines in that its binding is not purely competitive with Cl^- [438]. This finding has been interpreted as demonstrating that NH_3 binds to a second site on the Mn cluster, a site that sterically excludes amines larger than NH_3 and which does not bind Cl^- [438,439]. Because NH_3 is isoelectronic with H_2O [687], this second NH_3-specific site has been proposed to be a binding site for substrate H_2O [438,439].

If amines bind to the Mn complex, they should alter its magnetic properties. Indeed, microwave power saturation studies of Y_Z^+ have shown that amines disrupt the magnetic interaction between Mn and Y_Z^+ and that the extent of the disruption increases with the size of the amine [689]. Disruption is minimal for NH_3, however [688]. Studies of the S_2-state manganese EPR signals have found two coordination sites for NH_3 either on or near the Mn complex. One site is specific for NH_3 [427] and methylamine [428]. The extent of binding of NH_3 and methylamine to this site correlates inversely with the concentration of Cl^- [428,435,436]. Coordination occurs in the S_1 state and, with higher affinity, in the S_2 state [427,436]. Coordination stabilizes the S_2-state $g = 4.1$ EPR signal with respect to the multiline signal [427–429,435,436]. In the presence of 30% ethylene glycol, the enhanced $g = 4.1$ signal is identical to that produced by illumination of untreated samples at 130 K [427,428]. However, in the presence of 0.4 M sucrose [436,442] or in the absence of cryoprotectant [429], the signal narrows from approx. 360 Gauss to approx. 300 Gauss and shifts to g approx. 4.2. As discussed earlier (see subsection II-B.1), oriented NH_3-treated samples, prepared in the presence of 0.4 M sucrose, display approx. 16 partially resolved hyperfine lines spaced by approx. 36 Gauss [402,420]. Because Cl^- decreases the binding of NH_3 and methylamine to the site responsible for these alterations of the $g = 4.1$ EPR signal [428,435,436], this site has been equated with the Cl^- site identified in the steady-state inhibition studies mentioned above [428,436]. Indeed, the NH_3-induced resolution of hyperfine lines on the $g = 4.1$ EPR signal has been suggested to represent direct coordination of NH_3 to a Cl^- site on the Mn complex [402], as was concluded in the steady-state inhibition studies [437–439]. There are difficulties with equating the Cl^- sites identified by EPR and steady-state inhibition studies, however. First, many more amines interact with the Cl^- site in the steady-state inhibition studies [437–439] than in the EPR studies [427,428]. Second, NH_3 stabilizes the $g = 4.1$ signal at

concentrations that are considerably below those required to inhibit steady-state oxygen evolution [427].

The second NH_3-binding site identified in EPR studies is specific for NH_3 [427] and does not bind Cl^- [427,429,436,446]. Consequently, it has been equated with the Cl^--insensitive, NH_3-specific site identified in the steady-state inhibition studies. This site has a lower affinity for NH_3 than the Cl^--sensitive site [427,428, 436,442]. It binds NH_3 in the S_2 state, resulting in an altered multiline EPR signal having more lines and narrower hyperfine splittings (67.5 vs. 87.5 Gauss) than the unmodified signal [414,427–429,436,442,443 445,446] (see Fig. 9). The alteration of the hyperfine spacings was interpreted as demonstrating direct coordination of the Mn complex by one or more NH_3-derived ligands in the S_2 state [427,443] and a specific model for NH_3 binding involving formation of μ_2-imido bridges in the S_2 and S_3 states was proposed [444]. Electron Spin-Echo Envelope Modulation (ESEEM) experiments with $^{15}NH_3$ and $^{14}NH_3$ have confirmed that a single NH_3-derived ligand coordinates the Mn complex in the S_2 state [446,554]. On the basis of these data, an amido (NH_2) bridge between two Mn ions, or between one Mn and one Ca^{2+} ion, has been proposed [446,554]. The exchange of NH_3 into the coordination sphere of the Mn complex in the S_2 state has been shown by EPR studies to take place at temperatures as low as 198 K [429], accounting for earlier reports of coordination of NH_3 to this site in the S_1 state [436,442,445]. Because NH_3 and H_2O are isoelectronic, evidence for direct coordination of Mn by a NH_3-derived ligand has been taken as evidence for direct coordination of the Mn complex by substrate H_2O [427,428,438,439,443,446]. Indeed, because NH_3 exchanges into the coordination sphere of the Mn complex in the S_2 state and because H_2O is a weaker nucleophile than NH_3, substrate H_2O has been proposed to exchange into the coordination sphere of the Mn complex at the Cl^--insensitive NH_3-specific binding site in the more electron deficient S_3 state [427,428,443,478,567].

The hyperfine lines of the S_2-state multiline EPR signal are slightly broadened by $H_2^{17}O$ [436,457]. This broadening suggests direct coordination of Mn by ^{17}O, although a subtle alteration in the Mn environment caused by protein structural changes induced by replacing the solvent with $H_2^{17}O$ cannot be excluded. Direct coordination of Mn by ^{17}O could occur either by direct coordination of Mn by substrate $H_2^{17}O$, or by exchange of $H_2^{17}O$ into structural μ_2-oxo or μ_2-hydroxo bridges [30,31,428,496], as occurs in model compounds [692]. The NH_3-altered multiline signal is also broadened by $H_2^{17}O$ [436,445]. This could indicate that NH_3 exchanges only into a single substrate H_2O site in the S_2 state, or that either $H_2^{17}O$ or NH_3 (or both) exchange into structural μ_2-oxo bridges and not into substrate H_2O sites. Narrowing of the multiline hyperfine lines by ^2H_2O (observed by one group [458], but not by two others [396,399]) and recent ESEEM measurements conducted with ^2H_2O in the presence and absence of NH_3 [554], are also consistent either with direct coordination of the Mn complex by ^2H_2O, or with exchange of ^2H_2O into μ_2-hydroxo bridges. Exchangeable protons within 2–3 Å of the Mn complex have also been reported based on analyses of ENDOR spectra of the multiline signal obtained in the presence of ^1H_2O and ^2H_2O [440,441,693]. Nevertheless, because explanations other than direct coordination of Mn by H_2O can account for the EPR, ENDOR and ESEEM measurements conducted in the presence of ^2H_2O or $H_2^{17}O$, there remains no conclusive evidence that the Cl^--insensitive, NH_3-specific site identified by EPR studies is a binding site for substrate H_2O. Indeed, it has recently been suggested that it is not a substrate site [429] (see below).

Inhibition of steady-state oxygen evolution has been suggested to result from the occupation of a substrate site by NH_3 [38,427,428,435,442,443,446,687]. However, the amplitude of the NH_3-altered multiline EPR signal oscillates with a period of four in response to a series of flashes [429]. This demonstrates that the binding of NH_3 to the Cl^--insensitive site identified by EPR studies is not sufficient to block the S-state transitions, although a slowing of these transitions may account for the inhibition of oxygen evolution that is insensitive to Cl^- [429]. Two recent studies have noted a lack of correlation between the inhibition of steady-state oxygen evolution and the binding of NH_3 to the sites identified by EPR experiments [429,436]. One of these studies presented evidence that inhibition results from the slow binding of a second NH_3 molecule in the S_3 state [429], in agreement with an earlier luminescence study [687]. Both luminescence [686,687] and thermoluminescence [442] studies indicate that NH_3 blocks the $S_3 \rightarrow (S_4) \rightarrow S_0$ transition. The recent observation that NH_3 induces an approx. 100 Gauss-wide EPR signal in an 'S_2-plus-radical' state also suggests that NH_3 blocks this transition [456,485]. Similar signals observed in Ca^{2+}-depleted and Cl^--depleted samples have been attributed to modified forms of the S_3 state (see subsection II-B.2) and both Ca^{2+}-depletion and Cl^--depletion have been suggested to block the $S_3 \rightarrow (S_4) \rightarrow S_0$ transition (see subsection III-D). That NH_3 binds slowly in the S_3 state is suggested by failure of flash illumination to generate the approx. 100 Gauss-wide EPR signal in NH_3-treated samples [485].

It has been suggested that amines inhibit by binding in the S_3 state to the Cl^- site that was identified by EPR studies [38,427,429,436]. It has also been suggested that the water oxidizing complex may contain a third site for NH_3 and that NH_3 may inhibit by binding to this site in the S_3 state [38,429]. Amines have also

been proposed to inhibit by displacing a bridging Cl^- ion from the Mn cluster [437–439], or by altering the cluster's redox potential [438,439]. An NH_3-induced decrease in the redox potential of the S_2 state is suggested by the increased lifetime of the S_2-state in NH_3-treated samples as estimated by EPR [427,429], luminescence [687], thermoluminescence [442] and flash-induced O_2 yield [694] measurements.

It has recently been suggested that the Cl^--insensitive, NH_3-specific site identified by EPR studies is not a site for substrate H_2O [38,429], contrary to previous proposals [427,428,443]. Instead, substrate H_2O is suggested to bind at the Cl^--sensitive site [31,429] (see also the model presented in Refs. 695,696), or to the hypothesized third NH_3-binding site [38,429]. In one recent model [31,38,429], substrate H_2O exchanges for a Cl^- ion during the $S_3 \rightarrow S_4$ transition. In the lower S-states, substrate H_2O is proposed to coordinate to a nearby Ca^{2+} ion. The Cl^- ion, suggested to bind to Mn on the basis of the steady-state inhibition studies cited above, is proposed to influence the redox potential of the Mn complex and to prevent oxidation of water (or hydroxyl ions) in the S_1, S_2, or S_3 states [31,38,429, 567,695–697] (for further discussion, see subsection II-H). The close proximity of Mn and Ca^{2+} and the mutual interaction of these ions with Cl^-, is suggested to explain why the altered S_2-state multiline EPR signal observed in samples having Ca^{2+} replaced by Sr^{2+} [421,422,432] resembles the NH_3-altered multiline signal (compare Figs. 9 and 10). Such close proximity and mutual interactions may also explain why the 130–164 Gauss-wide EPR signal (subsection II-B.2) is observed in both Ca^{2+}-depleted [447,448,451–456,484] and Cl^--depleted [486,487] samples. This model, while intriguing, is speculative. There remains no direct spectroscopic proof that either Cl^- or H_2O occupy sites on the Mn complex, although recent EXAFS measurements on F^--inhibited samples or on samples having Cl^- substituted by Br^- have been interpreted as indicating that one Cl^- ion is ligated to the Mn complex in the S_1 state [543] (see subsection II-C.1).

It remains unclear how (or whether) the NH_3 sites identified in EPR studies correspond to those identified in the steady-state inhibition studies. It also remains unclear whether substrate H_2O coordinates to any of the identified sites. Indeed, it has recently been proposed that water oxidation may take place at a site that is physically removed from the Mn complex [566,593,659,698]. One such proposal [698] is based on a recent measurement of the rate that O_2 is released from flash-illuminated PS II membranes [699,700]. The released O_2 was detected with a bare metal electrode that was operated at a much less negative cathode potential than was employed in previous studies [701–705]. In this study, O_2 was found to be released from PS II much more slowly (30–130 ms) than the time required for the $S_3 \rightarrow (S_4) \rightarrow S_0$ transition to occur (approx. 1.2 ms). It was also found that the Mn complex could be oxidized through the S-states a second time, from S_0 to S_3, while O_2 or an O_2 precursor was still bound. This apparent ability of the Mn complex to become oxidized through a second round of S-state transitions before O_2 is released is difficult to reconcile with direct coordination of Mn by an O_2 precursor [698]. Recent electroluminescence measurements have also been interpreted in terms of a slow rate of O_2 release (with a half-time of 60–100 ms [594,603]). However, these slow rates of O_2 release contrast sharply with earlier measurements that found the rate to be comparable to that estimated for the $S_3 \rightarrow (S_4) \rightarrow S_0$ transition [701–705]. They also conflict with recent measurements of the rate of O_2 release as detected by photoacoustics [706,707], by EPR oximetry [708,709], by the flash-induced oxidation of mitochondrial cytochromes in anaerobic algal cells [710,711], by a Clark-type electrode [712] and by bare metal electrodes operated at various polarizing potentials [712,713,991, 992]. In some of these more recent studies, the slow release reported in Refs. 699,700 was attributed to an unidentified problem of electrode chemistry or to an unclean electrode [712,713].

High concentrations of Tris (e.g., 0.8 M) irreversibly inhibit oxygen evolution by releasing Mn(II) ions from the Mn complex [714,715]. Inhibition is facilitated by light [716,717], presumably because Tris preferentially reacts with the S_2 state [718]. Recent evidence indicates that Tris acts by reducing the Mn complex via the Cl^- site identified in steady-state inhibition studies and that this reaction also takes place in the S_1 state, although at a lower rate [719,720]. This process is suggested to be a four-electron reduction of the S_2 state to 'S_{-2}' and of the S_1 state to 'S_{-3}' [719,720]. Similar concentrations of many other primary amines (NH_3, methylamine, ethanolamine, dimethylamine and 2-amino-2-ethyl-1,3-propanediol) also reduce the Mn complex in darkness [719,720]. The reduction rate by Tris is 2-fold faster in the absence of the 24 and 17 kDa polypeptides [720]. Consequently, high concentrations of amines are proposed to act analogously to hydroxylamines (see subsection II-G.2) and to bulky reductants (e.g., hydroquinone, phenylenediamine and *N,N,N',N'*-tetramethyl-*p*-phenylenediamine) [567,720]. The latter reduce the Mn complex via a Cl^- site in the absence of the 24 and 17 kDa polypeptides [231,259, 271–276].

Future work must rigorously establish how low concentrations of amines reversibly inhibit steady-state oxygen evolution, how or whether the NH_3 sites identified in the EPR studies correspond to those identified in the steady-state inhibition studies and whether substrate H_2O molecules or Cl^- ions directly coordinate Mn ions. Factors governing the measured rate of O_2

release must also be clarified and the similarity between the altered S_2-state multiline EPR signals observed in Sr^{2+}-substituted and NH_3-treated samples must be explained.

II-G.2. Hydroxylamines

The reductive amines NH_2OH and NH_2NH_2 are isoelectronic with two molecules of H_2O and were long ago proposed to be substrate analogues [721–723]. As discussed earlier (see subsection II-A.2), at concentrations of 1–10 mM, NH_2OH irreversibly inhibits oxygen evolution by extracting Mn, presumably by reducing Mn to Mn(II) [272,349,350,353,354]. Approximately 25–40% of the 24 and 17 kDa polypeptides and approx. 5% of the 33 kDa polypeptide, are released concurrently. Hydroxylamine has also been reported to reversibly inhibit electron transfer between Y_Z and $P680^+$ [665,724–727]. This inhibition has been reported to require illumination [665]. However, this inhibition is difficult to reconcile with reports that illumination protects against inhibition, presumably by increasing the relative proportions of the higher S-states [231,728]. At much lower concentrations (50–200 μM, depending on the concentration of PS-II centers), NH_2OH has a negligible effect on the rate of steady-state O_2 evolution [729], but delays O_2 release [571,593,703,721,722,730–732], proton release [560–564], optical absorption changes in the visible [568,569,571] and ultraviolet [568–571] and the manifestation of the S_2-state multiline EPR signal [488,489,567], by two charge separations. Low concentrations of NH_2NH_2 [562–565,572,573,593,723,731, 733–735] and H_2O_2 [736,737] (see subsection II-G.3) cause a similar retardation of the S-state transitions. Low concentrations of H_2S [738] and acetone hydrazone [739,740], a potential protein labeling reagent [739], have also been proposed to function similarly. At low concentrations, NH_2OH has been reported to interact with the reducing side of PS II [488–490] and shift the EPR signal of the Q_AFe^{2+} complex to g approx. 2.1 [489,490]. However, the identity of the signal at g approx. 2.1 has been questioned [386,456]. At higher concentrations, NH_2OH causes the redox potential of cytochrome b-559 to substantially decrease [741] and interferes with herbicide binding and Q_B function [742,743].

From an examination of the ability of a series of NH_2OH and NH_2NH_2 derivatives to elicit a two-flash delay in O_2 release, a model for the dimensions of the substrate H_2O binding site was proposed, based on the assumption that NH_2OH and NH_2NH_2 bind to this site [723,731]. The proposed site would sterically restrict the access of *N*-methyl substituted compounds and particularly of *N,N*-dimethyl substituted compounds (also see [573]). The N_2 released from the oxidation of NH_2OH or NH_2NH_2 was detected by mass spectrometry, as was the O_2 released from the oxidation of water. As a result of these studies, a model for the mechanism of S-state retardation was proposed [722,731]. However, the N_2 that was detected has more recently been attributed to oxidation of NH_2OH or NH_2NH_2 by damaged PS-II centers that lack Mn [488,565,568].

Several mechanisms for the two-electron delay of the S-state transitions by NH_2OH and NH_2NH_2 have been proposed (for review, see Refs. 38,488,532,567, 570). Early models based on measurements of O_2 flash yields proposed that, in darkness, the S_1 state was either not reduced by NH_2OH [703], or was reduced by one electron [703,721,722,730,731]. More recently, EPR studies have been interpreted in terms of a two-electron reduction of the Mn complex in darkness, from the S_1 state to a stable 'S_{-1}' state [488,567]. Recent XANES spectra obtained with samples that lack the extrinsic 24 and 17 kDa polypeptides are consistent with this mechanism [544] (see subsection II-C.2). Flash-induced optical absorption changes in the visible and ultraviolet have been interpreted similarly [568–571] and H_2O_2 has been proposed to delay O_2 flash yields by the same mechanism [736,737] (see subsection II-G.3). However, the reduction mechanisms of NH_2OH and NH_2OH appear to differ: on the basis of O_2 flash yield measurements, NH_2OH appears to act as a single electron donor [593,732], while NH_2NH_2 appears to act as a two electron donor [572,593,735]. Both NH_2OH [571,593,732] and NH_2NH_2 [593,735] have been argued to produce a stable 'S_{-2}' state in darkness and the existence of an unstable 'S_{-3}' state has been suggested [277,488,719,720] (also see Ref. 593). In contrast to the recent data just described, interpretations of earlier O_2 flash yield [572] and proton release [560–564] measurements favored a stable association of one to four NH_2OH molecules with the Mn complex in the S_1 state, followed by a rapid reduction of the S_2 state to S_0 triggered by illumination. This mechanism agrees with an earlier proposal [703] and with X-ray absorption spectra that were obtained with samples that retained the extrinsic 24 and 17 kDa polypeptides [389,530,532–534] (see subsection II-C.2). Consistent with this mechanism, it has been proposed that NH_2OH and NH_2NH_2, in darkness, may reduce a redox-active component that is located near the Mn complex rather than the Mn complex itself [565,593,735] (also see Ref. 732). However, it has been questioned whether NH_2OH, NH_2NH_2 or any reduced redox-active protein-bound component could stably exist in close proximity to the Mn(III) or Mn(IV) ions of the S_1 state [488]. Some of the discrepancies between the observations and conclusions of the various NH_2OH studies may be caused by differences in the concentrations of PS II and NH_2OH employed and in the times allotted for reaction with NH_2OH (e.g., see discussions

in Refs. 38,488,532,564). The discrepancies have also been attributed to differences in sample pH or to differences in the concentrations of Ca^{2+} or Cl^- in the samples [696]. Alternatively, it has been suggested that the Mn complex may be in redox equilibrium with an unidentified redox-active component, with oxidation of the Mn complex being favored at room temperature and oxidation of the unidentified component being favored at the cryogenic temperatures that were employed for the X-ray absorption measurements [571]. This proposal does not account for the earlier O_2 release [572] or proton release [560–564] measurements, however, which were conducted at room temperature. A similar proposal has been made regarding the $S_2 \rightarrow S_3$ transition (see subsection II-F.2).

It has been proposed that the oxidation of NH_2OH or NH_2NH_2 alters the environment of the Mn complex, making it less susceptible to attack by these reductants during succeeding S-state cycles [572–574]. If this proposal is correct, the S_0 state formed by NH_2OH treatment (see subsection II-C.2) may not be equivalent to that formed during the $S_3 \rightarrow (S_4) \rightarrow S_0$ transition in untreated samples. Hydroxylamine reacts more readily with the S_2 state than with the S_1 state [445,489,572,593,735,744]. In contrast, O_2 release measurements have recently shown that both NH_2OH [593,744] and NH_2NH [593,735] react more rapidly with the S_2 state than with the S_3 state, even though the S_3 state is a stronger oxidant. These data have been interpreted as indicating that the Mn complex undergoes a significant structural rearrangement during the $S_2 \rightarrow S_3$ transition [593,735] (see subsection II-H).

Inhibition of steady-state oxygen evolution by NH_2OH is impeded by Cl^- in PS II complexes that retain the 24 and 17 kDa polypeptides [275,438,472]. At the concentrations of NH_2OH employed in these studies, inhibition would have resulted from extraction of Mn following its reduction to Mn(II). In contrast, Cl^- does not appear to impede the two-flash retardation of the S-state transitions induced by much lower concentrations of NH_2OH. This conclusion is based on measurements of proton release [563,564] or of optical absorption changes in the visible [571]. Although Cl^- has been asserted to protect against the delayed manifestation of the S_2-state multiline EPR signal caused by low concentrations of NH_2OH [428,435,488], the actual measurements that led to this assertion were performed with the bulkier *N,N*-dimethylhydroxylamine [488], a compound that is 300-fold less effective in promoting S-state delay than NH_2OH [488] (and see Refs. 723,731).

Because Cl^- impedes the rate of reduction of Mn by *N,N*-dimethylhydroxylamine [488], it was concluded that hydroxylamine and its derivatives interact with the Mn complex exclusively via the Cl^--sensitive amine binding site identified by EPR studies and not via the Cl^--insensitive, NH_3-specific site [428,435,488]. On the basis of this conclusion and because the latter site was assumed to be the binding site for substrate H_2O [427,428,443], it was concluded that NH_2OH and NH_2NH_2 should not be considered as substrate analogues [30,428,435,488]. This conclusion is not valid, however. Because it is based on data acquired only with bulky NH_2OH derivatives and because Cl^- does not impede the two-flash delays of proton release [563,564] or optical absorption changes in the visible [571] induced by NH_2OH, it seems likely that NH_2OH, like NH_3, interacts with the Mn complex via a second site that does not bind Cl^- and that sterically excludes bulky amines and hydroxylamine derivatives. Furthermore, as discussed above (see subsection II-G.1), the location of the binding site for substrate H_2O remains unknown and has recently been proposed to be a site where Cl^- binds. Finally, because the inhibition of steady-state oxygen evolution by NH_2OH is impeded by many anions, including SO_4^{2-} [275], an anion that does not protect against inhibition by other amines [428,437,438,532], it has been proposed that anions protect against NH_2OH inhibition by stabilizing the binding of the 24 and 17 kDa polypeptides to the PS-II core, rather than by (or in addition to) interacting with a binding site for Cl^- [275] (also see Ref. 745). In the absence of the 24 and 17 kDa polypeptides, 100 μM NH_2OH is sufficient to extract Mn [231,272,275–277], and no anion offers protection [275,277]. In contrast, Cl^- protects [275] against bulky reductants that gain access to the Mn complex in the absence of the 24 and 17 kDa polypeptides [231,271–273,275,276] (also see Ref. 720). In light of these data, it has recently been proposed that bulky amines, substituted hydroxylamines and other reductants interact with the Mn complex via a binding site for Cl^-, but that small amines such as NH_3, NH_2OH and NH_2NH_2 also react with Mn via an additional site that sterically excludes larger amines and that does not bind Cl^- [275,277]. This site may correspond to the Cl^--insensitive, 'NH_3-specific' site identified in the steady-state inhibition studies [437–439], and to the sterically-restricted site that was identified by mass spectrometry [723,731].

II-G.3. Hydrogen peroxide

As mentioned earlier (see subsection II-G.2), H_2O_2 delays O_2 release by two charge separations in intact samples [736,737]. In the experiments that demonstrated this delay, samples were incubated with 3–90 mM H_2O_2 and then were treated with catalase to decompose the unreacted H_2O_2 [736,737]. Because no O_2 was released during the first two charge separations, it was proposed that H_2O_2 reduces Mn in darkness from the S_1 state to the postulated 'S_{-1}' state [736,737]. Evidence for a much faster reduction of the

S_2 state to S_0 after a flash was also presented [736,737]. Similar concentrations of H_2O_2 extract Mn from samples that lack the 24 and 17 kDa polypeptides [231], that lack the 33 kDa polypeptide [746], or that have been depleted of Cl^- [747].

In intact samples that contain the 24 and 17 kDa polypeptides, a flash of light induces a catalytic decomposition of H_2O_2 in darkness [736,737]. If the concentration of H_2O_2 exceeds 1 mM, all of the O_2 produced following a flash is derived from H_2O_2, as determined by experiments conducted with $H_2^{18}O_2$ [737]. In the presence of 100–200 mM H_2O_2, more than 20 molecules of O_2 per PS II have been estimated to be generated in darkness following a single flash [737]. This catalase-like decomposition of H_2O_2 has been postulated to involve H_2O_2 alternately reducing the S_2 state to S_0 and oxidizing the S_0 state to S_2 [736,737], with one molecule of O_2 and two molecules of H_2O being formed for every 2 molecules of H_2O_2 consumed. Turnover of this $S_2 \rightarrow S_0 \rightarrow S_2$ cycle is believed to be limited by reduction of S_0 to S_{-1} by H_2O_2 and by the deactivation of S_2 to S_1 [736,737]. A slower catalytic cycling between S_1 and S_{-1} has also been postulated [696,736,748,749]. Although it has been presumed that the Mn complex remains intact during the catalytic decomposition of H_2O_2, it has not been demonstrated that subsequent removal of unreacted H_2O_2 restores normal photosynthetic oxygen evolution from water. Failure to restore normal H_2O-dependent O_2 evolution, with O_2 yields that oscillate with a period of four in response to a series of flashes, would indicate that the light-induced catalytic disproportionation of H_2O_2 does not involve the true S_2 and S_0 states of the Mn complex. It should be noted that inorganic model compounds that contain a single μ_2-oxo or di-μ_2-oxo bridged Mn dimer are capable of catalyzing the disproportionation of H_2O_2 [511,750–752] (also see Ref. 753) and a mechanistically similar disproportionation of H_2O_2 by a μ_2-oxo bridged Mn dimer has been proposed to occur in the Mn-containing catalases from *Thermus thermophilis* [754,755] and *Lactobacillus plantarum* [756,757]. If the Mn complex in PS II is comprised of two di-μ_2-oxo bridged Mn dimers (see Fig. 15), a single such dimer might give rise to the observed activity without the involvement of the true S-states.

It has recently been proposed that the H_2O_2-supported formation of O_2 by the postulated $S_2 \rightarrow S_0 \rightarrow S_2$ cycle takes place in darkness without being initiated by light [696,748,749,758]. Paradoxically, the steady-state rates of O_2 evolution reported [748,749], in terms of O_2 molecules evolved per PS-II center, are higher and more sustained than the rates previously attributed to this cycle when initiated by light [736,737]. The experiments were performed with PS II complexes that lack the 24 and 17 kDa polypeptides. Although H_2O_2 had earlier been shown to extract Mn in the absence of these polypeptides [231], the authors of the more recent studies report that incubation with 130 mM H_2O_2 does not extract Mn, as determined by the absence of the EPR signal of aqueous Mn^{2+} at room temperature [758]. The discrepancy between the two studies (Ref. 231 vs. Ref. 758) may be partially explained by differences in incubation times and whether Ca^{2+} was present during incubation; Ca^{2+} has recently been shown to stabilize the ligation environment of Mn in PS II complexes treated with NH_2OH [275,277,544]. However, the complete absence of the EPR signal of aqueous Mn^{2+} in the recent study [758] remains an unexplained discrepancy, especially because Mn^{2+} need not be released from PS II to exhibit this signal at room temperature [277]. An unambiguous determination of whether the S_0 and S_2 states participate in the catalytic disproportionation of H_2O_2 in darkness, or whether the Mn ions presumed to be involved are located in their native environments, will require further work. For example, if the Mn complex is unperturbed by 80–400 mM H_2O_2 in the absence of the 24 and 17 kDa polypeptides as asserted [748,749,758], it should be possible to observe normal photosynthetic O_2 evolution in these samples following removal of the unconsumed H_2O_2 by catalase. The discrepancy between the rates of H_2O_2-supported O_2 evolution attributed to the $S_0 \rightarrow S_2 \rightarrow S_0$ cycle in darkness [748,749,758] and after the cycle is initiated by light [736,737], should also be clarified. It should again be emphasized (see preceding paragraph) that inorganic model compounds [511,750–753] and Mn-catalases [754–757] that contain a single μ_2-oxo bridged Mn dimer can catalyze the disproportionation of H_2O_2 in darkness. The disproportionation of H_2O_2 by PS II in darkness may involve only a partially intact Mn cluster. It should also be noted that the disproportionation of H_2O_2 by PS II in darkness has recently been proposed not to involve the Mn complex; H_2O_2-supported O_2 evolution was inhibited by only approx. 40% in samples depleted of Mn by treatment with NH_2OH [759].

Mn-depleted PS-II centers catalyze the light-induced oxidation of H_2O_2 to O_2, but the reaction requires aqueous Mn^{2+} ions [378–380,736,760]. Consequently, the reaction is inhibited by EDTA. The free Mn^{2+} ions presumably serve as a redox mediator between H_2O_2 and Y_Z^+ [746,747].

II-H. The mechanism of water oxidation

From thermodynamic considerations, the mechanism of water oxidation is believed to involve either one concerted four-electron oxidation or two sequential two-electron oxidations with a peroxide intermediate [479,761]. The latter mechanism is considered to be the more likely [762]. These mechanisms are believed to involve the oxidations of deprotonated forms of water (e.g., OH^- or O^{2-} formed by the exchange of

substrate water molecules into μ_2-oxo bridges). They are also believed to be coupled with pK_a shifts of μ_2-oxo bridges or other protonatable groups associated with the Mn complex so that water oxidation is accompanied by proton release [30,479] (see also Ref. 38). The appropriate pK_a shifts of μ_2-oxo bridges have been proposed to arise from structural rearrangements of the Mn complex during the $S_4 \rightarrow S_0$ transition [30,387,479,502]. It has been proposed that the energetic favorability of water oxidation may be increased by binding the protons released during water oxidation to nearby basic amino-acid residues [30,479,761].

Sequential one-electron oxidations of water to form hydroxyl radical intermediates are considered to be energetically unfavorable [761]. Nevertheless, it has been argued that the mechanism of water oxidation could involve the formation of hydroxyl radicals if their association with the water oxidizing complex is sufficiently strong [597,655,656,763]. Indeed, it has recently been suggested that hydroxyl radicals are generated during the S-state oxidations and form covalent adducts with histidine [452] or tryptophan [589] residues. The formation of such adducts would have to be reversed during the $S_4 \rightarrow S_0$ transition and during the decay of the S_3 and/or S_2 states in darkness. Consequently, if the mechanism of water oxidation does involve the formation of covalent hydroxyl radical adducts of amino acid residues, some fairly exotic chemistry must take place during the catalytic cycle.

It is generally believed that water oxidation occurs during the $S_4 \rightarrow S_0$ transition. As mentioned in subsection II-D.1, flash-induced optical absorption changes in the ultraviolet have been interpreted in support of mechanisms of water oxidation that involve a concerted oxidation of substrate water during the $S_4 \rightarrow S_0$ transition [557,568,570,579,580,585,586,590]. However, these interpretations have been challenged [452,584,587,588, 595–597] (see subsection II-D.1). Mass spectrometry has been employed to address whether partial oxidation of substrate water takes place before the S_4 state is achieved. When chloroplasts in the presence of $H_2^{18}O$ were flashed to the S_3 state, rapidly washed with $H_2^{16}O$ and then flashed to the S_4 state, only $^{16}O_2$ was produced [764]. The reverse experiment was also performed: when samples in the presence of $H_2^{16}O$ were flashed to the S_3 state, mixed with $H_2^{18}O$ and then flashed to the S_4 state, $^{18}O_2$ was produced [765]. The mass spectrometry results were interpreted as demonstrating that water oxidation does not involve partially oxidized intermediates that are stably bound in the S_2 or S_3 states [764,765]. However, the possibility that the oxygen atoms of partially-oxidized intermediates are exchangeable with H_2O in the S_3 state cannot be excluded [31,388,597] and mechanisms involving a peroxide intermediate bound in the S_3 state (or earlier, see Ref. 388) have been proposed [574,596,597].

The mechanism of water oxidation is unknown. Numerous mechanisms have been proposed over the years (for recent reviews, see [30,387,496,500,503,504,511, 659,763]). As mentioned in subsection II-B.3, mechanisms have been advanced that are based on tetranuclear clusters structurally analogous to known model compounds [478,479,494,495,983] (also see the model of Moravsky and Khramov cited in Refs. 30,496). These and many other proposed mechanisms involve O–O bond formation between the oxygen atoms of μ_2-oxo bridges and/or terminal OH^- ligands of the Mn complex (e.g., Refs. 504,766–769,983). Model compounds that contain the resulting μ_2-peroxo bridging ligands between Mn ions have been prepared [770,771] (also see [769]). Some mechanisms predict that the Mn complex undergoes significant structural rearrangements during the $S_2 \rightarrow S_3$ and $S_3 \rightarrow S_0$ transitions [478,479, 494,495] or during the $S_1 \rightarrow S_2$ and $S_3 \rightarrow S_0$ transitions [495,497,500,501,506–508]. One of these involves the conversion between a distorted μ_3-oxo bridged Mn_4O_4 cubane structure and a μ_2-oxo bridged Mn_4O_6 adamantane structure [478,479]. Another involves the conversion between a μ_3-oxo bridged Mn_4O_2 'butterfly' structure and a distorted μ_3-oxo bridged Mn_4O_4 or Mn_4O_3Cl cubane structure [494,495] (and see Refs. 497,500,501,506–508). The Cl^--induced conversion of a Mn_4O_4 'butterfly' into a Mn_4O_3Cl cubane has been demonstrated [506]. No evidence for significant structural rearrangements during the $S_1 \rightarrow S_2$ or $S_2 \rightarrow S_3$ transitions have been observed in EXAFS analyses of samples poised in the S_1, S_2 and S_3 states [343,389,412,530,531,533,534]. However, the EXAFS spectra of the S_3-state samples were recorded at temperatures too high to permit resolution of the approx. 3.3 Å interaction [389,536,543]. Consequently, a significant change in the distance between two Mn dimers (or between a trimer and a monomer) during the $S_2 \rightarrow S_3$ transition would have escaped detection. Significant structural changes during the $S_2 \rightarrow S_3$ transition have been proposed based on the higher temperatures required for this transition to occur than for the $S_1 \rightarrow S_2$ transition [392,481,482] (see subsection II-D.1), based on the much slower reduction of the Mn complex in the S_3 state than in the S_2 state by hydroxylamine [593,744] and hydrazine [593,735] (see subsection II-G.2) and based on a three-fold larger reorganization parameter for the $S_2 \rightarrow S_3$ transition than for the $S_0 \rightarrow S_1$ or $S_1 \rightarrow S_2$ transitions calculated from classical Marcus electron transfer theory [591]. In addition, the activation energy of the $S_3 \rightarrow (S_4) \rightarrow S_0$ transition changes markedly below 279 K in spinach [591] and below 289 K in the cyanobacterium *Synechococcus vulcanus* [480]. This change in activation energy has been interpreted as indicated that the S_3 state can exist in two different structural configurations [480,591].

The protonation state of μ_2-oxo bridging ligands

critically influences the reactivities [751,752,772], redox potentials [773–776] and magnetic properties [777] of Mn complexes and can affect their nuclearity [778] (for reviews, see [387,502,504,511]). Consequently, factors that influence the pK_a values of the μ_2-oxo bridges and the pH in the vicinity of the Mn cluster are expected to profoundly influence water oxidation. Pecoraro and co-workers have recently demonstrated that di-μ_2-oxo bridged Mn(IV)-Mn(IV) dimers can catalyze the disproportionation of H_2O_2 to liberate O_2 and H_2O [511,751]. This reaction is exquisitely sensitive to the protonation of one μ_2-oxo bridging ligand [511,752]. Previous work by Boucher and Coe had shown that the acidification of di-μ_2-oxo bridged Mn(IV)-Mn(IV) dimers can liberate H_2O_2 [779]. On the basis of these known H_2O_2-producing and H_2O_2-disproportionating reactions of di-μ_2-oxo bridged Mn(IV)-Mn(IV) dimers, Pecoraro has recently suggested a speculative model for the mechanism of water oxidation in PS II [511] (see Fig. 18). This model assumes that the Mn ions are arranged as a bridged pair of di-μ_2-oxo bridged dimers, as proposed by Klein/Sauer and co-workers (Fig. 15). The S_2 state is assumed to consist of one Mn(III)-Mn(IV) dimer and one Mn(IV)-Mn(IV) dimer. The $S_2 \rightarrow S_3$ and $S_3 \rightarrow S_4$ transitions are proposed to correspond to the oxidations of an amino acid residue (e.g., histidine) and the Mn(III) ion, respectively. Upon oxidation of the Mn(III) ion during the $S_3 \rightarrow S_4$ transition, the proton from the oxidized histidine residue induces one Mn(IV)-Mn(IV) dimer to liberate a molecule of H_2O_2, which, before it diffuses out of the water-oxidizing complex, reacts with the second Mn(IV)-Mn(IV) dimer to form O_2. Peroxide intermediates have been proposed by many workers (reviewed in [387,502–504,511,659]), but this is the first proposal based on known reactions catalyzed by Mn structures that are believed to be present in PS II.

If the broad outline of Pecoraro's suggested mechanism for water oxidation is correct, H_2O_2 might be released from the water oxidizing complex under special circumstances. Indeed, there have been several reports of H_2O_2 formation by PS II membranes or inside-out thylakoids [695–697,780–785]. The formation of H_2O_2 appears to be stimulated by conditions that perturb the Mn complex. These include alkaline pH or low concentrations of Cl^- in the absence of the 24 and 17 kDa polypeptides [695,696,780,781,784], depletion of Cl^- in low concentrations of sucrose [783], treatment with compounds that destabilize the S_2 and S_3 states (e.g., with ADRY reagents) [786], acidification or 'ageing' of samples [782], mild heat denaturation [697] and treatment of samples with lauroylcholine chloride [990]. The H_2O_2 has been proposed to be produced by a 'short-circuiting' of the normal water oxidation process [567,695–697,758,783], or by the release of a peroxide intermediate of water oxidation [781–783]. Some workers have interpreted the formation of H_2O_2 as support for mechanisms of water oxidation that involve a peroxide intermediate bound in the S_2 or S_3 states [574,596,597]. Others attribute

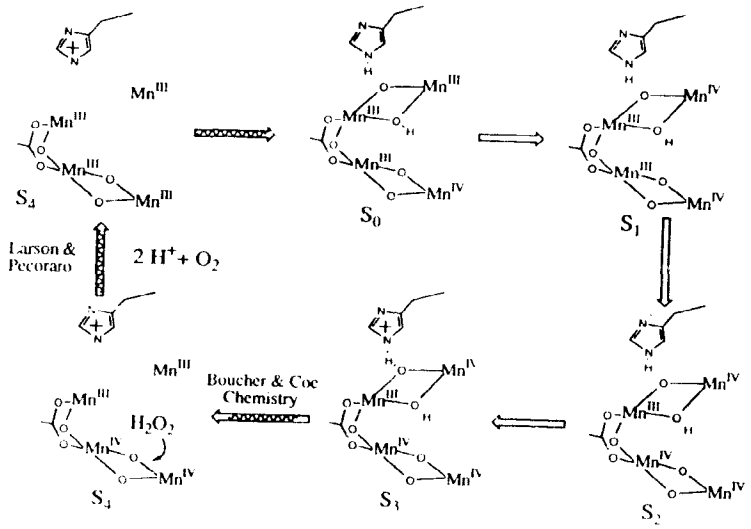

Fig. 18. A speculative mechanism for water oxidation in PS II proposed by V.L. Pecoraro [511] based on known reactions catalyzed by di-μ_2-oxo bridged Mn(IV)-Mn(IV) dimers and on the structural model of Klein, Sauer and co-workers (Figure 15). The S_2 state is assumed to consist of one Mn(III) and three Mn(IV) ions. Oxidation of a histidine residue during the $S_2 \rightarrow S_3$ transition is proposed to result in the protonation of one of the Mn(III)-Mn(IV) dimer's μ_2-oxo bridges. Oxidation of this dimer's Mn(III) ion during the $S_3 \rightarrow S_4$ transition could liberate H_2O_2 as described by Boucher and Coe for the reaction of di-μ_2-oxo bridged Mn(IV)-Mn(IV) dimers with acid [779]. The liberated H_2O_2 then reacts with the second Mn(IV)-Mn(IV) dimer to liberate O_2, as described by Larson and Pecoraro for the reaction of di-μ_2-oxo bridged Mn(IV)-Mn(IV) dimers with H_2O_2 [751,752]. Reprinted from Ref. 511 with permission (copyright 1992 by VCH, Inc.).

the presumed 'short-circuiting' of water oxidation to the oxidation of OH^- ions at a Cl^- site [38,567,695–697]. As noted in subsection II-G.1, Cl^- has been suggested to prevent the binding of water or hydroxyl ions to the Mn complex in the lower S-states and thereby prevent the premature oxidation of water or hydroxyl ions [31,38,429,567,695–697]. However, it should be noted that the H_2O_2 produced by PS II may not result from the oxidation of water: when PS II membranes were illuminated in the presence of $H_2^{18}O$, no significant incorporation of ^{18}O into H_2O_2 was detected [784]. It was proposed that the H_2O_2 resulted from the reduction of O_2 by the acceptor side of PS II [784]. Further clarification of the mechanism(s) of H_2O_2 production by PS II should be undertaken. Production of H_2O_2 by the Mn complex obviously could have mechanistic implications for the mechanism of water oxidation.

II-I. Specific residues for ligating manganese

The ligands to the manganese complex must stabilize the highly oxidizing S_3 state without stabilizing the more highly oxidizing S_4 state. When formed, the latter must immediately oxidize H_2O-derived ligands and revert to the S_0 state, liberating O_2 in the process. From considerations of Mn coordination chemistry and from studies of inorganic Mn compounds, the ligands to the Mn complex in PS II have been proposed to be primarily carboxylate residues in combination with μ_2-oxo or μ_2-hydroxo bridges [496,498,503]. Carboxylate ligands are favored because they can stabilize the higher oxidation states of Mn without being oxidized themselves [496,498]. Nevertheless, alkoxo groups from serine or threonine residues, phenoxo groups from tyrosine residues and imidazole groups from histidine residues could be possible coligands [495,496,498,501, 503,511]. Deprotonated [496] or deaminated [787] glutamine and asparagine residues have also been discussed as possible ligands and the possibility that a carboxylate ligand might be generated by the isomerization of an asparagine-glycine pair to form either an aspartate or isoaspartate residue [788] has been suggested [116]. Even arginine has been discussed as a possible ligand [368].

Electron Spin Echo Envelope Modulation (ESEEM) measurements have confirmed that the Mn ions are ligated primarily by ^{16}O atoms [398,446,554,789]. However, if the S_2 state multiline EPR signal arises from fewer than four Mn ions, this conclusion would pertain only to the Mn ions that give rise to the multiline signal. Ligation of Mn by carboxylate groups is supported by recent reports that carbodiimide modification of carboxylate residues in Mn-depleted PS II membranes appears to interfere with religation of Mn [790,791] (D.J. Blubaugh and G.M. Cheniae, personal communication) and to be suppressed in the presence of Mn^{2+} [791,792] (see subsection II-J.3). However, conformational changes induced by photoligation of Mn or by derivatization of residues located far from the Mn complex could also account for these observations (see subsection II-J.3). Although a histidine [452,454] or tryptophan [589] residue has been proposed to be oxidized during the $S_2 \rightarrow S_3$ transition and to give rise to the 130–164 Gauss-wide EPR signal in Ca^{2+}-depleted and Cl^--depleted preparations (see subsection II-B.2), models of its magnetic coupling to the Mn complex place it too far away from the Mn complex to directly ligate Mn [452,454,484,486] (at least in samples depleted of Ca^{2+} or Cl^-).

The possibility that one or more ligands to Mn are histidine residues onto which some delocalization of an oxidizing equivalent may occur (as proposed in earlier models [793,794]) is supported by several recent developments. First, ESEEM measurements on PS II complexes isolated from the cyanobacterium *Synechococcus elongatus* grown on $^{14}NO_3^-$ or $^{15}NO_3^-$ have demonstrated that nitrogen atoms are located in close proximity to the Mn ions that give rise to the S_2-state multiline EPR signal [389,398,554]. The authors of these studies favor direct ligation of these Mn ions by 1–2 histidine residues, but do not exclude the possibility that nitrogen atoms from non-histidine residues, or from the peptide backbone, interact with Mn ions through hydrogen bonds formed with μ_2-oxo bridges [389,398,554]. Direct ligation by histidine is favored by these authors because exchanging ^2H_2O for ^1H_2O does not affect the observed ^{14}N hyperfine couplings, even though ^2H forms weaker hydrogen bonds than ^1H [398,554]. The weakness of the ^{14}N and ^{15}N hyperfine couplings measured in the ESEEM experiments explains why exchanging ^{15}N for ^{14}N has no effect on the multiline signal measured in conventional EPR experiments [397,398]. In a second development, EPR measurements of the reduction of Y_Z^+ by exogenous Mn^{2+} in Mn-depleted PS II membranes indicate that Mn^{2+} binds more strongly to PS II at pH 7.5 than at pH 6 [366]. These results have been interpreted as suggesting that an endogenous Mn site contains a protonatable ligand with a pK_a between 6 and 7.5 [366], consistent with ligation of Mn by a histidine residue. Finally, chemical modification experiments have been interpreted in terms of ligation of Mn by histidine: modification of PS II membranes by diethyl pyrocarbonate (DEPC) has been reported to prevent photoligation of Mn to Mn-depleted PS II membranes [790,791,795–797] while prior Mn photoligation has been reported to suppress derivatization by [^{14}C]-DEPC [792] (also see [791] and subsection II-J.3). However, conformational changes induced by histidine derivatization, or by Mn photoligation, could also account for these observations (see subsection II-J.3).

II-J. The location of manganese in PS II

II-J.1 The relationship of the Mn complex to the 33 kDa polypeptide

Effects of removing the 33 kDa polypeptide on the Mn complex. Because several procedures for dissociating the extrinsic 33 kDa polypeptide from PS II also release Mn (see subsection I-B.4) and because some preparations of the isolated 33 kDa polypeptide have been found to contain bound Mn ions [798,799], attention was once focused on the 33 kDa polypeptide as providing the ligands for Mn in PS II (e.g., Ref. 800). However, this polypeptide can be removed from PS II without extracting the Mn complex [232,242,246,248, 251,252,265,404,801–805]. Furthermore, many such preparations have been reported to evolve oxygen in the presence of elevated concentrations of Cl^- (100–200 mM) and 5–20 mM Ca^{2+} [232,246,248,252, 265,802–805] (also see Ref. 251). While some studies have attributed the residual oxygen-evolving activities observed in these samples (10–45% compared to untreated samples) to incomplete removal of the 33 kDa polypeptide [362,806,807], a recent study showed that spinach PS II membranes depleted of > 99% of the 33 kDa polypeptide evolve oxygen at approx. 24% of the rate observed in untreated samples [248]) (the active PS-II centers in the preparations were suggested to evolve oxygen at approx. 55% the rate observed in untreated samples, based on relative quantum yield measurements [248]). In addition, three groups have deleted the *psb*O gene that encodes the 33 kDa polypeptide from the cyanobacterium *Synechocystis* sp. PCC 6803 [808–810] and a fourth has insertionally inactivated the *psb*O gene in *Synechococcus* sp. PCC 7942 [811]. The resulting organisms grow photoautotrophically. The *Synechocystis* mutants evolve oxygen at approx. 30% the rate of wild-type cells when 2,6-dichloro-*p*-benzoquinone (DCBQ) and potassium ferricyanide are employed as artificial PS II electron acceptors [808] and at 60–75% the rate of wild-type cells when CO_2 is employed as the electron acceptor [808–810]. The *Synechococcus* mutant is reported to evolve oxygen at the same rate as wild-type cells when CO_2 is employed as the electron acceptor [811]. Thylakoid membranes from one of the *Synechocystis* mutants retain 70–80% of their DCBQ/ferricyanide-supported activity when isolated in the presence of 0.5 M Cl^- (R.L. Burnap, personal communication). Thylakoid membranes from the *Synechococcus* mutant are reported to retain activity (approx. 75% compared to wild-type membranes) when supplemented with $MnCl_2$ and $CaCl_2$ [811]. The *Synechocystis* mutants are unable to grow in Ca^{2+}-depleted media [809] and are more susceptible to photoinhibition [809,810].

The ability of the cyanobacterial mutants to grow photoautotrophically and evolve oxygen demonstrates that the 33 kDa polypeptide is not required for the assembly and activation of the Mn cluster in cyanobacteria. However, the 33 kDa polypeptide may be required for the assembly and activation of the Mn complex in eukaryotes in vivo. A mutant of the eukaryotic alga *Chlamydomonas reinhardtii* that lacks this polypeptide is incapable of photoautotrophic growth, contains depressed steady-state levels of the intrinsic PS II polypeptides and evolves no oxygen [192,812]. Furthermore, during greening of *Euglena gracilis* cells, the acquisition of oxygen evolution activity correlates with the accumulation of the 33 kDa polypeptide [813]. The reasons for the apparently different requirements of the 33 kDa polypeptide for assembly of PS II or the Mn complex between prokaryotic and eukaryotic organisms are not understood. It has been suggested that concentrations of Ca^{2+} and Cl^- ions in cyanobacteria may be sufficiently high to permit assembly of the Mn complex, but that the concentrations of these ions may be too low in chloroplasts [248]. The Mn complex assembles in the absence of the 33 kDa polypeptide in vitro when 50 mM $CaCl_2$ is included in the incubation buffer [349,362,373] (also see [360,374]).

The 33 kDa polypeptide appears to cover and protect the Mn complex. In the absence of this polypeptide, two Mn ions become paramagnetically uncoupled [249,250] and are gradually released [232,245,246,251–253] unless the preparations are maintained in high concentrations of Cl^- (> 100 mM). In PS II membranes that have been depleted of the 33 kDa polypeptide, a surface-enhanced Raman scattering (SERS) signal at 225 cm^{-1} has been observed and attributed to the weakly bound Mn ions of the Mn complex [814,815]. When the preparations were incubated in 100 mM SO_4^{2-} instead of Cl^-, the signal was lost in parallel with the loss of oxygen evolution and apparently in parallel with the loss of the weakly bound Mn ions [814]. Because this signal was not observed in samples that retained the 33 kDa polypeptide, it was proposed that the 33 kDa polypeptide covers the Mn complex [814,815]. The vibrational mode that gives rise to the SERS signal is not a Mn–Cl mode [815] and has not been identified. It may be a vibrational mode that is affiliated with the Ag electrode used in the experiments and which depends on the presence of Mn and Cl^- at the PS II membrane surface [815].

The 33 kDa polypeptide optimizes the catalytic efficiency of the Mn complex. In the absence of this polypeptide, the extent of stable charge separation [805] and the rates of oxygen evolution [232,246,248, 251,252,265,802–805], electron transfer [273,548], and O_2 release (and possibly the rate of the $S_3 \rightarrow (S_4) \rightarrow S_0$ transition) [804], are significantly diminished. Also, the S_2 state is abnormally stable in these preparations, as determined from oxygen flash yield [804] and thermoluminescence [470,816] measurements. Nevertheless,

removal of the 33 kDa polypeptide in vitro induces only slight structural changes in the Mn complex, as determined by analyses of XANES and EXAFS data [253] and of the S_2-state multiline EPR signal [803,805] in samples that have been depleted of the 33 kDa polypeptide. However, there is some disagreement over the extent of these changes (see Ref. 803 vs. Ref. 805). The simplest interpretation of the observations described in this paragraph is that the extrinsic 33 kDa polypeptide covers, protects and influences the operation of the Mn complex without directly providing it with ligands (any ligands provided by the 33 kDa polypeptide would have to be functionally replaceable by Cl^- ions, water molecules or ligands from other polypeptides). Because no other extrinsic polypeptides are required for water oxidation (see subsection I-B), the Mn complex must bind to the lumenally-exposed surface of one or more of the intrinsic polypeptides of the PS-II core. Such a location is also suggested by the electrochromic shifts of carotenoid and chlorophyll *a* absorption bands that are produced by the S-state transitions (see subsection II-D.2). These shifts require that Mn ions are located in close proximity to the chlorophyll and carotenoid pigments, unless the electrochromic shifts result from pK_a shifts of amino-acid residues that are located far from the Mn complex [597,645] (see subsection II-H).

The binding domain of the 33 kDa polypeptide – cross-linking studies. Because the extrinsic 33 kDa polypeptide protects and influences the catalytic efficiency of the Mn complex, a determination of where this polypeptide binds to the PS-II core might be expected to help locate ligands to Mn. Crosslinking studies have demonstrated that the 33 kDa polypeptide can be specifically cross-linked to CP47 in spinach PS II membranes [222,283,817,818], in spinach PS II complexes that have been depleted of the LHCII antenna complex [282,817,819,820], and in PS II particles from *Synechococcus elongatus* [994]. The cross-linked residues are located in the 8 kDa amino-terminal domain of the 33 kDa polypeptide and in the 16.7 kDa carboxy-terminal domain of CP47, to the carboxy-terminal side of Met-359 and presumably in the large (approx. 190 residues) hydrophilic loop (see Fig. 5A, loop E) [818]. The amino-terminal 16–18 residues of the 33 kDa polypeptide had previously been shown to be involved in binding [236] (see subsection I-B.4).

Several of the cross-linked PS II complexes described in the previous paragraph have been reported to retain the ability to evolve oxygen [222,283,818]. One such complex was reported to resist extraction of Mn by alkaline pH [283]. However, this resistance has since been attributed to factors other than the cross-linking of the 33 kDa polypeptide with CP47 [222]. Cross-linking of the 33 kDa polypeptide to the a subunit of cytochrome *b*-559 and to the product of the *psb*I gene has recently been reported [821]. The latter study employed PS II complexes that had been depleted of the LHCII complex and the 24 and 17 kDa extrinsic polypeptides and made use of a cross-linking reagent that reacts with a wide variety of functional groups [821]. Possible cross-linking of the 33 kDa polypeptide to the D2 polypeptide has also been reported [820].

Crosslinking of the 33 kDa polypeptide to the D1/D2 heterodimer has also been reported [696,822,823]. In these studies, PS II particles were depleted of the extrinsic polypeptides, reconstituted with 33 kDa polypeptides that had been labeled with a photoaffinity cross-linking reagent, then illuminated with 254 nm light. The cross-linked complex, isolated by preparative gel electrophoresis in the presence of 1% SDS and 6 M urea, was found to include the D1, D2 and 33 kDa polypeptides plus variable quantities of a fourth, unidentified, approx. 34 kDa polypeptide [696,822,823]. The possibility that the cross-linked complex included small polypeptides (e.g., the *psb*I product or the cytochrome *b*-559 polypeptides) was not examined. The cross-linked complex was reported to retain approx. 4 Mn ions per P680 [696,822,823]. Because the isolated complex catalyzed H_2O_2-dependent O_2 evolution in darkness, previously attributed to a H_2O_2-induced cycling between the S_2 and S_0 states [696,748,749,758] (see subsection II-G.3), the cross-linked complex was proposed to contain the Mn complex in a partially active configuration that could cycle between these two S-states [696,822,823]. Consequently, the ligands to the Mn complex were proposed to be contributed solely by residues from the D1 and D2 polypeptides [696,822,823]. However, it is not clear whether the Mn ions presumed to be involved in the catalytic decomposition of H_2O_2 in the cross-linked complex were located in their native environments, whether their redox states corresponded to any of the S-states, or how many Mn ions were involved. As discussed in subsection II-G.3, the disproportionation of H_2O_2 can be catalyzed by model compounds that contain a single μ_2-oxo or di-μ_2-oxo bridged Mn dimer [511,750–752] and by catalases that contain a bridged Mn dimer at their catalytic site [754–757]. The H_2O_2-dependent O_2 evolution observed in the cross-linked complex might correspond to a μ_2-oxo bridged Mn dimer cycling between its Mn(III)-Mn(III) and Mn(II)-Mn(II) or Mn(IV)-Mn(IV) oxidation states. This activity may indicate that two Mn ions (perhaps the most tightly bound pair) are ligated by the D1/D2/I/cytochrome *b*-559 complex and perhaps by the D1/D2 heterodimer. However, the cross-linked complex must be isolated with procedures that are less harsh and preferably that preserve H_2O-supported O_2 evolution, before any definitive conclusions regarding the location of the Mn complex can be reached. It should be noted that the D1 polypeptide has not been cross-linked to

any polypeptide in unreconstituted preparations [222,282,283,817–820,824,825]. The D1 polypeptide appears to be unreactive to cross-linking reagents unless the preparations have been treated with specific detergents [824,825] or have been depleted of the 33, 24 and 17 kDa polypeptides [821].

The binding domain of the 33 kDa polypeptide – accessibility studies. Accessibility studies have also been employed to locate the binding domain of the 33 kDa polypeptide. Removing the 33 kDa polypeptide has been reported to increase the accessibility of PS II to antibodies directed against putative lumenal regions of the D1 polypeptide [826]. Removal of the 33 kDa polypeptide also increases the accessibility of CP47 to reagents that modify free amino groups [817,827], increases the susceptibility of CP43 to extraction by linolenic acid [828] and increases the accessibility of CP47 [829], CP43 [830] and the α subunit of cytochrome *b*-559 [198] to digestion by trypsin. The modified amino groups on CP47 have been localized to the large (approx. 190 residue) hydrophilic loop that is believed to be located on the lumenal side of the thylakoid membrane [130,818,827] (see Fig. 5A, loop E). The modified residues lie between Lys-304 and Lys-321 and between Lys-389 and Lys-438 [818,827]. The accessibility of CP47 to a monoclonal antibody directed against an epitope within a 32-residue segment of this hydrophilic loop (Pro-360 to Ser-391) is also increased by the removal of the 33 kDa polypeptide, but only if all four Mn ions are also removed [130,827,829,831]. The accessibility is not increased [829] if only the two more weakly bound Mn ions are removed (e.g., by incubating samples depleted of the 33 kDa polypeptide with low concentrations of Cl^- [232,245,246,251–253]). The latter observation has been interpreted as indicating that removal of the two most tightly-bound Mn ions is accompanied by polypeptide conformational changes [130,827,829,831]. These conformational changes may be the reverse of those that are believed to accompany the formation of the Mn complex during photoactivation (see subsection II-A.3).

The binding domain of the 33 kDa polypeptide – other studies. Interactions between the 33 kDa polypeptide and the core polypeptides of PS II have been examined by methods other than cross-linking. A specific interaction between the 33 kDa polypeptide and the D1, D2, or cytochrome *b*-559 polypeptides has been proposed based the successful purification of the D1/D2/I/cytochrome *b*-559 complex by affinity chromatography using the 33 kDa polypeptide as an immobilized ligand [832]. Such an interaction was also proposed based on a report that the isolated 33 kDa polypeptide binds to the isolated D1/D2/I/cytochrome *b*-559 complex [833]. A specific interaction between the 33 kDa polypeptide and cytochrome *b*-559 has been proposed on the basis of a radiation inactivation study [834] and a specific interaction between the 33 kDa polypeptide and the D2 polypeptide has been proposed based on the observation that changing Tyr-160 to Phe in the D2 polypeptide of *Synechocystis* sp. PCC 6803 [65,66] destabilizes the binding of the 33 kDa polypeptide to isolated PS II particles [835].

Taken together, the data described in this subsection indicate that the 33 kDa polypeptide interacts with or shields essentially all of the intrinsic polypeptides of the PS-II core. On the basis of these data, none of the intrinsic polypeptides can be excluded as possible sources of ligands to the Mn complex.

II-J.2 The relationship of the Mn complex to Y_Z and Y_D

Some constraints on the location of the Mn complex have been provided by the identifications of Y_D as Tyr-161 of the D2 polypeptide [65,66] and Y_Z as Tyr-161 of the D1 polypeptide [67,68]. These identifications place Y_Z and Y_D in nearly the same membrane plane as the presumed location of P680 in models of the D1/D2 heterodimer (see Figs. 1 and 4). This location is in agreement with work demonstrating that electron transfer from Y_Z to $P680^+$ is not electrogenic [55] and is consistent with a Y_Z–P680 distance of 10–15 Å estimated from the broadening of the EPR spectrum of $P680^+$ by Y_Z^+ [681]. At least one Mn ion must be in close proximity to Y_Z because of the rapid oxidation of Mn by Y_Z^+ during the S-state transitions (e.g., approx. 30 and approx. 110 μs for the $S_0 \rightarrow S_1$ and $S_1 \rightarrow S_2$ transitions, respectively [480,570,580,582], see subsection II-D.1). The proximity of the Mn complex to both Y_Z and Y_D is indicated by microwave power saturation studies [32,341,551,688,836–839] and spin-lattice relaxation time measurements [552,789,840,841] of Y_D^+ and Y_Z^+ and saturation-recovery measurements of Y_D^+ [842,843]. These studies have demonstrated that there is magnetic coupling between the Mn complex and both Y_Z^+ and Y_D^+. The coupling between Mn and Y_Z^+ is stronger than that between Mn and Y_D^+ [32,836], indicating that the Mn complex is closer to Y_Z than to Y_D. Consequently, the Mn complex must be located asymmetrically with respect to the central axis of symmetrical models of the D1/D2 heterodimer (see Figs. 1 and 4). The distance between Y_Z and the Mn complex has been estimated to be > 10 Å because the linewidth of the EPR signal of Y_Z^+ is not changed when the Mn complex is removed [60]. This distance has also been estimated to be 8–15 Å based on analyzing the temperature-dependence of electron transfer from Mn to Y_Z^+ in terms of classical Marcus electron transfer theory [591]. The distance between Y_D and the Mn complex has been estimated to be 30–40 Å based on the temperature-dependence of the relaxation rate of Y_D^+ [552,841]. The non-heme Fe^{2+} ion contributes to the relaxation of Y_D^+ [841–845]. From the relaxation rate of Y_D^+ measured in Mn-depleted samples, the distance

between Y_D and the non-heme Fe^{2+} ion has been estimated to be $\geqslant 38$ Å [843] (also see Ref. 845). This estimate agrees with that predicted from the crystal structures [20–22] of reaction centers from purple non-sulfur bacteria. From studies of the relaxation of Y_D^+ in the presence of the exogenously added relaxation enhancers $(Dy^{3+}\text{-EDTA})^-$ and Dy^{3+}-HEDTA, Y_D has been estimated to be located approx. 25 Å [838] or approx. 20 Å [846] from the lumenal surface of the PS-II core polypeptides in the absence of the extrinsic polypeptides. Recent electroluminescence measurements indicate that electron transfer from Mn to Y_Z^+ is electrogenic, but spans only approx. 5% of the hydrophobic core of the thylakoid membrane [603]. Consequently, if the distance estimates based on the relaxation enhancements of Y_D^+ caused by $(Dy^{3+}\text{-EDTA})^-$ and Dy^{3+}-HEDTA are correct and if Y_Z and Y_D are located symmetrically in the D1/D2 heterodimer, then at least part of the Mn complex must be located deep within the PS-II core, far from the lumenal surface of the intrinsic polypeptides. Further investigation of this point seems warranted.

Based on the distance estimates described in the preceding paragraph, many of the ligands to the Mn complex could be provided by residues in the lumenally-exposed regions of the D1 and D2 polypeptides (see Fig. 4). In support of this supposition, removal of the Mn complex exposes Y_D^+ [348,489,847] and Y_Z^+ [271,273,348,366,760,848,849] to exogenous reductants such as benzidine and NH_2OH. However, because the intrinsic polypeptides of PS II are likely to be extensively entwined, like those of the reaction centers of purple non-sulfur bacteria [20–22], none of the intrinsic polypeptides that comprise the core of PS II can legitimately be excluded as providing some of the ligands to the Mn complex on the basis of these data.

II-J.3 The relationship of the Mn complex to the intrinsic polypeptides

The LF-1 mutant of Scenedesmus obliquus. Several lines of circumstantial evidence have been used to implicate the D1 polypeptide as providing some of the ligands to the Mn complex. Much of this evidence is based on studies of the LF-1 mutant of the green alga *Scenedesmus obliquus*. This mutant assembles PS II complexes that do not evolve oxygen [850–854] and cannot be photoactivated with exogenous Mn and Ca^{2+} ions [795,796]. Normal Y_D^+ and $Q_A^-Fe^{2+}$ EPR signals can be generated in PS II membranes from the mutant, however [837]. Thylakoid membranes [850–852] and PS II membranes [795] from the LF-1 mutant contain only 25–40% of the Mn found in wild-type preparations. The residual Mn ions do not permit the formation of the S_2 state, as determined by EPR [837] and thermoluminescence [795] measurements and do not interact magnetically with Y_D^+ [837]. The extent of inhibition by Mn^{2+} ions of DPC-supported DCIP reduction in Mn-depleted LF-1 PS II membranes is approx. 50% that in Mn-depleted wild-type membranes [795,796] (for further discussion of this assay, see later in this subsection). These data were interpreted as indicating that LF-1 PS II complexes contain half the number of high affinity Mn sites as wild-type complexes [795,796]. The full complement of such sites could be generated by treating LF-1 PS II membranes with various proteinases [796]. A small surface-enhanced Raman scattering (SERS) peak at 225 cm^{-1} was detected in LF-1 PS II membranes following removal of the 33 kDa extrinsic polypeptide [815]. This signal, previously attributed to the weakly bound Mn ions of the Mn complex [814] (see subsection II-J.1), decays far more rapidly in LF-1 than in wild-type preparations [815].

Thylakoid membranes [850–852,854,855] and PS II particles [853] from the LF-1 mutant were found to contain a protein that is approx. 2 kDa larger than in wild-type preparations. This protein was subsequently determined to be the D1 polypeptide [855]. Its larger size in the LF-1 mutant results from a failure to cleave a 1.5–2.0 kDa fragment from the carboxy-terminus of the polypeptide's precursor form [856,857]. This failure is caused by the absence or inactivation of the processing enzyme that normally cleaves the D1 polypeptide between Ala-344 and position 345 [143–146,858]. The addition of the processing enzyme from spinach [145], pea [146] or wild-type *Scenedesmus* [146,858] to PS II membranes from the LF-1 mutant results in the processing of the D1 polypeptide [145,146,858]. The processed complexes can reportedly be photoactivated [146,858], but whether the extent of photoactivation is significant has been disputed [796]. The carboxy-terminal extension of the unprocessed D1 polypeptide has no known function (see the discussion in Ref. 146). It is not present in *Euglena gracilis* [859,860] and can be deleted from *Synechocystis* sp. PCC 6803 without effect [17,19,880,996]. (More recently, the carboxy-terminal extension has also been deleted from *Chlamydomonas reinhardtii*, also without apparent effect [997,998].) In contrast, when Ser-345 of *Synechocystis* 6803 was changed to proline (but not when changed to alanine or arginine), the processing of the carboxy-terminus was prevented and no functional Mn complex was assembled [17,19,996]. Consequently, the failure to post-translationally cleave the carboxy-terminal extension of the D1 polypeptide correlates with the failure to assemble a functional Mn complex. This correlation has led some authors to suggest that the D1 polypeptide provides ligands to the Mn complex (e.g., [852,853,855]). So has the rapid loss of the SERS signal [815] and the lower apparent number of high-affinity Mn sites in LF-1 PS II membranes [795,796]. However, none of these data necessarily imply that the D1 polypeptide contributes ligands to the Mn complex.

Because the polypeptides that comprise the core of PS II may be extensively entwined, the 1.5–2.0 kDa extension of the unprocessed polypeptide may disrupt the entire lumenal domain of PS II. Such a disruption would likely prevent the assembly of a functional Mn complex and alter the properties of all Mn sites in PS II. It should be noted that the extrinsic 24 and 17 kDa polypeptides appear to bind only weakly to LF-1 PS II complexes [854] and that cytochrome *b*-559 in these complexes is predominantly in a low potential form [837,850–852].

The light-induced iodination of preparations containing Mn. A specific light-induced iodination of the D1 polypeptide in PS II membranes depleted of Cl^- has been reported [861,862]. Iodination was reported to involve the formation of monoiodotyrosine [862] and to be suppressed by Cl^-, F^- and acetate [861]. Because these anions compete for a common site that is believed to be on the Mn complex [439] (see subsection II-G.1), it was proposed that the Mn complex oxidizes I^- at a Cl^- site on the Mn complex and that the oxidized iodine labels a nearby residue of the D1 polypeptide [861]. Based on partial proteolysis of ^{125}I-labeled Cl^--depleted PS II membranes, it was proposed that Tyr-161 of the D1 polypeptide was specifically iodinated [862]. The same residue appeared to be iodinated in Mn-depleted samples [862]. No sequence analyses of iodinated peptides were reported to support this assignment, however and the iodinated tryptic fragment seems too small (7.7 kDa) to be assigned to the fragment that includes Tyr-161 (8.9 kDa) (see Fig. 5 of Ref. 862). Because the labeled residue is part of the D1 polypeptide, it was proposed that the Mn complex must bind to the D1 polypeptide [861,862]. However, if the polypeptides that comprise the lumenal domain of PS II are entwined, the iodinated residue(s) will not necessarily be located on the same polypeptide as those that ligate the Mn complex.

The loss of Mn following photoinhibition. A correlation between the loss of Mn ions and the degradation of the D1 polypeptide following photoinhibition of thylakoid membranes from spinach has been reported [863,864]. On the basis of this correlation it was suggested that the Mn complex is ligated by the D1 polypeptide [863]. However, this correlation does not imply that the D1 polypeptide provides ligands to Mn. Disassembly of the PS-II core structure, which also accompanies the degradation of the D1 polypeptide following photoinhibition [864], would undoubtedly cause the destruction of the Mn complex and the release of Mn^{2+} ions irrespective of what polypeptides provide ligands to the Mn complex. It has recently been reported that the loss of Mn ions correlates with hypothetical conformational changes in PS II that precede the degradation of the D1 polypeptide [984].

Chemical modification of PS II. Chemical modification and steady-state electron transfer studies have been interpreted as demonstrating that the D1 polypeptide provides some of the ligands to the Mn complex. As mentioned in subsection II-I, chemical modification of histidine residues in Mn-depleted PS II membranes has been reported to prevent the ligation [791,792] and photoactivation [792] of the Mn complex. In addition, photoligation of Mn ions has been reported to suppress the labeling of PS II membrane preparations by [^{14}C]-DEPC [792]. Although it was claimed that the photoligation of Mn ions suppressed [^{14}C]-DEPC labeling of both the D1 polypeptide and a approx. 60 kDa D1/D2 heterodimer, the individual bands of neither the D1 polypeptide nor the D2 polypeptide can be individually discerned in the published fluorogram because of overlapping bands from the LHCII antenna complex. Consequently, the conclusions, that the labeling of the D1 polypeptide was suppressed by Mn and, consequently, that the D1 polypeptide contributes histidine ligands to the Mn complex, are not necessarily correct. The experiments should be repeated with purified PS II complexes that lack the LHCII polypeptides so that the bands of the individual D1 and D2 polypeptides can be resolved. Nevertheless, the Mn-induced suppression of [^{14}C]-DEPC labeling of the D1/D2 heterodimer would be consistent with Mn ligation by residues from either of the D1 or D2 polypeptides, assuming that no small polypeptides are present in the approx. 60 kDa complex observed in the fluorogram. However, the Mn-induced suppression of labeling could also be caused by conformational changes that accompany the photoligation of Mn ions (see below and subsection II-A.3).

Submicromolar concentrations of Mn^{2+} have been reported to inhibit electron donation by 1,5-diphenylcarbazide (DPC) to Mn-depleted PS II membranes or complexes, as assayed by the photoreduction of 2,6-dichlorophenolindophenol (DCIP) [381] or silicomolybdate (SiMo) [795]. This inhibition has been employed by several authors as an assay for the ligation of Mn^{2+} to one or more of the endogenous Mn sites in Mn-depleted preparations [381,790–792,795–797]. Chemical modification of histidine residues with DEPC [790–792,795–797] or carboxylate residues with 1-ethyl-3-[(3-dimethylamino)propyl]carbodiimide (EDC) [790, 791,797], or digestion with various proteinases [790,797], partially abolishes the ability of Mn^{2+} to inhibit electron donation by DPC. In addition, millimolar concentrations of Mn^{2+} ions protect PS II membranes from modification by DEPC and EDC [791,792]. Most of this work has been conducted by Seibert and coworkers.

Seibert and co-workers argue that the modification-susceptible histidine and carboxylate residues coordinate one or more of the Mn ions of the Mn complex [790,791,795–797]. By analyzing the Mn^{2+}-induced in-

hibition of DPC-supported DCIP reduction in samples treated with DEPC and/or EDC plus various combinations of proteinases, Seibert and co-workers argue that they have detected four separate endogenous Mn sites, although they do not exclude the possibility that these four 'sites' may be four individual ligands in the first site occupied by a Mn^{2+} ion during the photoactivation process [791,797]. According to the interpretations of Seibert and co-workers, half of these four sites include histidine residues that are susceptible to modification by DEPC [790,791,795–797], while the remaining half include carboxylate residues that are susceptible to modification by EDC [790,791,797]. One of the sites that contains a DEPC-susceptible histidine residue is sensitive to digestion by subtilisin [790,797], while the other is sensitive to digestion by carboxypeptidase A, *Staphylococcus aureus* V8 proteinase and trypsin [790,797]. One of the sites that contains an EDC-susceptible carboxylate residue is sensitive to digestion by trypsin [790,797], but only in the absence of the extrinsic 33 kDa polypeptide [797]. The histidine and carboxylate sites are proposed to be affiliated with the strongly and weakly bound Mn ions of the Mn complex, respectively; both carboxylate sites are uncovered when PS II membranes depleted of the 33 kDa polypeptide are incubated in the presence of low concentrations of Cl^- [791] (conditions that cause the release of two Mn ions [232,245,246,251–253]), whereas the two histidine sites remain protected under these conditions [791]. Both of the histidine sites appear to be occluded in the LF-1 mutant of *Scenedesmus obliquus* [795,796] and can be uncovered by digestion with various proteinases [796] (see above). Both of the carboxylate sites are accessible in LF-1 PS II membranes [791]. One of the DEPC-susceptible histidine residues has been proposed to be His-337 of the D1 polypeptide [790,797]. The other has been suggested to be His-92 of the D1 polypeptide [790,797] or His-62, His-88 or His-337 of the D2 polypeptide [797].

The interaction between Mn^{2+} and DPC was originally reported to be competitive [381]. However, this interaction has recently been proposed to be non-competitive under the conditions employed for the assay (200 μM DPC and < 10 μM Mn^{2+}) [791]. Consequently, Mn^{2+} ions and DPC are proposed to bind to separate sites on PS II [791]. The inhibition of electron donation by DPC has been proposed to result from the ligation of a Mn^{3+} ion generated by the oxidation of Mn^{2+} by Y_Z^+: the bound Mn^{3+} ion is presumed to prevent the oxidation of DPC by Y_Z^+ [791] (D.J. Blubaugh and G.M. Cheniae, personal communication). However, the Mn^{2+}-induced inhibition in the DPC/Mn^{2+} inhibition assay is never more than approx. 50%, even in the presence of saturating concentrations of Mn^{2+} ions (10–100 μM). The high residual DPC-supported DCIP reduction rates observed in maximally inhibited samples at saturating light intensities have been proposed to result from DPC donation to Y_D^+ [791] (also see Ref. 365). The reduction of Y_D^+ by DPC has been reported [276]. In addition, both Mn^{2+} and DPC have been reported to reduce both Y_Z^+ (with K_m values of 10 μM for Mn^{2+} and 42 μM for DPC) and an unidentified component that was presumed to be Y_D^+ (with K_m values of 200 μM for Mn^{2+} and 2.0 mM for DPC) [365].

Because the nature of the interaction between Mn^{2+} and DPC appears to be complex [791] and possibly to be complicated by the multiple turnovers that are required for the steady-state DPC/Mn^{2+} inhibition assay (e.g., see [354,365,366,791]), the Mn binding properties of the chemically modified and proteinase-treated preparations should be characterized by independent methods. These should include flash-induced measurements of the reduction of Y_Z^+ by Mn^{2+}. The reduction of Y_Z^+ can be monitored by the decay of its EPR signal [366], by the decay of its optical absorption spectrum in the ultraviolet [68] or visible [981], or by monitoring the ability of Mn^{2+} to block charge recombination between Q_A^- and Y_Z^+ in samples that lack Q_B or contain DCMU [368]. It should be noted that, while Mn^{2+} was reported to bind more weakly to PS II membranes at pH 7.7 than at pH 6.1 on the basis of the DPC/Mn^{2+} inhibition assay [381], the opposite conclusion was reached on the basis of flash-induced EPR measurements of the decay of Y_Z^+ [366] (see subsection II-1).

Seibert and co-workers have proposed that all four endogenous Mn sites are located on the D1/D2/I/cytochrome *b*-559 complex. This proposal is based on DPC/Mn^{2+} inhibition assays conducted with silicomolybdate as the electron acceptor [795]. The same degree of inhibition of DPC donation by Mn^{2+} was observed in these complexes as in Mn-depleted PS II membranes (approx. 50% inhibition) [795]. However, in view of the complexity of this assay in the more intact PS II membrane preparations [791] and because the donor side of D1/D2/I/cytochrome *b*-559 complexes appears to be severely disrupted (for example, no direct evidence for the formation of Y_Z^+ in such complexes has been presented [184,185] (see subsection I-B.2)), the proposal that all four Mn sites are located on the D1/D2/I/cytochrome *b*-559 complex should be interpreted cautiously until confirmed by independent methods.

Although Seibert and co-workers interpret their data in terms of direct coordination of Mn ions by the DEPC-susceptible histidine and EDC-susceptible carboxylate residues [790,791,795–797], it is possible to explain their data without invoking direct coordination of Mn by these residues. Polypeptide conformational rearrangements near Y_Z, induced by the ligation of Mn^{3+}, could be involved in blocking electron donation

TABLE II

Lumenal residues in the D1 and D2 polypeptides that directly or indirectly influence water oxidation

Cells were grown in liquid media. Cells that grew photoautotrophically with normal doubling times (as determined by the optical density of the cultures at 730 nm) are denoted '+.' Cells that exhibited impaired photoautotrophic growth are denoted '+(slow).' Where known, an estimate of the cell doubling time relative to wild-type is given. The doubling time of wild-type cells was 14–20 h, depending on growth conditions. Cells that were unable to grow photoautotrophically (and, therefore, required glucose for propagation) are denoted '–.' The maximal light-saturated rates of O_2 evolution were measured with whole cells in growth media supplemented with 0.3–1.0 mM 2,6-dichloro-*p*-benzoquinone and 1 mM $K_3Fe(CN)_6$. Except where noted, the PS II content of cells, relative to wild-type, was estimated from the yield of variable fluorescence in the presence of 40 μM DCMU and 20 mM NH_2OH after cells had been preincubated with 0.2–0.3 mM *p*-benzoquinone and 0.3–1.0 mM $K_3Fe(CN)_6$ [19,368] (H.-A. Chu, A.P. Nguyen and R.J. Debus, unpublished).

Mutation	Photoautotrophic growth	O_2 evolution (% wild-type)	PS II content (% wild-type)
D2 polypeptide:			
Glu-70 → Gln [a]	–	approx. 30	approx. 35 [c]
→ Val [a]	–	0	0
D1 polypeptide:			
Asp-59 → Glu [b]	+	approx. 70	50–70
→ Asn [b]	+(slow, 1.3×)	20–30	50–60
→ Val [c]	+(slow, 3.3×)	approx. 10	approx. 30
Asp-61 → Glu [b]	+	80–95	≥ 80
→ Asn [b,c]	+(slow, 2.1×)	approx. 15	≥ 70
→ Ala [b]	+(slow, 3.0×)	approx. 10	≥ 70
→ Val [c]	+(slow, 2.2×)	approx. 5	approx. 75
Glu-65 → Asp [b]	+	80–90	≥ 70
→ Gln [b,c]	+(slow, 1.9×)	10–20	≥ 60
→ Ala [b]	+(slow, 2.7×)	approx. 10	≥ 80
→ Leu [c]	+(slow, 4.0×)	approx. 10	approx. 100
Asp-170 → Glu [b,c]	+	(50–60) [b] (60–100) [c]	≥ 85
→ His [c]	+(slow)	20–40	≥ 80
→ Cys [c]	–	20–30	≥ 70
→ Tyr [c]	–	10–20	≥ 50
→ Arg [c]	–	10–20	≥ 60
→ Met [c]	–	10–20	≥ 70
→ Trp [c]	–	3–5	5–10
→ Asn [b,c]	–	(3–9) [b] (0–2) [c]	≥ 60
→ Ala [b,c]	–	0	≥ 70
→ Ser [c]	–	0	≥ 70
→ Phe [c]	–	0	approx. 10
→ Val [b]	–		
→ Leu [b]	–		
→ Thr [b]			
Glu-189 → Asp [b]	–	0	approx. 100
→ Gln [b,c]	+	approx. 50	≥ 70
His-190 → Asp [c]	–	0	
→ Asn [b]	–	0	≥ 70
→ Gln [b,c]	–	0	approx. 100
→ Tyr [b]	–	0	10–20
→ Leu [b,c]	–	0	approx. 20
His-332 → Asn [b]	–	0	approx. 30
→ Gln [b]	–	approx. 10	30–40
→ Tyr [b]	–	0	
→ Leu [b,c]	–	0	approx. 10
Glu-333 → Asp [b]	–	0	approx. 5
→ Gln [b,c]	+(slow, 3.3×)	approx. 20	≥ 60
His-337 → Asn [b]	+(very slow)	approx. 6	20–30
→ Gln [b]	+(very slow)	6–18	30–40
→ Tyr [b,c]	–		approx. 10
→ Leu [b,c]	–	(3–5) [b] (approx. 20) [c]	(approx. 20) [b] (approx. 35) [c]

TABLE II (continued)

Mutation	Photoautotrophic growth	O_2 evolution (% wild-type)	PS II content (% wild-type)
Asp-342 → Glu [b]	+(slow, 1.2×)	approx. 15	approx. 70
→ Asn [b]	–	0	approx. 15
→ Ala [b]	–	0	10–15
→ Val [c]	–		
Ala-344 → Stop [d]	–		
Ser-345 → Ala [c]	+		
→ Pro [c]	–	0	20–30
→ Arg [c]	+		
→ Stop [c]	+		100

[a] Mutants constructed by Vermaas and co-workers [867].
[b] Mutations constructed by Debus and co-workers [871,873] (H.-A. Chu, A.P. Nguyen and R.J. Debus, unpublished).
[c] Mutations constructed by Nixon and Diner [17,19,368,996].
[d] Mutation constructed by Nixon and Diner [880,996].
[e] Measured from [^{14}C]DCMU binding assays [867].

by DPC to Y_Z^+. Protease digestion or chemical modification at sites located far from the Mn complex could prevent or alter these conformational rearrangements, thereby allowing full or partial access of DPC to Y_Z^+ in the presence of ligated Mn^{3+}. As a precedent for such a mechanism, conformational rearrangements are believed to occur following the oxidation of the first Mn^{2+} ion by Y_Z^+ during the assembly of the Mn cluster [349,359,362] (see subsection II-A.3). These conformational changes may explain why the presence of a functional Mn complex both facilitates the rebinding of the extrinsic polypeptides [232–234,278,279] and shields Y_D^+ and Y_Z^+ from exogenous reductants [271,273,348, 366,489,760,847–849]. Conformational changes are also believed to accompany the extraction of the two most tightly-bound Mn ions [130,827,829,831] (see subsection II-J.1). These conformational changes may explain why the extrinsic polypeptides are more easily extracted in the absence of the Mn complex [231,234,279]. The unprocessed carboxy-terminus of the D1 polypeptide in the LF-1 mutant of *Scenedesmus obliquus* may interfere with conformational changes induced by the ligation of a Mn^{3+} ion that would otherwise restrict the access of DPC to Y_Z^+ and lead to the assembly of a functional Mn complex. The mechanism of Mn^{2+} inhibition of electron donation by DPC to Y_Z^+ must be further clarified if the DPC/Mn^{2+} inhibition assay is to be employed to identify ligands of the Mn complex.

Site-directed mutagenesis of PS II. Site-directed mutagenesis has begun to play an active role in the search for ligands to the Mn or Ca^{2+} ions of PS II. Most published work has focused on conserved residues in the D1 and D2 polypeptides (see Fig. 3). Several models for the ligation of Mn and Ca^{2+} by these polypeptides have been advanced [32,35,114,116,787,865]. Some of these models were developed from computer-assisted modeling based on the structures [20–22] of reaction centers from purple non-sulfur bacteria [35,114,116]. However, none of the proposed models is compelling. For example, the C_2 symmetry believed to be present in the membrane-spanning regions of the D1/D2 heterodimer (e.g., Figs. 1 and 4) and which led to the identification of Y_Z and Y_D [65–68], does not appear to extend to the lumenal regions of these polypeptides in terms of amino acid residues. Also, the structures of the bacterial reaction centers provide limited insight: not only do these reaction centers fail to evolve oxygen, there is little similarity between the sequences of the lumenal regions of the D1 and D2 polypeptides and the corresponding regions of the L and M polypeptides of the bacterial reaction centers. Furthermore, the D1 and D2 polypeptides have many more residues in these regions than the L and M polypeptides. Finally, recent work indicates that the pigment content of the D1/D2 heterodimer differs from that of bacterial reaction centers [13,135–140,866] (see subsection I-B.1).

Because of the lack of compelling models, several groups have constructed mutations at nearly every residue in the lumenal regions of the D1 and D2 polypeptides that could conceivably (see subsection II-I) ligate Mn or Ca^{2+} ions. These mutations have been constructed in the cyanobacterium *Synechocystis* sp. PCC 6803. Of the 30 conserved lumenal residues targeted in the D2 polypeptide [18], including all lumenal carboxylate and histidine residues, only mutations at Glu-70 (in the sequence numbering system from spinach) abolished photoautotrophic growth [18,867] (see Table II). However, changing His-189 to Leu moderately impaired photoautotrophic growth [868]. Of the 30 lumenal conserved residues targeted in the D1 polypeptide, including all 21 lumenal carboxylate, histidine and tyrosine residues, only mutations at Asp-59, Asp-61, Glu-65, Asp-170, Glu-189, His-190, His-332,

Glu-333, His-337 and Asp-342 abolished or impaired photoautotrophic growth (See Refs. 17,19,869–871 and H.-A Chu, A.P Nguyen and R.J. Debus, unpublished data; also see Table II).

The first residue identified as a potential ligand to the Mn complex was Glu-70 of the D2 polypeptide [867]. This work was carried out by Vermaas and co-workers. Cells having Glu-70 changed to Gln or Val are unable to grow photoautotrophically [867] (see Table II). Nevertheless, cells and thylakoid membranes from the Glu-70 → Gln mutant evolve oxygen at low rates in the presence of added electron acceptors. The rate of oxygen evolution was observed to decline rapidly during illumination. This apparent photoinactivation was diminished by the addition of Mn^{2+} ions, but not by the addition of Ca^{2+} ions. Thylakoid membranes from other mutants (e.g., Pro-162 → Leu in the D2 polypeptide) were similarly photoinactivated [867,872], but the addition of Mn^{2+} ions had no protective effect [867]. Because the presence of exogenous Mn^{2+} ions diminished the rate of photoinactivation in the Glu-70 → Gln mutant, but not in the Pro-162 → Leu mutant, Glu-70 of the D2 polypeptide was proposed to be a ligand to the Mn complex [867]. The substitution of Gln for Glu was proposed to weaken the binding of one Mn ion in the higher S states. Loss of a Mn(IV) ion seems unlikely, since this would require the formation of a penta-coordinate intermediate with considerable loss of ligand field stabilization energy [498,503]. Such considerations are less significant for Mn(III) ions, however [498,503]. Because of the conformational rearrangements in the Mn environment that are believed to accompany the S-state transitions [38,387, 427,429,443,477–479] (see subsections II-G.1 and II-H), a lower affinity for Mn(III) in a higher S-state in the Glu-70 → Gln mutant is conceivable. Nevertheless, explanations other than ligation of Mn by Glu-70 are possible. For example, exogenous Mn^{2+} ions may slow the photoinactivation of the Glu-70 → Gln mutant by donating electrons to Y_Z^+. The electron donor DPC has been demonstrated to slow photoinactivation in the Glu-70 → Gln mutant [867] and in other mutants of *Synechocystis* 6803 [867,872], presumably by donating to Y_Z^+. Insufficient access of Mn^{2+} ions to the donor side of PS II may account for the inability of Mn^{2+} ions to slow photoinactivation in the Pro-162 → Leu mutant. A rigorous determination of whether Glu-70 of the D2 polypeptide is a ligand to the Mn complex will require spectroscopic analyses of oxygen-evolving PS II complexes isolated from the Glu-70 → Gln mutant and from mutants having other residues substituted for Glu-70. Until recently, no suitable preparation from *Synechocystis* sp. PCC 6803 was available. Fortunately, highly-active oxygen-evolving preparations capable of exhibiting the S_2-state multiline EPR signal have been developed recently [209,415,993] (also see Ref. 963).

Recently, attention has been focused on the D1 polypeptide. Photoautotrophic growth was completely abolished when Asp-170 was replaced with 12 out of 14 other residues or when Asp-342 was replaced with Gln, Ala or Val [17,19,367,368,869–871,873] (H.-A. Chu, A.P. Nguyen and R.J. Debus, unpublished) (see below and Table II). In contrast, replacing Asp-170 or Asp-342 with Glu had little effect. Photoautotrophic growth was moderately impaired when Asp-59 was replaced with Asn or Val, when Asp-61 was replaced with Asn, Ala or Val, or when Glu-65 was replaced with Gln, Ala or Leu [17,19,871] (H.-A Chu, A.P Nguyen and R.J. Debus, unpublished) (see Table II). In contrast, replacing Asp-59 or Asp-61 with Glu or replacing Glu-65 with Asp had little effect. Based on the criteria that eliminating a carboxylate ligand to Mn or Ca^{2+} should impair photoautotrophic growth, while changing the size of the carboxylate ligand might not, Asp-59, Asp-61, Glu-65, Asp-170 and Asp-342 could potentially coordinate Mn or Ca^{2+} ions. However, other effects caused by these mutations, such as destabilized binding of the 33 kDa extrinsic polypeptide or conformational changes in the PS-II core, might also account for the impairment or abolition of photoautotrophic growth. Interestingly, photoautotrophic growth was completely abolished when Glu-189 or Glu-333 was replaced with Asp (H.-A Chu, A.P Nguyen and R.J. Debus, unpublished), but was either unaffected (Glu-189) or was only impaired (Glu-333) when either residue was replaced with Gln [17,19] (H.-A Chu, A.P Nguyen and R.J. Debus, unpublished) (Table II). As mentioned in the preceding paragraph, to demonstrate that any of these residues ligates Mn or Ca^{2+} ions will require spectroscopic analyses of isolated PS II complexes. Such analyses have recently been reported for mutations constructed at Asp-170 of the D1 polypeptide [367,368,873,981].

The effects of mutations constructed at Asp-170 of the D1 polypeptide have been examined in detail by Nixon and Diner [367,368,981] and by Debus, Barry and co-workers [873]. Only cells having Asp-170 replaced with Glu or His were able to grow photoautotrophically, with the Asp → His mutant exhibiting considerably impaired growth (see Table II). The PS-II content of most of the 14 mutants was 70–100% that of wild-type cells, when expressed on a chlorophyll basis. Many non-photoautotrophic mutants evolved oxygen, although at low rates (see Table II). The latter mutants exhibited oxygen flash yields that oscillated with the normal period of four [368]. From considerations of manganese coordination chemistry (see subsection II-I), those mutants able to evolve oxygen contained a potential Mn ligand in place of Asp-170. The highest rates of oxygen evolution were exhibited by residues with the lowest pK_a values [368]. The S_2-state decay times in whole cells of those mutants able to evolve oxygen,

TABLE III

Further characteristics of mutants having Asp-170 of the D1 polypeptide substituted by other residues

Mutation	S_2 decay time in whole cells ($S_2Q_B \rightarrow S_1Q_B$) (s) [a]	K_m for Mn^{2+} binding to Mn-depleted PS II particles (μM) [a]	Mn content of Mn-containing PS II particles (Mn per 2 cyt *b*-599 hemes) [b]
wild-type	20 ± 5	1	4.0 (3.8–4.2) [c]
Asp → Glu	65 ± 5	2	3.3 (3.1–3.6) [c]
→ His	45 ± 5	2–10	
→ Cys		1	
→ Tyr	55 ± 5	20–40	
→ Arg	30 ± 5	5	
→ Met	65 ± 10	20	
→ Trp			
→ Asn		50	1.4 (1.2–1.7) [c]
→ Ala		50	
→ Ser		60	

[a] From Ref. 368.
[b] From Ref. 873.
[c] Range.

measured in the absence of DCMU, differed from those in wild-type cells by no more than a factor of three [368] (see Table III). (In the absence of DCMU, the S_2 state decay time primarily represents charge recombination between Q_B^- and the S_2 state).

All of the non-photoautotrophic mutants having residues substituted for Asp-170 were unable to rapidly reduce Y_Z^+ [367,368,873]. In PS II particles isolated by a procedure that retains high rates of oxygen evolution in wild-type particles [209], the Mn content of the Asp → Asn mutant was only 30–40% that of wild-type particles, while the Mn content of the Asp → Glu mutant was 75–90% [873] (see Table III). The K_m for binding Mn^{2+} ions to Mn-depleted PS II particles from 11 mutants was estimated by Nixon and Diner from the ability of different concentrations of exogenous Mn^{2+} ions to block charge recombination between Q_A^- and Y_Z^+ [367,368]. The estimated K_m values were 1 μM and 2 μM were for the wild type and Asp → Glu particles, respectively and 50–60 μM for the Asp → Asn, Asp → Ser and Asp → Ala particles [368] (see Table III). Because oxygen evolution or high affinity binding of Mn^{2+} ions was observed only when position 170 of the D1 polypeptide contained a potential metal ligand [368] and because the Mn content of the Asp → Asn mutant was significantly diminished compared to wild-type preparations [873], it was concluded that Asp-170 is critical for the assembly or stability of the Mn complex [368,873,981]. Because the reduction of Y_Z^+ by Mn^{2+} was impaired in Mn-depleted particles, it was further proposed that Asp-170 participates in the first step in the assembly of the Mn complex [368,981]. It was also concluded that Asp-170 might serve as a ligand to the final Mn complex [368,873]. However, if Asp-170 ligates Mn, because of the similarities of the S_2 state decay times in those mutants able to evolve oxygen [368] (see Table III), this residue must have little influence on the redox potential of the Mn complex and consequently must occupy only a terminal coordination site. It cannot be excluded that the altered properties of the mutants are caused indirectly by global conformational changes induced by the mutations. However, the ability of the Asp → His mutant to grow photoautotrophically (Table II) and the similarity of the K_m values in the mutants containing Glu, His, Cys and Arg (Table III), suggest that the altered properties of the mutants are more likely to be caused directly by the different properties of the residues substituted for Asp-170. Furthermore, the observed alterations (e.g., loss of activity and metal binding) are typical of those reported in other proteins when putative ligands to metal ions are changed (e.g., Refs. 874–879). Nevertheless, a determination of whether Asp-170 of the D1 polypeptide coordinates the Mn complex (or a Ca^{2+} ion that is intimately associated with the complex) will require further spectroscopic analysis of intact, isolated PS II particles. For example, if Asp-170 ligates Mn, ESEEM spectra should reveal additional Mn ligation by nitrogen in the Asp-170 → His mutant and EXAFS spectra should reveal Mn ligation by sulfur in the Asp-170 → Cys mutant.

Preliminary analyses of Mn-depleted PS II particles isolated from mutants having Asp-342 replaced with Val indicate that the high affinity (K_m = 1 μM) Mn^{2+} binding site is intact in this mutant, but that no functional Mn complexes can be assembled [17,870,880]. The properties of this mutant resemble those of the LF-1 mutant of *Scenedesmus obliquus* (see earlier in this subsection). Properties similar to those of the Asp-342 → Val mutant were also found when the processing of the carboxy-terminal extension was prevented by replacing Ser-345 with Pro [17,19,996] and when Ala-344 was replaced by a stop codon, so that the polypeptide terminated at Leu-343 [880,996]. On the basis of the latter result, the free carboxylate group of Ala-344, the carboxy-terminal residue of the mature D1 polypeptide, has been proposed to ligate the Mn complex [17,870,880,996].

Replacing His-190 with Asp or Gln slowed electron transfer from Y_Z to $P680^+$ by a factor of 200 [17,19], consistent with proposals that His-190 serves as a hydrogen bond acceptor for Y_Z [35,65,114,116,122]. Replacing His-332 with Leu, Asn, Gln or Tyr completely abolished photoautotrophic growth [17,19,880] (H.-A Chu, A.P Nguyen and R.J. Debus, unpublished) (see Table II). The properties of PS II particles of the His-332 → Leu mutant resemble those of the Asp-342 → Val, Ala-344 → Stop and Ser-345 → Pro mutants [17,19,880]. These results could be consistent with His-332 serving as a redox-active component of the water

oxidizing complex or as a ligand to the Mn cluster. Replacing His-337 with Leu or Tyr also abolished photoautotrophic growth [17,19] (H.-A Chu, A.P Nguyen and R.J. Debus, unpublished), while replacing this residue with Asn or Gln only impaired photoautotrophic growth, although severely (H.-A Chu, A.P Nguyen and R.J. Debus, unpublished). These results could be consistent with His-337 serving as a terminal ligand to the Mn cluster. However, spectroscopic analyses will be required to determine the relationships of His-332 and His-337 to the water oxidizing complex.

To summarize, while a steadily accumulating body of indirect evidence has been interpreted as suggesting that the D1 and D2 polypeptides provide ligands to the Mn complex (see subsection II-J.2 and earlier in this subsection), only Glu-70 of the D2 polypeptide and Asp-59, Asp-61, Glu-65, Asp-170, His-332, His-337, Asp-342 and Ala-344 of the D1 polypeptide have been identified as potential ligands to Mn (or Ca^{2+}) by site-directed mutagenesis experiments. Of these, detailed spectroscopic analyses have been reported only for Asp-170 of the D1 polypeptide [367,368,873,981], while preliminary analyses have been reported only for His-332, Asp-342 and the free carboxylate group of Ala-344 [17,19,880]. The fact that some or all of the mutations at Asp-59, Asp-61, Glu-65 and His-337 retain some level of photoautotrophic growth indicates that, should they ligate Mn, they must occupy only terminal coordination sites. An alternative possibility is that mutation of these residues interferes with the water oxidizing complex only indirectly by inducing conformational changes in the PS-II core. One consequence of such conformational changes could be destabilized binding of the 33 kDa polypeptide. Weaker binding of the 33 kDa polypeptide has been observed in a mutant having the Y_D tyrosine changed to Phe [835].

It should be emphasized that there is currently no solid experimental evidence that excludes any of the other intrinsic polypeptides of the PS-II core as potentially contributing ligands to the Mn complex. Indeed, in the Klein/Sauer model (Fig. 15), only 10 of the 24 coordination sites on the four Mn ions are filled by μ_2-oxo bridges, leaving 14 positions to be filled by water, Cl^- or amino-acid residues. Numerous acidic residues suitable for ligating Mn (or Ca^{2+}) are located in the lumenally-exposed regions of CP47 [130], CP43 [130,162] and the α-subunit of cytochrome *b*-559 [196–199]. Furthermore, the hydrophilic carboxy-terminal region of the 4.2 kDa product of the *psb*I gene contains such residues [297,299]. Preliminary accounts of mutations constructed in the large (approx. 190 residue) hydrophilic loop of CP47 have been reported [818,881] (see Fig. 5A, loop E). Changing the basic residue pairs Arg-286/Arg-287, Arg-357/Arg-358, Arg-385/Arg-386 and Arg-422/Lys-423 to Gly/Gly pairs in *Synechocystis* sp. PCC 6803 did not abolish photoautotrophic growth [881], but the Arg-384/Arg-385 → Gly/Gly mutation led to a approx. 50% loss in oxygen evolution activity [818]. Deletion mutations have also been reported for CP47 [882] and CP43 [883,884]. Segments ranging in length from 6 to 17 residues have been deleted from the approx. 190 residue hydrophilic loop of CP47 [882] (Fig. 5A, loop E) and from the approx. 130 residue hydrophilic loop of CP43 [883,884] (Fig. 5B, loop E). Photoautotrophic growth was abolished by all deletions in CP43 (Gln-289 to Val-306, Arg-307 to Ala-313, Asn-314 to Thr-322, Gly-334 to Met-343, Phe-345 to Glu-354, Trp-352 to Asn-360, Gly-364 to Asp-370, Gln-375 to Ala-386) [884]. Photoautotrophic growth was abolished and no stably assembled PS II complexes were detected when the segment extending from Gly-351 to Thr-365 was deleted from CP47 [882]. The epitope of the monoclonal antibody that recognizes CP47 only in the absence of the two most tightly bound Mn ions [130,827,829,831] (between Pro-360 and Ser-391) overlaps this region (see subsection II-J.1). Photoautotrophic growth was not affected when the segment extending from Arg-384 to Val-392 was deleted from CP47 [882]. However, the mutant contained approx. 65% fewer PS II complexes [882].

On the basis of directed mutations (Arg-68 → Leu and Pro-63 → Thr) and segment deletions (deletions of 18–20 residue-long segments) in the hydrophilic 37-residue carboxy-terminal domain of the α subunit of cytochrome *b*-559 in *Synechocystis* sp. PCC 6803, Pakrasi and co-workers have reported that the region between Asp-52 and Ile-71 influences oxygen evolution [18]. In contrast, Tae and Cramer have reported that changing Arg-68 or Arg-59 to Gln, either individually or simultaneously, has no significant effect on photoautotrophic growth rates, oxygen evolution activity or low-temperature fluorescence spectra [885]. Deletion of the carboxy-terminal 31 residues decreased photoautotrophic growth and oxygen evolution rates dramatically, to approx. 15% of those measured for wild-type cells [885]. However, the PS-II content of this mutant (estimated on a chlorophyll basis from [^{14}C]-DCMU binding assays) was also estimated to be approx. 15% compared to wild-type cells [885]. Consequently, the small fraction of PS-II centers in this mutant appears to be fully functional. It was concluded that the carboxy-terminal 31 residues of the α subunit of cytochrome *b*-559 have little influence on water oxidation and contribute no ligands to Mn or Ca^{2+} ions, but that the absence of these residues decreases the stability of PS II or the probability of correctly assembling functional PS II complexes [885].

III. Calcium

For recent comprehensive reviews of calcium in PS II, see [37,38,270,886]. A role for Ca^{2+} in PS II was

first observed in photosynthetic membranes from cyanobacteria [887–894]. A role for Ca^{2+} in PS II from higher plants was demonstrated when Ca^{2+} was found to reverse the inhibition of oxygen evolution caused by the depletion of the extrinsic 24 and 17 kDa polypeptides from PS II membranes [260–262]. These polypeptides were subsequently shown to substantially increase the apparent affinity of Ca^{2+} for sites in PS II [318,474,802,895–897]. Further work established that the presence of the 24 kDa polypeptide is sufficient to enhance binding of the Ca^{2+} ion(s) involved in oxygen evolution [259,895,897].

III-A. Stoichiometry and affinity

Atomic absorption measurements have demonstrated that PS II membranes [235,344,475,898–901] and core complexes [902] from higher plants contain 2–3 non-adventitiously bound Ca^{2+} ions per P680. All but one Ca^{2+} ion can be extracted by washing with 1–2 M NaCl in the presence of 1 mM EGTA and the ionophore A23187 (20 μM) [898,902], or by incubation with 10–20 mM sodium citrate at pH 3 [475]. The extrinsic 24 and 17 kDa polypeptides are lost during treatment with NaCl (see subsection I-B.4). These polypeptides are also dissociated from PS II during treatment with sodium citrate at pH 3, but reassociate when the pH is raised to pH 6.5 [235,274,903]. Consequently, samples depleted of Ca^{2+} by treatment with sodium citrate at pH 3 retain the 24 and 17 kDa polypeptides. Extraction of the final remaining Ca^{2+} ion requires more stringent conditions: 150 minutes of incubation with 2 M NaCl, 1 mM EGTA and 20 μM A23187 at pH 5, followed by repeated washings with 1 mM EGTA and 20 μM A23187 at pH 6 [902] (and see Ref. 898). All Ca^{2+} ions in PS II can also be removed by quantitatively replacing them with La^{3+} or Dy^{3+} [476] (see subsection III-B). The lanthanide ions can then be removed to yield PS II preparations that lack both Ca^{2+} and lanthanide ions [476].

Earlier procedures to extract Ca^{2+} employed less stringent conditions and used the extent of inhibition of oxygen evolution as an assay for the completeness of extraction. All procedures involved washing PS II membranes with 1–2 M NaCl in either light [895,897,904] or darkness [214,260,404,474,802,905] to extract the 24 and 17 kDa polypeptides, thereby rendering the Ca^{2+} ions more labile and/or more accessible to extraction. In some cases EDTA (1–5 mM) [404,802] or EGTA (10–50 μM [895,904] or 5–10 mM [214,474,897]) was included in the wash or added subsequently. Illumination was found to facilitate extraction [802,895,897,904,905], usually in samples that were not washed concurrently with both NaCl and chelating agents. However, one study reported that illumination was an absolute requirement for extraction, even in the presence of 10 mM EGTA [897]. Subsequent work demonstrated that the effectiveness of Ca^{2+} extraction by treatment with NaCl and EGTA depends on the redox state of the Mn complex [477]. These observations presumably explain why illumination was reported to facilitate extraction in the earlier studies. The ease of extraction descends in the order $S_3 > S_2$, $S_0 > S_1$ [477]. Based on these observations, it was proposed that the affinity of PS II for Ca^{2+} depends on the redox state of the Mn complex, with the S_1 state possessing the highest affinity and the S_3 state possessing the least [477]. It was also proposed that the accessibility of the Ca^{2+} site (or sites) depends on the redox state of the Mn complex and is greatest in the S_3 state [477]. The possible relevance of the Ca^{2+} pump of the sarcoplastic reticulum to PS II was suggested [477] because changes in Ca^{2+} affinity and accessibility take place during the catalytic cycling of this enzyme [906]. It has recently been suggested that the apparent S-state dependent affinity of PS II for Ca^{2+} may result from an S-state-dependent binding of the extrinsic polypeptides [37]. However, this possibility was rejected in an earlier study [477]. There has been considerable controversy concerning the relative effectiveness of these earlier procedures in removing all traces of Ca^{2+} (see subsection III-C and see the discussion in Ref. 421). Those employing EDTA or EGTA plus some degree of illumination are presumed to have extracted all but the one most tenaciously bound Ca^{2+} ion, but this supposition has not been tested by atomic absorption measurements.

Efforts to determine the affinity of Ca^{2+} for PS II have relied on measuring oxygen evolution in Ca^{2+}-depleted samples as a function of added Ca^{2+}. The most recent determinations were performed on spinach PS-II core complexes depleted of all but 0.26 Ca^{2+} ions per P680 [902]. This study yielded three apparent K_m values: 1–4 μM, 67–97 μM and 2.7–7 mM [902]. These K_m values have been interpreted in terms of three separate Ca^{2+} sites. However, the three values may also reflect a heterogeneity of fewer sites. Other determinations have been performed on samples either known [898,907] or now presumed [895,908] (see above) to have been depleted of all but one Ca^{2+} ion per P680. These studies have yielded apparent K_m values of 50–100 μM and 1–7 mM [895,898,907,908], in agreement with the two weaker values determined in the most recent study [902]. These two weaker values have been interpreted as representing either two Ca^{2+} sites [898,902], or a single Ca^{2+} site [895] having a K_m value that is determined by the redox state of the Mn complex [421,477]. It was suggested that the K_m = 50–100 μM and K_m = 1–7 mM sites may correspond to the same site, but in samples poised in the S_1 and S_0 states before extraction of Ca^{2+}, respectively [421,477]. In support of a single site characterized by two K_m

values, the K_m = 1–7 mM site can reportedly be converted into the K_m = 50–100 μM site by raising the pH of the sample from 5.1 to 6.2 [908]. It should be noted that all of these binding studies were performed in the presence of 10–40 mM NaCl. Because Na^+ has been shown to compete with Ca^{2+} for a common site on PS II (with a K_i of approx. 8 mM) [909,910], the true K_m values could be much lower. When Na^+ ions were excluded from similar Ca^{2+}-rebinding experiments by employing tetramethylammonium cation as a counterion to Cl^-, an apparent K_m value of 20–30 μM was determined, compared to approx. 350 μM in control samples containing 30 mM NaCl [274,909,910]. No lower-affinity Ca^{2+} site was detected in these experiments [274]. It should also be noted that all of the reported K_m values were determined in the absence of the 24 kDa polypeptide; the true affinity of Ca^{2+} could be much greater in native PS II complexes. Alternatively, removal of the 24 kDa polypeptide may expose Ca^{2+} site(s) to Na^+ ions; the apparent decrease in Ca^{2+} affinity may result from competition between Ca^{2+} and Na^+ rather than from any direct or indirect structural influence of the 24 kDa polypeptide on one or more Ca^{2+} sites. The 24 and 17 kDa polypeptides form an apparent diffusion barrier to Ca^{2+} rebinding in darkness [274,474–476] and may similarly shield the Ca^{2+} site(s) from Na^+. In the presence of the 24 and 17 kDa polypeptides, the rebinding of Ca^{2+} to PS II is a slow process (40–60 min) [274,474–476]. It has been proposed to involve the reversible dissociation of the 24 and 17 kDa polypeptides [274]. (K_m values for Ca^{2+} rebinding determined in the presence of the 24 and 17 kDa polypeptides by one set of workers [903,907] are suspect because no account was taken of the slowness of Ca^{2+} rebinding in the presence of these polypeptides [474–476]).

To summarize, PS II contains 1 high-affinity and 1–2 lower affinity sites for Ca^{2+} per P680. The apparent affinity for Ca^{2+} of at least the latter 1–2 site(s) is modulated by the redox state of the Mn cluster [477], although whether this reflects an S-state-dependent affinity for Ca^{2+}, or an S-state-dependent accessibility of the Ca^{2+} site(s), remains unknown. The Ca^{2+} in the highest-affinity site can be removed only by relatively harsh procedures [898,902] or by treatments with lanthanides [476] (see subsection III-B), whereas the Ca^{2+} in the 1–2 lower affinity sites can be removed by a number of relatively mild procedures. Occupancy of the 1–2 lower-affinity sites by Ca^{2+} is not required for assembly of the Mn complex, but is required for the complex to yield O_2 [349,354,375] (see subsections II-A.3 and III-C). There is evidence that the 1–2 lower-affinity sites are created during formation of the functional Mn complex [362]. At least one Ca^{2+} site can be occupied by lanthanides in the absence of the Mn complex, as determined from the paramagnetic effect of Dy^{3+} on the EPR signal and relaxation properties of Y_D^+ in samples having Ca^{2+} quantitatively replaced by Dy^{3+} [476]. In addition to inhibiting oxygen evolution, removal of Ca^{2+} from the 1–2 lower-affinity sites has also been reported to slow the oxidation of Y_Z by $P680^+$ [487] (also see Refs. 628,630,638) and see subsection III-C), although Ca^{2+} is not required for this electron transfer step to proceed [902], at least in samples poised in the lower S-states [487] (see subsection III-C). Depletion of Ca^{2+} may inhibit electron transfer from Y_Z to $P680^+$ more severely in cyanobacteria than in higher plants [893,911], (see subsections III-C and III-E). There is currently no conclusive evidence that the Ca^{2+} ion in the highest-affinity site has any role in either oxygen evolution or PS II photochemistry: removal of Ca^{2+} from the lower-affinity site (or sites) is sufficient to inhibit oxygen evolution and PS II core complexes depleted of all but 0.26 Ca^{2+} per P680 were able to generate Y_Z^+ upon illumination at room temperature [902]. However, these samples were unable to oxidize the Mn complex at 210 K [902] and samples that had been depleted of all Ca^{2+} ions by treatment with La^{3+} or Dy^{3+} were unable to oxidize the Mn complex at 200 K, even when the Dy^{3+} ions were subsequently removed, leaving no Ca^{2+} or Dy^{3+} ions in the preparation [476] (see subsection III-B). Whether any of these Ca^{2+}-depleted samples were able to oxidize the Mn complex at higher temperatures was not investigated. The samples depleted of all but 0.26 Ca^{2+} per P680 were reported to photooxidize Mn^{2+} during the initial steps of photoactivation [912]. However, it was also reported that the presence of Ca^{2+} in the highest-affinity site is required for assembly of the Mn complex in Mn-depleted preparations [912].

It should be noted that Katoh and co-workers disagree with the majority view, expressed above, that the weakly bound Ca^{2+} ion(s) are essential for water oxidation. They have reported that treatment with 1–2 M NaCl removes no Ca^{2+} ions from PS II membranes in either light or darkness, even when the NaCl-washed membranes are subsequently incubated with 2 mM EGTA [900]. Oxygen evolution was inhibited by approx. 50% in these samples, and was largely restored by the addition of 5 mM Ca^{2+} [900]. They have also reported that only approx. 1 Ca^{2+} ion per P680 is present in highly purified PS II preparations from spinach [11,900], including one preparation that retains the 24 and 17 kDa polypeptides [11]. They also find only approx. 1 Ca^{2+} in PS II complexes isolated from the cyanobacterium *Synechococcus clongatus* [286,899, 913,995] and from a mutant of rice that lacks chlorophyll *b* [344]. The activities of the higher-plant preparations that contained only approx. 1 Ca^{2+} per P680 were significantly inhibited by washing with 1.5 M NaCl [11,344] or by incubating with sodium citrate at pH 3 [903,907]. No further Ca^{2+} was extracted by these

treatments, but significant activity appeared to be restored by the addition of Ca^{2+} [11,344,903,907]. On the basis of these results, Katoh and co-workers argue that procedures employed to remove Ca^{2+} inactivate oxygen evolution by inducing structural perturbations that are unrelated to the removal of Ca^{2+} ions, but which can be compensated for by the subsequent addition of Ca^{2+} ions [11,900,903]. They have proposed that the structural perturbation may be the removal of the 24 kDa polypeptide [11,900]. However, other workers have shown that rebinding the 24 and 17 kDa polypeptides to NaCl-washed samples does not restore activity in the absence of Ca^{2+} [447,474,896]. Furthermore, Katoh and co-workers have recently shown that binding these polypeptides to citrate-treated samples does not restore activity in the absence of Ca^{2+} [903]. Consequently, the hypothetical structural perturbations that cause the loss of oxygen evolution remain undefined. The reasons for the discrepancies between the results of Katoh and co-workers and the rest of the work discussed in this review remain unclear. However, many of the preparations of Katoh and co-workers appear to have significantly lower oxygen evolution activities than those of other workers (for a detailed discussion of this point, see Ref. 914). The presence of significant amounts of Ca^{2+}-deficient inactive centers would lead to underestimation of the number of Ca^{2+} ions bound to and readily removed from, active centers. In the remainder of this review, the majority viewpoint, that the weakly-bound Ca^{2+} ion(s) are essential for water oxidation, will be adopted.

III-B. Other metal ions at the Ca^{2+} site(s)

The lower-affinity Ca^{2+} site(s) can be occupied by several metal ions other than Na^+ and Ca^{2+}. (For a comprehensive discussion, see Ref. 37). Both Sr^{2+} [260,372,894] and vanadyl ions (VO^{2+}) [483] can substitute for Ca^{2+} and support oxygen evolution, but the steady-state rates are lower. In the case of Sr^{2+}, the slower steady-state rate has been attributed to a slowing of the $S_3 \rightarrow (S_4) \rightarrow S_0$ transition [421,432] and at least one other S-state transition [487]. Substitution of Sr^{2+} for Ca^{2+} results in a modified S_2-state multiline EPR signal that has narrower hyperfine spacings [421,432] (see Fig. 10). Both K^+ and Cs^+, like Na^+, have been shown to inhibit oxygen evolution by being weakly competitive with Ca^{2+} (with K_i values of 5–10 mM) [909,910]. The Cd^+ ion is a more strongly competitive inhibitor (K_i approx. 0.3 mM) [910]. Photoactivation studies showed that Mn^{2+} also inhibits oxygen evolution by competing for this site(s) [349,354,362, 371,375] and a mathematical model for the photoactivation process predicts that Mn^{2+} binds to the Ca^{2+} site with a K_d of approx. 90 μM [354]. Finally, La^{3+} has an even greater affinity for this site(s) than Ca^{2+} [476,548]. The effects of La^{3+} on PS II are not limited to inhibiting oxygen evolution by competing for Ca^{2+} sites. The La^{3+} ion also releases the 24 and 17 kDa polypeptides, even in the presence of excess Ca^{2+} ions [548]. In the absence of excess Ca^{2+} ions, La^{3+} releases the 33 kDa polypeptide and approx. 60% of the Mn complex unless approx. 200 mM Cl^- is present during exposure to La^{3+} [476,548]. It has recently been reported that all Ca^{2+} in PS II can be quantitatively replaced by La^{3+} or Dy^{3+} without loss of Mn [476]. The resulting samples can be reconstituted with the 24 and 17 kDa polypeptides but do not evolve oxygen and oxidize a chlorophyll molecule rather than the Mn complex when illuminated at 200 K [476]. Magnetic coupling between Y_D^+ and Dy^{3+} was reported in these samples [476]. This coupling was observed even in the absence of the Mn complex [476]. Consequently, the Ca^{2+} site occupied by Dy^{3+} in the Mn-depleted samples may correspond to the most tightly-bound Ca^{2+} site. From the magnitude of the magnetic coupling between Dy^{3+} and Y_D^+, the distance between this Ca^{2+} site and Y_D^+ could be as large as 40 Å, however [476].

III-C. Influence of Ca^{2+} on the S-state transitions

Extraction of Ca^{2+} from the lower-affinity site(s) reversibly inhibits oxygen evolution by disrupting normal cycling of the Mn complex through the S-states. The identity of the S-state transition blocked in the absence of Ca^{2+} has been a major point of controversy. Blockage of the $S_1 \rightarrow S_2$ transition has been proposed on the basis of EPR studies [9,214,600,601,805,902,915], blockage of the $S_2 \rightarrow S_3$ transition has been proposed on the basis of thermoluminescence measurements [362,375,422,449,916], blockage of the $S_3 \rightarrow S_4$ transition has been proposed on the basis of EPR studies [421,447,454,487], luminescence measurements [432, 904] and an earlier thermoluminescence study [802] and blockage of the $S_4 \rightarrow S_0$ transition has been proposed based on other EPR studies [455] (also see Ref. 448). In addition, the $S_0 \rightarrow S_1$ transition has been proposed to be blocked in samples depleted of Ca^{2+} while poised in the S_0 state [421,477,483] and one set of workers argues that Ca^{2+} is not required for any of the S-state transitions to proceed (see subsection III-A).

The basis for concluding that the $S_0 \rightarrow S_1$ transition is blocked in samples depleted of the lower-affinity Ca^{2+} ion(s) while poised in the S_0 state was the inability to generate the S_2-state multiline EPR signal during illumination at 200 K [483]. The samples were depleted of Ca^{2+} at pH 8.3 [483]. Incubation in darkness at this pH has been proposed to reduce samples from the S_1 state to the S_0 state [483,917]. However, this pH has been argued to diminish the quantum yield of S-state turnover (increase the 'miss' parameter) rather than generate the S_0 state [587,620]. Indeed, the flash-in-

duced yield of cytochrome *b*-559 oxidation has recently been found to increase significantly above pH 7.5 [215], perhaps accounting for the increased 'miss' parameter reported in Ref. 620. Consequently, it is not clear that the samples depleted of Ca^{2+} at pH 8.3 were poised in the S_0 state, although a weak multiline-like EPR signal observed in the Ca^{2+}-depleted samples prior to illumination [483] suggests that some modification of the Mn complex had occurred during Ca^{2+} depletion. Further work will be required to establish whether the $S_0 \rightarrow S_1$ transition is blocked in the absence of Ca^{2+}.

The basis for concluding that the $S_1 \rightarrow S_2$ transition is blocked in samples depleted of the lower-affinity Ca^{2+} ion(s) is also the inability to generate the S_2-state multiline EPR signal at 200 K [9,214,805,902,915] or at higher temperatures in the presence of DCMU [214]. Some workers have reported that a chlorophyll molecule is oxidized instead of the Mn complex when these samples are illuminated at 200 K [214] (also see Ref. 902), but others report no significant oxidation of chlorophyll at 200 K in samples that were treated similarly [421]. Proponents of a block at the $S_3 \rightarrow S_4$ transition have argued that the high concentrations of chelating agents employed by most workers unable to generate the multiline signal (1–10 mM EDTA or EGTA) perturbs the relaxation properties of the Mn complex sufficiently to preclude observation of the signal [421,432,454]. Proponents of a block at the $S_3 \rightarrow S_4$ transition observe a normal multiline signal when only 50 μM EGTA is employed to extract Ca^{2+} [421,432,454], or when samples extracted with 5 mM EGTA are subsequently resuspended in the presence of 50 μM EGTA [421]. However, the argument that high concentrations of chelating agents precludes the formation of the multiline signal has been weakened by a recent observation: the addition of 10 mM EGTA to a sample that had been depleted of Ca^{2+} in the presence of 50 μM EGTA decreased the amplitude of the multiline signal by only approx. 20% [454].

The proponents of a block at either the $S_1 \rightarrow S_2$ or $S_2 \rightarrow S_3$ transitions argue that 50 μM EGTA, employed to extract Ca^{2+} by proponents of a block at the $S_3 \rightarrow S_4$ transition, is insufficient to sequester all of the large amount of adventitious Ca^{2+} known (e.g., Refs. 260,449,476,899) to be associated with PS II membranes. Consequently, these authors argue that the multiline signal observed by the proponents of a block at the $S_3 \rightarrow S_4$ transition arises from adventitious Ca^{2+} that has repopulated the Ca^{2+} site(s). Indeed, it has been argued [270,274] that the observation of a normal multiline signal in these samples shows that adventitious Ca^{2+} had rebound to PS II because this signal is not observed in most Cl^--depleted preparations [214,433,434,487,519] (see subsection III-D) and because the binding of Cl^- to PS II has been reported to require the prior binding of Ca^{2+} [274,910]. (However, it is not clear that no multiline signal could have been generated in the Ca^{2+}/Cl^--depleted samples that were used in the ordered binding experiments: the Cl^- ions were removed by an incubation in a Cl^--free buffer [274,910]; see subsection III-D.) The luminescence and EPR experiments supporting a block at the $S_3 \rightarrow S_4$ transition were originally performed with samples that had been extracted with only 50 μM EGTA [421,432,904]. Unfortunately, the Ca^{2+} contents of these samples were not determined by atomic absorption measurements. Nevertheless, samples extracted with 5 mM EGTA and subsequently resuspended in 50 μM EGTA exhibit a normal multiline signal [421] (see preceding paragraph). Furthermore, samples extracted with only 50 μM EGTA exhibit the 130–160 Gauss-wide EPR signal that has been attributed to a modified form of the S_3 state [454] (see subsection II-B.2). This signal has been observed in citrate-treated samples [448,455,456,484] that are believed to contain only 1 Ca^{2+} ion per P680 on the basis of atomic absorption measurements performed on similarly prepared samples [475].

Because the S_1 state predominates in dark-adapted samples, blockage of the $S_1 \rightarrow S_2$ transition should prevent the oxidation of Mn by Y_Z^+. Under these circumstances Y_Z^+ should be reduced by Q_A^- with a half-time of 80–120 ms [68,178] or by Q_B with a halftime of approx. 20 sec [70]. Because Y_Z^+ is normally reduced by Mn in the S_1 state with a half-time of approx. 100 μs (see subsection II-D.1), blockage of the $S_1 \rightarrow S_2$ transition should be manifested as a dramatically slower decay of Y_Z^+ when detected following a single flash-induced charge separation. Indeed, the reduction of Y_Z^+ was observed to slow dramatically in several EPR studies that involved averaging many flash-induced measurements [260,601,905], but not in others [404,600]. The reasons for the discrepancy between these various studies remain unclear. However, the conclusion of one of the studies that reported a slower decay of Y_Z^+ has been challenged [421,432].

Further characterization of the dark-stable approx. 26-line multiline and 130–160 Gauss-wide EPR signals recently detected in Ca^{2+}-depleted samples (see subsection II-B.1 and II-B.2) should help clarify the controversy over which S-state transition is blocked in the absence of the weakly-bound Ca^{2+} ions. For example, generation of the altered multiline signal in Ca^{2+}-depleted samples demonstrates that oxidation of the Mn complex to at least a modified S_2 state can take place under some circumstances. As discussed in subsection II-B.1, the modified multiline signal has been reported in samples either washed with NaCl and high concentrations of EDTA or EGTA in the presence of light [447,449,452,453], or in samples incubated with 10–20 mM sodium citrate at pH 3 in darkness [423,448, 450,982].

As discussed in subsection II-B.2, the 130–160 Gauss-wide EPR signal has been attributed to a modified form of the S_3 state, or to an organic radical that is magnetically coupled with the Mn complex when the latter is poised in a modified S_2 state. It has also been proposed that the 130–160 Gauss-wide signal arises from a modified S_4 state [448,455,484]. The block at the $S_4 \rightarrow S_0$ transition was proposed on grounds that, when samples were poised in the dark-stable S_2 state, generation of the 130–160 Gauss-wide signal required two turnovers in a substantial fraction of the PS II centers [455,484]. Furthermore, the loss of the altered multiline signal reportedly did not correlate with the formation of the 130–160 Gauss signal [455]. These results were explained in terms of a 'hidden' reductant that is formed in a substantial fraction of samples during Ca^{2+} depletion and that must be oxidized before the 130–160 Gauss-wide signal can be generated [448,455,484]. No explanation has been offered to explain why the yield of this 'hidden' reductant is so variable [484]. The nature and variable yield of the unidentified 'hidden' reductant should be investigated. This reductant was reported to rapidly reduce approx. 50% of Y_D^+ when Ca^{2+} was added to samples that had been depleted of Ca^{2+} by incubation with sodium citrate at pH 3 [448,484]. A similar reduction of approx. 50% of Y_D^+ was reported when Ca^{2+} was added to samples that had been depleted of Ca^{2+} at pH 8.3 [483]. However, a similar reduction of Y_D^+ has not been reported in samples depleted of Ca^{2+} at pH 6.5. Description of the 130–160 Gauss-wide EPR signal as a modified form of the S_4 state seems largely a matter of semantics, however, since even the proponents of a block at the $S_4 \rightarrow S_0$ transition agree that the 130–160 Gauss-wide signal arises from an organic radical interacting with the Mn complex when the Mn ions are poised their S_2-state oxidation levels [448,455,484].

Blockage of the $S_2 \rightarrow S_3$ transition has been proposed based on interpretations of thermoluminescence flash yield data [422,449,916]. However, generation of the 130–160 Gauss-wide EPR signal, whatever its origin, is difficult to reconcile with these interpretations. Standard interpretations of thermoluminescence require that the thermoluminescence yield should oscillate in response to a series of flashes if any electrons can be extracted from the donor side of PS II once the S_2 state has been achieved [674,918,919] (for review, see Refs. 675–677). Generation of the 130–160 Gauss-wide signal concurrently with the disappearance of the multiline signal [447,448,452,454] demonstrates that at least one electron can be extracted from the donor side of PS II once the S_2 state is achieved. However, no thermoluminescence oscillations have been observed in Ca^{2+}-depleted preparations that exhibit the 130–160 Gauss-wide EPR signal [422,449,453,916], even when both the thermoluminescence and the EPR measurements were performed in the same laboratory [453]. The thermoluminescence and EPR data are, therefore, in direct conflict, even if the 130–160 Gauss-wide EPR signal arises from a precursor to the S_3 state [453], or from an organic component that becomes reversibly oxidized when the normal $S_2 \rightarrow S_3$ transition is blocked [453]. The reasons for the discrepancy between the thermoluminescence and EPR data are unknown. One possibility is that extraction of Ca^{2+} modifies the acceptor side of PS II. For example, treatment with 2 M NaCl has been reported to abolish the binary oscillations of Q_B semiquinone formation in response to a series of flashes [585,905,920]. Such an alteration in Q_B function or Q_B^- stability would likely lead to misinterpretations of the thermoluminescence flash yield data. However, such an alteration of the properties of the PS II electron acceptors would have to be reversed by the addition of Ca^{2+} [422,449,453]. Other possible explanations have also been advanced [38,447,454]. Further characterization of the EPR properties of samples that have been analyzed by thermoluminescence is needed. It would be helpful if the EPR and thermoluminescence measurements were performed in the same laboratory on samples that have been depleted of Ca^{2+} by a variety of methods.

Differences between Ca^{2+}-extraction procedures may underlie the controversy over which S-state transition is blocked. For example, no multiline signal of any kind (other than what might be attributed to PS-II centers containing residual weakly-bound Ca^{2+} ions) has been reported in samples depleted of Ca^{2+} in darkness with high concentrations of chelating agents at pH 6.0–6.5 [9,214,421,902] (unless the concentration of chelating agent was lowered to approx. 50 μM after the Ca^{2+} ions were extracted [421]), even when the samples were illuminated at 273 K with continuous light in the presence of DCMU [214]. Perhaps the extraction of Ca^{2+} in darkness at pH 6.0–6.5 and the presence of high concentrations of chelating agents, traps the Mn complex in an altered S_1 configuration that, depending on the temperature of illumination, is unable to advance to the S_2 state, or advances to an S_2 state that yields only a broad and unrecognizable EPR signal. Similarly, the extraction of Ca^{2+} during illumination may trap the Mn complex in an S_2 or S_3-like configuration that resists being altered by chelating agents when deactivated to the S_1 state. Different trapped configurations of the Mn complex could explain why illumination at 200 K in the presence of 10 mM EGTA generates very little multiline signal in samples depleted of Ca^{2+} with 5 mM EGTA in darkness [421], yet generates a substantial multiline signal in samples depleted of Ca^{2+} with 50 μM EGTA during illumination [454]. Alternate configurations of the Mn complex in the S_1 state have been proposed previously [120,459,460,921]. Moreover, as discussed earlier,

conformational rearrangements in the Mn environment are believed to accompany the S-state transitions [31,38,387,427,443,477–479] (see subsections II-G.1 and II-H), even at temperatures as low as 198 K [429]. Furthermore, 'structural orderings' have been postulated to accompany the formation of the multiline signal based on the negative activation entropies estimated for the $S_1 \rightarrow S_2$ transition [480] and for the conversion of the S_2-state $g = 4.1$ EPR signal to the multiline signal [418]. As mentioned in subsection II-C.1, X-ray absorption measurements indicate that structural rearrangements in the Mn environment take place when Ca^{2+} is extracted by treatment with sodium citrate at pH 3 [424] (M.J. Latimer, V.J. DeRose, V.K. Yachandra, I. Mukerji, K. Sauer and M.P. Klein, personal communication). Structural changes have also been suggested to accompany the extraction of Ca^{2+} at pH 8.3 [483]. It would be of interest to determine whether similar structural rearrangements are observed in samples depleted of Ca^{2+} by other methods.

It has recently been proposed that Y_Z can no longer be oxidized once the modified S_3 state (or the 'S_2-plus-radical' state) is formed in Ca^{2+}-depleted samples [38,487]. This proposal is based on an inability to accumulate significant quantities of Y_Z^+ in Ca^{2+}-depleted samples, as determined by EPR measurements conducted with both continuous and flash illumination [487] and by flash-induced optical absorption measurements in the ultraviolet that failed to detect the absorption changes characteristic of Y_Z^+ formation (J. Lavergne and A. Boussac, quoted in Ref. 487). Electron transfer from Y_Z to $P680^+$ was slowed to 20–40 μs in the same Ca^{2+}-depleted samples [487] (also see Refs. 628,630,638). It was argued that electron transfer from Y_Z to $P680^+$ is slowed even further after the putative histidine radical of the modified S_3 state is formed, so that further charge separations result in the reduction of $P680^+$ by Q_A^- rather than by Y_Z [38,487]. Electrostatic interactions involving an extra positive charge associated with the modified S_3 state [452] were postulated to cause the further slowing of electron transfer from Y_Z to $P680^+$ once the modified S_3 state is achieved [38,487]. The earlier luminescence data that were originally interpreted as demonstrating the formation of both Y_Z^+ and the S_3 state in Ca^{2+}-depleted samples [432,904] have been reinterpreted in accordance with the new model [38,487].

The proposed inability to generate Y_Z^+ in Ca^{2+}-depleted samples once the modified S_3 state is formed [38,487] is very intriguing, particularly since the same phenomenon has also been proposed to occur in Cl^--depleted samples [38,487] (see subsection III-D). However, the reported failure to accumulate the EPR signal of Y_Z^+ in Ca^{2+}-depleted samples [487] conflicts with other studies. In some studies, 0.5–0.6 Y_Z^+ per P680 was detected as a flash-induced transient that decayed in hundreds of milliseconds [260,271,600–602,905,922]. In other studies, the EPR spectrum of approx. 0.5 [600], 0.75 ± 0.10 [214] or 0.8 ± 0.1 [456] Y_Z^+ per P680 was generated by continuous illumination. In the latter study [456], Y_Z^+ was distinguished from Y_D^+ on the basis of the different microwave power saturation characteristics of the EPR signals of two radicals in the presence of the Mn complex (see subsection II-J.2). Similar amounts of Y_Z^+ were also generated by continuous illumination of samples that had been depleted of Ca^{2+} with sodium citrate at pH 3 [424,456,916]. The substantial quantities of Y_Z^+ observed in these studies are unlikely to have resulted from incomplete removal of Ca^{2+} ions because in Ca^{2+}-sufficient samples the reduction of Y_Z^+ by the Mn complex is too rapid to be resolved in most EPR experiments (30–1200 μs, see subsection II-D.1). The reasons for the discrepancies in the amount of Y_Z^+ generated in different studies need to be clarified.

III-D. Relationship between Ca^{2+}-depletion and Cl^--depletion

For reviews of Cl^- in PS II, see Refs. 38,270,690,691, also see Ref. 33. The binding of Ca^{2+} and Cl^- ions to PS II has been reported to be a rapid, ordered equilibrium process, with the binding of Cl^- requiring the prior binding of Ca^{2+} [274,910]. Chloride ions can be competitively displaced from PS II (possibly from a site on the Mn complex, see subsection II-G.1) by F^- [439], acetate [439] and many primary amines [437–439]. Chloride ions have also been removed by alkaline pH [685,923–926], by treatment with 25–100 mM SO_4^{2-} [241,437,466,471,927], or by extended incubation in Cl^--free buffers [404,928,929]. All of these treatments reversibly inactivate oxygen evolution. However, SO_4^{2-}, which displaces Cl^- ions from PS II in a non-competitive fashion [241,438,927], irreversibly inactivates approx. 25% of the PS II centers [241,438,927,929]. Sulfate also releases a similar percentage of the Mn cluster as Mn^{2+} ions [929] and releases a fraction of the 24 and 17 kDa extrinsic polypeptides [745]. Chloride can be functionally replaced by Br^- and, to a lesser extent, by NO_3^- or I^- [434,461,472,473,923,928]. However, the $S_3 \rightarrow (S_4) \rightarrow S_0$ transition is slowed in the presence of NO_3^- [471]. (It has been reported that SO_4^{2-}, HPO_4^{2-} and Mes anions can functionally replace Cl^- in the cyanobacterium *Synechococcus elongatus* [930,931]). Extraction of Cl^- by extended incubation in Cl^--free buffers produces different effects than extraction by the more stringent conditions of alkaline pH or SO_4^{2-} (see discussion in Ref. 38). The S_2-state multiline EPR signal can be generated in the former samples [404,928], but not in the latter [214,433,434,487,519], even though a modified S_2 state is formed in the latter samples [433,434,466–470,932,933] (see below). The S_2 state is

also abnormally stable in the latter preparations [433,434,468–470,932–935].

The number of Cl^- ions required for oxygen evolution in PS II (per P680) is not known. A Cl^-/PS II stoichiometry of approx. 5 was estimated on the basis of $^{35}Cl^-$-binding studies conducted with Cl^--depleted thylakoid membranes that were incubated with $^{36}Cl^-$ during illumination [924]. Recent experiments conducted with $^{36}Cl^-$ indicate that illuminated PS II membranes contain at least one Cl^- ion per P680 that exchanges very slowly with Cl^- ions in solution (half-time of several hours) [936]. The slowly exchanging Cl^- ions were rapidly lost when the extrinsic 24 and 17 kDa polypeptides were removed [936]. A single class of tightly-bound but rapidly exchangeable Cl^- ions in PS II has been inferred from recent ^{35}Cl-NMR line broadening experiments [937]. Earlier ^{35}Cl-NMR data that were interpreted in terms of multiple classes of rapidly exchangeable Cl^- sites [938,939] are now considered to have been compromised by a systematic instrument irregularity [937]. The rapidly exchangeable Cl^- ions appear to bind more tightly in the S_2 and S_3 states than in the S_0 and S_1 states [610] (also see Ref. 940). From Cl^- titrations of the restoration of oxygen evolution to Cl^--depleted chloroplasts and sub-chloroplast particles, it was concluded that Cl^- functions at a single catalytic site [472]. However, from Cl^- titrations of F^--inhibited PS II membranes, it was concluded that Cl^- binds to two sites: the restoration of the multiline EPR signal required 11-fold less Cl^- than the restoration of oxygen evolution [928]. From a study of the onset of Cl^--depletion caused by SO_4^{2-}, NO_3^- and acetate, it was also concluded that PS-II centers contain two Cl^- sites [471]. It was proposed that the displacement of Cl^- from one of these sites slows the $S_3 \rightarrow (S_4) \rightarrow S_0$ transition, whereas displacement of Cl^- from the other completely inactivates oxygen evolution [471]. Nitrate was proposed to act at only the first site, SO_4^{2-} was proposed to act at the second site and acetate was proposed to act at either site [471]. The two Cl^- sites identified in these studies were considered to be present simultaneously in the same PS-II centers [471,928]. An intriguing alternate possibility is that the two sites appear in different S-states, so that only a single site is present at any given time [38,486]. In one recent model, a single Cl^- ion exchanges between two sites during the S state cycle [31,38] (see subsection III-G). One of these sites is proposed to be on a Ca^{2+} ion, while the other is proposed to be on the Mn complex [31,38].

A considerable number of studies have concluded that the depletion of Cl^- with alkaline pH or SO_4^{2-} blocks the $S_2 \rightarrow S_3$ transition [433,466–470,933]. However, as mentioned in subsection II-B.2, a new EPR signal centered at g approx. 2 and reported to have a linewidth of 160 ± 20 Gauss [486] or < 90 Gauss [487] has recently been reported in Cl^--depleted [486,487], F^--treated [486] and NH_3-treated samples [456,485]. This signal superficially resembles the 130–160 Gauss-wide signal observed in Ca^{2+}-depleted samples and has also been attributed to a modified form of the S_3 state [485–487] or to an 'S_2-plus-radical' state [456]. The conclusions of the earlier Cl^--depletion studies must reevaluated. In one of the earlier studies, the addition of Cl^- ions to Cl^--depleted samples immediately after a flash yielded the multiline signal in darkness, demonstrating the presence of an altered 'EPR-silent' S_2 state [433]. Because this signal was also generated when Cl^- was immediately added to samples that had been given two or more flashes, it was concluded that the $S_2 \rightarrow S_3$ transition was blocked in the absence of Cl^- [433]. These data would be consistent with the formation of a modified S_3 or 'S_2-plus-radical' state if the addition of Cl^- led to a rapid deactivation of this state in addition to a conversion of the altered 'EPR-silent' S_2 state to the normal S_2 state. The addition of Ca^{2+} has been observed to cause a similar rapid deactivation of the 'S_2-plus-radical' state in Ca^{2+}-depleted samples [447]. Fluorescence measurements [466,467], luminescence measurements [467] and optical absorption measurements of the decay of $P680^+$ [468,487] in Cl^--depleted samples indicate that only two electrons are rapidly transferred from the donor side of PS II to $P680^+$ in response to a series of flashes. These data were interpreted in terms of formation of the state $Y_Z^+S_2$, with the $S_2 \rightarrow S_3$ transition being either blocked or slowed considerably. How to reconcile these data with the observation of the 90–160 Gauss-wide EPR signal is less obvious. However, several possible explanations have been suggested.

One explanation, suggested by Nugent and coworkers [456], is that the 90–160 Gauss-wide EPR signal arises from an interaction between Y_Z^+ and the modified S_2 state Mn complex. If so, there would be no contradiction between the earlier studies and the observation of the new EPR signal. A second possible explanation is that, following the formation of the $Y_Z^+S_2$ state, Y_Z^+ is slowly reduced by a donor side component to yield the 'S_2-plus-radical' state. Both the fluorescence [466] and the optical absorption data [468,487] showed that one of the two oxidized donors to $P680^+$ was slowly reduced in darkness, with half-times of approx. 120 ms [466] (or approx. 300 ms [468]) and several seconds (see Refs. 466,468, also see Ref. 487). The slowly-reduced donor was presumed to be Y_Z^+ [466,468]. A slow reduction of Y_Z^+ by an organic component in competition with Q_A^- or Q_B could form the 'S_2-plus-radical' state. Because of the time delay between the flashing and freezing of EPR samples, a slow transition from the $Y_Z^+S_2$ state to the modified S_3 (or 'S_2-plus-radical') state could give rise to the 90–160 Gauss-wide EPR signal even if only the $Y_Z^+S_2$ state

could be formed rapidly in response to a series of flashes. This explanation was previously advanced to explain earlier thermoluminescence data that were interpreted as indicating that a modified S_3 state could be formed in Cl^--depleted samples [932].

A third explanation, proposed by Rutherford and co-workers [38,487], is particularly intriguing in that it may account for the similarities between Ca^{2+}-depleted and Cl^--depleted samples. In Cl^--depleted samples, two charge separations are proposed to rapidly generate the modified S_3 (or 'S_2-plus-radical') state [38,487]. As proposed for Ca^{2+}-depleted preparations [38,487] (see subsection III-C), it is proposed that Y_Z cannot be oxidized by $P680^+$ once the 'S_2-plus-radical' state is formed in Cl^--depleted preparations [38,487]. This proposal is based on an inability to accumulate significant quantities of Y_Z^+ in Cl^--depleted samples, as determined by averaging many flash-induced EPR transients [487]. In agreement with this observation, an earlier study reported that only 0.3–0.4 Y_Z^+ per P680 could be generated by continuous illumination of samples depleted of Cl^- by treatment with SO_4^{2-} or ammonia [602]. However, higher yields of Y_Z^+ were implied in other studies of SO_4^{2-}-treated [437], acetate-treated [632] or NH_3-treated [437,456] samples (also see Ref. 688). A significant fraction of Y_D^+ has been reported to decay rapidly in darkness in Cl^--depleted samples [487,928]. In some of the earlier studies, a rapidly decaying Y_D^+ may have been misidentified as Y_Z^+. However, Y_Z^+ was distinguished from Y_D^+ in one of the earlier studies [437] on the basis of the different microwave power saturation characteristics of the EPR signals of these two species (see subsection II-J.2). The proposal that Y_Z cannot be oxidized by $P680^+$ in the presence of the 'S_2-plus-radical' state would be consistent with the earlier Cl^--depletion studies if the donor that is slowly reduced in darkness [466,468,487] is a component of the 'S_2-plus-radical' state and if this state decays more rapidly than the normal S_3 state. In Ca^{2+}-depleted samples, the 'S_2-plus-radical' state decays more rapidly than the normal S_3 state in the absence of the 24 and 17 kDa extrinsic polypeptides [447,454,904].

Acetate-treated samples, like samples depleted of Cl^- with alkaline pH or SO_4^{2-}, rapidly transfer only two electrons from the donor side of PS II to $P680^+$ in response to a series of flashes [631,633]. In response to subsequent flashes, $P680^+$ is reduced by Q_A^- in competition with an unidentified electron donor [633]. Under these circumstances, the EPR signal of $P680^+$ is broadened from approx. 8 Gauss to approx. 14 Gauss [632]. Rutherford and co-workers have suggested that the first two flashes generate the 'S_2-plus-radical' state and that the putative histidine radical of this state causes the broadening of the $P680^+$ EPR signal [487]. The histidine radical was estimated to be located approx. 8.5 Å from $P680^+$ [487]. It would be tempting to speculate that the putative histidine radical could be His-190 of the D1 polypeptide (see Fig. 4). If His-190 acts as a hydrogen bond acceptor for Y_Z, as proposed [35,65,114,116,122], the oxidation of His-190 would be expected to change the redox potential of Y_Z. As noted in subsection II-J.3, replacing His-190 of the D1 polypeptide with Asp or Gln has been observed to slow electron transfer from Y_Z to $P680^+$ by a factor of 200 [17,19].

It should be determined if the 90–160 Gauss-wide EPR signal of the 'S_2-plus-radical' state is observed in acetate treated samples after two charge separations. It should also be determined if the EPR signal of $P680^+$ is broadened in samples depleted of Ca^{2+} or Cl^- or in samples treated with F^- or NH_3. In this regard it should be noted that the approx. 100 Gauss-wide 'S_2-plus-radical' state signal observed in NH_3-treated samples apparently cannot be generated by flash illumination [485]. Furthermore, the properties of this signal have been suggested to reflect the binding of NH_3 to the NH_3-specific site (see subsection II-G.1), rather than to the Cl^- site, of the water oxidizing complex [456]. A comparison of the properties of the altered multiline EPR signal, the 'S_2-plus-radical' EPR signal and the potentially broadened $P680^+$ EPR signal in samples depleted of Ca^{2+} or Cl^-, or treated with a variety of anions or amines, should yield further insight into the connections between Ca^{2+}, Cl^- and ligand exchange reactions in the water oxidizing complex. Each type of sample should be prepared by a variety of methods and their Ca^{2+} contents should be determined by atomic absorption spectroscopy or by an equivalent analytical method. The formation and stability of Y_D^+ and the rates and temperature dependencies of all electron transfer reactions involving the Mn complex, Y_Z, P680 and all other redox active donor-side components should also be examined.

III-E. Location of Ca^{2+} in PS II

For a recent discussion of this topic, see Ref. 37. The altered lineshapes of the S_2-state multiline EPR signals observed in Ca^{2+}-extracted [423,424,447–456] (see Fig. 11) and Sr^{2+}-reconstituted [415,421,422,432] (see Fig. 10) samples have been taken as evidence that at least one Ca^{2+} ion is located close to the Mn complex, particularly because an NH_3-derived ligand has been shown to coordinate the Mn complex during the $S_1 \rightarrow S_2$ transition [446,554] and because NH_3-treated and Sr^{2+}-substituted samples exhibit altered multiline signals that are superficially similar (compare Figs. 9 and 10). The apparent creation of the lower-affinity Ca^{2+} site(s) during the formation of the functional Mn cluster [362] and the apparent dependence of Ca^{2+} affinity on the redox state of the Mn cluster

[477], also suggests that one or more Ca^{2+} ions may be located near the Mn complex. Further evidence that Ca^{2+} and Mn may be located in close proximity is suggested by recent data demonstrating that Ca^{2+} stabilizes the ligation environment of the Mn complex, protecting the complex against the loss of Mn^{2+} ions produced by the action of NH_2OH and other reductants [275–277,544]. Finally, as discussed earlier, based on EXAFS measurements, one group has proposed that a Ca^{2+} ion is located approx. 3.3 Å from Mn [389,543] (M.J. Latimer, V.J. DeRose, V.K. Yachandra, I. Mukerji, K. Sauer and M.P. Klein, personal communication), while another group has suggested that a Ca^{2+} ion may be located approx. 4.35 Å from Mn [535]. Several authors [510,535,539,548,549] have noted the possible relevance of the Mn^{2+}-Ca^{2+} dinuclear site in concanavalin A [546,547] to PS II and some [34,37] have also pointed out that the Ca^{2+} site in concanavalin A is created by the ligation of Mn^{2+} [941], a situation similar to that in PS II.

Because Ca^{2+} and the Mn complex are believed to be located in close proximity, many of the ligands to Ca^{2+} are expected to be contributed by the D1 and D2 polypeptides (see subsection II-J.3). However, none of the intrinsic polypeptides can be excluded as possible sources of ligands. As mentioned in subsection II-J.3, numerous acidic residues suitable for ligating Ca^{2+} are located in the lumenally-exposed regions of CP47 [130], CP43 [130,162] and the α-subunit of cytochrome *b*-559 [196–199] and in the hydrophilic carboxy-terminal region of the 4.2 kDa product of the *psb*.I gene [297,299]. In light of the low rates of oxygen evolution reported in its absence [232,246,248,251,252,265,802–805], the 33 kDa polypeptide also cannot be excluded as a possible source of ligands. Not even the 24 kDa polypeptide can be excluded [37] because the affinity of Ca^{2+} for PS II has only been measured in its absence (see subsection III-A). Finally, it has been pointed out [37] that no data exist to exclude the possibility that polar groups of carbohydrates or lipids contribute ligands to Ca^{2+} in PS II.

The specific and reversible extraction of Ca^{2+} by sodium citrate at pH 3 [475] has been considered to be consistent with the ligation of Ca^{2+} by carboxylate residues in PS II [37,38,270,422,475], particularly because the efficiency of extraction is half-maximal at pH 4.0 [475]. However, the short incubation at pH 3 causes the reversible dissociation of the 24 and 17 kDa extrinsic polypeptides [235,274,903], thereby increasing the accessibility of Ca^{2+} to citrate as a chelating agent. Consequently, the significance of the reversible Ca^{2+} extraction at pH 3 to the ligation of Ca^{2+} in PS II is unclear.

High-resolution crystal structures of many Ca^{2+}-binding proteins are available (reviewed in Refs. 942–944). An analysis of 27 Ca^{2+} binding sites in 17 structures refined to resolutions of ≤ 2.3 Å has recently been reported [943]. All 182 Ca^{2+} ligands in these 27 sites are oxygen atoms. Of these, 29%, 18%, 6% and 2% are contributed by side-chain oxygens from Asp, Glu, Asn and Gln residues, respectively, while 23% are contributed by peptide carbonyl oxygens and 20% are contributed by immobilized H_2O molecules [943]. The Asp and Glu residues ligate with either one or both side-chain oxygens. The most common Ca^{2+} coordination number is seven, but coordination numbers of six or eight are not uncommon. The oxygen ligands are generally arranged approximately as a pentagonal bipyramid. The average Ca^{2+}-O distance is 2.4 Å, but the distances generally range from 2.1 to 2.6 Å [943,944]. All 27 sites contain at least one peptide carbonyl oxygen as a ligand [943].

Calcium-binding proteins are generally grouped into two categories: those that possess the 'Helix-Loop-Helix' (HLH) motif (also known as the 'EF hand' motif, reviewed in Refs. 942,945–948), and those that do not. In proteins that possess the HLH motif, the residues that coordinate the Ca^{2+} ion are located in a contiguous stretch of 12 residues that connects two α-helices. The HLH motif is very highly conserved and consensus sequences are available [949–952]. The Ca^{2+}-binding sites of proteins that do not possess the HLH motif are exceedingly diverse [943]. In most of these 'non-HLH' proteins, a majority of the ligating residues are located in a contiguous stretch of 10–15 residues. In many cases, all of the ligating residues are located in this stretch, as in HLH proteins [943]. However, in some non-HLH proteins, none of the ligating residues are located in the same region of the polypeptide sequence. No correlation exists between Ca^{2+} affinity and the geometry of the site or whether the ligating residues are part of a contiguous stretch of the polypeptide chain [943]. However, the Ca^{2+} affinity does correlate with the number of H_2O molecules in the Ca^{2+} coordination sphere [943]. The sites with the highest affinities contain 0–1 ligating H_2O molecules, while the sites with the lowest affinities contain 1–3 ligating H_2O molecules [943]. Nearly all HLH sites contain one carbonyl oxygen and one ligating H_2O molecule, while non-HLH sites contain 1–3 carbonyl oxygens and 0–4 ligating H_2O molecules. All HLH sites contain a bidentate Glu residue, while few non-HLH sites contain Glu residues [943]. None of the HLH sites contain bidentate Asp residues, while many non-HLH sites contain bidentate Asp residues [943].

Most non-HLH Ca^{2+}-binding sites are located in Ω loops or portions of Ω loops [943]. An Ω loop is a 6–16-residue loop that is located on the surface of a protein, contains no regular repeating secondary structure and whose termini are ≤ 10 Å apart [953]. All HLH Ca^{2+}-binding sites are located in Ω loops if the restriction on regular secondary structure that defines

Ω loops is relaxed slightly [943,953]. Most Ca^{2+}-binding loops contain Asx turns, although other reverse turns are also found [943]. An Asx turn involves a hydrogen bond between a side-chain oxygen of an Asp or Asn residue at position 'n' and the peptide amide nitrogen of the residue at position '$n + 2$' [954–957]. (Occasionally the Asx residue is Ser, Thr or Cys [955]). In Ca^{2+}-binding proteins, the Asx residue is usually Asp, occasionally Asn and rarely Ser [943]. The Asx residue generally ligates the Ca^{2+} ion with one or two side-chain oxygens. The vast majority of Asx-turns in Ca^{2+}-binding proteins have a Pro or Gly residue located immediately adjacent to the turn and within three residues of the Asx residue [943]. In conjunction with the Asx turn, these residues facilitate folding the Ca^{2+}-binding loop around the Ca^{2+} ion to correctly position oxygen ligands [943]. Extensive networks of hydrogen bonds are found in Ca^{2+}-binding sites. These stabilize the conformation of the Ca^{2+}-binding loop, correctly position the ligating H_2O molecules and other oxygen ligands and help counteract electrostatic repulsion between negatively charged Asp and Glu residues that may be juxtaposed in the ligation site. The ability of Asp and Glu residues to form multiple hydrogen bonds, in addition to their negative charge, explains the prevalence of these residues in Ca^{2+}-binding sites [943].

Numerous authors have examined PS II polypeptides for sequences that resemble the HLH consensus sequence. Such sequences have been found in the D1 [422,787,865], D2 [865] and 33 kDa [227,958] polypeptides. The similarities with the HLH consensus sequence are weak, although the similarity is strongest for the identified region of the 33 kDa polypeptide. Proteins with the HLH motif have been shown to bind ^{45}Ca when transferred to nitrocellulose membranes after being denatured and subjected to gel electrophoresis [959]. When similar experiments were performed on PS II membranes, the only non-LHCII polypeptide that bound ^{45}Ca was an unidentified protein of 33 kDa and the binding was very weak [960]. Recently, PS II polypeptides were examined for sequences that resemble the contiguous Ca^{2+}-binding loops of several non-HLH Ca^{2+}-binding proteins [37]. Vaguely similar sequences were found in the 33 kDa polypeptide and in the lumenally exposed regions of CP47, CP43 and the D1 and D2 polypeptides [37].

III-F. Ca^{2+} in cyanobacteria

The influence of Ca^{2+} on electron transfer and oxygen evolution in cyanobacteria may differ from that in plants. For example, depletion of Ca^{2+} from cyanobacterial cells or PS II membranes has been reported to block electron transfer from Y_Z to $P680^+$, as measured by flash-induced optical absorption changes (even after only a single flash) [911] or by chlorophyll *a* fluorescence in the presence of DCMU [893]. However, this conclusion has been challenged [633] and a narrow version of the 130–160 Gauss-wide EPR signal of the 'S_2-plus-radical' state (see subsection II-B.2) has recently been observed in Ca^{2+}-depleted PS II particles from *Synechocystis* sp. PCC 6803 [415]. The narrow linewidth of this signal (< 90 Gauss) resembles that of the signal observed in NH_3-treated [456,485] or some Cl^--depleted [487] preparations from higher plants (see subsection II-B.2). In higher plants, the depletion of the weakly-bound Ca^{2+} ion(s) reversibly slows electron transfer from Y_Z to $P680^+$ [487] (also see Refs. 628,630,638 and see subsection III-C).

The requirement for Ca^{2+} in cyanobacteria may also be different from the requirement in plants and may differ between different species of cyanobacteria. Early studies on the non-thermophilic cyanobacteria *Phormidium luridum* [887–889] and *Anacystis nidulans* [890–892,961] indicated that approx. 30 mM Ca^{2+} is required to maintain the stability and oxygen-evolving activity of PS II membranes. However, active PS II complexes from *Anacystis nidulans* have more recently been isolated in the presence of high concentrations of Na^+ (added as approx. 300 mM sodium citrate) [962]. Highly-purified PS II complexes from *Synechocystis* sp. PCC 6803 have also been reported to require either 20–50 mM Ca^{2+} [209,415,963] or approx. 300 mM Na^+ [963] for maximal activity. The ability of *Anacystis nidulans* and many other cyanobacteria to substitute Na^+ for Ca^{2+} has also been inferred from studies conducted on intact cells [964–966]. Other cyanobacteria apparently have an absolute requirement for Ca^{2+} [966], while at least one, *Synechocystis* sp. PCC 6714, apparently has an absolute requirement for Na^+; Ca^{2+} reportedly does not substitute [967]. (However, thylakoid membranes from this organism have been reported to require > 5 mM Ca^{2+} for maximal oxygen-evolving activity [968].)

Highly purified PS II preparations from thermophilic cyanobacteria do not require added Ca^{2+} for maximal activity. Although some procedures for isolating PS II complexes from *Synechococcus elongatus* employ buffers that contain 20 mM $CaCl_2$ [168,287], highly active PS II preparations have been isolated from this organism [343,969–971,995], from *Synechococcus lividus* [972], from *Synechococcus vulcanus* [285,289,480], from *Mastigocladus laminosus* [634] and from *Phormidium laminosum* [288] in buffers that contain 5–35 mM Na^+ and/or 5–10 mM Mg^{2+}, but no added Ca^{2+} ions. However, the preparations from *Phormidium laminosum* have been reported to be most active and stable in the presence of either 10 mM Mg^{2+} or Ca^{2+} [288,334] and some preparations from *Synechococcus elongatus* show slight (approx. 15%) enhancements in activity in the presence of 5 mM Ca^{2+} [286].

The Ca^{2+} required for oxygen evolution appears to have a lower-affinity for PS II in cyanobacteria than in higher plants. This Ca^{2+} is easily lost from some cyanobacteria during cell breakage [889] and appears to be readily extracted from highly-purified PS-II complexes from the thermophilic cyanobacterium *Synechococcus elongatus* by treatment with 1 mM EDTA [911,973] or by gel filtration [930,931]. Activity can be restored by the addition of Ca^{2+} [930,931,973], Na^+ [930,931], or Mg^{2+} [930,931] ions. An apparent K_m value for Ca^{2+} was estimated to be approx. 130 μM (measured in the presence of 10–25 mM Na^+), while the optimum concentrations of Na^+ or Mg^{2+} were found to vary considerably depending on whether Cl^-, SO_4^{2-}, or HPO_4^{2-} was present as the counterion [930,931]. Highly-purified PS-II complexes from *Synechococcus elongatus* have been reported to contain approx. 1 tightly-bound Ca^{2+} ion (per P680) that resists extraction by chelex resin [286,899,913,995]. It was proposed that this Ca^{2+} ion is essential for oxygen evolution [286,913], but atomic absorption measurements on samples further extracted with EDTA were inconclusive [913]. It should be noted that these complexes were isolated by Katoh and co-workers, who, in conflict with other workers, maintain that highly purified PS II preparations from spinach also contain only approx. 1 Ca^{2+} ion per P680 [11,900] (see subsection III-A). Nevertheless, this group's most recent preparation of PS II particles from *Synechococcus* appears to contain approx. 1 Ca^{2+} ion per P680 and to exhibit phenomenally high rates of oxygen evolution at 45°C [995].

The apparently lower-affinity of Ca^{2+} for PS II in cyanobacteria may reflect the absence of the 24 and 17 kDa polypeptides. It has been suggested that cyanobacteria may contain higher concentrations of Ca^{2+} and Cl^- ions than chloroplasts [248]. Higher concentrations of these ions in cyanobacteria may obviate the need for the 24 and 17 kDa polypeptides (see subsections I-B.4 and III-A). The apparent ability of Na^+ or Mg^{2+} to substitute for Ca^{2+} in cyanobacteria contrasts with the specific requirement for Ca^{2+} in higher plants, where Na^+ is a competitive inhibitor of oxygen evolution [909,910] and Mg^{2+} is neither an activator nor an inhibitor [37] (see subsection III-B). Clarification of the role of Ca^{2+} or other cations in cyanobacteria will require rigorous extraction procedures. The Ca^{2+} contents of the extracted samples should be determined by atomic absorption spectroscopy or by an equivalent analytical method. A variety of cyanobacteria should be examined to ascertain whether the cation requirements of thermophilic cyanobacteria differ from those of non-thermophilic cyanobacteria. Clarification of the cation requirements of cyanobacteria is essential if the amino-acid residues that coordinate Ca^{2+} ions in higher plants are to be identified from directed mutagenesis studies performed with cyanobacterial genes. Alternatively, mutants could be constructed in eukaryotic organisms. Mutations have recently been constructed in the D1 polypeptide of the alga *Chlamydomonas reinhardtii* [974,975,985,997,998].

III-G. The role of Ca^{2+} in oxygen evolution

Despite its requirement in the S-state transitions, the specific role of Ca^{2+} in oxygen evolution remains unclear. Because the appearance and/or stability of the S_2-state multiline EPR signal is altered when Ca^{2+} is removed [423,424,447–456] (see subsection II-B.1 and Fig. 11) or replaced with Sr^{2+} [415,421,422,432] (see Fig. 10) and because the structure of the Mn complex can be severely disrupted when Ca^{2+} is replaced with La^{3+} [548] (see subsection III-B), Ca^{2+} has been proposed to stabilize the structure of the Mn complex [34,37,39,422,448,474,475,548] or to influence its redox behavior [34,37,422,511,549]. Indeed, recent evidence indicates that Ca^{2+} stabilizes the ligation of the Mn complex, protecting it against the loss of Mn^{2+} ions produced by the actions of NH_2OH or other reductants [275–277,544]. Calcium has also been proposed to protect the Mn complex against chelation by EDTA, EGTA and citrate [454]. The proposed structural influence of Ca^{2+} has been likened to that of the Zn^{2+} ion in Cu/Zn superoxide dismutase [37,474]. The Zn^{2+} ion in this protein influences the redox potential of the Cu^{2+} ion by sharing an imidazole bridging ligand with it [976,977]. Whether Ca^{2+} has a mechanistic role in water oxidation remains unknown. It has been proposed to function in deprotonation events coupled to S state-dependent conformational changes or pK_a shifts of carboxylate groups [452,477]. Indeed, a deprotonation event that is believed to normally accompany the $S_2 \rightarrow S_3$ transition does not appear to occur in the absence of Ca^{2+}, as indicated by the presence of an electrochromic shift in the optical absorption spectrum of this transition in Ca^{2+}-depleted samples [452] (see subsection II-D.2 and Fig. 16). Calcium has also been proposed to govern the accessibility of H_2O to the Mn cluster [31,448,455,865]. In one recent model, Ca^{2+} is proposed to coordinate substrate H_2O in the lower S-states and to exchange it for a Cl^- ion on the Mn complex just prior to water oxidation [31]. This model is of great interest in light of the ubiquitous appearance of H_2O as a ligand to Ca^{2+} in Ca^{2+}-binding proteins (see subsection III-E) and in light of the many data that suggest that Ca^{2+} and Mn are located in close proximity.

IV. Concluding remarks

I have tried to describe the controversies that currently envelop the Mn and Ca^{2+} ions in PS II and to point out issues that should be clarified or reexamined. Such issues include the relationship between the pro-

tons released into the lumen and deprotonation events at the site of water oxidation, the identity of the component that is oxidized during the $S_2 \rightarrow S_3$ transition in intact preparations, the identity of the radical in the modified S_3 or 'S_2-plus-radical' state observed in Ca^{2+}-or Cl^--depleted samples and in samples treated with NH_3, the source of the 90–160 Gauss-wide EPR signal observed in this state, whether an organic component other than Y_Z is oxidized with high quantum yield in Mn-depleted preparations, the relationship between the S_2-state multiline and $g = 4.1$ EPR signals, the S_1-state EPR signal and the NMR proton relaxation enhancement data, the relationship between extraction conditions and how Ca^{2+}-depletion and Cl^--depletion disrupt the S-state transitions, the mechanism of amine-induced inhibition of water oxidition and whether substrate water binds at the NH_3-specific site, the Cl^--sensitive site or elsewhere. Further examination of altered multiline, 'S_2-plus-radical' and broadened $P680^+$ EPR signals in samples depleted of Ca^{2+} or Cl^- or treated with a variety of inhibitory anions or amines should yield further insight into the connection between Ca^{2+}, Cl^- and ligand/substrate exchange reactions during the S-state cycle. Examination of samples prepared by a variety of methods and routinely analyzed for Ca^{2+} content by atomic absorption spectroscopy or equivalent analytical methods should be undertaken. The temperature-dependencies of the S-state transitions in these samples and whether particular S-state transitions are blocked or merely slowed considerably should also be determined. The relationship between the 'S_2-plus-radical' EPR signals and a similar signal reported in Tris-washed, NH_2OH-treated samples should also be explored.

A clearer picture of the structure of the Mn complex is beginning to emerge because of what seems to be a growing consensus among the various groups that apply X-ray absorption spectroscopy to intact preparations that are poised in the S_1 state. Continuing advances in the synthesis of inorganic model compounds that potentially mimic the structure or reactivity of the Mn complex are contributing significantly to this picture. Future X-ray absorption studies will undoubtedly focus on samples having Ca^{2+} or Cl^- exchanged for other ions and on samples treated with NH_3 or other inhibitors. Further application of L-edge X-ray absorption spectroscopy [978,979], magnetic susceptibility and ESEEM and ENDOR spectroscopies should provide further insight into the structure and operation of the Mn complex. The application of site-directed mutagenesis to the search for the amino-acid residues that ligate Mn and Ca^{2+} is only beginning and is currently being extended to polypeptides other than D1 and D2 and to organisms other than cyanobacteria. The recent development of highly-active oxygen-evolving PS II preparations from *Synechocystis* sp. PCC 6803 will give a major impetus to these studies. The coming decade will see major advances on many fronts.

Acknowledgements

I am deeply grateful to the many individuals who spent time discussing their results and ideas with me over the past several years. I am particularly indebted to C.F. Yocum, G.T. Babcock, W.F. Beck, B.A. Diner, G.W. Brudvig and A.W. Rutherford. I am also grateful to L.-E. Andréasson, W.H. Armstrong, B.A. Barry, D.J. Blubaugh, T.M. Bricker, R.D. Britt, R.L. Burnap, G.M. Cheniae, S.P. Cramer, W.A. Cramer, J.P. Dekker, J.C. de Paula, V.J. DeRose, G.C. Dismukes, W.D. Frasch, M.M. Grush, A. Haddy, Ö. Hannson, Y. Inoue, M.J. Latimer, J. Lavergne, W. Junge, M.P. Klein, P.J. Nixon, J.H.A. Nugent, T.-A. Ono, H.B. Pakrasi, V.L. Pecoraro, J.E. Penner-Hahn, G. Renger, P.O. Sandusky, K. Sauer, M. Seibert, R.R. Sharp, S. Styring, B. Svensson, H.H. Thorp, W.F.J. Vermaas and V.K. Yachandra. I would also like to thank many of the above individuals, their co-workers, plus M. Ikeuchi, N. Murata, Ki. Satoh, T. Vänngård and their co-workers, for sending preprints of (then) unpublished manuscripts. Finally, I would like to thank C.F. Yocum, B.A. Barry, T. Bricker, G.W. Brudvig, W.A. Cramer, B.A. Diner, A.W. Rutherford, K. Sauer and an anonymous reviewer for critical comments on all or part of this manuscript. Work in my laboratory is funded by the National Institutes of Health (GM-43496).

References

1 Stewart, A.C. and Bendall, D.S. (1979) FEBS Lett. 107, 308–312.
2 Berthold, D.A., Babcock, G.T. and Yocum, C.F. (1981) FEBS Lett. 134, 231–234.
3 Yamamoto, Y., Ueda, T., Shinkai, H. and Nishimura, M. (1982) Biochim. Biophys. Acta 679, 347–350.
4 Kuwabara, T. and Murata, N. (1982) Plant Cell Physiol. 23, 533–539.
5 a Tang, X.-S. and Satoh, Ki (1985) FEBS Lett. 179, 60–64.
5 b Ikeuchi, M., Yuasa, M. and Inoue, Y. (1985) FEBS Lett. 185, 316–322.
6 Ghanotakis, D.F. and Yocum, C.F. (1986) FEBS Lett. 197, 244–248.
7 Ikeuchi, M. and Inoue, Y. (1986) Arch. Biochem. Biophys. 247, 97–107.
8 Franzén, L.-G., Styring, S., Étienne, A.-L., Hansson, Ö. and Vernotte, C. (1986) Photobiochem. Photobiophys. 13, 15–28.
9 Ghanotakis, D.F., Demetriou, D.M. and Yocum, C.F. (1987) Biochim. Biophys. Acta 891, 15–21.
10 Yamada, Y., Tang, X.-S., Itoh, S. and Satoh, Ki. (1987) Biochim. Biophys. Acta 891, 129–137.
11 Enami, I., Kamino, K., Shen, J.-R., Satoh, Ka. and Katoh, S. (1989) Biochim. Biophys. Acta 977, 33–39.
12 Haag, E., Irrgang, K.-D., Boekema, E.J. and Renger, G. (1990) Eur. J. Biochem. 189, 47–53.
13 Van Leeuwen, P.J., Nieveen, M.C., Van de Meent, E.J., Dekker, J.P. and Van Gorkom, H.J. (1991) Photosynth. Res. 28, 149–153.
14 Hallick, R.B. (1989) Plant Mol. Biol. Report. 7, 266–275.

15 Wolfe, K.H. (1991) in The Photosynthetic Apparatus: Molecular Biology and Operation (Bogorad, L. and Vasil, I.K., eds.), pp. 467–482, Academic Press, San Diego.
16 Erickson, J.M. and Rochaix, J.-D. (1992) in The Photosystems: Structure, Function and Molecular Biology (Barber, J., ed.), pp. 101–177, Elsevier, Amsterdam.
17 Diner, B.A., Nixon, P.J. and Farchaus, J.W. (1991) Curr Opin. Struct. Biol. 1, 546–554.
18 Pakrasi, H.B. and Vermaas, W.F.J. (1992) in The Photosystems: Structure, Function and Molecular Biology (Barber, J., ed.), pp. 231–257, Elsevier Science Publishers B.V., Amsterdam.
19 Nixon, P.J., Chisholm, D.A. and Diner, B.A. (1992) in Plant Protein Engineering (Shewry, P. and Gutteridge, S., eds.), pp. 93–141, Cambridge University Press, Cambridge.
20 Deisenhofer, J., Epp, O., Miki, K., Huber, R. and Michel, H. (1985) Nature 318, 618–624.
21 Allen, J.P., Feher, G., Yeates, T.O., Komiya, H. and Rees, D.C. (1987) Proc. Natl. Acad. Sci. USA 84, 6162–6166.
22 Chang, C.-H., El-Kabbani, O., Tiede, D., Norris, J. and Schiffer, M. (1991) Biochemistry 30, 5352–5360.
23 Huber, R. (1989) EMBO J. 8, 2125–2147.
24 Deisenhofer, J. and Michel, H. (1989) EMBO J. 8, 2149–2170.
25 Feher, G., Allen, J.P., Okamura, M.Y. and Rees, D.C. (1989) Nature 339, 111–116.
26 El-Kabbani, O., Chang, C.-H., Tiede, D., Norris, J. and Schiffer, M. (1991) Biochemistry 30, 5361–5369.
27 Deisenhofer, J. and Michel, H. (1991) Annu. Rev. Biophys. Biophys. Chem. 20, 247–266.
28 Deisenhofer, J. and Michel, H. (1991) Annu. Rev. Cell Biol. 7, 1–23.
29 Michel, H. and Deisenhofer, J. (1988) Biochemistry 27, 1–7.
30 Brudvig, G.W., Beck, W.F. and De Paula, J.C. (1989) Annu. Rev. Biophys. Biophys. Chem. 18, 25–46.
31 Rutherford, A.W. (1989) Trends Biochem. Sci. 14, 227–232.
32 Babcock, G.T., Barry, B.A., Debus, R.J., Hoganson, C.W., Atamian, M., McIntosh, L., Sithole, I. and Yocum, C.F. (1989) Biochemistry 28, 9557–9565.
33 Hansson, Ö. and Wydrzynski, T. (1990) Photosynth. Res. 23, 131–162.
34 Ghanotakis, D.F. and Yocum, C.F. (1990) Annu. Rev. Plant Physiol. Plant Mol. Biol. 41, 255–276.
35 Andersson, B. and Styring, S. (1991) Curr. Top. Bioenerg. 16, 1–81.
36 Vermaas, W.F.J. and Ikeuchi, M. (1991) in The Photosynthetic Apparatus: Molecular Biology and Operation (Bogorad, L. and Vasil, I.K., eds.), pp. 25–111, Academic Press, San Diego.
37 Yocum, C.F. (1991) Biochim. Biophys. Acta 1059, 1–15.
38 Rutherford, A.W., Zimmermann, J.-L. and Boussac, A. (1992) in The Photosystems: Structure, Function and Molecular Biology (Barber, J., ed.), pp. 179–229, Elsevier, B.V., Amsterdam.
39 Babcock, G.T. (1987) in New Comprehensive Biochemistry: Photosynthesis (Amesz, J., ed.), pp. 125–158, Elsevier, Amsterdam.
40 Green, B.R. (1988) Photosynth. Res. 15, 3–32.
41 Chitnis, P.R. and Thornber, J.P. (1988) Photosynth. Res. 16, 41–63.
42 Bassi, R., Rigoni, F. and Giacometti, G.M. (1990) Photochem. Photobiol. 52, 1187–1206.
43 Green, B.R., Pichersky, E. and Kloppstech, K. (1991) Trends Biochem. Sci. 16, 181–186.
44 Allen, J.F. (1992) Biochim. Biophys. Acta 1098, 275–335.
45 Kühlbrandt, W. and Wang, D.N. (1991) Nature 350, 130–134.
46 Glazer, A.M. (1989) J. Biol. Chem. 264, 1–4.
47 Schirmer, T., Bode, W. and Huber, R. (1987) J. Mol. Biol. 196, 677–695.
48 Duerring, M., Huber, R., Bode, W., Ruembeli, R. and Zuber, H. (1990) J. Mol. Biol. 211, 633–644.
49 Duerring, M., Schmidt, G.B. and Huber, R. (1991) J. Mol. Biol. 217, 577–592.
50 Renger, G. (1992) in The Photosystems: Structure, Function and Molecular Biology (Barber, J., ed.), pp. 45–99, Elsevier, Amsterdam.
51 Wasielewski, M.R., Johnson, D.G., Seibert, M. and Govindjee (1989) Proc. Natl. Acad. Sci. USA 86, 524–528.
52 Wasielewski, M.R., Johnson, D.G., Govindjee, Preston, C. and Seibert, M. (1989) Photosynth. Res. 22, 89–99.
53 Jankowiak, R., Tang, D., Small, G.J. and Seibert, M. (1989) J. Phys. Chem. 93, 1649–1654.
54 Nuijs, A.M., Van Gorkom, H.J., Plijter, J.J. and Duysens, L.N.M. (1986) Biochim. Biophys. Acta 848, 167–175.
55 Trissl, H.-W., Breton, J., Deprez, J. and Leibl, W. (1987) Biochim. Biophys. Acta 893, 306–319.
56 Schatz, G.H., Brock, H. and Holzwarth, A.R. (1987) Proc. Natl. Acad. Sci. USA 84, 8414–8418
57 Eckert, H.-J., Wiese, N., Bernarding, J., Eichler, H.-J. and Renger, G. (1988) FEBS Lett. 240, 153–158.
58 Trissl, H.-W. and Leibl, W. (1989) FEBS Lett. 244, 85–88.
59 Leibl, W., Breton, J., Deprez, J. and Trissl, H.-W. (1989) Photosynth. Res. 22, 257–275.
60 Hoganson, C.W. and Babcock, G.T. (1988) Biochemistry 27, 5848–5855.
61 Gerken, S., Brettel, K., Schlodder, E. and Witt, H.T. (1988) FEBS Lett. 237, 69–75.
62 Barry, B.A. and Babcock, G.T. (1987) Proc. Natl. Acad. Sci. USA 84, 7099–7103.
63 Barry, B.A. and Babcock, G.T. (1988) Chem. Scripta 28A, 117–122.
64 Barry, B.A., El-Deeb, M.K., Sandusky, P.O. and Babcock, G.T. (1990) J. Biol. Chem. 265, 20139–20143.
65 Debus, R.J., Barry, B.A., Babcock, G.T. and McIntosh, L. (1988) Proc. Natl. Acad. Sci. USA 85, 427–430.
66 Vermaas, W.F.J., Rutherford, A.W. and Hansson, Ö. (1988) Proc. Natl. Acad. Sci. USA 85, 8477–8481.
67 Debus, R.J., Barry, B.A., Sithole, I., Babcock, G.T. and McIntosh, L. (1988) Biochemistry 27, 9071–9074.
68 Metz, J.G., Nixon, P.J., Rögner, M., Brudvig, G.W. and Diner, B.A. (1989) Biochemistry 28, 6960–6969.
69 Bowes, J.M. and Crofts, A.R. (1980) Biochim. Biophys. Acta 590, 373–384.
70 Robinson, H.H. and Crofts, A.R. (1983) FEBS Lett. 153, 221–226.
71 Crofts, A.R. and Wraight, C.A. (1983) Biochim. Biophys. Acta 726, 149–185.
72 Crofts, A.R., Robinson, H.H. and Snozzi, M. (1984) in Advances in Photosynthesis Research (Sybesma, C., ed.), Vol. I, pp. 461–468, Martinus Nijhoff/Dr. W. Junk, The Hague.
73 Vermaas, W.F.J., Arntzen, C.J., Gu, L.-Q. and Yu, C.-A. (1983) Biochim. Biophys. Acta 723, 266–275.
74 Oettmeier, W. and Soll, H.-J. (1983) Biochim. Biophys. Acta 724, 287–290.
75 Vermaas, W.F.J. and Arntzen, C.J. (1983) Biochim. Biophys. Acta 725, 483–491.
76 Mathis, P. and Rutherford, A.W. (1987) in New Comprehensive Biochemistry: Photosynthesis (Amesz, J., ed.), pp. 63–96, Elsevier, Amsterdam.
77 Diner, B.A., Petrouleas, V. and Wendoloski, J.J. (1991) Physiol. Plant. 81, 423–436.
78 Mets, L. and Thiel, A. (1989) in Target Sites of Herbicide Action (Böger, P. and Sandmann, G., eds.), pp. 1–24, CRC Press, Boca Raton.
79 Bowyer, J.R., Camilleri, P. and Vermaas, W.F.J. (1991) in Herbicides (Baker, N.R. and Percival, M.P., eds.), pp. 27–85, Elsevier, Amsterdam.
80 Oettmeier, W. (1992) in The Photosystems: Structure, Function

and Molecular Biology (Barber, J., ed.), pp. 349–408, Elsevier, Amsterdam.
81 Sinning, I. (1992) Trends Biochem. Sci. 17, 150–154.
82 Feher, G. and Okamura, M.Y. (1992) Annu. Rev. Biochem.61, 861–896.
83 McPherson, P.H., Okamura, M.Y. and Feher, G. (1990) Biochim. Biophys. Acta 1016, 289–292.
84 Diner, B.A., Schenck, C.C. and De Vitry, C. (1984) Biochim. Biophys. Acta 766, 9–26.
85 Rutherford, A.W., Boussac, A. and Zimmermann, J.-L. (1991) New J. Chem. 15, 491–500.
86 Vermaas, W.F.J., Renger, G. and Dohnt, G. (1984) Biochim. Biophys. Acta 764, 194–202.
87 Styring, S. and Rutherford, A.W. (1987) Biochemistry 26, 2401–2405.
88 Vass, I., Deák, Z. and Hideg, É. (1990) Biochim. Biophys. Acta 1017, 63–69.
89 Kok, B., Forbush, B. and McGloin, M.P. (1970) Photochem. Photobiol. 11, 457–475.
90 Forbush, B., Kok, B. and McGloin, M.P. (1971) Photochem. Photobiol. 14, 307–321.
91 Joliot, P., Barbieri, G. and Chabaud, R. (1969) Photochem. Photobiol. 10, 309–329.
92 Joliot, P. and Kok, B. (1975) in Bioenergetics of Photosynthesis (Govindjee, ed.), pp. 387–412, Academic Press, New York.
93 Radmer, R. and Cheniae, G.M. (1977) in Primary Processes of Photosynthesis (Barber, J., ed.), pp. 303–348, Elsevier, Amsterdam.
94 Nugent, J.H.A., Diner, B.A. and Evans, M.C.W. (1981) FEBS Lett. 124, 241–244.
95 Evans, M.C.W., Diner, B.A. and Nugent, J.H.A. (1982) Biochim. Biophys. Acta 682, 97–105.
96 Rutherford, A.W. and Mathis, P. (1983) FEBS Lett. 154, 328–334.
97 Rutherford, A.W. and Zimmermann, J.-L. (1984) Biochim. Biophys. Acta 767, 168–175.
98 Rutherford, A.W., Zimmermann, J.-L. and Mathis, P. (1984) in Advances in Photosynthesis Research (Sybesma, C., ed.), Vol. I, pp. 445–448, Marinus Nijhoff/Dr W. Junk, The Hague.
99 Zimmermann, J.-L. and Rutherford, A.W. (1986) Biochim. Biophys. Acta 851, 416–423.
100 Hallahan, B.J., Ruffle, S.V., Bowden, S.J. and Nugent, J.H.A. (1991) Biochim. Biophys. Acta 1059, 181–188.
101 Diner, B.A. and Petrouleas, V. (1988) Biochim. Biophys. Acta 895, 107–125.
102 Debus, R.J., Feher, G. and Okamura, M.Y. (1986) Biochemistry 25, 2276–2287.
103 Nam, H.K., Austin, R.H. and Dismukes, G.C. (1984) Biochim. Biophys. Acta 765, 301–308.
104 Buchanan, S.K. and Dismukes, G.C. (1987) Biochemistry 26, 5049–5055.
105 Kirmaier, C., Holten, D., Debus, R.J., Feher, G. and Okamura, M.Y. (1986) Proc. Natl. Acad. Sci. USA 83, 6407–6411.
106 Agalidis, I., Nuijs, A.M. and Reiss-Husson, F. (1987) Biochim. Biophys. Acta 890, 242–250.
107 Liu, N.L., Van Kan, P.J.M. and Hoff, A.J. (1991) FEBS Lett. 289, 23–28.
108 Klimov, V.V., Dolan, E., Shaw, E.R. and Ke, B. (1980) Proc. Natl. Acad. Sci. USA 77, 7227–7231.
109 MacMillan, F., Gleiter, H., Renger, G. and Lubitz, W. (1990) in Current Research in Photosynthesis (Baltscheffsky, M., ed.), Vol. I, pp. 531–534, Kluwer, Dordrecht.
110 Petrouleas, V. and Diner, B.A. (1987) Biochim. Biophys. Acta 893, 126–137.
111 Diner, B.A. and Petrouleas, V. (1987) Biochim. Biophys. Acta 893, 138–148.
112 Diner, B.A. and Petrouleas, V. (1990) Biochim. Biophys. Acta 1015, 141–149.
113 Semin, B.K., Loviagina, E.R., Aleksandrov, A.Y., Kaurov, Y.N. and Novakova, A.A. (1990) FEBS Lett. 270, 184–186.
114 Svensson, B., Vass, I. and Styring, S. (1991) Z. Naturforsch. 46c, 765–776.
115 Ko, K. (1990) Nucleic Acids Res. 18, 375.
116 Svensson, B., Vass, I., Cedergren, E. and Styring, S. (1990) EMBO J. 9, 2051–2059.
117 Babcock, G.T. and Sauer, K. (1973) Biochim. Biophys. Acta 325, 483–503.
118 Velthuys, B.R. and Visser, J.W.M. (1975) FEBS Lett. 55, 109–112.
119 Kawamori, A., Satoh, J.-I., Inui, T. and Satoh, Ki. (1987) FEBS Lett. 217, 134–138.
120 Nugent, J.H.A., Demetriou, C. and Lockett, C.J. (1987) Biochim. Biophys. Acta 894, 534–542.
121 Inui, T., Kawamori, A., Kuroda, G., Ono, T.-A. and Inoue, Y. (1989) Biochim. Biophys. Acta 973, 147–152.
122 Vass, I. and Styring, S. (1991) Biochemistry 30, 830–839.
123 Buser, C.A., Thompson, L.K., Diner, B.A. and Brudvig, G.W. (1990) Biochemistry 29, 8977–8985.
124 Vass, I., Deák, Z., Jegerschöld, C. and Styring, S. (1990) Biochim. Biophys. Acta 1018, 41–46.
125 Evelo, R.G., Dikanov, S.A. and Hoff, A.J. (1989) Chem. Phys. Lett. 157, 25–30.
126 Evelo, R.G., Hoff, A.J., Dikanov, S.A. and Tyryshkin, A.M. (1989) Chem. Phys. Lett. 161, 479–484.
127 Van Mieghem, F.J.E., Satoh, Ki. and Rutherford, A.W. (1991) Biochim. Biophys. Acta 1058, 379–385.
128 Ghanotakis, D.F., Waggoner, C.M., Bowlby, N.R., Demetriou, D.M., Babcock, G.T. and Yocum, C.F. (1987) Photosynth. Res. 14, 191–199.
129 Bowlby, N.R., Ghanotakis, D.F., Yocum, C.F., Petersen, J. and Babcock, G.T. (1988) in Light-Energy Transduction in Photosynthesis: Higher Plant and Bacterial Models (Stevens, S.E., Jr. and Bryant, D.A., eds.), pp. 215–226, American Socieity of Plant Physiologists, Rockville.
130 Bricker, T.M. (1990) Photosynth. Res. 24, 1–13.
131 Svensson, B., Vass, I. and Styring, S. (1991) Z. Naturforsch. 46c, 62–73.
132 Nanba, O. and Satoh, Ki. (1987) Proc. Natl. Acad. Sci. USA 84, 109–112.
133 Barber, J., Chapman, D.J. and Telfer, A. (1987) FEBS Lett. 220, 67–73.
134 Akabori, K., Tsukamoto, H., Tsukihara, J., Nagatsuka, T., Motokawa, O. and Toyoshima, Y. (1988) Biochim. Biophys. Acta 932, 345–357.
135 Dekker, J.P., Bowlby, N.R. and Yocum, C.F. (1989) FEBS Lett. 254, 150–154.
136 Kobayashi, M., Maeda, H., Watanabe, T., Nakane, H. and Satoh, Ki. (1990) FEBS Lett. 260, 138–140.
137 Gounaris, K., Chapman, D.J., Booth, P., Crystall, B., Giorgi, L.B., Klug, D.R., Porter, G. and Barber, J. (1990) FEBS Lett. 265, 88–92.
138 Nagatsuka, T., Fukuhara, S., Akabori, K. and Toyoshima, Y. (1991) Biochim. Biophys. Acta 1057, 223–231.
139 Montoya, G., Yruela, I. and Picorel, R. (1991) FEBS Lett. 283, 255–258.
140 Tang, X.-S., Fushimi, K. and Satoh, Ki. (1990) FEBS Lett. 273, 257–260.
141 Takahashi, M.-A., Shiraishi, T. and Asada, K. (1988) FEBS Lett. 240, 6–8.
142 Takahashi, Y., Nakane, H., Kojima, H. and Satoh, Ki. (1990) Plant Cell Physiol. 31, 273–280.

143 Inagaki, N., Fujita, S. and Satoh, Ki. (1989) FEBS Lett. 246, 218–222.
144 Fujita, S., Inagaki, N., Ono, T.-A., Inoue, Y. and Satoh, Ki. (1989) FEBS Lett. 255, 1–4.
145 Inagaki, N., Fujita, S. and Satoh, Ki. (1990) in Current Research in Photosynthesis (Baltscheffsky, M., ed.), Vol. III, pp. 763–766, Kluwer, Dordrecht.
146 Bowyer, J.R., Packer, J.C.L., McCormack, B.A., Whitelegge, J.P., Robinson, C. and Taylor, M.A. (1992) J. Biol. Chem. 267, 5424–5433.
147 Mattoo, A.K. and Edelman, M. (1987) Proc. Natl. Acad. Sci. USA 84, 1497–1501.
148 Telfer, A., Marder, J.B. and Barber, J. (1987) Biochim. Biophys. Acta 893, 557–563.
149 Marder, J.B., Telfer, A. and Barber, J. (1988) Biochim. Biophys. Acta 932, 362–365.
150 Michel, H.P., Hunt, D.F., Shabanowitz, J. and Bennett, J. (1988) J. Biol. Chem. 263, 1123–1130.
151 Elich, T.D., Edelman, M. and Mattoo, A.K. (1992) J. Biol. Chem. 267, 3523–3529.
152 Shipton, C.A. and Barber, J. (1991) Proc. Natl. Acad. Sci. USA 88, 6691–6695.
153 Misra, A.N., Hall, S.G. and Barber, J. (1991) Biochim. Biophys. Acta 1059, 239–242.
154 Barbato, R., Shipton, C.A., Giacometti, G.M. and Barber, J. (1991) FEBS Lett. 290, 162–166.
155 Shipton, C.A. and Barber, J. (1992) Biochim. Biophys. Acta 1099, 85–90.
156 Barber, J. and Andersson, B. (1992) Trends Biochem. Sci. 17, 61–66.
157 Prášil, O., Adir, N. and Ohad, I. (1992) in The Photosystems: Structure, Function and Molecular Biology (Barber, J., ed.), pp. 295–348, Elsevier, Amsterdam.
158 De Vitry, C., Diner, B.A. and Lemoine, Y. (1987) in Progress in Photosynthesis Research (Biggins, J., ed.), Vol. II, pp. 105–108, Martinus Nijhoff, Dordrecht.
159 Gounaris, K., Pick, U. and Barber, J. (1987) FEBS Lett. 211, 94–98.
160 Golden, S.S. and Stearns, G.W. (1988) Gene 67, 85–96.
161 Carpenter, S.D., Charité, J., Eggers, B. and Vermaas, W.F.J. (1990) FEBS Lett. 260, 135–137.
162 Sayre, R.T. and Wrobel-Boerner, E. (1990) Plant Physiol. 93, 22a.
163 Salter, A.H., Virgin, I., Hagman, Å. and Andersson, B. (1992) Biochemistry 31, 3990–3998.
164 Dekker, J.P., Betts, S.D., Yocum, C.F. and Boekema, E.J. (1990) Biochemistry 29, 3220–3225.
165 Rögner, M., Chisholm, D.A. and Diner, B.A. (1991) Biochemistry 30, 5387–5395.
166 Yamaguchi, N., Takahashi, Y. and Satoh, Ki. (1988) Plant Cell Physiol. 29, 123–129.
167 Barbato, R., Race, H.L., Friso, G. and Barber, J. (1991) FEBS Lett. 286, 86–90.
168 Dekker, J.P., Boekema, E.J., Witt, H.T. and Rögner, M. (1988) Biochim. Biophys. Acta 936, 307–318.
169 Vermaas, W.F.J., Ikeuchi, M. and Inoue, Y. (1988) Photosynth. Res. 17, 97–113.
170 Chapman, D.J., Gounaris, K. and Barber, J. (1988) Biochim. Biophys. Acta 933, 423–431.
171 Gounaris, K., Chapman, D.J. and Barber, J. (1988) FEBS Lett. 240, 143–147.
172 Chapman, D.J., Vass, I. and Barber, J. (1991) Biochim. Biophys. Acta 1057, 391–398.
173 Mathis, P., Satoh, Ki. and Hansson, Ö. (1989) FEBS Lett. 251, 241–244.
174 Satoh, Ki., Hansson, Ö. and Mathis, P. (1990) Biochim. Biophys. Acta 1016, 121–126.
175 Booth, P.J., Crystall, B., Giorgi, L.B., Barber, J., Klug, D.R. and Porter, G. (1990) Biochim. Biophys. Acta 1016, 141–152.
176 Diner, B.A., De Vitry, C. and Popot, J.-L. (1988) Biochim. Biophys. Acta 934, 47–54.
177 Van Gorkom, H.J. (1974) Biochim. Biophys. Acta 347, 439–442.
178 Dekker, J.P., Van Gorkom, H.J., Brok, M. and Ouwehand, L. (1984) Biochim. Biophys. Acta 764, 301–309.
179 Schatz, G.H. and Van Gorkom, H.J. (1985) Biochim. Biophys. Acta 810, 283–295.
180 Klimov, V.V., Klevanik, A.V., Shuvalov, V.A. and Krasnovsky, A.A. (1977) FEBS Lett. 82, 183–186.
181 Nakane, H., Iwaki, M., Satoh, Ki. and Itoh, S. (1991) Plant Cell Physiol. 32, 1165–1171.
182 Liu, B.-L., Hoff, A.J., Gu, L.-Q., Li, L.-B. and Zhou, P.-Z. (1991) Photosynth. Res. 30, 95–106.
183 Gunner, M.R., Robertson, D.E. and Dutton, P.L. (1986) J. Phys. Chem. 90, 3783–3795.
184 Petersen, J., Dekker, J.P., Bowlby, N.R., Ghanotakis, D.F., Yocum, C.F. and Babcock, G.T. (1990) Biochemistry 29, 3226–3231.
185 Frank, H.A., Hansson, Ö. and Mathis, P. (1989) Photosynth. Res. 20, 279–289.
186 Ghanotakis, D.F., De Paula, J.C., Demetriou, D.M., Bowlby, N.R., Petersen, J., Babcock, G.T. and Yocum, C.F. (1989) Biochim. Biophys. Acta 974, 44–53.
187 Yamagishi, A. and Katoh, S. (1984) Biochim. Biophys. Acta 765, 118–124.
188 Yamagishi, A. and Katoh, S. (1985) Biochim. Biophys. Acta 807, 74–80.
189 Boska, M., Yamagishi, A. and Sauer, K. (1986) Biochim. Biophys. Acta 850, 226–233.
190 Bowden, S.J., Hallahan, B.J., Ruffle, S.V., Evans, M.C.W. and Nugent, J.H.A. (1991) Biochim. Biophys. Acta 1060, 89–96.
191 Carpenter, S.D. and Vermaas, W.F.J. (1988) in Light-Energy Transduction in Photosynthesis: Higher Plant and Bacterial Models (Stevens, S.E.,Jr. and Bryant, D.A., eds.), pp. 327–331, American Society of Plant Physiologists, Rockville.
192 De Vitry, C., Olive, J., Drapier, D., Recouvreur, M. and Wollman, F.-A. (1989) J. Cell Biol. 109, 991–1006.
193 Widger, W.R., Cramer, W.A., Hermodson, M. and Herrmann, R.G. (1985) FEBS Lett. 191, 186–190.
194 Willey, D.L. and Gray, J.C. (1989) Curr. Genet. 15, 213–220.
195 Herrmann, R.G., Alt, J., Schiller, B., Widger, W.R. and Cramer, W.A. (1984) FEBS Lett. 176, 239–244.
196 Tae, G.-S., Black, M.T., Cramer, W.A., Vallon, O. and Bogorad, L. (1988) Biochemistry 27, 9075–9080.
197 Vallon, O., Tae, G.-S., Cramer, W.A., Simpson, D., Hoyer-Hansen, G. and Bogorad, L. (1989) Biochim. Biophys. Acta 975, 132–141.
198 Tae, G.-S. and Cramer, W.A. (1989) FEBS Lett. 259, 161–164.
199 Cramer, W.A., Furbacher, P.N., Szczepaniak, A. and Tae, G.-S. (1990) in Current Research in Photosynthesis (Baltscheffsky, M., ed.), Vol. III, pp. 221–230, Kluwer, Dordrecht.
200 Cramer, W.A., Theg, S.M. and Widger, W.R. (1986) Photosynth. Res. 10, 393–403.
201 Babcock, G.T., Widger, W.R., Cramer, W.A., Oertling, W.A. and Metz, J.G. (1985) Biochemistry 24, 3638–3645.
202 Miyazaki, A., Shina, T., Toyoshima, Y., Gounaris, K. and Barber, J. (1989) Biochim. Biophys. Acta 975, 142–147.
203 Buser, C.A., Diner, B.A. and Brudvig, G.W. (1992) Biochemistry, in press.
204 Lam, E., Baltimore, B., Ortiz, W., Chollar, S., Melis, A. and Malkin, R. (1983) Biochim. Biophys. Acta 724, 201–211.
205 Murata, N., Miyao, M., Omata, T., Matsunami, H. and Kuwabara, T. (1984) Biochim. Biophys. Acta 765, 363–369.
206 Yamamoto, Y., Tabata, K., Isogai, Y., Nishimura, M., Okayama,

S., Matsuura, K. and Itoh, S. (1984) Biochim. Biophys. Acta 767, 493–500.
207 Briantais, J.-M., Vernotte, C., Miyao, M., Murata, N. and Picaud, M. (1985) Biochim. Biophys. Acta 808, 348–351.
208 De Paula, J.C., Innes, J.B. and Brudvig, G.W. (1985) Biochemistry 24, 8114–8120.
209 Noren, G.H., Boerner, R.J. and Barry, B.A. (1991) Biochemistry 30, 3943–3950.
210 Cramer, W.A. and Whitmarsh, J. (1977) Annu. Rev. Plant Physiol. 28, 133–172.
211 Thompson, L.K., Miller, A.-F., Buser, C.A., De Paula, J.C. and Brudvig, G.W. (1989) Biochemistry 28, 8048–8056.
212 Larsson, C., Jansson, C., Ljungberg, U., Åkerlund, H.-E. and Andersson, B. (1984) in Advances in Photosynthesis Research (Sybesma, C., ed.), Vol. I, pp. 363–366, Martinus Nijhoff/Dr. W. Junk, The Hague.
213 Ghanotakis, D.F., Yocum, C.F. and Babcock, G.T. (1986) Photosynth. Res. 9, 125–134.
214 De Paula, J.C., Li, P.M., Miller, A.-F., Wu, B.W. and Brudvig, G.W. (1986) Biochemistry 25, 6487–6494.
215 Buser, C.A., Diner, B.A. and Brudvig, G.W. (1992) Biochemistry, in press.
216 Thompson, L.K. and Brudvig, G.W. (1988) Biochemistry 27, 6653–6658.
217 Whitmarsh, J. and Cramer, W.A. (1978) Biochim. Biophys. Acta 501, 83–93.
218 Butler, W.L. and Matsuda, H. (1983) in The Oxygen Evolving System of Photosynthesis (Inoue, Y., Crofts, A.R., Govindjee, Murata, N., Renger, G. and Satoh, Ki., eds.), pp. 113–122, Academic Press, Tokyo.
219 Cananni, O. and Havaux, M. (1990) Proc. Natl. Acad. Sci. USA 87, 9295–9299.
220 Oh-oka, H., Tanaka, S., Wada, K., Kuwabara, T. and Murata, N. (1986) FEBS Lett. 197, 63–66.
221 Tyagi, A., Hermans, J., Steppuhn, J., Jansson, C., Vater, F. and Herrmann, R.G. (1987) Mol. Gen. Genet. 207, 288–293.
222 Enami, I., Kaneko, M., Kitamura, N., Koike, H., Sonoike, K., Inoue, Y. and Katoh, S. (1991) Biochim. Biophys. Acta 1060, 224–232.
223 Murata, N., Miyao, M. and Kuwabara, T. (1983) in The Oxygen Evolving System of Photosynthesis (Inoue, Y., Crofts, A.R., Govindjee, Murata, N., Renger, G. and Satoh, Ki., eds.), pp. 213–222, Academic Press, Tokyo.
224 Cammarata, K.V., Tamura, N., Sayre, R.T. and Cheniae, G.M. (1984) in Advances in Photosynthesis Research (Sybesma, C., ed.), Vol. I, pp. 311–320, Martinus Nijhoff/Dr. W. Junk Publishers, The Hague.
225 Millner, P.A., Gogel, G. and Barber, J. (1987) Photosynth. Res. 13, 185–198.
226 Andersson, B., Larsson, C., Jansson, C., Ljungberg, U. and Åkerlund, H.-E. (1984) Biochim. Biophys. Acta 766, 21–28.
227 Wales, R., Newman, B.J., Pappin, D. and Gray, J.C. (1989) Plant Mol. Biol. 12, 439–451 (erratum, Plant. Mol. Biol. 13, 257).
228 Borthakur, D. and Haselkorn, R. (1989) Plant Mol. Biol. 13, 427–439.
229 Tanaka, S. and Wada, K. (1988) Photosynth. Res. 17, 255–266.
230 Tanaka, S., Kawata, Y., Wada, K. and Hamaguchi, K. (1989) Biochemistry 28, 7188–7193.
231 Ghanotakis, D.F., Topper, J.N. and Yocum, C.F. (1984) Biochim. Biophys. Acta 767, 524–531.
232 Kuwabara, T., Miyao, M., Murata, T. and Murata, N. (1985) Biochim. Biophys. Acta 806, 283–289.
233 Miyao, M. and Murata, N. (1989) Biochim. Biophys. Acta 977, 315–321.
234 Kavelaki, K. and Ghanotakis, D.F. (1991) Photosynth. Res. 29, 149–155.
235 Shen, J.-R. and Inoue, Y. (1991) Plant Cell Physiol. 33, 453–457.
236 Eaton-Rye, J.J. and Murata, N. (1989) Biochim. Biophys. Acta 977, 219–226.
237 Völker, M., Ono, T.-A., Inoue, Y. and Renger, G. (1985) Biochim. Biophys. Acta 806, 25–34.
238 Åkerlund, H.-E. and Jansson, C. (1981) FEBS Lett. 124, 229–232.
239 Yamamoto, Y., Doi, M., Tamura, N. and Nishimura, M. (1981) FEBS Lett. 133, 265–268.
240 Kuwabara, T. and Murata, N. (1983) Plant Cell Physiol. 24, 741–747.
241 Sandusky, P.O., Selvius-DeRoo, C.L., Hicks, D.B., Yocum, C.F., Ghanotakis, D.F. and Babcock, G.T. (1983) in The Oxygen Evolving Complex of Photosynthesis (Inoue, Y., Crofts, A.R., Govindjee, Murata, N., Renger, G. and Satoh, Ki., eds.), pp. 189–199, Academic Press, Tokyo.
242 Ono, T.-A. and Inoue, Y. (1983) FEBS Lett. 164, 255–260.
243 Ono, T.-A. and Inoue, Y. (1984) FEBS Lett. 166, 381–384.
244 Miyao, M. and Murata, N. (1983) FEBS Lett. 164, 375–378.
245 Miyao, M. and Murata, N. (1984) Biochim. Biophys. Acta 765, 253–257.
246 Miyao, M. and Murata, N. (1984) FEBS Lett. 170, 350–354.
247 Stewart, A.C., Ljungberg, U., Åkerlund, H.-E. and Andersson, B. (1985) Biochim. Biophys. Acta 808, 353–362.
248 Bricker, T.M. (1992) Biochemistry 31, 4623–4628.
249 Mavankal, G., McCain, D.C. and Bricker, T.M. (1986) FEBS Lett. 202, 235–239.
250 Mavankal, G., McCain, D.C. and Bricker, T.M. (1987) in Progress in Photosynthesis Research (Biggins, J., ed.), Vol. I, pp. 661–664, Martinus Nijhoff, Dordrecht.
251 Ono, T.-A. and Inoue, Y. (1984) FEBS Lett. 168, 281–286.
252 Ono, T.-A. and Inoue, Y. (1985) Biochim. Biophys. Acta 806, 331–340.
253 Cole, J.L., Yachandra, V.K., McDermott, A.E., Guiles, R.D., Britt, R.D., Dexheimer, S.L., Sauer, K. and Klein, M.P. (1987) Biochemistry 26, 5967–5973.
254 Mayfield, S.P., Rahire, M., Frank, G., Zuber, H. and Rochaix, J.-D. (1987) Proc. Natl. Acad. Sci. USA 84, 749–753.
255 Jansen, T., Rother, C., Steppuhn, J., Reinke, H., Beyreuther, K., Jansson, C., Andersson, B. and Herrmann, R.G. (1987) FEBS Lett. 216, 234–240.
256 Wales, R., Newman, B.J., Rose, S.A., Pappin, D. and Gray, J.C. (1989) Plant Mol. Biol. 13, 573–582.
257 Åkerlund, H.-E., Jansson, C. and Andersson, B. (1982) Biochim. Biophys. Acta 681, 1–10.
258 Miyao, M. and Murata, N. (1983) Biochim. Biophys. Acta 725, 87–93.
259 Waggoner, C.M. and Yocum, C.F. (1987) in Progress in Photosynthesis Research (Biggins, J., ed.), Vol. I, pp. 685–688, Martinus Nijhoff, Dordrecht.
260 Ghanotakis, D.F., Babcock, G.T. and Yocum, C.F. (1984) FEBS Lett. 167, 127–130.
261 Miyao, M. and Murata, N. (1984) FEBS Lett. 168, 118–120.
262 Nakatani, H.Y. (1984) Biochem. Biophys. Res. Commun. 120, 299–304.
263 Andersson, B., Critchley, C., Ryrie, I.J., Jansson, C., Larsson, C. and Anderson, J.M. (1984) FEBS Lett. 168, 113–117.
264 Akabori, K., Imaoka, A. and Toyoshima, Y. (1984) FEBS Lett. 173, 36–40.
265 Miyao, M. and Murata, N. (1985) FEBS Lett. 180, 303–308.
266 Ghanotakis, D.F. and Yocum, C.F. (1985) Photosynth. Res. 7, 97–114.
267 Murata, N. and Miyao, M. (1985) Trends Biochem. Sci. 10, 122–124.
268 Murata, N. and Miyao, M. (1987) in Progress in Photosynthesis Research (Biggins, J., ed.), Vol. I, pp. 453–462, Martinus Nijhoff, Dordrecht.

269 Andersson, B. and Åkerlund, H.-E. (1987) in The Light Reactions (Barber, J., ed.), pp. 379–420, Elsevier Science Publishers B.V., Amsterdam.
270 Yocum, C.F. (1992) in Manganese Redox Enzymes (Pecoraro, V.L., ed.), pp. 71–83, VCH, New York.
271 Ghanotakis, D.F., Babcock, G.T. and Yocum, C.F. (1984) Biochim. Biophys. Acta 765, 388–398.
272 Tamura, N. and Cheniae, G.M. (1985) Biochim. Biophys. Acta 809, 245–259.
273 Tamura, N., Radmer, R., Lantz, S., Cammarata, K.V. and Cheniae, G.M. (1986) Biochim. Biophys. Acta 850, 369–379.
274 Waggoner, C.M. (1989) Ph.D. Dissertation, University of Michigan, Ann Arbor.
275 Mei, R. and Yocum, C.F. (1990) in Current Research in Photosynthesis (Baltscheffsky, M., ed.), Vol. I, pp. 729–732, Kluwer, Dordrecht.
276 Tamura, N., Inoué, H. and Inoue, Y. (1990) Plant Cell Physiol. 31, 469–477.
277 Mei, R. and Yocum, C.F. (1991) Biochemistry 30, 7836–7842.
278 Becker, D.W., Callahan, F.E. and Cheniae, G.M. (1985) FEBS Lett. 192, 209–214.
279 Ono, T.-A., Kajikawa, H. and Inoue, Y. (1986) Plant Physiol. 80, 85–90.
280 Kuwabara, T., Murata, T., Miyao, M. and Murata, N. (1986) Biochim. Biophys. Acta 850, 146–155.
281 Miyao, M., Fujimura, Y. and Murata, N. (1988) Biochim. Biophys. Acta 936, 465–474.
282 Enami, I., Mochizuki, Y., Takahashi, S., Kakuno, T., Horio, T., Satoh, Ka. and Katoh, S. (1990) Plant Cell Physiol. 31, 725–729.
283 Enami, I., Miyaoka, T., Mochizuki, Y., Shen, J.-R., Satoh, Ka. and Katoh, S. (1989) Biochim. Biophys. Acta 973, 35–40.
284 Bowes, J.M., Stewart, A.C. and Bendall, D.S. (1983) Biochim. Biophys. Acta 725, 210–219.
285 Koike, H. and Inoue, Y. (1985) Biochim. Biophys. Acta 807, 64–73.
286 Ohno, T., Satoh, Ka. and Katoh, S. (1986) Biochim. Biophys. Acta 852, 1–8.
287 Rögner, M., Dekker, J.P., Boekema, E.J. and Witt, H.T. (1987) FEBS Lett. 219, 207–211.
288 Bendall, D.S., Bowes, J.M., Stewart, A.C. and Taylor, M.E. (1988) Methods Enzymol. 167, 272–281.
289 Koike, H., Mamada, K., Ikeuchi, M. and Inoue, Y. (1989) FEBS Lett. 244, 391–396.
290 Shen, J.-R., Ikeuchi, M. and Inoue, Y. (1992) FEBS Lett. 301, 145–149.
291 Ljungberg, U., Henrysson, T., Rochester, C.P., Åkerlund, H.-E. and Andersson, B. (1986) Biochim. Biophys. Acta 849, 112–120.
292 Henrysson, T., Ljungberg, U., Franzén, L.-G., Andersson, B. and Åkerlund, H.-E. (1987) in Progress in Photosynthesis Research (Biggins, J., ed.), Vol. II, pp. 125–128, Martinus Nijhoff, Dordrecht.
293 Ikeuchi, M. and Inoue, Y. (1988) Plant Cell Physiol. 29, 1233–1239.
294 Schröder, W.P., Henrysson, T. and Åkerlund, H.-E. (1988) FEBS Lett. 235, 289–292.
295 Murata, N., Miyao, M., Hayashida, N., Hidaka, T. and Sugiura, M. (1988) FEBS Lett. 235, 283–288.
296 Webber, A.N., Hird, S.M., Packman, L.C., Dyer, T.A. and Gray, J.C. (1989) Plant Mol. Biol. 12, 141–151.
297 Ikeuchi, M. and Inoue, Y. (1988) FEBS Lett. 241, 99–104.
298 Ikeuchi, M., Takio, K. and Inoue, Y. (1989) FEBS Lett. 242, 263–269.
299 Webber, A.N., Packman, L., Chapman, D.J., Barber, J. and Gray, J.C. (1989) FEBS Lett. 242, 259–262.
300 Ikeuchi, M., Koike, H. and Inoue, Y. (1989) FEBS Lett. 251, 155–160.
301 Ikeuchi, M., Koike, H. and Inoue, Y. (1989) FEBS Lett. 253, 178–182.
302 Ikeuchi, M., Koike, H., Mamada, K., Takio, K. and Inoue, Y. (1990) in Current Research in Photosynthesis (Baltscheffsky, M., ed.), Vol. I, pp. 347–350, Kluwer, Dordrecht.
303 Koike, H., Ikeuchi, M., Hiyama, T., Mamada, K. and Inoue, Y. (1990) in Current Research in Photosynthesis (Baltscheffsky, M., ed.), Vol. I, pp. 351–354, Kluwer, Dordrecht.
304 Gray, J.C., Webber, A.N., Hird, S.M., Willey, D.L. and Dyer, T.A. (1990) in Current Research in Photosynthesis (Baltscheffsky, M., ed.), Vol. III, pp. 461–468, Kluwer, Dordrecht.
305 Gray, J.C., Dunn, P.J.P., Eccles, C.J., Hird, S.M., Last, D.I., Newman, B.J. and Willey, D.L. (1987) in Plant Molecular Biology (von Wettstein, D. and Chua, N.-H., eds.), pp. 105–113, Plenum Press, New York.
306 Cushman, J.C., Christopher, D.A., Little, M.C., Hallick, R.B. and Price, C.A. (1988) Curr. Genet. 13, 173–180.
307 Cantrell, A. and Bryant, D.A. (1988) Photosynth. Res. 16, 65–81.
308 Nyhus, K.J. and Pakrasi, H.B. (1989) in Techniques and New Developments in Photosynthesis Research (Barber, J. and Malkin, R., eds.), pp. 469–472, Plenum Press, New York.
309 Ikeuchi, M., Eggers, B., Shen, G., Webber, A.N., Yu, J., Hirano, A., Inoue, Y. and Vermaas, W.F.J. (1991) J. Biol. Chem. 266, 11111–11115.
310 Farchaus, J.W. and Dilley, R.A. (1986) Arch. Biochem. Biophys. 244, 94–101.
311 Hird, S.M., Dyer, T.A. and Gray, J.C. (1986) FEBS Lett. 209, 181186.
312 Westhoff, P., Farchaus, J.W. and Herrmann, R.G. (1986) Curr. Genet. 11, 165–169.
313 Ljungberg, U., Åkerlund, H.-E., Larsson, C. and Andersson, B. (1984) Biochim. Biophys. Acta 767, 145–152.
314 Ljungberg, U., Åkerlund, H.-E. and Andersson, B. (1986) Eur. J. Biochem. 158, 477–482.
315 Lautner, A., Klein, R., Ljungberg, U., Reiländer, H., Bartling, D., Andersson, B., Reinke, H., Beyreuther, K. and Herrmann, R.G. (1988) J. Biol. Chem. 263, 10077–10081.
316 Webber, A.N., Packman, L.C. and Gray, J.C. (1989) FEBS Lett. 242, 435–438.
317 Stockhaus, J., Höfer, M., Renger, G., Westhoff, P., Wydrzynski, T. and Willmitzer, L. (1990) EMBO J. 9, 3013–3021.
318 Merritt, S., Ernfors, P., Ghanotakis, D.F. and Yocum, C.F. (1987) in Progress in Photosynthesis Research (Biggins, J., ed.), Vol. I, pp. 689–692, Martinus Nijhoff, Dordrecht.
319 Bowlby, N.R. (1989) Ph.D. Dissertation, University of Michigan, Ann Arbor.
320 Bowlby, N.R., Petersen, J., Babcock, G.T. and Yocum, C.F. (1990) in Current Research in Photosynthesis (Baltscheffsky, M., ed.), Vol. I, pp. 539–542, Kluwer, Dordrecht.
321 Nilsson, F., Andersson, B. and Jansson, C. (1990) Plant Mol. Biol. 14, 1051–1054.
322 Michel, H.P. and Bennett, J. (1987) FEBS Lett. 212, 103–108.
323 Dedner, N., Meyer, H.E., Ashton, C. and Wildner, G.F. (1988) FEBS Lett. 236, 77–82.
324 Abdel-Mawgood, A. and Dilley, R.A. (1990) Plant Mol. Biol. 14, 445–446.
325 Mayes, S.R. and Barber, J. (1990) Nucleic Acids Res. 18, 194.
326 Debus, R.J., Feher, G. and Okamura, M.Y. (1985) Biochemistry 24, 2488–2500.
327 Camm, E.L. and Green, B.R. (1989) Biochim. Biophys. Acta 974, 180–184.
328 Henrysson, T., Schröder, W.P., Spangfort, M. and Åkerlund, H.-E. (1989) Biochim. Biophys. Acta 977, 301–308.
329 Barbato, R., Rigoni, F., Giardi, M.T. and Giacometti, G.M. (1989) FEBS Lett. 251, 147–154.
330 Reuter, R.A., White, L.S. and Berg, S.P. (1990) in Current

Research in Photosynthesis (Baltscheffsky, M., ed.), Vol. I, pp. 671–674, Kluwer, Dordrecht.
331 Pichersky, E. and Green, B.R. (1990) in Current Research in Photosynthesis (Baltscheffsky, M., ed.), Vol. III, pp. 553–556, Kluwer, Dordrecht.
332 Morishige, D.T. and Thornber, J.P. (1992) Plant Physiol. 98, 238–245.
333 Stewart, A.C., Steczkowski, M. and Ljungberg, U. (1985) FEBS Lett. 193, 175–179.
334 Rolfe, S.A. and Bendall, D.S. (1989) Biochim. Biophys. Acta 973, 220–226.
335 Steinmetz, A.A., Castroviejo, M., Cayre, R.T. and Bogorad, L. (1986) J. Biol. Chem. 261, 2485–2488.
336 Nixon, P.J., Gounaris, K., Coomber, S.A., Hunter, C.N., Dyer, T.A. and Barber, J. (1989) J. Biol. Chem. 264, 14129–14135.
337 Mayes, S.R., Cook, K.M. and Barber, J. (1990) FEBS Lett. 262, 49–54.
338 Cheniae, G.M. (1980) Methods Enzymol. 69, 349–363.
339 Amesz, J. (1983) Biochim. Biophys. Acta 726, 1–12.
340 Cheniae, G.M. and Martin, I.F. (1971) Plant Physiol. 47, 568–575.
341 Yocum, C.F., Yerkes, C.T., Blankenship, R.E., Sharp, R.R. and Babcock, G.T. (1981) Proc. Natl. Acad. Sci. USA 78, 7507–7511.
342 Ke, B., Inoué, H., Babcock, G.T., Fang, Z.-X. and Dolan, E. (1982) Biochim. Biophys. Acta 682, 297–306.
343 McDermott, A.E., Yachandra, V.K., Guiles, R.D., Cole, J.L., Dexheimer, S.L., Britt, R.D., Sauer, K. and Klein, M.P. (1988) Biochemistry 27, 4021–4031.
344 Shen, J.-R., Satoh, Ka. and Katoh, S. (1988) Biochim. Biophys. Acta 936, 386–394.
345 Cheniae, G.M. and Martin, I.F. (1970) Biochim. Biophys. Acta 197, 219–239.
346 Stewart, A.C. and Bendall, D.S. (1981) Biochem. J. 194, 877–887.
347 Pauly, S. and Witt, H.T. (1992) Biochim. Biophys. Acta 1099, 211–218.
348 Babcock, G.T., Ghanotakis, D.F., Ke, B. and Diner, B.A. (1983) Biochim. Biophys. Acta 723, 276–286.
349 Tamura, N. and Cheniae, G.M. (1987) Biochim. Biophys. Acta 890, 179–194.
350 Miller, A.-F. and Brudvig, G.W. (1990) Biochemistry 29, 1385–1392.
351 Klimov, V.V., Allakhverdiev, S.I., Shuvalov, V.A. and Krasnovsky, A.A. (1982) Dokl. Akad. Nauk SSSR 263, 1001–1005 (Engl. Transl., Dokl. Biophys. 263, 60–63).
352 Klimov, V.V., Allakhverdiev, S.I., Shuvalov, V.A. and Krasnovsky, A.A. (1982) FEBS Lett. 148, 307–312.
353 Miyao, M. and Inoue, Y. (1991) Biochim. Biophys. Acta 1056, 47–56.
354 Miller, A.-F. and Brudvig, G.W. (1989) Biochemistry 28, 8181–8190.
355 Cheniae, G.M. and Martin, I.F. (1971) Biochim. Biophys. Acta 253, 167–181.
356 Radmer, R. and Cheniae, G.M. (1971) Biochim. Biophys. Acta 253, 182–186.
357 Inoue, Y., Kobayashi, Y., Sakamoto, E. and Shibata, K. (1975) Plant Cell Physiol. 16, 327–336.
358 Yamashita, T., Inoue, Y., Kobayashi, Y. and Shibata, K. (1978) Plant Cell Physiol. 19, 895–900.
359 Ono, T.-A. and Inoue, Y. (1987) Plant Cell Physiol. 28, 1293–1299.
360 Anan'ev, G.M., Shafiyev, M.A., Isayenko, T.V. and Klimov, V.V. (1988) Biofizika 33, 265–269 (Engl. Transl., Biophysics 33, 285–289).
361 Tamura, N. and Cheniae, G.M. (1987) in Progress in Photosynthesis Research (Biggins, J., ed.), Vol. I, pp. 621–624, Martinus Nijhoff, Dordrecht.
362 Tamura, N. and Cheniae, G.M. (1988) in Light-Energy Transduction in Photosynthesis: Higher Plant and Bacterial Models (Stevens, S.E.,Jr. and Bryant, D.A., eds.), pp. 227–242, American Society of Plant Physiologists, Rockville.
363 Miyao-Tokutomi, M. and Inoue, Y. (1992) Biochemistry 31, 526–532.
364 Miyao, M. and Inoue, Y. (1991) Biochemistry 30, 5379–5387.
365 Blubaugh, D.J. and Cheniae, G.M. (1990) Biochemistry 29, 5109–5118.
366 Hoganson, C.W., Ghanotakis, D.F., Babcock, G.T. and Yocum, C.F. (1989) Photosynth. Res. 22, 285–293.
367 Nixon, P.J. and Diner, B.A. (1990) in Proceedings of the Twelfth Annual International Conference of the IEEE Engineering in Medicine and Biology Society (Pedersen, P.C. and Onarai, B., eds.), pp. 1732–1734, IEEE, New York.
368 Nixon, P.J. and Diner, B.A. (1992) Biochemistry 31, 942–948.
369 Yamashita, T. and Tomita, G. (1974) Plant Cell Physiol. 15, 69–82.
370 Yamashita, T. and Tomita, G. (1976) Plant Cell Physiol. 17, 571–582.
371 Ono, T.-A. and Inoue, Y. (1983) Biochim. Biophys. Acta 723, 191–201.
372 Pistorius, E.K. and Schmid, G.H. (1984) FEBS Lett. 171, 173–178.
373 Tamura, N. and Cheniae, G.M. (1986) FEBS Lett. 200, 231–236.
374 Shafiyev, M.A., Anan'ev, G.M., Allakhverdiev, S.I., Smolova, T.N. and Klimov, V.V. (1988) Biofizika 33, 61–65 (Engl. Transl., Biophysics 33, 61–65).
375 Tamura, N., Inoue, Y. and Cheniae, G.M. (1989) Biochim. Biophys. Acta 976, 173–181.
376 Yamashita, T. and Ashizawa, A. (1985) Arch. Biochem. Biophys. 238, 549–557.
377 Tamura, N., Kamachi, H., Hokari, N., Masumoto, H. and Inoué, H. (1991) Biochim. Biophys. Acta 1060, 51–58.
378 Boussac, A., Picaud, M. and Étienne, A.-L. (1986) Photobiochem. Photobiophys. 10, 201–211.
379 Inoué, H. and Wada, T. (1987) Plant Cell Physiol. 28, 767–773.
380 Inoué, H., Akanori, H. and Noguchi, M. (1987) Plant Cell Physiol. 28, 1339–1343.
381 Hsu, B.-D., Lee, J.-Y. and Pan, R.-L. (1987) Biochim. Biophys. Acta 890, 89–96.
382 Hoganson, C.W., Casey, P.A. and Hansson, Ö. (1991) Biochim. Biophys. Acta 1057, 399–406.
383 Conjeaud, H. and Mathis, P. (1980) Biochim. Biophys. Acta 590, 353–359.
384 Conjeaud, H. and Mathis, P. (1986) Biophys. J. 49, 1215–1221.
385 Brudvig, G.W. (1989) in Advanced EPR: Applications in Biology and Biochemistry (Hoff, A.J., ed.), pp. 839–863, Elsevier, Amsterdam.
386 Miller, A.-F. and Brudvig, G.W. (1991) Biochim. Biophys. Acta 1056, 1–18.
387 Brudvig, G.W., Thorp, H.H. and Crabtree, R.H. (1991) Acc. Chem. Res. 24, 311–316.
388 Vänngard, T., Hansson, Ö. and Haddy, A. (1992) in Manganese Redox Enzymes (Pecoraro, V.L., ed.), pp. 105–118, VCH, New York.
389 Sauer, K., Yachandra, V.K., Britt, R.D. and Klein, M.P. (1992) in Manganese Redox Enzymes (Pecoraro, V.L., ed.), pp. 141–175, VCH, New York.
390 Dismukes, G.C. and Siderer, Y. (1980) FEBS Lett. 121, 78–80.
391 Dismukes, G.C. and Siderer, Y. (1981) Proc. Natl. Acad. Sci. USA 78, 274–278.
392 Brudvig, G.W., Casey, J.L. and Sauer, K. (1983) Biochim. Biophys. Acta 723, 366–371.
393 Aasa, R., Hansson, Ö. and Vänngård, T. (1987) in Progress in

Photosynthesis Research (Biggins, J., ed.), Vol. I, pp. 577–580, Martinus Nijhoff, Dordrect.
394 Hansson, Ö., Aasa, R. and Vänngård, T. (1987) Biophys. J. 51, 825–832.
395 Brudvig, G.W., Casey, J.L. and Sauer, K. (1983) in The Oxygen Evolving System of Photosynthesis (Inoue, Y., Crofts, A.R., Govindjee, Murata, N., Renger, G. and Satoh, Ki., eds.), pp. 159–164, Academic Press, Tokyo.
396 Yachandra, V.K., Guiles, R.D., Sauer, K. and Klein, M.P. (1986) Biochim. Biophys. Acta 850, 333–342.
397 Andréasson, L.-E. (1989) Biochim. Biophys. Acta 973, 465–467.
398 DeRose, V.J., Yachandra, V.K., McDermott, A.E., Britt, R.D., Sauer, K. and Klein, M.P. (1991) Biochemistry 30, 1335–1341.
399 Haddy, A., Aasa, R. and Andréasson, L.-E. (1989) Biochemistry 28, 6954–6959.
400 Haddy, A., Aasa, R. and Hansson, Ö. (1990) in Current Research in Photosynthesis (Baltscheffsky, M., ed.), Vol. I, pp. 777–780, Kluwer, Dordrecht.
401 Rutherford, A.W. (1985) Biochim. Biophys. Acta 807, 189–201.
402 Kim, D.H., Britt, R.D., Klein, M.P. and Sauer, K. (1992) Biochemistry 31, 541–547.
403 Zimmermann, J.-L. and Rutherford, A.W. (1984) Biochim. Biophys. Acta 767, 160–167.
404 Franzén, L.-G., Hansson, Ö. and Andréasson, L.-E. (1985) Biochim. Biophys. Acta 808, 171–179.
405 Andréasson, L.-E. and Hansson, Ö. (1982) Biochim. Biophys. Acta 679, 261–268.
406 Cooper, S.R., Dismukes, G.C., Klein, M.P. and Calvin, M. (1978) J. Am. Chem. Soc. 100, 7248–7252.
407 Hagen, K.S., Armstrong, W.H. and Hope, H. (1988) Inorg. Chem. 27, 967–969.
408 Dismukes, G.C., Ferris, K. and Watnick, P. (1982) Photobiochem. Photobiophys. 3, 243–256.
409 Andréasson, L.-E., Hansson, Ö. and Vänngård, T. (1983) Chem. Scripta 21, 71–74.
410 Hansson, Ö., Andréassor, L.-E. and Vänngård, T. (1984) in Advances in Photosynthesis Research (Sybesma, C., ed.), Vol. I, pp. 307–310, Marinus Nijhoff/Dr. W. Junk, The Hague.
411 Goodin, D.B., Yachandra, V.K., Britt, R.D., Sauer, K. and Klein, M.P. (1984) Biochim. Biophys. Acta 767, 209–216.
412 Yachandra, V.K., Guiles, R.D., McDermott, A.E., Cole, J.L., Britt, R.D., Dexheimer, S.L., Sauer, K. and Klein, M.P. (1987) Biochemistry 26, 5974–5981.
413 Atkinson, Y.E. and Evans, M.C.W. (1984) in Advances in Photosynthesis Research (Sybesma, C., ed.), Vol. I, pp. 139–142, Martinus Nijhoff/Dr. W. Junk, The Hague.
414 Aasa, R., Andréasson, L.-E., Lagenfelt, G. and Vänngård, T. (1987) FEBS Lett. 221, 245–248.
415 Kirilovsky, D.L., Boussac, A.G.P., Van Mieghem, F.J.E., Ducruet, J.-M.R.C., Sétif, P.R., Yu, J., Vermaas, W.F.J. and Rutherford, A.W. (1992) Biochemistry 31, 2099–2107.
416 Haddy, A., Dunham, W.R., Sands, R.H. and Aasa, R. (1992) Biochim. Biophys. Acta 1099, 25–34.
417 Casey, J.L. and Sauer, K. (1984) Biochim. Biophys. Acta 767, 21–28.
418 De Paula, J.C., Beck, W.F., Miller, A.-F., Wilson, R.B. and Brudvig, G.W. (1987) J. Chem. Soc. Faraday Trans. I 83, 3635–3651.
419 Cole, J., Yachandra, V.K., Guiles, R.D., McDermott, A.E., Britt, R.D., Dexheimer, S.L., Sauer, K. and Klein, M.P. (1987) Biochim. Biophys. Acta 890, 395–398.
420 Kim, D.H., Britt, R.D., Klein, M.P. and Sauer, K. (1990) J. Am. Chem. Soc. 112, 9389–9391.
421 Boussac, A. and Rutherford, A.W. (1988) Biochemistry 27, 3476–3483.
422 Ono, T.-A. and Inoue, Y. (1989) Arch. Biochem. Biophys. 275, 440–448.
423 Ono, T.-A. and Inoue, Y. (1990) Biochim. Biophys. Acta 1015, 373–377.
424 Ono, T.-A., Kusunoki, M., Matsushita, T., Oyanagi, H. and Inoue, Y. (1991) Biochemistry 30, 6836–6841.
425 Sonoike, K. and Katoh, S. (1989) Biochim. Biophys. Acta 976, 210–213.
426 Zimmermann, J.-L. and Rutherford, A.W. (1986) Biochemistry 25, 4609–4615.
427 Beck, W.F. and Brudvig, G.W. (1986) Biochemistry 25, 6479–6486.
428 Beck, W.F. and Brudvig, G.W. (1988) Chem. Scripta 28A, 93–98.
429 Boussac, A., Rutherford, A.W. and Styring, S. (1990) Biochemistry 29, 24–32.
430 Andréasson, L.-E. (1990) in Current Research in Photosynthesis (Baltscheffsky, M., ed.), Vol. I, pp. 785–788, Kluwer, Dordrecht.
431 Pace, R.J., Smith, P., Bramley, R. and Stehlik, D. (1991) Biochim. Biophys. Acta 1058, 161–170.
432 Boussac, A. and Rutherford, A.W. (1988) Chem. Scripta 28A, 123–126.
433 Ono, T.-A., Zimmermann, J.-L., Inoue, Y. and Rutherford, A.W. (1986) Biochim. Biophys. Acta 851, 193–201.
434 Ono, T.-A., Nakayama, H., Gleiter, H., Inoue, Y. and Kawamori, A. (1987) Arch. Biochem. Biophys. 256, 618–624.
435 Beck, W.F. and Brudvig, G.W. (1988) J. Am. Chem. Soc. 110, 1517–1523.
436 Andréasson, L.-E., Hansson, Ö. and von Schenck, K. (1988) Biochim. Biophys. Acta 936, 351–360.
437 Sandusky, P.O. and Yocum, C.F. (1983) FEBS Lett. 162, 339–343.
438 Sandusky, P.O. and Yocum, C.F. (1984) Biochim. Biophys. Acta 766, 603–611.
439 Sandusky, P.O. and Yocum, C.F. (1986) Biochim. Biophys. Acta 849, 85–93.
440 Kawamori, A., Inui, T., Ono, T.-A. and Inoue, Y. (1989) FEBS Lett. 254, 219–224.
441 Kawamori, A. and Inui, T. (1990) in Current Research in Photosynthesis (Baltscheffsky, M., ed.), Vol. I, pp. 765–768, Kluwer, Dordrecht.
442 Ono, T.-A. and Inoue, Y. (1988) Arch. Biochem. Biophys. 264, 82–92.
443 Beck, W.F., De Paula, J.C. and Brudvig, G.W. (1986) J. Am. Chem. Soc. 108, 4018–4022.
444 Beck, W.F. and Brudvig, G.W. (1987) in Progress in Photosynthesis Research (Biggins, J., ed.), Vol. I, pp. 499–502, Martinus Nijhoff, Dordrecht.
445 Andréasson, L.-E. and Hansson, Ö. (1987) in Progress in Photosynthesis Research (Biggins, J., ed.), Vol. I, pp. 503–510, Martinus Nijhoff, Dordrecht.
446 Britt, R.D., Zimmermann, J.-L., Sauer, K. and Klein, M.P. (1989) J. Am. Chem. Soc. 111, 3522–3532.
447 Boussac, A., Zimmermann, J.-L. and Rutherford, A.W. (1989) Biochemistry 28, 8984–8989.
448 Sivaraja, M., Tso, J. and Dismukes, G.C. (1989) Biochemistry 28, 9459–9464.
449 Ono, T.-A. and Inoue, Y. (1990) in Current Research in Photosynthesis (Baltscheffsky, M., ed.), Vol. I, pp. 741–744, Kluwer, Dordrecht.
450 Ono, T.-A. and Inoue, Y. (1990) in Current Research in Photosynthesis (Baltscheffsky, M., ed.), Vol. I, pp. 701–708, Kluwer, Dordrecht.
451 Boussac, A., Zimmermann, J.-L. and Rutherford, A.W. (1990) in Current Research in Photosynthesis (Baltscheffsky, M., ed.), Vol. I, pp. 713–716, Kluwer, Dordrecht.
452 Boussac, A., Zimmermann, J.-L., Rutherford, A.W. and Lavergne, J. (1990) Nature 347, 303–306.
453 Ono, T.-A. and Inoue, Y. (1990) Biochim. Biophys. Acta 1020, 269–277.

454 Boussac, A., Zimmermann, J.-L. and Rutherford, A.W. (1990) FEBS Lett. 277, 69–74.
455 Tso, J., Sivaraja, M. and Dismukes, G.C. (1991) Biochemistry 30, 4734–4739.
456 Hallahan, B.J., Nugent, J.H.A., Warden, J.T. and Evans, M.C.W. (1992) Biochemistry 31, 4562–4573.
457 Hansson, Ö., Andréasson, L.-E. and Vänngård, T. (1986) FEBS Lett. 195, 151–154.
458 Nugent, J.H.A. (1987) Biochim. Biophys. Acta 893, 184–189.
459 De Paula, J.C. and Brudvig, G.W. (1985) J. Am. Chem. Soc. 107, 2643–2648.
460 Beck, W.F., De Paula, J.C. and Brudvig, G.W. (1985) Biochemistry 24, 3035–3043.
461 Haddy, A. and Vänngård, T. (1990) in Current Research In Photosynthesis (Baltscheffsky, M., ed.), Vol. I, pp. 753–756, Kluwer, Dordrecht.
462 Butler, W.F., Calvo, R., Fredkin, D.R., Isaacson, R.A., Okamura, M.Y. and Feher, G. (1984) Biophys. J. 45, 947–973.
463 Rutherford, A.W., Zimmermann, J.-L. and Mathis, P. (1984) FEBS Lett. 165, 156–162.
464 Vermaas, W.F.J. and Rutherford, A.W. (1984) FEBS Lett. 175, 243–248.
465 Rutherford, A.W. (1987) in Progress in Photosynthesis Research (Biggins, J., ed.), Vol. I, pp. 277–283, Martinus Nijhoff, Dordrecht.
466 Itoh, S., Yerkes, C.T., Koike, H., Robinson, H.H. and Crofts, A.R. (1984) Biochim. Biophys. Acta 766, 612–622.
467 Theg, S.M., Jursinic, P.A. and Homann, P.H. (1984) Biochim. Biophys. Acta 766, 636–646.
468 Ono, T.-A., Conjeaud, H., Gleiter, H., Inoue, Y. and Mathis, P. (1986) FEBS Lett. 203, 215–219.
469 Rózsa, Zs. and Demeter, S. (1987) Photochem. Photobiol. 45, 525–528.
470 Vass, I., Ono, T.-A. and Inoue, Y. (1987) Biochim. Biophys. Acta 892, 224–235.
471 Sinclair, J. (1984) Biochim. Biophys. Acta 764, 247–252.
472 Kelley, P.M. and Izawa, S. (1978) Biochim. Biophys. Acta 502, 198–210.
473 Critchley, C., Baianu, I.C., Govindjee and Gutowsky, H.S. (1982) Biochim. Biophys. Acta 682, 436–445.
474 Ghanotakis, D.F., Topper, J.N., Babcock, G.T. and Yocum, C.F. (1984) FEBS Lett. 170, 169–173.
475 Ono, T.-A. and Inoue, Y. (1988) FEBS Lett. 227, 147–152.
476 Bakou, A., Buser, C., Dandulakis, G., Brudvig, G.W. and Ghanotakis, D.F. (1992) Biochim. Biophys. Acta 1099, 131–136.
477 Boussac, A. and Rutherford, A.W. (1988) FEBS Lett. 236, 432–436.
478 Brudvig, G.W. and Crabtree, R.H. (1986) Proc. Natl. Acad. Sci. USA 83, 4586–4588.
479 Brudvig, G.W. and De Paula, J.C. (1987) in Progress in Photosynthesis Research (Biggins, J., ed.), Vol. I, pp. 491–498, Martinus Nijhoff, Dordrecht.
480 Koike, H., Hanssum, B., Inoue, Y. and Renger, G. (1987) Biochim. Biophys. Acta 893, 524–533.
481 Koike, H. and Inoue, Y. (1987) in Progress in Photosynthesis Research (Biggins, J., ed.), Vol. I, pp. 645–648, Martinus Nijhoff, Dordrecht.
482 Styring, S. and Rutherford, A.W. (1988) Biochim. Biophys. Acta 933, 378–387.
483 Lockett, C.J., Demetriou, C., Bowden, S.J. and Nugent, J.H.A. (1990) Biochim. Biophys. Acta 1016, 213–218.
484 Tso, J., Sivaraja, M., Philo, J.S. and Dismukes, G.C. (1991) Biochemistry 30, 4740–4747.
485 Andréasson, L.-E. and Lindberg, K. (1992) Biochim. Biophys. Acta 1100, 177–183.
486 Baumgarten, M., Philo, J.S. and Dismukes, G.C. (1990) Biochemistry 29, 10814–10822.
487 Boussac, A., Sétif, P. and Rutherford, A.W. (1992) Biochemistry 31, 1224–1234.
488 Beck, W.F. and Brudvig, G.W. (1987) Biochemistry 26, 8285–8295.
489 Sivaraja, M. and Dismukes, G.C. (1986) Biochemistry 27, 3467–3475.
490 Sivaraja, M. and Dismukes, G.C. (1988) Biochemistry 27, 6297–6306.
491 Dismukes, G.C. and Damoder, R. (1985) Biophys. J. 47, 166a.
492 De Paula, J.C., Beck, W.F. and Brudvig, G.W. (1986) J. Am. Chem. Soc. 108, 4002–4009 (erratum, J. Am. Chem. Soc. 109, 6565).
493 Sheats, J.E., UnniNair, B.C., Petrouleas, V., Artandi, S., Czernuszewicz, R.S. and Dismukes, G.C. (1987) in Progress in Photosynthesis Research (Biggins, J., ed.), Vol. I, pp. 721–724, Martinus Nijhoff, Dordrecht.
494 Vincent, J.B. and Christou, G. (1987) Inorg. Chim. Acta 136, L41–L43.
495 Christou, G. and Vincent, J.B. (1988) Biochim. Biophys. Acta 895, 259–274.
496 Brudvig, G.W. and Crabtree, R.H. (1989) Prog. Inorg. Chem. 37, 99–142.
497 Christou, G. and Vincent, J.B. (1988) in Metal Clusters in Proteins (Que, L., Jr., ed.), pp. 238–255, American Chemical Society, Washington, D.C.
498 Pecoraro, V.L. (1988) Photochem. Photobiol. 48, 249–264.
499 Wieghardt, K. (1989) Angew. Chem. Int. Ed. Engl. 28, 1153–1172.
500 Christou, G. (1989) Acc. Chem. Res. 22, 328–335.
501 Vincent, J.B. and Christou, G. (1989) Adv. Inorg. Chem. 33, 197–257.
502 Thorp, H.H. and Brudvig, G.W. (1991) New J. Chem. 15, 479–490.
503 Larson, E.J. and Pecoraro, V.L. (1992) in Manganese Redox Enzymes (Pecoraro, V.L., ed.), pp. 1–28, VCH, New York.
504 Armstrong, W.H. (1992) in Manganese Redox Enzymes (Pecoraro, V.L., ed.), pp. 261–286, VCH, New York.
505 Chan, M.K. and Armstrong, W.H. (1991) J. Am. Chem. Soc. 113, 5055–5057.
506 Wang, S., Folting, K., Streib, W.E., Schmitt, E.A., McCusker, J.K., Hendrickson, D.N. and Christou, G. (1991) Angew. Chem. Int. Ed. Engl. 30, 305–306.
507 Libby, E., McCusker, J.K., Schmitt, E.A., Folting, K., Hendrickson, D.N. and Christou, G. (1991) Inorg. Chem. 30, 3846–3495.
508 Hendrickson, D.N., Christou, G., Schmitt, E.A., Libby, E., Bashkin, J.S., Wang, S., Tsai, H.-L., Vincent, J.B., Boyd, P.D.W., Huffman, J.C., Folting, K., Li, Q. and Streib, W.E. (1992) J. Am. Chem. Soc. 114, 2455–2471.
509 Kessissoglou, D.P., Kirk, M.L., Bender, C.J., Lah, M.S. and Pecoraro, V.L. (1989) J. Chem. Soc., Chem. Commun. 84–86.
510 Pecoraro, V.L., Kessissoglou, D.P., Li, X., Lah, M.S., Saadeh, S.M., Bender, C.J., Bonadies, J.A. and Larson, E. (1990) in Current Research in Photosynthesis (Baltscheffsky, M., ed.), Vol. I, pp. 709–712, Kluwer, Dordrecht.
511 Pecoraro, V.L. (1992) in Manganese Redox Enymes (Pecoraro, V.L., ed.), pp. 197–231, VCH, New York.
512 Li, X., Kessissoglou, D.P., Kirk, M.L., Bender, C.J. and Pecoraro, V.L. (1988) Inorg. Chem. 27, 1–3.
513 Messerschmidt, A., Rossi, A., Ladenstein, F., Huber, R., Bolognesi, M., Gatti, G., Marchesini, A., Petruzzelli, R. and Finazzi-Agró, A. (1989) J. Mol. Biol. 206, 513–529.
514 Messerschmidt, A., Ladenstein, R., Huber, R., Bolognesi, M., Avigliano, L., Petruzzelli, R., Rossi, A. and Finazzi-Agró, A. (1992) J. Mol. Biol. 224, 179–205.
515 Que, L.Jr. and True, A.E. (1990) Prog. Inorg. Chem. 38, 97–200.
516 Saadeh, S.M., Lah, M.S. and Pecoraro, V.L. (1991) Inorg. Chem. 30, 8–15

517 Brudvig, G.W. (1988) in Metal Clusters in Proteins (Que, L., Jr., ed.), pp. 221–237, American Chemical Society, Washington, D.C..

518 Sivaraja, M., Philo, J.S., Lary, J. and Dismukes, G.C. (1989) J. Am. Chem. Soc. 111, 3221–3225.

519 Imaoka, A., Akabori, K., Yanagi, M., Izumi, K., Toyoshima, Y., Kawamori, A., Nakayama, H. and Sato, J. (1986) Biochim. Biophys. Acta 848, 201–211.

520 Bonvoisin, J., Blondin, G., Girerd, J.-J. and Zimmermann, J.-L. (1992) Biophys. J. 61, 1076–1086

521 Dexheimer, S.L., Sauer, K. and Klein, M.P. (1990) in Current Research in Photosynthesis (Baltscheffsky, M., ed.), Vol. I, pp. 761–764, Kluwer, Dordrecht.

522 Dexheimer, S.L. and Klein, M.P. (1992) J. Am. Chem. Soc. 114, 2821–2826.

523 Srinivasan, A.N. and Sharp, R.R. (1986) Biochim. Biophys. Acta 850, 211–217.

524 Srinivasan, A.N. and Sharp, R.R. (1986) Biochim. Biophys. Acta 851, 369–376.

525 Srinivasan, A.N. and Sharp, R.R. (1987) in Progress in Photosynthesis Research (Biggins, J., ed.), Vol. I, pp. 553–556, Martinus Nijhoff, Dordrecht.

526 Yeh, S., Bayburt, T.H. and Sharp, R.R. (1990) in Current Research in Photosynthesis (Baltscheffsky, M., ed.), Vol. I, pp. 821–824, Kluwer, Dordrecht.

527 Sharp, R.R. (1992) in Manganese Redox Enzymes (Pecoraro, V.L., ed.), pp. 177–196, VCH, New York.

528 Kirby, J.A., Robertson, A.S., Smith, J.P., Thompson, A.C., Cooper, S.R. and Klein, M.P. (1981) J. Am. Chem. Soc. 103, 5529–5537.

529 Yachandra, V.K., Guiles, R.D., McDermott, A.E., Britt, R.D., Dexheimer, S.L., Sauer, K. and Klein, M.P. (1986) Biochim. Biophys. Acta 850, 324–332.

530 Guiles, R.D., Yachandra, V.K., McDermott, A.E., Britt, R.D., Dexheimer, S.L., Sauer, K. and Klein, M.P. (1987) in Progress in Photosynthesis Research (Biggins, J., ed.), Vol. I, pp. 561–564, Marinus Nijhoff, Dordrecht.

531 Guiles, R.D., Zimmermann, J.-L., McDermott, A.E., Yachandra, V.K., Cole, J.L., Dexheimer, S.L., Britt, R.D., Wieghardt, K., Bossek, U., Sauer, K. and Klein, M.P. (1990) Biochemistry 29, 471–485.

532 Guiles, R.D., Yachandra, V.K., McDermott, A.E., Cole, J.L., Dexheimer, S.L., Britt, R.D., Sauer, K. and Klein, M.P. (1990) Biochemistry 29, 486–496.

533 Guiles, R.D., Yachandra, V.K., McDermott, A.E., DeRose, V.J., Zimmermann, J.-L., Sauer, K. and Klein, M.P. (1990) in Current Research in Photosynthesis (Baltscheffsky, M., ed.), Vol. I, pp. 789–792, Kluwer, Dordrecht.

534 Sauer, K., Guiles, R.D., McDermott, A.E., Cole, J.L., Yachandra, V.K., Zimmermann, J.-L., Klein, M.P., Dexheimer, S.L. and Britt, R.D. (1988) Chem. Scripta 28A, 87–91.

535 Penner-Hahn, J.E., Fronko, R.M., Pecoraro, V.L., Yocum, C.F., Betts, S.D. and Bowlby, N.R. (1990) J. Am. Chem. Soc. 112, 2549–2557.

536 Penner-Hahn, J.E., Fronko, R.M., Waldo, G.S., Yocum, C.F., Bowlby, N.R. and Betts, S.D. (1990) in Current Research in Photosynthesis (Baltscheffsky, M., ed.), Vol. I, pp. 797–800, Kluwer, Dordrecht.

537 George, G.N., Prince, R.C. and Cramer, S.P. (1989) Science 243, 789–791.

538 Prince, R.C., Cramer, S.P. and George, G.N. (1990) in Current Research in Photosynthesis (Baltscheffsky, M., ed.) Vol. I, pp. 685–692, Kluwer, Dordrecht.

539 Bonadies, J.A., Kirk, M.L., Lah, M.S., Kessissoglou, D.P., Hatfield, W.E. and Pecoraro, V.L. (1989) Inorg. Chem. 28, 2037–2044.

540 Corrie, A.R., Evans, M.C.W., Hubbard, J.A.M., Strange, R.W and Hasnain, S.S. (1990) in Current Research in Photosynthesis (Baltscheffsky, M., ed.), Vol. I, pp. 793–796, Kluwer, Dordrecht.

541 Kusunoki, M., Ono, T.-A., Suzuki, M., Uehara, A., Matsushita, T., Oyanoagi, H. and Inoue, Y. (1990) in Current Research in Photosynthesis (Baltscheffsky, M., ed.), Vol. I, pp. 801–804, Kluwer, Dordrecht.

542 Kusunoki, M., Ono, T.-A., Matsushita, T., Oyanagi, H. and Inoue, Y. (1990) J. Biochem. 108, 560–567.

543 Yachandra, V.K., DeRose, V.J., Latimer, M.J., Mukerji, I., Sauer, K. and Klein, M.P. (1991) Photochem. Photobiol. 53, 98s–99s.

544 Riggs, P.J., Mei, R., Yocum, C.F. and Penner-Hahn, J.E. (1992) J. Am. Chem. Soc., submitted.

545 Larson, E., Lah, M.S., Li, X., Bonadies, J.A. and Pecoraro, V.L. (1992) Inorg. Chem. 31, 373–378.

546 Hardman, K.D., Agarwal, R.C. and Freiser, M.J. (1982) J. Mol. Biol. 157, 69–86.

547 Becker, J.W., Reeke, G.N.,Jr., Wang, J.L., Cunningham, B.A. and Edelman, G.M. (1975) J. Biol. Chem. 250, 1513–1524.

548 Ghanotakis, D.F., Babcock, G.T. and Yocum, C.F. (1985) Biochim. Biophys. Acta 809, 173–180.

549 Bonadies, J.A., Maroney, M.J. and Pecoraro, V.L. (1989) Inorg. Chem. 28, 2044–2051.

550 Kirby, J.A., Goodin, D.B., Wydrzynski, T., Robertson, A.S. and Klein, M.P. (1981) J. Am. Chem. Soc. 103, 5537–5542.

551 Styring, S.A. and Rutherford, A.W. (1988) Biochemistry 27, 4915–4923.

552 Evelo, R.G., Styring, S., Rutherford, A.W. and Hoff, A.J. (1989) Biochim. Biophys. Acta 973, 428–442.

553 Thorp, H.H. (1992) Inorg. Chem. 31, 1585–1588.

554 Britt, R.D., DeRose, V.J., Yachandra, V.K., Kim, D.H., Sauer, K. and Klein, M.P. (1990) in Current Research in Photosynthesis (Baltscheffsky, M., ed.), Vol. I, pp. 769–772, Kluwer, Dordrecht.

555 Petrouleas, V. and Diner, B.A. (1986) Biochim. Biophys. Acta 849, 264–275.

556 Brudvig, G.W. (1987) J. Bioenerg. Biomemb. 19, 91–104.

557 Dekker, J.P. (1992) in Manganese Redox Enzymes (Pecoraro, V.L., ed.), pp. 85–103, VCH, New York.

558 Thorp, H.H., Sarneski, J.E., Kulawiec, R.J., Brudvig, G.W., Crabtree, R.H. and Papaefthymiou, G.C. (1991) Inorg. Chem. 30, 1153–1155.

559 Rappaport, F. and Lavergne, J. (1991) Biochemistry 30, 10004–10012.

560 Förster, V. and Junge, W. (1985) Photochem. Photobiol. 41, 191–194.

561 Förster, V. and Junge, W. (1985) FEBS Lett. 186, 153–157.

562 Förster, V. and Junge, W. (1986) Photosynth. Res. 9, 197–210.

563 Förster, V. and Junge, W. (1987) in Progress in Photosynthesis Research (Biggins, J., ed.), Vol. I, pp. 511–514, Martinus Nijhoff, Dordrecht.

564 Förster, V. and Junge, W. (1988) Chem. Scripta 28A, 111–116.

565 Renger, G., Bader, K.P. and Schmid, G.H. (1990) Biochim. Biophys. Acta 1015, 288–294.

566 Renger, G., Messinger, J. and Hanssum, B. (1990) in Current Research in Photosynthesis (Baltscheffsky, M., ed.), Vol. I, pp. 845–848, Kluwer, Dordrecht.

567 Brudvig, G.W. and Beck, W.F. (1992) in Manganese Redox Enzymes (Pecoraro, V.L., ed.), pp. 119–140, VCH Publishers, Inc., New York.

568 Saygin, Ö. and Witt, H.T. (1985) Photobiochem. Photobiophys. 10, 71–82.

569 Witt, H.T., Schlodder, E., Brettel, K. and Saygin, Ö. (1986) Photosynth. Res. 10, 453–471.

570 Saygin, Ö. and Witt, H.T. (1987) Biochim. Biophys. Acta 893, 452–469 (erratum, Biochim. Biophys. Acta 932, 177).
571 Kretschmann, H., Pauly, S. and Witt, H.T. (1991) Biochim. Biophys. Acta 1059, 208–214.
572 Hanssum, B. and Renger, G. (1985) Biochim. Biophys. Acta 810, 225–234.
573 Hanssum, B. and Renger, G. (1987) in Progress in Photosynthesis Research (Biggins, J., ed.), Vol. I, pp. 515–518, Martinus Nijhoff, Dordrecht.
574 Renger, G. (1988) Chem. Scripta 28A, 105–109.
575 Pulles, M.P.J., Van Gorkom, H.J. and Willemsen, J.G. (1976) Biochim. Biophys. Acta 449, 536–540.
576 Mathis, P. and Haveman, J. (1977) Biochim. Biophys. Acta 461, 167–181.
577 Velthuys, B.R. (1981) in Photosynthesis (Akoyunoglou, G., ed.), Vol. II, pp. 75–85, Balaban International Science Services, Philadelphia.
578 Renger, G. and Weiss, W. (1983) Biochim. Biophys. Acta 722, 1–11.
579 Dekker, J.P., Van Gorkom, H.J., Wensink, J. and Ouwehand, L. (1984) Biochim. Biophys. Acta 767, 1–9.
580 Dekker, J.P., Plijter, J.J., Ouwehand, L. and Van Gorkom, H.J. (1984) Biochim. Biophys. Acta 767, 176–179.
581 Renger, G. and Weiss, W. (1986) Biochem. Soc. Trans. 14, 17–20.
582 Renger, G. and Weiss, W. (1986) Biochim. Biophys. Acta 850, 184–196.
583 Lavergne, J. (1986) Photochem. Photobiol. 43, 311–317.
584 Lavergne, J. (1987) Biochim. Biophys. Acta 894, 91–107.
585 Dekker, J.P., Plijter, J.J. and Van Gorkom, H.J. (1987) in Progress in Photosynthesis Research (Biggins, J., ed.), Vol. I, pp. 533–536, Martinus Nijhoff, Dordrecht.
586 Kretschmann, H., Dekker, J.P., Saygin, Ö. and Witt, H.T. (1988) Biochim. Biopnys. Acta 932, 358–361.
587 Renger, G. and Hanssum, B. (1988) Photosynth. Res. 16, 243–259.
588 Lavergne, J. (1989) Photochem. Photobiol. 50, 235–241.
589 Lavergne, J. (1991) Biochim. Biophys. Acta 1060, 175–188.
590 Dekker, J.P. and Van Gorkom, H.J. (1987) J. Bioenerg. Biomemb. 19, 125–142.
591 Renger, G. and Hanssum, B. (1992) FEBS Lett. 299, 28–32.
592 Witt, H.T., Saygin, Ö., Brettel, K. and Schlodder, E. (1987) in Progress in Photosynthesis Research (Biggins, J., ed.), Vol. I, pp. 523–531, Martinus Nijhoff, Dordrecht.
593 Messinger, J., Wacker, U. and Renger, G. (1991) Biochemistry 30, 7852–7862.
594 Van Leeuwen, P.J., Vos, M.H. and Van Gorkom, H.J. (1990) Biochim. Biophys. Acta 1018, 173–176.
595 Vincent, J.B. and Christou, G. (1986) FEBS Lett. 207, 250–252.
596 Renger, G. (1987) Angew. Chem. Int. Ed. Engl. 26, 643–660.
597 Renger, G. (1987) Photosynthetica 21, 203–224.
598 Babcock, G.T., Blankenship, R.E. and Sauer, K. (1976) FEBS Lett. 61, 286–289.
599 Boska, M. and Sauer, K. (1984) Biochim. Biophys. Acta 765, 84–87.
600 Boska, M., Blough, N.V. and Sauer, K. (1985) Biochim. Biophys. Acta 808, 132–139.
601 Cole, J. and Sauer, K. (1987) Biochim. Biophys. Acta 891, 40–48.
602 Babcock, G.T., Buttner, W.T., Ghanotakis, D.F., O'Malley, P.J., Yerkes, C.T. and Yocum, C.F. (1984) in Advances in Photosynthesis Research (Sybesma, C., ed.), Vol. I, pp. 243–252, Martinus Nijhoff/Dr. W. Junk, The Hague.
603 Vos, M.H., Van Gorkom, H.J. and Van Leeuwen, P.J. (1991) Biochim. Biophys. Acta 1056, 27–39.
604 Lavergne, J. (1984) FEBS Lett. 173, 9–14.
605 Saygin, Ö. and Witt, H.T. (1984) FEBS Lett. 176, 83–87.
606 Lavergne, J. (1985) Physiol. Vég. 23, 411–423.
607 Saygin, O. and Witt, H.T. (1985) FEBS Lett. 187, 224–226.
608 Velthuys, B.R. (1988) Biochim. Biophys. Acta 933, 249–257.
609 Dismukes, G.C. and Mathis, P. (1984) FEBS Lett. 178, 51–54.
610 Preston, C. and Pace, R.J. (1985) Biochim. Biophys. Acta 810, 388–391.
611 Dismukes, G.C. (1986) Photochem. Photobiol. 43, 99–115.
612 Mauzerall, D.C. (1972) Proc. Natl. Acad. Sci. USA 69, 1358–1362.
613 Sonneveld, A., Rademaker, H. and Duysens, L.N.M. (1979) Biochim. Biophys. Acta 548, 536–551.
614 Deprez, J., Dobek, A., Geacintov, N.E., Paillotin, G. and Breton, J. (1983) Biochim. Biophys. Acta 725, 444–454.
615 Van Best, J.A. and Mathis, P. (1978) Biochim. Biophys. Acta 503, 178–188.
616 Brettel, K. and Witt, H.T. (1983) Photobiochem. Photobiophys. 6, 253–260.
617 Schlodder, E., Brettel, K., Schatz, G.H. and Witt, H.T. (1984) Biochim. Biophys. Acta 765, 178–185.
618 Brettel, K., Schlodder, E. and Witt, H.T. (1984) Biochim. Biophys. Acta 766, 403–415.
619 Eckert, H.-J., Renger, G. and Witt, H.T. (1984) FEBS Lett. 167, 316–320.
620 Meyer, B., Schlodder, E., Dekker, J.P. and Witt, H.T. (1989) Biochim. Biophys. Acta 974, 36–43.
621 Schlodder, E., Brettel, K. and Witt, H.T. (1985) Biochim. Biophys. Acta 808, 123–131.
622 Schlodder, E. and Meyer, B. (1987) Biochim. Biophys. Acta 890, 23–31.
623 Thompson, L.K., Miller, A.-F., De Paula, J.C. and Brudvig, G.W. (1988) Isr. J. Chem. 28, 121–128.
624 Conjeaud, H., Mathis, P. and Paillotin, G. (1979) Biochim. Biophys. Acta 546, 280–291.
625 Reinman, S., Mathis, P., Conjeaud, H. and Stewart, A. (1981) Biochim. Biophys. Acta 635, 429–433.
626 Renger, G. and Eckert, H.-J. (1981) Biochim. Biophys. Acta 638, 161–171.
627 Boska, M., Sauer, K., Buttner, W. and Babcock, G.T. (1983) Biochim. Biophys. Acta 722, 327–330.
628 Åkerlund, H.-E., Brettel, K. and Witt, H.T. (1984) Biochim. Biophys. Acta 765, 7–11.
629 Renger, G., Völker, M. and Weiss, W. (1984) Biochim. Biophys. Acta 766, 582–591.
630 Völker, M., Eckert, H.-J. and Renger, G. (1987) Biochim. Biophys. Acta 890, 66–76.
631 Saygin, Ö., Gerken, S., Meyer, B. and Witt, H.T. (1986) Photosynth. Res. 9, 71–78.
632 Bock, C.H., Gerken, S., Stehlik, D. and Witt, H.T. (1988) FEBS Lett. 227, 141–146.
633 Gerken, S., Dekker, J.P., Schlodder, E. and Witt, H.T. (1989) Biochim. Biophys. Acta 977, 52–61.
634 Frei, R., Eckert, H.-J., Renger, G. and Bachofen, R. (1988) Biochim. Biophys. Acta 932, 258–267.
635 Eckert, H.-J. and Renger, G. (1988) FEBS Lett. 236, 425–431.
636 Reinman, S. and Mathis, P. (1981) Biochim. Biophys. Acta 635, 247–258.
637 Diner, B.A. and De Vitry, C. (1984) in Advances in Photosynthesis Research (Sybesma, C., ed.), Vol. I, pp. 407–411, Martinus Nijhoff/Dr. W. Junk, The Hague.
638 Renger, G., Eckert, H.-J. and Völker, M. (1989) Photosynth. Res. 22, 247–256.
639 Fowler, C.F. (1977) Biochim. Biophys. Acta 462, 414–421.
640 Saphon, S. and Crofts, A.R. (1977) Z. Naturforsch. 32c, 617–626.
641 Velthuys, B.R. (1980) FEBS Lett. 115, 167–170.

642 Förster, V., Hong, Y.-Q. and Junge, W. (1981) Biochim. Biophys. Acta 638, 141–152.
643 Förster, V. and Junge, W. (1985) Photochem. Photobiol. 41, 183–190.
644 Diedrich-Glaubitz, R., Völker, M., Renger, G. and Gräber, P. (1987) in Progress in Photosynthesis Research (Biggins, J., ed.), Vol. I, pp. 519–522, Martinus Nijhoff Publishers, Dordrecht.
645 Renger, G., Wacker, U. and Völker, M. (1987) Photosynth. Res. 13, 167–189.
646 Wille, B. and Lavergne, J. (1982) Photobiochem. Photobiophys. 4, 131–144.
647 Bowes, J.M. and Crofts, A.R. (1978) Z. Naturforsch. 33c, 271–275.
648 Bowes, J.M. and Crofts, A.R. (1981) Biochim. Biophys. Acta 637, 464–472.
649 Lavergne, J. and Rappaport, F. (1990) in Current Research in Photosynthesis (Baltscheffsky, M., ed.), Vol. I, pp. 873–876, Kluwer, Dordrecht.
650 Jahns, P., Lavergne, J., Rappaport, F. and Junge, W. (1991) Biochim. Biophys. Acta 1057, 313–319.
651 Jahns, P. and Junge, W. (1992) Biochemistry, 31, 7398–7403.
652 Maróti, P. and Wraight, C.A. (1988) Biochim. Biophys. Acta 934, 314–328.
653 Maróti, P. and Wraight, C.A. (1988) Biochim. Biophys. Acta 934, 329–347.
654 McPherson, P.H., Okamura, M.Y. and Feher, G. (1988) Biochim. Biophys. Acta 934, 348–368.
655 Renger, G. (1977) FEBS Lett. 81, 223–228.
656 Renger, G. (1978) in Photosynthetic Oxygen Evolution (Metzner, H., Ed.), pp. 229–248, Academic Press, London.
657 Wacker, U., Haag, E. and Renger, G. (1990) in Current Research in Photosynthesis (Baltscheffsky, M., ed.), Vol. I, pp. 869–872, Kluwer, Dordrecht.
658 Lübbers, K. and Junge, W. (1990) in Current Research in Photosynthesis (Baltscheffsky, M., ed.), Vol. I, pp. 877–880, Kluwer, Dordrecht.
659 Renger, G. and Wydrzynski, T. (1991) Biol. Metals 4, 73–80.
660 Jahns, P. and Junge, W. (1992) Biochemistry, 31, 7390–7397.
661 Jahns, P., Polle, A. and Junge, W. (1988) EMBO J. 7, 589–594.
662 Jahns, P. and Junge, W. (1989) FEBS Lett. 253, 33–37.
663 Jahns, P. and Junge, W. (1990) Eur. J. Biochem. 193, 731–736.
664 Rao, P.S., Simic, M. and Hayon, E. (1975) J. Phys. Chem. 13, 1260–1263.
665 Weiss, W. and Renger, G. (1986) Biochim. Biophys. Acta 850, 173–183.
666 Bansal, K.M. and Sellers, R.M. (1975) J. Phys. Chem. 79, 1775–1780.
667 Okamura, M.Y., Isaacson, R.A. and Feher, G. (1979) Biochim. Biophys. Acta 546, 394–417.
668 Klimov, V.V., Dolan, E. and Ke, B. (1980) FEBS Lett. 112, 97–100.
669 Ono, T.-A. and Inoue, Y. (1991) FEBS Lett. 278, 183–186.
670 Ono, T.-A. and Inoue, Y. (1991) Biochemistry 30, 6183–6188.
671 Allakhverdiev, S.I., Klimov, V.V. and Demeter, S. (1992) FEBS Lett. 297, 51–54.
672 Ono, T.-A. and Inoue, Y. (1992) Biochim. Biophys. Acta 1099, 185–192.
673 Demeter, S., Rózsa, Zs., Vass, I. and Sallai, A. (1985) Biochim. Biophys. Acta 809, 369–378.
674 Koike, H., Siderer, Y., Ono, T.-A. and Inoue, Y. (1986) Biochim. Biophys. Acta 850, 89–89.
675 Sane, P.V. and Rutherford, A.W. (1986) in Light Emission by Plants and Bacteria (Govindjee, Amesz, J. and Fork, D.C., eds.), pp. 329–360, Academic Press, Orlando.
676 Demeter, S. and Govindjee (1989) Physiol. Plant. 75, 121–130.
677 Vass, I. and Inoue, Y. (1992) in The Photosystems: Structure, Function and Molecular Biology (Barber, J., ed.), pp. 259–294, Elsevier, Amsterdam.
678 Diner, B.A. and Bowes, J.M. (1981) in Photosynthesis (Akoyunoglou, G., ed.), Vol. III, pp. 875–883, Balaban International Science Services, Philadelphia.
679 Satoh, Ki. and Mathis, P. (1981) Photobiochem. Photobiophys. 2, 189–198.
680 Yerkes, C.T., Babcock, G.T. and Crofts, A.R. (1983) FEBS Lett. 158, 359–363.
681 Hoganson, C.W. and Babcock, G.T. (1989) Biochemistry 28, 1448–1454.
682 Rutherford, A.W. and Inoue, Y. (1984) FEBS Lett. 165, 163–170.
683 Blubaugh, D.J., Atamian, M., Babcock, G.T., Golbeck, J.H. and Cheniae, G.M. (1991) Biochemistry 30, 7586–7597.
684 Noren, G.H. and Barry, B.A. (1992) Biochemistry 31, 3335–3342.
685 Izawa, S., Heath, R.L. and Hind, G. (1969) Biochim. Biophys. Acta 180, 388–398.
686 Velthuys, B.R. and Amesz, J. (1975) Biochim. Biophys. Acta 376, 162–168.
687 Velthuys, B.R. (1975) Biochim. Biophys. Acta 396, 392–401.
688 Yocum, C.F. and Babcock, G.T. (1981) FEBS Lett. 130, 99–102.
689 Ghanotakis, D.F., O'Malley, P.J. and Babcock, G.T. (1983) in The Oxygen Evolving System of Photosynthesis (Inoue, Y., Crofts, A.R., Govindjee, Murata, N., Renger, G. and Satoh, Ki., eds.), pp. 91–101, Academic Press, Tokyo.
690 Govindjee and Homann, P.H. (1989) in Highlights of Modern Biochemistry (Kotyk, A., Škoda, J., Pačes, V. and Kostka, V., eds.), pp. 933–961, VSP, Utrecht.
691 Coleman, W.J. (1990) Photosynth. Res. 23, 1–27.
692 Sheats, J.E., Czernuszewicz, R.S., Dismukes, G.C., Rheingold, A.L., Petrouleas, V., Stubbe, J., Armstrong, W.H., Beer, R.H. and Lippard, S.J. (1987) J. Am. Chem. Soc. 109, 1435–1444.
693 Baumgarten, M., Tso, J., Marino, J., Sivaraja, M., Lin, C.P., Dismukes, G.C., Sheats, J.E., Gast, P. and Philo, J.S. (1990) in Current Research in Photosynthesis (Baltscheffsky, M., ed.), Vol. I, pp. 953–956, Kluwer, Dordrecht.
694 Delrieu, M.J. (1976) Biochim. Biophys. Acta 440, 176–188.
695 Fine, P.L. and Frasch, W.D. (1990) in Current Research in Photosynthesis (Baltscheffsky, M., ed.), Vol. I, pp. 905–908, Kluwer, Dordrecht.
696 Frasch, W.D. (1992) in Manganese Redox Enzymes (Pecoraro, V.L., ed.), pp. 47–70, VCH, New York.
697 Thompson, L.K., Blaylock, R., Sturtevant, J.M. and Brudvig, G.W. (1989) Biochemistry 28, 6686–6695.
698 Sauer, K. (1990) in Current Research in Photosynthesis (Baltscheffsky, M., ed.), Vol. I, pp. 675–684, Kluwer Academic Publishers, Dordrecht.
699 Plijter, J.J., Aalbers, S.E., Barends, J.-P.F., Vos, M.H. and Van Gorkom, H.J. (1988) Biochim. Biophys. Acta 935, 299–311.
700 Van Gorkom, H.J., Van Leeuwen, P.J., Vos, M.H. and Barends, J.-P.F. (1990) in Current Research in Photosynthesis (Baltscheffsky, M., ed.), Vol. I, pp. 693–700, Kluwer Academic Publishers, Dordrecht.
701 Joliot, P., Hofnung, M. and Chabaud, R. (1966) J. Chim. Phys. 63, 1423–1441.
702 Étienne, A.-L. (1968) Biochim. Biophys. Acta 153, 895–897.
703 Bouges-Bocquet, B. (1973) Biochim. Biophys. Acta 292, 772–785.
704 Sinclair, J. and Arnason, T. (1974) Biochim. Biophys. Acta 368, 393–400.
705 Arnason, T. and Sinclair, J. (1976) Biochim. Biophys. Acta 430, 517–523.
706 Cananni, O., Malkin, S. and Mauzerall, D.C. (1988) Proc. Natl. Acad. Sci. USA 85, 4725–4729.
707 Mauzerall, D.C. (1990) Plant Physiol. 94, 278–283.
708 Strzalka, K., Walczak, T., Sarna, T. and Swartz, H.M. (1990) Arch. Biochem. Biophys. 281, 312–318.

709 Tang, X.-S., Moussavi, M. and Dismukes, G.C. (1991) J. Am. Chem. Soc. 113, 5914–5915.
710 Lavergne, J. (1989) Proc. Natl. Acad. Sci. USA 86, 8768–8772.
711 Lavergne, J. (1990) in Current Research in Photosynthesis (Baltscheffsky, M., ed.), Vol. I, pp. 893–896, Kluwer Academic Publishers, Dordrecht.
712 Jursinic, P.A. and Dennenberg, R.J. (1990) Biochim. Biophys. Acta 1020, 195–206.
713 Meunier, P.C. and Popovic, R. (1991) Photosynth. Res. 28, 33–39.
714 Lozier, R., Baginsky, M. and Butler, W.L. (1971) Photochem. Photobiol. 14, 323–328.
715 Blankenship, R.E. and Sauer, K. (1974) Biochim. Biophys. Acta 357, 252–266.
716 Ikehara, N. and Sugahara, K. (1969) Bot. Mag. Tokyo 82, 271–277.
717 Cheniae, G.M. and Martin, I.F. (1978) Biochim. Biophys. Acta 502, 321–344.
718 Frasch, W.D. and Cheniae, G.M. (1980) Plant Physiol. 65, 735–745.
719 Beck, W.F., Sears, J., Brudvig, G.W., Kulawiec, R.J. and Crabtree, R.H. (1989) Tetrahedron 45, 4903–4911.
720 Rickert, K.W., Sears, J., Beck, W.F. and Brudvig, G.W. (1991) Biochemistry 30, 7888–7894.
721 Bennoun, P. and Bouges, B. (1972) in Proceedings of the Second International Congress on Photosynthesis Research, Vol. I (Forti, G., Avron, M. and Melandri, A., eds.), pp. 569–576, Dr. W. Junk, The Hague.
722 Radmer, R. and Ollinger, O. (1982) FEBS Lett. 144, 162–166.
723 Radmer, R. and Ollinger, O. (1983) FEBS Lett. 152, 39–43.
724 Den Haan, G.A., Duysens, L.N.M. and Egberts, D.J.N. (1974) Biochim. Biophys. Acta 368, 409–421.
725 Den Haan, G.A., Gorter De Vries, H. and Duysens, L.N.M. (1976) Biochim. Biophys. Acta 430, 265–281.
726 Jursinic, P.A. and Govindjee (1982) Photosynth. Res. 3, 161–177.
727 Ghanotakis, D.F. and Babcock, G.T. (1983) FEBS Lett. 153, 231–234.
728 Sharp, R.R. and Yocum, C.F. (1981) Biochim. Biophys. Acta 635, 90–104.
729 Bennoun, P. and Joliot, A. (1969) Biochim. Biophys. Acta 189, 85–94.
730 Bouges, B. (1971) Biochim. Biophys. Acta 234, 103–112.
731 Radmer, R. (1983) in The Oxygen Evolving System of Photosynthesis (Inoue, Y., Crofts, A.R., Govindjee, Murata, N., Renger, G. and Satoh, Ki., eds.), pp. 135–144, Academic Press, Inc., Tokyo.
732 Messinger, J., Pauly, S. and Witt, H.T. (1991) Z. Naturforsch. 46c, 1033–1038.
733 Kok, B. and Velthuys, B.R. (1977) in Research in Photobiology (Castellani, A., ed.), pp. 111–119, Plenum Press, New York.
734 Radmer, R. and Ollinger, O. (1981) Biochim. Biophys. Acta 637, 80–87.
735 Messinger, J. and Renger, G. (1990) FEBS Lett. 277, 141–146.
736 Velthuys, B.R. and Kok, B. (1978) Biochim. Biophys. Acta 502, 211–221.
737 Mano, J., Takahashi, M.-A. and Asada, K. (1987) Biochemistry 26, 2495–2501.
738 Sivaraja, M., Hunziker, D. and Dismukes, G.C. (1988) Biochim. Biophys. Acta 936, 228–235.
739 Tso, J., Petrouleas, V. and Dismukes, G.C. (1990) Biochemistry 29, 7759–7767.
740 Vass, I., Tso, J. and Dismukes, G.C. (1990) Biochemistry 29, 7767–7773.
741 Cramer, W.A. and Böhme, H. (1972) Biochim. Biophys. Acta 256, 358–369.
742 Jursinic, P.A. and Stemler, A. (1983) Plant Physiol. 73, 703–708.
743 Renger, G., Hagemann, R. and Fromme, R. (1986) FEBS Lett. 203, 210–214.
744 Franck, F. and Schmid, G.H. (1989) Biochim. Biophys. Acta 977, 215–218.
745 Homann, P.H. (1988) Plant Physiol. 88, 194–199.
746 Berg, S.P. and Seibert, M. (1987) Photosynth. Res. 13, 3–17.
747 Sandusky, P.O. and Yocum, C.F. (1988) Biochim. Biophys. Acta 936, 149–156.
748 Frasch, W.D. and Mei, R. (1987) Biochim. Biophys. Acta 891, 8–14.
749 Frasch, W.D. and Mei, R. (1987) Biochemistry 26, 7321–7325.
750 Mathur, P., Crowder, M. and Dismukes, G.C. (1987) J. Am. Chem. Soc. 109, 5227–5233.
751 Larson, E.J. and Pecoraro, V.L. (1991) J. Am. Chem. Soc. 113, 7809–7810.
752 Larson, E.J., Riggs, P.J., Penner-Hahn, J.E. and Pecoraro, V.L. (1992) J. Chem. Soc., Chem. Commun. 102–103.
753 Rush, J.D. and Maskos, Z. (1990) Inorg. Chem. 29, 897–905.
754 Khangulov, S.V., Goldfeld, M.G., Gerasimenko, V.V., Andreeva, N.E., Barynin, V.V. and Grebenko, A.I. (1990) J. Inorg. Biochem. 40, 279–292.
755 Khangulov, S.V., Barynin, V.V. and Antonyuk-Barynina, S.V. (1990) Biochim. Biophys. Acta 1020, 25–33.
756 Waldo, G.S., Fronko, R.M. and Penner-Hahn, J.E. (1991) Biochemistry 30, 10486–10490.
757 Penner-Hahn, J.E. (1992) in Manganese Redox Enzymes (Pecoraro, V.L., ed.), pp. 29–45, VCH, New York.
758 Frasch, W.D., Mei, R. and Sanders, M.A. (1988) Biochemistry 27, 3715–3719.
759 Quensel, J. and Åkerlund, H.-E. (1990) in Current Research in Photosynthesis (Baltscheffsky, M., ed.), Vol. I, pp. 897–900, Kluwer, Dordrecht.
760 Velthuys, B.R. (1983) in The Oxygen Evolving System of Photosynthesis (Inoue, Y., Crofts, A.R., Govindjee, Murata, N., Renger, G. and Satoh, Ki., eds.), pp. 83–90, Academic Press, Tokyo.
761 Krishtalik, L.I. (1986) Biochim. Biophys. Acta 849, 162–171.
762 Krishtalik, L.I. (1990) Bioelectrochem. Bioenerg. 23, 249–263.
763 Volkov, A.G. (1989) Bioelectrochem. Bioenerg. 21, 3–24.
764 Radmer, R. and Ollinger, O. (1986) FEBS Lett. 195, 285–289.
765 Bader, K.P., Thibault, P. and Schmid, G.H. (1987) Biochim. Biophys. Acta 893, 564–571.
766 Micklitz, W., Bott, S.G., Bentsen, J.G. and Lippard, S.J. (1989) J. Am. Chem. Soc. 111, 372–374.
767 Dismukes, G.C., Sheats, J.E., Mathur, P. and Czernuszewicz, R.S. (1990) in Current Research in Photosynthesis (Baltscheffsky, M., ed.), Vol. I, pp. 773–776, Kluwer Academic Publishers, Dordrecht.
768 Chan, M.K. and Armstrong, W.H. (1990) J. Am. Chem. Soc. 112, 4985–4986.
769 Stibrany, R.T. and Gorun, S.M. (1990) Angew. Chem. Int. Ed. Engl. 29, 1156–1158.
770 Bhula, R., Gainsford, G.J. and Weatherburn, D.C. (1988) J. Am. Chem. Soc. 110, 7550–7552.
771 Bossek, U., Weyhermüller, T., Wieghardt, K., Nuber, B. and Weiss, J. (1990) J. Am. Chem. Soc. 1990, 6387–6388.
772 Larson, E.J. and Pecoraro, V.L. (1991) J. Am. Chem. Soc. 113, 3810–3818.
773 Thorp, H.H., Sarneski, J.E., Brudvig, G.W. and Crabtree, R.H. (1989) J. Am. Chem. Soc. 111, 9249–9250.
774 Thorp, H.H., Brudvig, G.W. and Bowden, E.F. (1990) J. Electroanal. Chem. 290, 293–301.
775 Manchanda, R., Thorp, H.H., Brudvig, G.W. and Crabtree, R.H. (1991) Inorg. Chem. 30, 494–497.
776 Kalsbeck, W.A., Thorp, H.H. and Brudvig, G.W. (1991) J. Electroanal. Chem. 314, 335–343.

777 Hagen, K.S., Westmoreland, T.D., Scott, M.J. and Armstrong, W.H. (1989) J. Am. Chem. Soc. 111, 1907–1909.
778 Sarneski, J.E., Thorp, H.H., Brudvig, G.W., Crabtree, R.H. and Schulte, G.K. (1990) J. Am. Chem. Soc. 112, 7255–7260.
779 Boucher, L.J. and Coe, C.G. (1975) Inorg. Chem. 14, 1289–1295.
780 Schröder, W.P. and Åkerlund, H. E. (1986) Biochim. Biophys. Acta 848, 359–363.
781 Schröder, W.P. and Åkerlund, H.-E. (1987) in Progress in Photosynthesis Research (Biggins, J., ed.), Vol. I, pp. 665–668, Martinus Nijhoff, Dordrecht.
782 a Anan'ev, G.M. and Klimov, V.V. (1988) Dokl. Akad. Nauk SSSR 298, 1007–1011 (Engl. Transl., Dokl Biochem. 298, 22–25).
782 b Anan'ev, G.M. and Klimov, V.V. (1989) Biokhimiya 54, 1587–1597 (English translation: Biochemistry (USSR) 54, 1295–1303).
783 Wydrzynski, T., Ångström, J. and Vänngård, T. (1989) Biochim. Biophys. Acta 973, 23–28.
784 Schröder, W.P. and Åkerlund, H.-E. (1990) in Current Research in Photosynthesis (Baltscheffsky, M., ed.), Vol. I, pp. 901–904, Kluwer, Dordrecht.
785 Bradley, R.L., Long, K.M. and Frasch, W.D. (1991) FEBS Lett. 286, 209–213.
786 Sayre, R.T. and Homann, P.H. (1979) Arch. Biochem. Biophys. 196, 525–533.
787 Dismukes, G.C. (1988) Chem. Scripta 28A, 99–104.
788 Aswad, D.W. and Johnson, B.A. (1987) Trends Biochem. Sci. 12, 155–158.
789 Britt, R.D., Sauer, K. and Klein, M.P. (1987) in Progress in Photosynthesis (Biggins, J., ed.), Vol. I, pp. 573–576, Martinus Nijhoff, Dordrecht.
790 Preston, C. and Seibert, M. (1990) in Current Research in Photosynthesis (Baltscheffsky, M., ed.), Vol. I, pp. 925–928, Kluwer, Dordrecht.
791 Preston, C. and Seibert, M. (1991) Biochemistry 30, 9615–9624.
792 Tamura, N., Ikeuchi, M. and Inoue, Y. (1989) Biochim. Biophys. Acta 973, 281–289.
793 Kambara, T. and Govindjee (1985) Proc. Natl. Acad. Sci. USA 82, 6119–6123.
794 Padhye, S., Kambara, T., Hendrickson, D.N. and Govindjee (1986) Photosynth. Res. 9, 103–112.
795 Seibert, M., Tamura, N. and Inoue, Y. (1989) Biochim. Biophys. Acta 974, 185–191.
796 Preston, C. and Seibert, M. (1989) Photosynth. Res. 22, 101–113.
797 Preston, C. and Seibert, M. (1991) Biochemistry 30, 9625–9633.
798 Abramowicz, D.A. and Dismukes, G.C. (1984) Biochim. Biophys. Acta 765, 318–328.
799 Yamamoto, Y., Shinkai, H., Isogai, Y., Matsuura, K. and Nishimura, M. (1984) FEBS Lett. 175, 429–432.
800 Barber, J. (1984) Trends Biochem. Sci. 9, 79–80.
801 Franzén, L.-G. and Andréasson, L.-E. (1984) Biochim. Biophys. Acta 765, 166–170.
802 Ono, T.-A. and Inoue, Y. (1986) Biochim. Biophys. Acta 850, 380–389.
803 Styring, S., Miyao, M. and Rutherford, A.W. (1987) Biochim. Biophys. Acta 890, 32–38.
804 Miyao, M., Murata, N., Lavorel, J., Maison-Peteri, B., Boussac, A. and Étienne, A.-L. (1987) Biochim. Biophys. Acta 890, 151–159.
805 Miller, A.-F., De Paula, J.C. and Brudvig, G.W. (1987) Photosynth. Res. 12, 205–218.
806 Hunziker, D., Abramowicz, D.A., Damoder, R. and Dismukes, G.C. (1987) Biochim. Biophys. Acta 890, 6–14.
807 Camm, E.L., Green, B.R., Allred, D.R. and Staehelin, L.A. (1987) Photosynth. Res. 13, 69–80.
808 Burnap, R.L. and Sherman, L.A. (1991) Biochemistry 30, 440–446.
809 Philbrick, J.B., Diner, B.A. and Zilinskas, B.A. (1991) J. Biol. Chem. 266, 13370–13376.
810 Mayes, S.R., Cook, K.M., Self, S.J., Zhang, Z. and Barber, J. (1991) Biochim. Biophys. Acta 1060, 1–12.
811 Bockholt, R., Masepohl, B. and Pistorius, E.K. (1991) FEBS Lett. 294, 59–63.
812 Mayfield, S.P., Bennoun, P. and Rochaix, J.-D. (1987) EMBO J. 6, 313–318.
813 Mizobuchi, A. and Yamamoto, Y. (1989) Biochim. Biophys. Acta 977, 26–32.
814 Seibert, M. and Cotton, T.M. (1985) FEBS Lett. 182, 34–38.
815 Seibert, M., Cotton, T.M. and Metz, J.G. (1988) Biochim. Biophys. Acta 934, 235–246.
816 Vass, I., Ono, T.-A. and Inoue, Y. (1987) FEBS Lett. 211, 215–220.
817 Bricker, T.M., Odom, W.R. and Queirolo, C.B. (1988) FEBS Lett. 231, 111–117.
818 Odom, W.R. and Bricker, T.M. (1992) Biochemistry, 31, 5616–5620.
819 Enami, I., Satoh, Ka. and Katoh, S. (1987) FEBS Lett. 226, 101–165.
820 Enami, I., Mochizuki, Y., Kaneko, M., Kakuno, T., Horio, T., Satoh, Ka. and Katoh, S. (1990) in Current Research in Photosynthesis (Baltscheffsky, M., ed.), Vol. I, pp. 319–322, Kluwer, Dordrecht.
821 Enami, I., Ohta, S., Mitsuhashi, S., Takahashi, S., Ikeuchi, M. and Kate , S. (1992) Plant Cell Physiol. 33, 291–297.
822 Frasch, W.D., Green, J.P. and Mei, R. (1988) in Light-Energy Transduction in Photosynthesis: Higher Plant and Bacterial Models (Stevens, S.E., Jr. and Bryant, D.A., eds.), pp. 373–376, American Society of Plant Physiologists, Rockville.
823 Mei, R., Green, J.P., Sayre, R.T. and Frasch, W.D. (1989) Biochemistry 28, 5560–5567.
824 Adir, N. and Ohad, I. (1986) Biochim. Biophys. Acta 850, 264–274.
825 Adir, N. and Ohad, I. (1988) J. Biol. Chem. 263, 283–289.
826 Sayre, R.T., Andersson, B. and Bogorad, L. (1986) Cell 47, 601–608.
827 Frankel, L.K. and Bricker, T.M. (1990) in Current Research in Photosynthesis (Baltscheffsky, M., ed.), Vol. I, pp. 639–642, Kluwer, Dordrecht.
828 Garstka, M. and Kaniuga, Z. (1991) Physiol. Plant. 82, 271–277.
829 Bricker, T.M. and Frankel, L.K. (1987) Arch. Biochem. Biophys. 256, 295–301.
830 Isogai, Y., Yamamoto, Y. and Nishimura, M. (1985) FEBS Lett. 187, 240–244.
831 Frankel, L.K. and Bricker, T.M. (1989) FEBS Lett. 257, 279–282.
832 Gounaris, K., Chapman, D.J. and Barber, J. (1988) FEBS Lett. 234, 374–378.
833 Gounaris, K., Chapman, D.J. and Barber, J. (1990) in Current Research in Photosynthesis (Baltscheffsky, M., ed.), Vol. I, pp. 327–330, Kluwer, Dordrecht.
834 Takahashi, M.-A. and Asada, K. (1991) Biochim. Biophys. Acta 1059, 361–364.
835 Noren, G.H., Boerner, R.J., Bixby, K.A. and Barry, B.A. (1991) Biophys. J. 59, 145a.
836 Warden, J.T., Blankenship, R.E. and Sauer, K. (1976) Biochim. Biophys. Acta 423, 462–478.
837 Rutherford, A.W., Seibert, M. and Metz, J.G. (1988) Biochim. Biophys. Acta 932, 171–176.
838 Innes, J.B. and Brudvig, G.W. (1989) Biochemistry 28, 1116–1125.
839 Isogai, Y., Nishimura, M., Iwaki, M. and Itoh, S. (1988) Biochim. Biophys. Acta 936, 259–268.
840 De Groot, A., Plijter, J.J., Evelo, R.G., Babcock, G.T. and Hoff, A.J. (1986) Biochim. Biophys. Acta 848, 8–15.

841 Bosch, M.K., Evelo, R.G., Styring, S., Rutherford, A.W. and Hoff, A.J. (1991) FEBS Lett. 292, 279–283.
842 Beck, W.F., Innes, J.B. and Brudvig, G.W. (1990) in Current Research in Photosynthesis (Baltscheffsky, M., ed.), Vol. I, pp. 817–820, Kluwer, Dordrecht.
843 Hirsh, D.J., Beck, W.F., Innes, J.B. and Brudvig, G.W. (1992) Biochemistry 31, 532–541.
844 Beck, W.F., Innes, J.B., Lynch, J.B. and Brudvig, G.W. (1991) J. Magn. Reson. 91, 12–29.
845 Evelo, R.G. and Hoff, A.J. (1991) J. Magn. Reson. 95, 495–508.
846 Isogai, Y., Itoh, S. and Nishimura, M. (1990) Biochim. Biophys. Acta 1017, 204–208.
847 Lozier, R.H. and Butler, W.L. (1973) Photochem. Photobiol. 17, 133–137.
848 Yerkes, C.T. and Babcock, G.T. (1980) Biochim. Biophys. Acta 590, 360–372.
849 Ghanotakis, D.F., Yerkes, C.T. and Babcock, G.T. (1982) Biochim. Biophys. Acta 682, 21–31.
850 Metz, J.G., Wong, J. and Bishop, N.I. (1980) FEBS Lett. 114, 61–66.
851 Metz, J.G. and Bishop, N.I. (1980) Biochem. Biophys. Res. Commun. 94, 560–566.
852 Bishop, N.I. (1983) in The Oxygen Evolving System of Photosynthesis (Inoue, Y., Crofts, A.R., Govindjee, Murata, N., Renger, G. and Satoh, K., eds.) pp. 177–187, Academic Press Inc., Tokyo.
853 Metz, J.G. and Seibert, M. (1984) Plant Physiol. 76, 829–832.
854 Metz, J.G., Bricker, T.M. and Seibert, M. (1985) FEBS Lett. 185, 191–196.
855 Metz, J.G., Pakrasi, H.B., Seibert, M. and Arntzen, C.J. (1986) FEBS Lett. 205, 269–274.
856 Diner, B.A., Ries, D.F., Cohen, B.N. and Metz, J.G. (1988) J. Biol. Chem. 263, 8972–8980.
857 Taylor, M.A., Nixon, P.J., Todd, C.M., Barber, J. and Bowyer, J.R. (1988) FEBS Lett. 235, 109–116.
858 Taylor, M.A., Packer, J.C.L. and Bowyer, J.R. (1988) FEBS Lett. 237, 229–233.
859 Karabin, G.D., Farley, M. and Hallick, R.B. (1984) Nucleic Acids Res. 12, 5801–5812.
860 Keller, M. and Stutz, E. (1984) FEBS Lett. 175, 173–177.
861 Ikeuchi, M., Koike, H. and Inoue, Y. (1988) Biochim. Biophys. Acta 932, 160–169.
862 Ikeuchi, M. and Inoue, Y. (1988) Plant Cell Physiol. 29, 695–705.
863 Virgin, I., Styring, S. and Andersson, B. (1988) FEBS Lett. 233, 408–412.
864 Hundal, T., Virgin, I., Styring, S. and Andersson, B. (1990) Biochim. Biophys. Acta 1017, 235–341.
865 Coleman, W.J. and Govindjee (1987) Photosynth. Res. 13, 199–223.
866 Gounaris, K., Chapman, D.J. and Barber, J. (1989) Biochim. Biophys. Acta 973, 296–301.
867 Vermaas, W.F.J., Charité, J. and Shen, G. (1990) Biochemistry 29, 5325–5332.
868 Madsen, C. and Vermaas, W.F.J. (1991) in Third International Congress of Plant Molecular Biology: Program and Abstracts (Hallick, R.B., ed.), Abst. 1879, International Society for Plant Molecular Biology, Athens, GA.
869 Diner, B.A., Nixon, P.J., Metz, J.G., Rögner, M. and Chisholm, D.A. (1990) Biophys. J. 57, 405a.
870 Nixon, P.J. and Diner, B.A. (1991) Photochem. Photobiol. 53, 71S.
871 Debus, R.J., Nguyen, A.P., Conway, A.B. and Chu, H.-A. (1991) Biophys. J. 59, 143a.
872 Van der Bolt, F. and Vermaas, W.F.J. (1992) Biochim. Biophys. Acta 1098, 247–254.
873 Boerner, R.J., Nguyen, A.P., Barry, B.A. and Debus, R.J. (1992) Biochemistry 31, 6660–6672.
874 Makaroff, C.A., Paluh, J.L. and Zalkin, H. (1986) J. Biol. Chem. 261, 11416–11423.
875 Nakai, M., Ishiwatari, H., Asada, A., Bogaki, M., Kawai, K., Tanaka, Y. and Matsubara, H. (1990) J. Biochem. 108, 798–803.
876 Haiech, J., Kilhoffer, M.-C., Lukas, T.J., Craig, T.A., Roberts, D.M. and Watterson, D.M. (1991) J. Biol. Chem. 266, 3427–3431.
877 Rothery, R.A. and Weiner, J.H. (1991) Biochemistry 30, 8296–8305.
878 Minagawa, J., Mogi, T., Gennis, R.B. and Anraku, Y. (1992) J. Biol. Chem. 267, 2096–2104.
879 Lemieux, L.J., Calhoun, M.W., Thomas, J.W., Ingledew, W.J. and Gennis, R.B. (1992) J. Biol. Chem. 267, 2105–2113.
880 Nixon, P.J. and Diner, B.A. (1992) J. Cell Biochem. 16D, 118.
881 Putnam-Evans, C. and Bricker, T.M. (1991) Plant Physiol. 96, 115a.
882 Eaton-Rye, J.J. and Vermaas, W.F.J. (1991) Plant Mol. Biol. 17, 1165–1177.
883 Kuhn, M. and Vermaas, W.F.J. (1991) Plant Physiol. 96, 165a.
884 Kuhn, M. and Vermaas, W.F.J. (1991) in Third International Congress of Plant Molecular Biology: Program and Abstracts (Hallick, R.B., ed.), Abst. 1869, International Society for Plant Molecular Biology, Athens, GA.
885 Tae, G.-S. and Cramer, W.A. (1992) Biochemistry 31, 4066–4074.
886 Homann, P.H. (1989) in The Role of Calcium in Biological Systems, Vol. V (Anghileri, L.J., ed.), pp. 79–96, CRC Press, Boca Raton.
887 Binder, A., Tel-Or, E. and Avron, M. (1976) Eur. J. Biochem. 67, 187–196.
888 Piccioni, R.G. and Mauzerall, D.C. (1976) Biochim. Biophys. Acta 423, 605–609.
889 Piccioni, R.G. and Mauzerall, D.C. (1978) Biochim. Biophys. Acta 504, 384–397.
890 Brand, J.J. (1979) FEBS Lett. 103, 114–117.
891 England, R.R. and Evans, E.H. (1981) FEBS Lett. 134, 175–177.
892 England, R.R. and Evans, E.H. (1983) Biochem. J. 210, 473–476.
893 Brand, J.J., Mohanty, P. and Fork, D.C. (1983) FEBS Lett. 155, 120–124.
894 Pistorius, E.K. (1983) Eur. J. Biochem. 135, 217–222.
895 Boussac, A., Maison-Peteri, B., Étienne, A.-L. and Vernotte, C. (1985) Biochim. Biophys. Acta 808, 231–234.
896 Ghanotakis, D.F., Babcock, G.T. and Yocum, C.F. (1985) FEBS Lett. 192, 1–3.
897 Miyao, M. and Murata, N. (1986) Photosynth. Res. 10, 489–496.
898 Cammarata, K.V. and Cheniae, G.M. (1987) Plant Physiol. 84, 587–595.
899 Katoh, S., Satoh, Ka., Ohno, T., Shen, J.-R and Kashino, Y. (1987) in Progress in Photosynthesis (Biggins, J., ed.), Vol. I, pp. 625–628, Martinus Nijhoff, Dordrecht.
900 Shen, J.-R., Satoh, Ka. and Katoh, S. (1988) Biochim. Biophys. Acta 933, 358–364.
901 Fromme, R. and Renger, G. (1990) Z. Naturforsch. 45c, 373–378.
902 Kalosaka, K., Beck, W.F., Brudvig, G.W. and Cheniae, G.M. (1990) in Current Research in Photosynthesis (Baltscheffsky, M., ed.), Vol. I, pp. 721–724, Kluwer, Dordrecht.
903 Shen, J.-R. and Katoh, S. (1991) Plant Cell Physiol. 32, 439–446.
904 Boussac, A., Maison-Peteri, B., Vernotte, C. and Étienne, A.-L. (1985) Biochim. Biophys. Acta 808, 225–230.
905 Dekker, J.P., Ghanotakis, D.F., Plijter, J.J., Van Gorkom, H.J. and Babcock, G.T. (1984) Biochim. Biophys. Acta 767, 515–523.
906 Glynn, I.M. and Karlish, S.J.D. (1990) Annu. Rev. Biochem. 59, 171–205.
907 Shen, J.-R. and Katoh, S. (1990) in Current Research in Photosynthesis (Baltscheffsky, M., ed.), Vol. I, pp. 737–740, Kluwer, Dordrecht.
908 Homann, P.H. (1988) Biochim. Biophys. Acta 934, 1–13.
909 Waggoner, C.M., Pecoraro, V.L. and Yocum, C.F. (1989) FEBS Lett. 244, 237–240.

910 Waggoner, C.M. and Yocum, C.F. (1990) in Current Research in Photosynthesis (Baltscheffsky, M., ed.), Vol. I, pp. 733–736, Kluwer, Dordrecht.
911 Satoh, Ka. and Katoh, S. (1985) FEBS Lett. 190, 199–203.
912 Blubaugh, D.J. and Cheniae, G.M. (1990) Plant Physiol. 93, 22.
913 Kashino, Y., Satoh, Ka. and Katoh, S. (1986) FEBS Lett. 205, 150–154.
914 Boussac, A. and Rutherford, A.W. (1992) Photosynth. Res. 32, 207–209.
915 Blough, N.V. and Sauer, K. (1984) Biochim. Biophys. Acta 767, 377–381.
916 Ono, T.-A. and Inoue, Y. (1989) Biochim. Biophys. Acta 973, 443–449.
917 Plijter, J.J., De Groot, A., Van Dijk, M.A. and Van Gorkom, H.J. (1986) FEBS Lett 195, 313–318.
918 Rutherford, A.W., Crofts, A.R. and Inoue, Y. (1982) Biochim. Biophys. Acta 682, 457–465.
919 Rutherford, A.W., Renger, G., Koike, H. and Inoue, Y. (1984) Biochim. Biophys. Acta 767, 548–556.
920 Wensink, J., Dekker, J.P. and Van Gorkom, H.J. (1984) Biochim. Biophys. Acta 765, 147–155.
921 Delrieu, M.J. and Rosengard, F. (1991) Biochim. Biophys. Acta 1057, 78–88.
922 Ghanotakis, D.F., Babcock, G.T. and Yocum, C.F. (1984) in Advances in Photosynthesis Research (Sybesma, C., ed.), Vol. I, pp. 279–282, Martinus Nijhoff/Dr. W. Junk, The Hague.
923 Hind, G., Nakatani, H.Y. and Izawa, S. (1969) Biochim. Biophys. Acta 172, 277–289.
924 Theg, S.M. and Homann, P.H. (1982) Biochim. Biophys. Acta 679, 221–234.
925 Izawa, S., Muallem, A. and Ramaswamy, N.K. (1983) in The Oxygen Evolving System of Photosynthesis (Inoue, Y., Crofts, A.R., Govindjee, Murata, N., Renger, G. and Satoh, Ki., eds.), pp. 293–302, Academic Press, Tokyo.
926 Homann, P.H. (1985) Biochim. Biophys. Acta 809, 311–319.
927 Sandusky, P.O. (1985) Ph.D. Dissertation, University of Michigan, Ann Arbor.
928 Damoder, R., Klimov, V.V. and Dismukes, G.C. (1986) Biochim. Biophys. Acta 848, 378–391.
929 Wydrzynski, T., Baumgart, F., MacMillan, F. and Renger, G. (1990) Photosynth. Res. 25, 59–72.
930 Pauly, S., Schlodder, E. and Witt, H.T. (1990) in Current Research in Photosynthesis (Baltscheffsky, M., ed.), Vol. I, pp. 745–748, Kluwer, Dordrecht.
931 Pauly, S., Schlodder, E. and Witt, H.T. (1992) Biochim. Biophys. Acta 1099, 203–210.
932 Homann, P.H., Gleiter, H., Ono, T.-A. and Inoue, Y. (1986) Biochim. Biophys. Acta 850, 10–20.
933 Inoue, Y. (1987) in Progress in Photosynthesis Research (Biggins, J., ed.), Vol. I, pp. 637–644, Martinus Nijhoff Publishers, Dordrecht.
934 Muallem, A., Farineau, J., Lainé-Böszörményi, M. and Izawa, S. (1981) in Photosynthesis (Akoyunoglou, G., ed.), Vol. II, pp. 435–443, Balaban International Science Services, Philadelphia.
935 Muallem, A. and Lainé-Böszörményi, M. (1981) Photochem. Photobiol. 2, 337–345.
936 Lindberg, K., Wydrzynski, T., Vänngård, T. and Andréasson, L.-E. (1990) FEBS Lett. 264, 153–155.
937 Wydrzynski, T., Åkerlund, H.-E., Baumgart, F., Renger, G. and Vänngård, T. (1990) Biochim. Biophys. Acta 1018, 55–60.
938 Coleman, W.J., Govindjee and Gutowsky, H.S. (1987) Biochim. Biophys. Acta 894, 443–452.
939 Coleman, W.J., Govindjee and Gutowsky, H.S. (1987) Biochim. Biophys. Acta 894, 453–459.
940 Shachar-Hill, Y., Beck, W.F. and Brudvig, G.W. (1989) FEBS Lett. 254, 184–188.
941 Kalb, A.J. and Levitzki, A. (1968) Biochem. J. 109, 669–672.
942 Strynadka, N.C.J. and James, M.N.G. (1989) Annu. Rev. Biochem. 58, 951–998.
943 McPhalen, C.A., Strynadka, N.C.J. and James, M.N.G. (1991) Adv. Protein Chem. 42, 77–144.
944 Strynadka, N.C.J. and James, M.N.G. (1991) Current Opinion in Struct. Biol. 1, 905–914.
945 Kretsinger, R.H. (1987) Cold Spring Harbor Symp. Quant. Biol. 52, 499–510.
946 Boguta, G., Stepkowski, D. and Bierzynski, A. (1988) J. Theor. Biol. 135, 41–61.
947 Persechini, A., Moncrief, N.D. and Kretsinger, R.H. (1989) Trends Neurosci. 12, 462–467.
948 Heizmann, C.W. and Hunziker, W. (1991) Trends Biochem. Sci. 16, 98–103.
949 Szebenyi, D.M.E. and Moffat, K. (1986) J. Biol. Chem. 261, 8761–8777.
950 Vyas, N.K., Vyas, M.N. and Quiocho, F.A. (1987) Nature 327, 635–638.
951 Boguta, G. and Bierzynski, A. (1988) Biophys. Chem. 133, 137.
952 Godzik, A. and Sander, C. (1989) Protein Engineering 2, 589–596.
953 Leszczynki, J.F. and Rose, G.D. (1986) Science 234, 849–855.
954 Rees, D.C., Lewis, M. and Lipscomb, W.N. (1983) J. Mol. Biol. 168, 367–387.
955 Baker, E.N. and Hubbard, R.E. (1984) Prog. Biophys. Molec. Biol. 44, 97–179.
956 Richardson, J.S. and Richardson, D.C. (1989) in Prediction of Protein Structure and the Principles of Protein Conformation (Fasman, G.D., ed.), pp. 1–98, Plenum Press, New York.
957 Abbadi, A., Mcharfi, M., Aubry, A., Prémilat, S., Boussard, G. and Marraud, M. (1991) J. Am. Chem. Soc. 113, 2729–2735.
958 Burnap, R.L., Webb, R. and Sherman, L.A. (1990) in Current Research in Photosynthesis (Baltscheffsky, M., ed.), Vol. I, pp. 255–258, Kluwer, Dordrecht.
959 Maruyama, K., Mikawa, T. and Ebashi, S. (1984) J. Biochem. 95, 511–519.
960 Webber, A.N. and Gray, J.C. (1989) FEBS Lett. 249, 79–82.
961 Yu, C.M.-C. and Brand, J.J. (1980) Biochim. Biophys. Acta 591, 483–487.
962 Pakrasi, H.B. and Sherman, L.A. (1984) Plant Physiol. 74, 742–745.
963 Burnap, R.L., Koike, H., Sotiropoulou, G., Sherman, L.A. and Inoue, Y. (1989) Photosynth. Res. 22, 123–130.
964 Brand, J.J. and Becker, D.W. (1984) J. Bioenerg. Biomemb. 16, 239–249.
965 Becker, D.W. and Brand, J.J. (1985) Plant Physiol. 79, 552–558.
966 Brand, J.J. and Becker, D.W. (1988) Methods Enzymol. 167, 280–285.
967 Zhao, J. and Brand, J.J. (1988) Arch. Biochem. Biophys. 264, 657–664.
968 Astier, C., Styring, S., Maison-Peteri, B. and Étienne, A.-L. (1986) Photobiochem. Photobiophys. 11, 37–47.
969 Schatz, G.H. and Witt, H.T. (1984) Photobiochem. Photobiophys. 7, 1–14.
970 Schatz, G.H. and Witt, H.T. (1984) Photobiochem. Photobiophys. 7, 77–89.
971 Katoh, S. (1988) Methods Enzymol. 167, 263–269.
972 Smutzer, G. and Wang, J.H. (1984) Biochim. Biophys. Acta 766, 240–244.
973 Satoh, Ka. and Katoh, S. (1985) Biochim. Biophys. Acta 806, 221–229.
974 Przibilla, E., Heiss, S., Johanningmeier, U. and Trebst, A. (1991) The Plant Cell 3, 169–174.
975 Roffey, R.A., Golbeck, J.H., Hille, C.R. and Sayre, R.T. (1991) Proc. Natl. Acad. Sci. USA 88, 9122–9126.
976 Tainer, J.A., Getzoff, E.D., Beem, K.M., Richardson, J.S. and Richardson, D.C. (1982) J. Mol. Biol. 160, 181–217.

977 Lamer, J.A., Getzoff, E.D., Richardson, J.S. and Richardson, D.C. (1983) Nature 306, 284–287.
978 Cramer, S.P., Siddons, P., Smith, G., Prince, R.C., George, G.N. and Chen, C. (1989) J. Inorg. Biochem. 36, 248.
979 Cramer, S.P., De Groot, F.M.F., Ma, Y., Chen, C.T., Sette, F., Kipke, C.A., Eichhorn, D.M., Chan, M.K., Armstrong, W.H., Libby, E., Christou, G., Brooker, S., McKee, V., Mullins, O.C. and Fuggle, J.C. (1991) J. Am. Chem. Soc. 113, 7937–7940.
980 Rigoni, F., Barbato, R., Friso, G. and Giacometti, M. (1992) Biochem. Biophys. Res. Commun. 184, 1094–1100.
981 Diner, B.A. and Nixon, P.J. (1992) Biochim. Biophys. Acta 1101, 134–138.
982 Shen, J.-R., Ono, T.-A. and Inoue, Y. (1992) Photosynth. Res. 32, 71–78.
983 Proserpio, D.M., Hoffmann, R. and Dismukes, G.C. (1992) J. Am. Chem. Soc. 114, 4374–4382.
984 Van Wijk, K.J., Andersson, B. and Styring, S. (1992) Biochem. Biophys. Acta 1100, 207–215.
985 Whitelegge, J., Maung, T., Tahtakran, S. and Erickson, J.M. (1992) in Third International Congress of Plant Molecular Biology: Program and Abstracts (Hallick, R.B., ed.), Abstr. 1865, International Society for Plant Molecular Biology, Athens, GA.
986 Barry, B.A. (1992) Photochem. Photobiol., in press.
987 Virgin, I., Salter, A.H., Hagman, Å., Vass, I., Styring, S. and Andersson, B. (1992) Biochim. Biophys. Acta 1101, 139–142.
988 Pichersky, E., Subramaniam, R., White, M.J., Reid, J., Aebersold, R. and Green, B.R. (1991) Mol. Gen. Genet. 227, 277–284.
989 Demeter, S., Rózsa, Zs., Vass, I. and Hideg, É. (1985) Biochim. Biophys. Acta 809, 379–387.
990 Ananyev, G., Wydrzynski, T., Renger, G. and Klimov, V.V. (1992) Biochim. Biophys. Acta 1100, 303–311.
991 Schulder, R., Bader, K.P. and Schmid, G.H. (1990) Z. Naturforsch 45c, 1117–1126.
992 Lavorel, J. (1992) Biochem. Biophys. Acta 1101, 33–40.
993 Nilsson, F., Gounaris, K., Styring, S. and Andersson, B. (1992) Biochim. Biophys. Acta 1100, 251–258.
994 Kashino, Y., Enami, I., Igarashi, S. and Katoh, S. (1992) Plant Cell Physiol. 33, 259–266.
995 Ichimura, T., Miyairi, S., Satoh, Ka. and Katoh, S. (1992) Plant Cell Physiol. 33, 299–305.
996 Nixon, P.J., Trost, J.T. and Diner, B.A. (1992) Biochemistry, in press.
997 Schrader, S. and Johanningmeier, U. (1992) Plant Mol. Biol. 19, 251–256.
998 Lers, A., Heifetz, P.B., Boynton, J.E., Gillham, N.W. and Osmond, C.B. (1992) J. Biol. Chem., in press.
999 Boussac, A. and Rutherford, A.W. (1992) Biochemistry, 31, 7441–7445.